New Mexico Department of Transportation

Research Bureau

Innovation in Transportation

Strengthening Reinforced Concrete Bridges in New Mexico Using Fiber Reinforced Polymers: A Compendium of Four Reports

Prepared by:
University of New Mexico
Albuquerque, NM

Prepared for:
New Mexico Department of Transportation
Research Bureau
Santa Fe, NM

In Cooperation with:
The US Department of Transportation
Federal Highway Administration

Report NM06TT-01

MARCH 2008

STRENGTHENING REINFORCED CONCRETE BRIDGES IN NEW MEXICO USING FIBER REINFORCED POLYMERS: A COMPILATION OF FOUR REPORTS

I. Structural Analysis and Evaluation of Bridges 7930, 7931, 7937 and 7938 in Tucumcari

II. Design Method for Strengthening K-Frame Bridges Using FRP

III. Implementation of FRP Design Alternative to K-Frame Bridge

IV. Guidelines for Using FRP Technology for Strengthening Bridges

by

M. M. Reda Taha
K. K. Choi
M. Azarbayejani
University of New Mexico
Department of Civil Engineering

Prepared for:
New Mexico Department of Transportation, Research Bureau

A Report on Research Sponsored by:
New Mexico Department of Transportation, Research Bureau

In Cooperation with the
U.S. Department of Transportation, Federal Highway Administration

March 2008

NMDOT, Research Bureau
7500-B Pan American Freeway NE
Albuquerque, NM 87109

Form DOT F 1700.7 (8-72)

1. Report No. NM06TT-01	**2. Government Accession No.**	**3. Recipient's Catalog No.**
4. Title and Subtitle Strengthening Reinforced Concrete Bridges in New Mexico Using Fiber Reinforced Polymers Report I: Structural Analysis and Evaluation of Bridges (7930, 7931, 7937 and 7938) in Tucumcari		**5. Report Date** March 2008 **6. Performing Organization Code**
7. Author(s) M. M. Reda Taha, K. K. Choi, M. Azarbayejani		**8. Performing Organization Report No.**
9. Performing Organization Name and Address University of New Mexico Department of Civil Engineering Albuquerque, NM 87131		**10. Work Unit No. (TRAIS)** **11. Contract or Grant No.** CO4961
12. Sponsoring Agency Name and Address Research Bureau New Mexico Department of Transportation 7500-B Pan American Freeway NE Albuquerque, NM 87109		**13. Type of Report and Period Covered** **14. Sponsoring Agency Code**
15. Supplementary Notes		

16. Abstract

The objective of this report is to provide detailed evaluation of the structural capacity of the concrete frame bridges #7930, 7931, 7937 and 7938 at Tucumcari, New Mexico and evaluate their need for strengthening. Finite Element (FE) analysis using SAP 2000® was performed to estimate the moment and shear force demand and compare it to the existing capacity of the four bridges on I-40 at Tucumcari. The structural analysis and the strength evaluation were performed according to ASSHTO LRFD Bridge Design Specification with 2006 Interim Revision (AASHTO 2006).

The investigations showed that the four bridges do not meet the AASHTO requirements and need strengthening. The structural evaluation showed that the four bridges require strengthening at the top side (negative moment side) of the K-Frame joint. The report provides detailed information about the locations that require strengthening.

17. Key Words: Concrete frame bridges, AASHTO LRFD Bridge Design Specification, Fiber reinforced polymers.		**18. Distribution Statement** Available from NMDOT Research Bureau	
19. Security Classif. (of this report) None	**20. Security Classif. (of this page)** None	**21. No. of Pages** 54	**22. Price**

PREFACE

The purpose of this research is to evaluate the structural capacity of the concrete frame bridges #7930, 7931, 7937 and 7938 at Tucumcari, New Mexico and evaluate their need for strengthening to meet AASHTO safety requirements.

NOTICE

DISCLAIMER

ABSTRACT

The objective of this report is to provide detailed evaluation of the structural capacity of the concrete frame bridges #7930, 7931, 7937 and 7938 at Tucumcari, New Mexico and evaluate their need for strengthening. Finite Element (FE) analysis using SAP 2000® was performed to estimate the moment and shear force demand and compare it to the existing capacity of the four bridges on I-40 at Tucumcari. The structural analysis and the strength evaluation were performed according to ASSHTO LRFD Bridge Design Specification with 2006 Interim Revision (AASHTO 2006).

The investigations showed that the four bridges do not meet the AASHTO requirements and need strengthening. The structural evaluation showed that the four bridges require strengthening at the top side (negative moment side) of the K-Frame joint. The report provides detailed information about the locations that require strengthening.

TABLE OF CONTENTS

Report I: Structural Analysis and Evaluation of Bridges 7930, 7931, 7937 and 7938 in Tucumcari

TABLES

FIGURES

OBJECTIVE

The objective of this report is to provide details regarding the process of evaluation of the structural capacity of the concrete frame bridges 7930, 7931, 7937 and 7938 at Tucumcari and evaluate their need for strengthening. Finite Element (FE) analysis using SAP 2000® was performed to estimate the moment and shear force demand and compare it to the existing capacity of the four bridges on I-40 at Tucumcari. The structural analysis and the strength evaluation were performed according to ASSHTO LRFD Bridge Design Specification with 2006 Interim Revision (1).

DESCRIPTION OF BRIDGES

Bridges 7930, 7931, 7937 and 7938 at Tucumcari are four reinforced concrete K-Frame bridges located on Interstate I-40. Photos representing the four bridges are presented in Fig. 1 to Fig. 6. The four bridges have similar configurations and material properties as shown by their structural plans (Figs. 7 to 8). Each bridge consists of 5 to 6 K-frames (Bridge 7930 is composed of six reinforced concrete K-frames whiles the others three bridges 7931, 7937 and 7938 are composed of reinforced concrete 5 K-frames), reinforced concrete transverse beams, and a reinforced concrete deck. Asphalt overlay was used on bridges 7937 and 7938 while 7930 and 7931 did not have asphalt. It was noted that bridge 7931 was skewed by 7 degrees. Each K-frame has a rectangular-shaped cross-section the depth of which varies along the length of the bridge. Moreover, the longitudinal and transverse reinforcements vary along the length of the bridge.

During the last two decades since the bridges were constructed, the size and weight of trucks passing over I-40 increased dramatically. Therefore, it is expected that the moment and shear demand by the current traffic according to AASHTO 2006 (1) might exceed the bridge capacity. Our analysis aimed at investigating the moment and shear capacity of the four bridges compared to the current traffic loads according to AASHTO 2006 (1).

FIGURE 1 Tucumcari bridge 7930.

FIGURE 2 Tucumcari bridge 7931.

FIGURE 3 Tucumcari bridge 7937.

FIGURE 4 Tucumcari bridge 7938.

FIGURE 5 Tucumcari bridge 7930 showing tension cracking at the bottom of the deck at the K-frame connection.

FIGURE 6 Supporting condition at the end of the girder of bridge 7937.

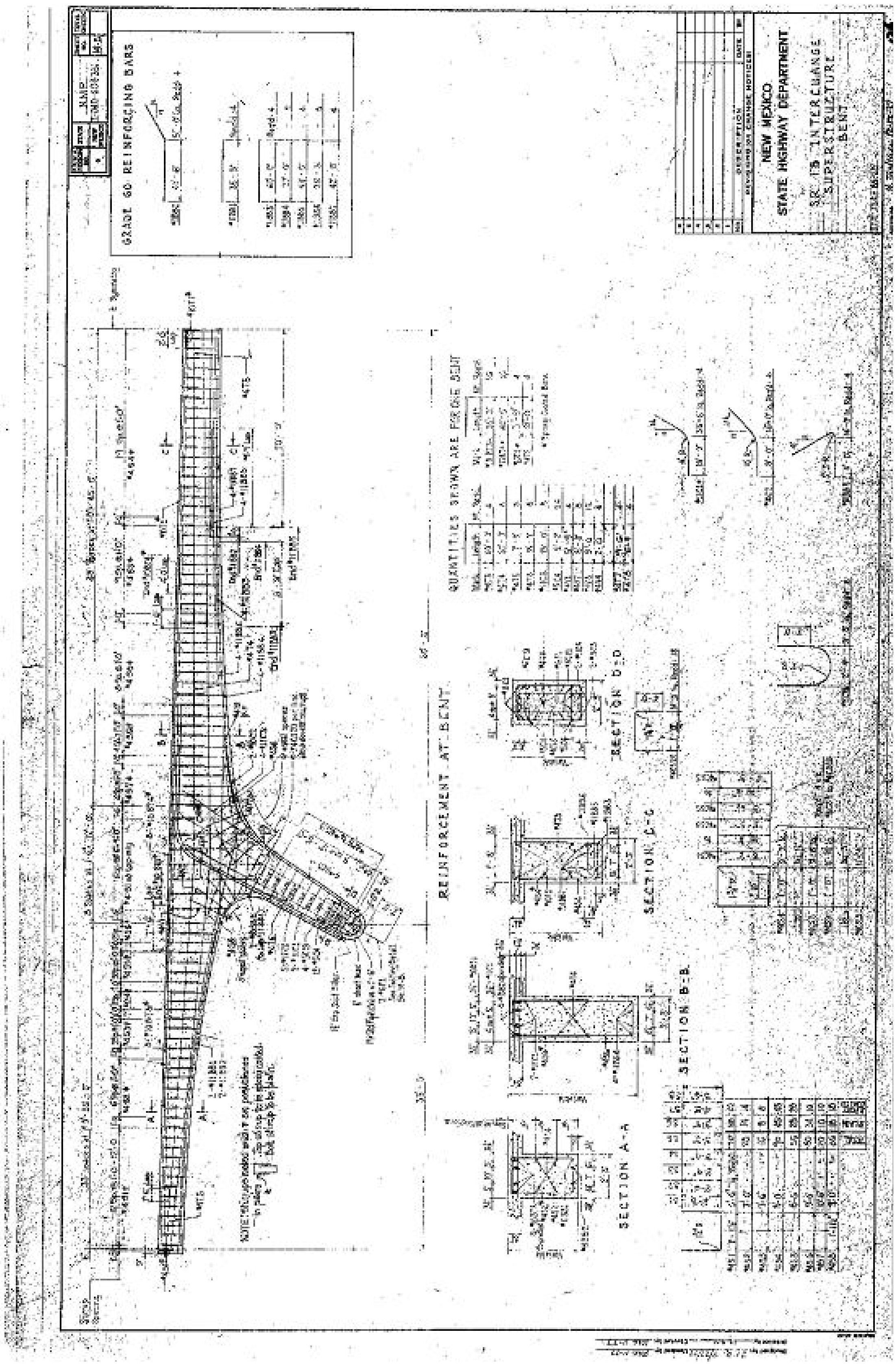

FIGURE 7 Structural drawing of bridges 7930 and 7931.

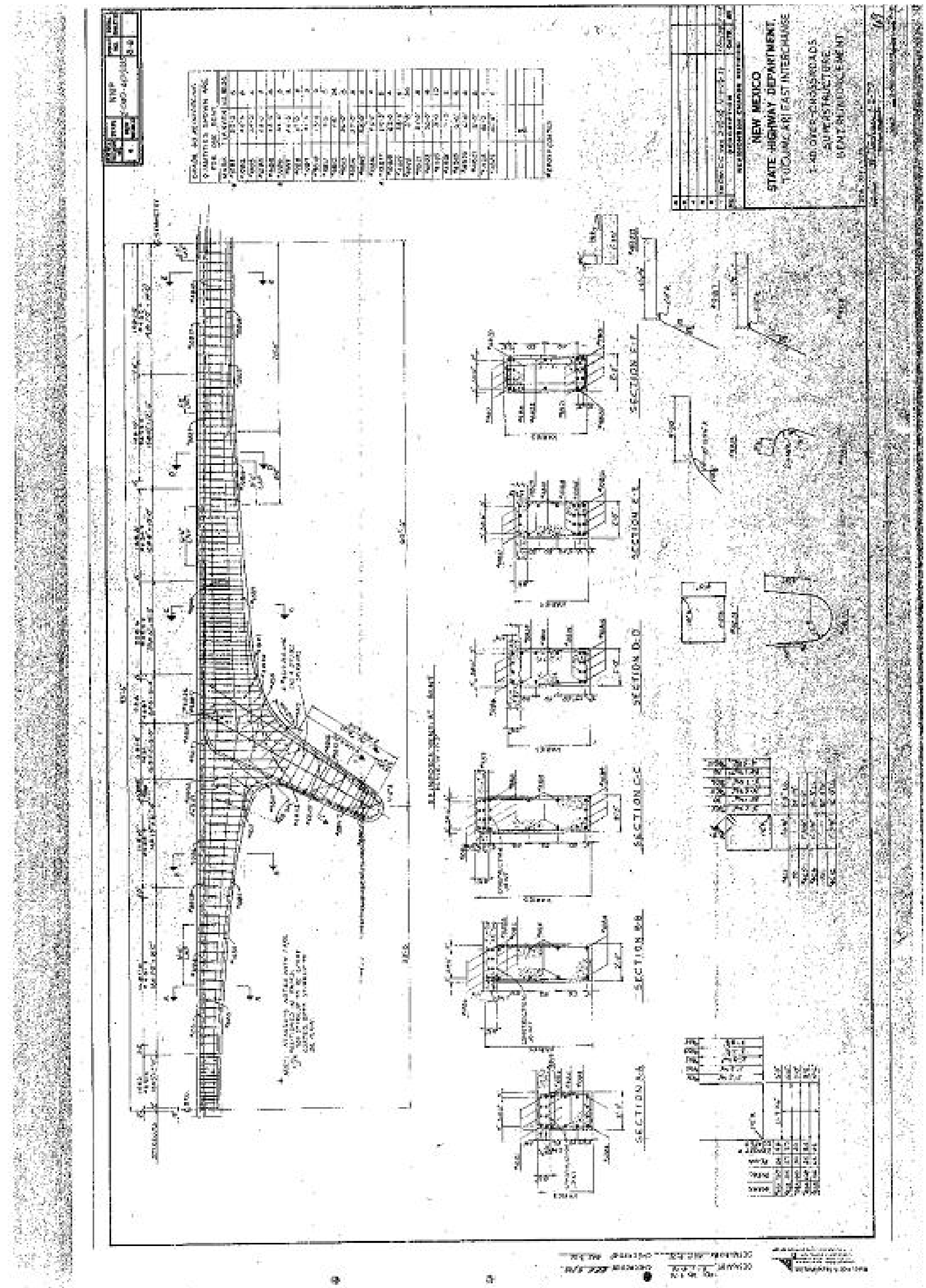

FIGURE 8 Structural drawing of bridges 7937 and 7938.

BRIDGE LOADING

Four different types of New Mexico Legal trucks were used in the FE analysis, in addition to Design truck by AASHTO and Tandem load. These four trucks included NMDOT Two-Axle Legal load truck, NMDOT Three-Axle Legal load truck, NMDOT Five-Axle Legal load truck, and NMDOT Permit truck P327-B. Characteristics of each truck including axle loading are presented in Fig. 9. Moreover, the distance between the two 145,000N axles in the AASHTO design truck was used as a variable from 4.3 m to 9.0 m as specified in AASHTO (1).

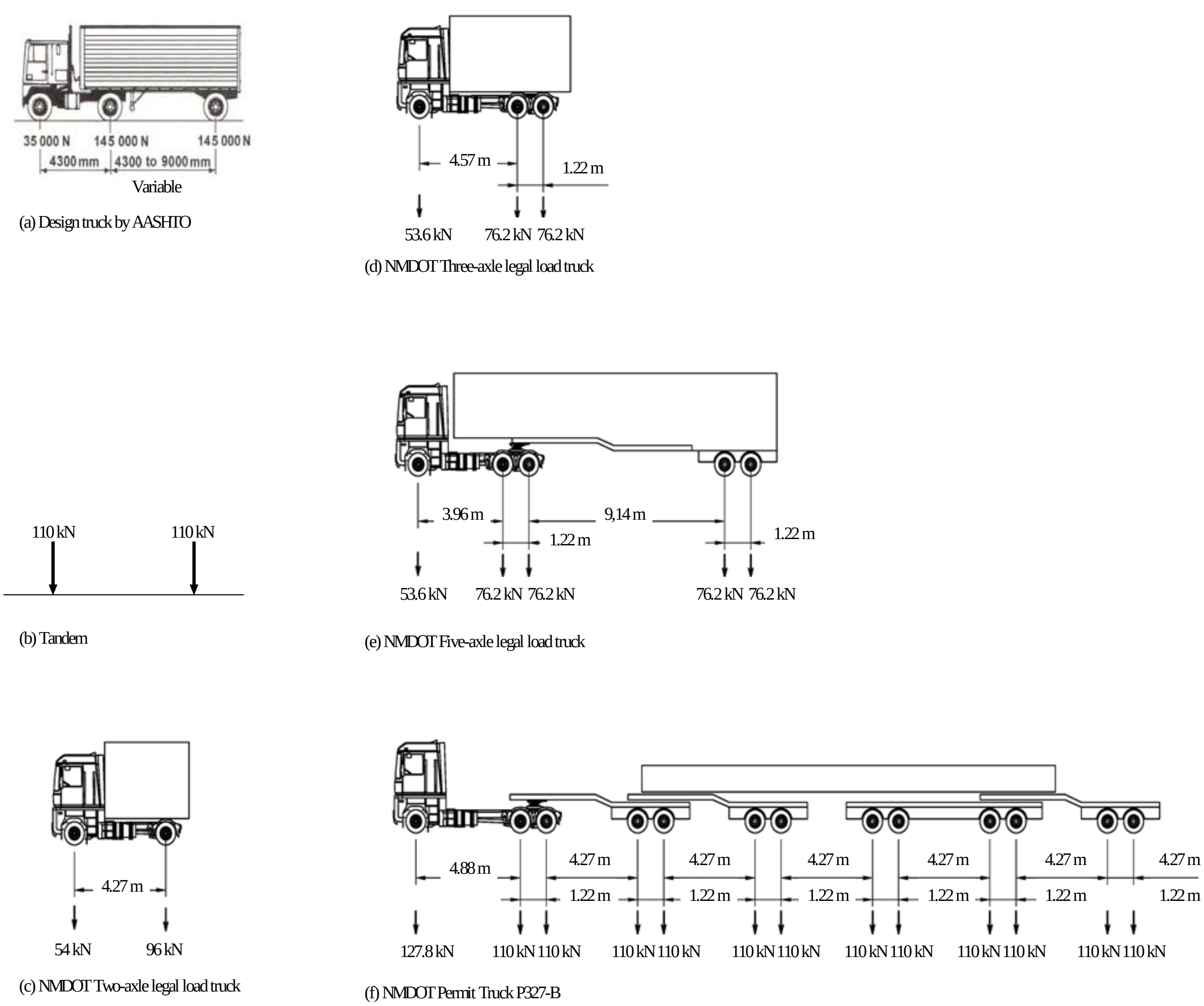

FIGURE 9 Characteristics of trucks used in FE analysis.

Furthermore, a 9.3 kN/m, uniformly distributed design lane load in the longitudinal direction was also considered as specified by AASHTO (1). The dynamic load allowance was computed to be (1.33) and was applied to the truck and tandem loads to consider the dynamic effect of traffic load. Finally, dead loads including self weight of the K-frames, concrete deck weight, rail load and asphalt weight were also included in the FE analysis.

LIVE LOAD DISTRIBUTION

In computing the total load on each K-frame bridge, traffic (live) load distribution between the frames needed to be calculated. The load distribution factors of the exterior and interior frames were computed separately. According to AASHTO (1), for exterior frames, the load distribution factors for moment and shear can be simply defined by using Eq. (1).

$$R = \frac{N_L}{N_b} + \frac{X_{ext}\sum^{N_L} e}{\sum^{N_L} x^2} \tag{1}$$

where

R = reaction on exterior beam in terms of lanes

N_L = number of loaded lanes under consideration

e = eccentricity of a design truck or a design lane load from the center of gravity of the pattern of frames (mm)

x = horizontal distance from the center of gravity of the pattern of frames to each frame (mm)

X_{ext} = horizontal distance from the center of gravity of the pattern of frames to the exterior frame (mm)

N_b = number of beams of frames.

The width of bridges 7930, 7931, 7937 and 7938 is 14.22 m, 11.78 m, 11.38 m, and 11.38 m, respectively. Therefore, four design lanes for bridge 7930 and three design lanes for the other bridges needed to be considered. Moreover, for exterior frames, the multiple presence factors m needed to be applied to address the effect of multiple presence of live load. The multiple presence factors are defined in Table 1 according to AASHTO (1). Finally, the load distribution factor is determined as a maximum value among the product of R [Eq. (1)] and m values (Table 1) using different N_L values.

TABLE 1 Multiple presence factors *m*.

Number of loaded lanes, N_L	Multiple presence factors *m*
1	1.20
2	1.00
3	0.85
> 3	0.65

For interior beams, the load distribution factors for moment and shear can be defined by Eqs. (2) and (3) respectively.

For moment

One design lane loaded

$$R = 0.06 + \left(\frac{S}{4300}\right)^{0.4}\left(\frac{S}{L}\right)^{0.3}\left(\frac{K_g}{Lt_s^3}\right)^{0.1} \qquad (2a)$$

Two or more design lane loaded

$$R = 0.075 + \left(\frac{S}{2900}\right)^{0.6}\left(\frac{S}{L}\right)^{0.2}\left(\frac{K_g}{Lt_s^3}\right)^{0.1} \quad (2b)$$

<u>For shear</u>

One design lane loaded

$$R = 0.36 + \frac{S}{7600} \quad (3a)$$

Two or more design lane loaded

$$R = 0.2 + \frac{S}{3600} - \left(\frac{S}{10700}\right)^{2.0} \quad (3b)$$

where:

S = spacing of supporting components (mm)

L = span length of deck (mm)

K_g $[= n(I + Ae_g{}^2)]$ = longitudinal stiffness parameter (mm^4)

n = ratio between modulus of elasticity of beam material and modulus of elasticity of deck material

I = moment of inertia of beam

e_g = distance between the centers of gravity of the basic beam and deck (mm)

t_s = depth of concrete slab (mm).

As defined in Eq. (4), the load distribution factor of interior beams may vary according to its location along the length of the beams because the depth of beams varies along the length of the beams. It is also noted that the multiple presence factors need not be applied to interior beams because Eq. (4) already considers such multiple presence effect.

Finally, the skew of bridge 7931 needs to be considered in the load calculation. In such case, the load distribution factor needs to be revised by the following correction factor.

$$1.0 + 0.2\left(\frac{Lt_s^{\ 3}}{K_g}\right)^{0.3} \tan\theta \tag{4}$$

where θ = skew angle.

FINITE ELEMENT (FE) ANALYSIS

Static structural analysis was performed for the four K-frame bridges. Considering the diaphragm action of bridges due to transverse beams and deck, each K-frame was analyzed as a separate frame instead of using an entire bridge model. Then, the load distribution between each frame was considered by using load distribution factors described above. Since the dead load (deck, asphalt, and bar railing load) was different in interior and exterior girders, two finite element models for each bridge were developed: one mode for interior frames and one model for exterior frames.

In general, bridge structures are analyzed assuming linear elastic behavior unless cracking is evident. No indication of cracks in the K-frames indicated the need for cracked/non-linear analysis. Therefore, according to AASHTO, the elastic material behavior was assumed in the FE analysis and the stiffness of the girder was calculated using an undamaged cross-section. Non-linear moving load analysis for live load was considered in order to identify the maximum effect of all moving loads considered in the analysis. Fig. 10 shows the FE model used in SAP 2000®. 58 nodes and 12 nodes were used to model the girder and inclined columns, respectively. Also 57 and 12 frame elements were used to model the girder and inclined columns, respectively. The girders and the columns were assumed to be monolithic, and enabling moment transfer. At each node, the FE model had the same depth of real K-frames shown in drawing.

Figures 11 and 12 show the moment and shear distribution of an exterior beam of bridge 7930 for several sources of loading: self weight of girders, Deck, design truck by AASHTO, Tandem, and NMDOT Permit truck P327-B. As shown in the figures, for moving load, the maximum and minimum effect was obtained directly from the non-linear moving load analysis in SAP 2000®.

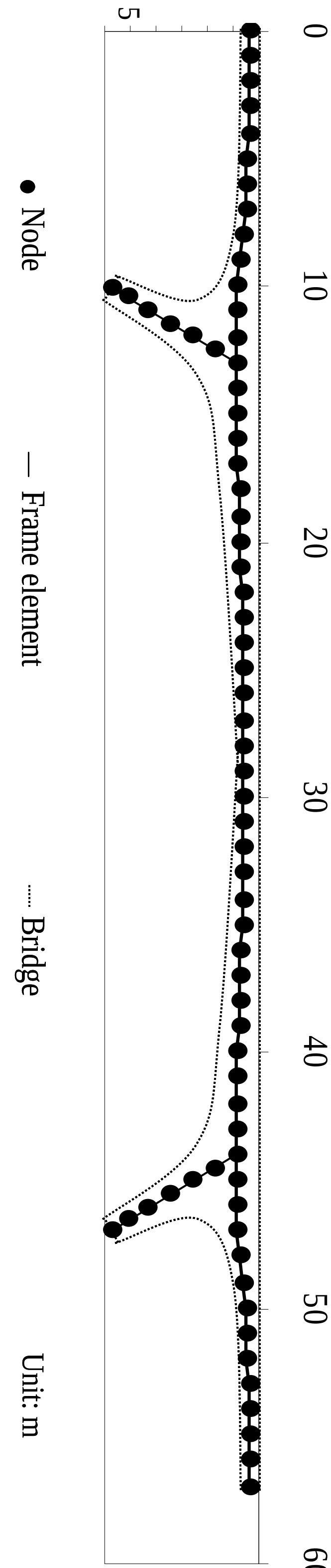

FIGURE 10 FE model showing nodes and frame elements.

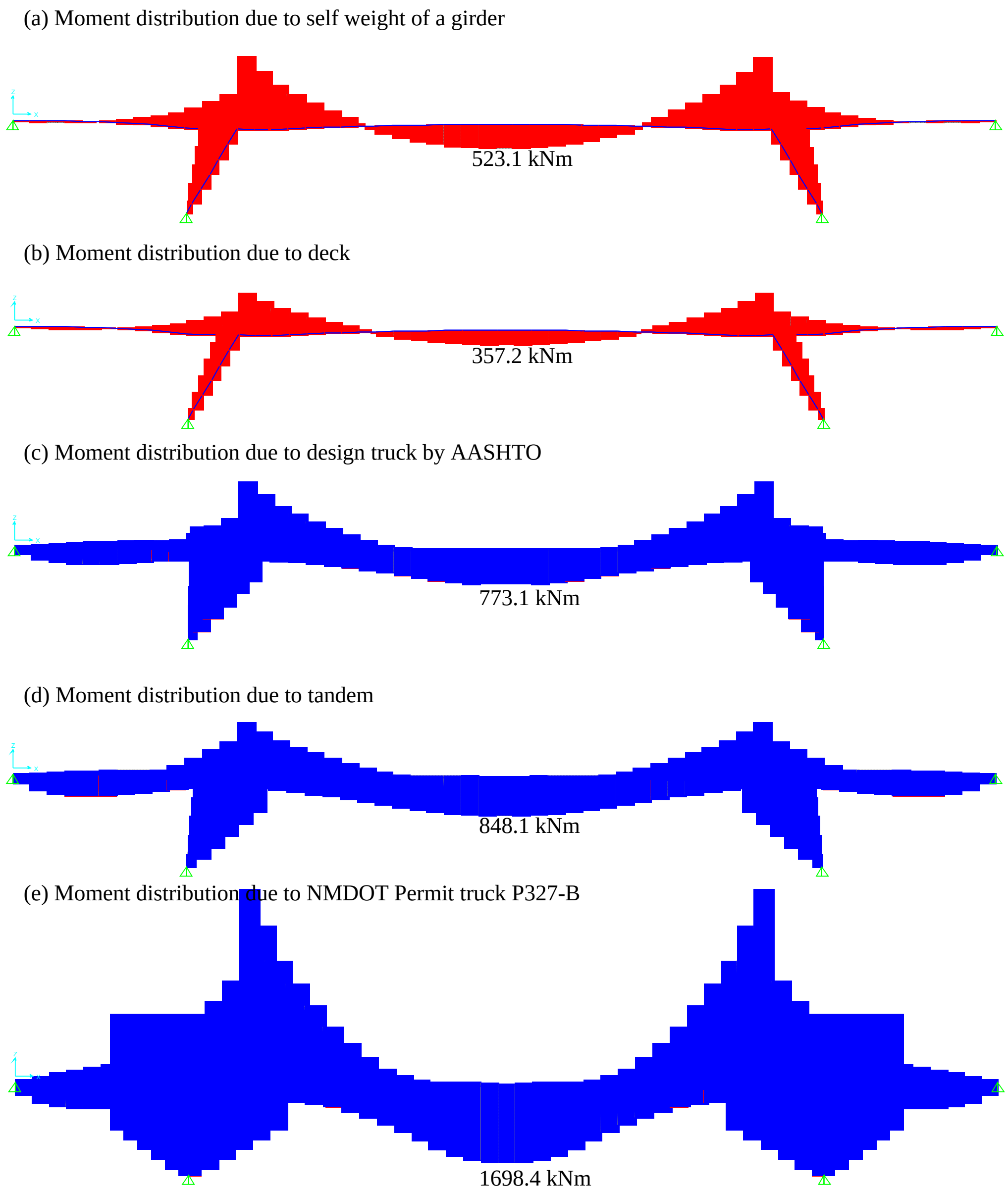

FIGURE 11 Moment distribution of an exterior beam of bridge 7937.

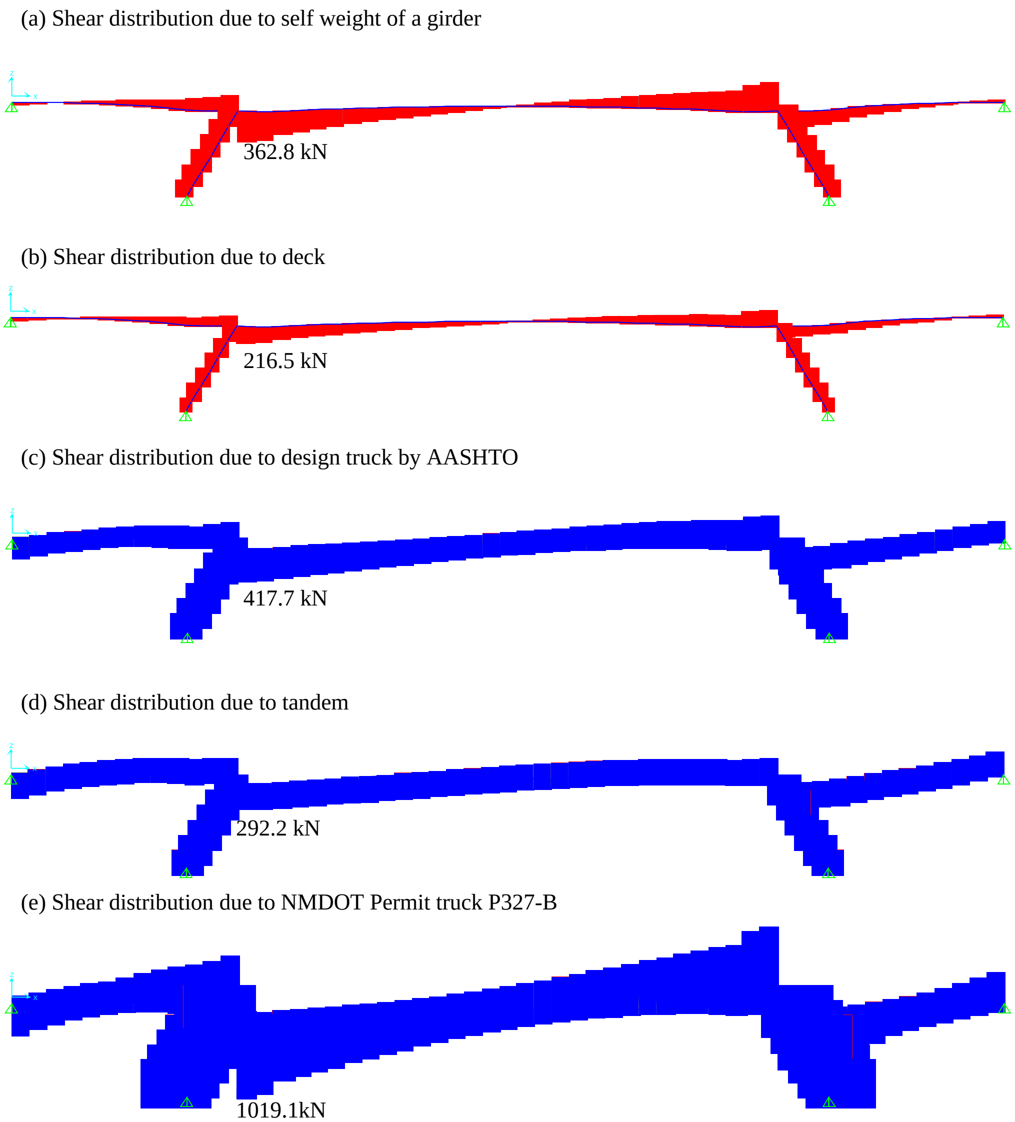

FIGURE 12 Shear distribution of an exterior beam of bridge 7937.

LOAD COMBINATIONS

The final shear and moment effects from all load cases were obtained from SAP 2000®. These values needed to be combined to represent the final straining action affecting the bridge structure. Based on AASHTO (1), several load combinations needed to be considered. This includes *Strength I* and *Strength II* load combinations which can be described as

Strength I

Factored load = 0.9*(Self weight of girder and deck load) + 0.65*(Asphalt and railing) + 1.75*Maximum moving loads and design lane load (5a)

Strength II

Factored load = 0.9*(Self weight of girder and deck load) + 0.65*(Asphalt and railing) + 1.35*Maximum moving loads and design lane load (5b)

Here, "*maximum moving loads and design lane load*" was defined as the maximum moment (or shear) of moving trucks and tandem plus design lane load. According to AASHTO, *Strength I* and *II* combinations include the basic load combination relating to the normal vehicular use of the bridges without wind and load combination relating to the use of the bridge by owner-specified special design vehicles, evaluation permit trucks, or both without wind. Therefore, in *Strength I*, AASHTO design truck and Tandem load were considered in calculation of "maximum moving loads and design lane load" while in *Strength II*, in addition to AASHTO design truck and Tandem load, NMDOT legal trucks (Two-Axle Legal load truck, NMDOT Three-Axle Legal load truck, NMDOT Five-Axle Legal load truck, NMDOT Permit truck P327-B) were considered.

BRIDGE CARRYING CAPACITY

The K-frames are reinforced concrete structures. The cross sectional dimensions and reinforcing details are provided in Figures 7 and 8 showing the as-built drawings. The flexural strength of the K-frames was defined according to AASHTO (1) specification (section 5) as

$$M_n = A_s f_y (d - a/2) \tag{6}$$

where:

A_s = area of tension reinforcement

f_y = yield strength of reinforcing bars

a = depth of the equivalent stress block determined based on compressive strength of concrete.

The shear capacity of the cross-section of girders was evaluated according to AASHTO (1) specification (section 5) as

$$V_n = V_c + V_s \tag{7}$$

where:

V_c = shear resistance of concrete

V_s = shear resistance of transverse reinforcement.

In this investigation, for simplicity, V_c is evaluated by using ACI 318 (2) design provision.

$$V_c = 0.33\sqrt{f'_c} \text{ (MPa)} \tag{8}$$

$$V_s = \frac{A_v f_{vy} d_v}{s} \tag{9}$$

where:

A_v = area of transverse reinforcement

f_{vy} = yield strength of transverse reinforcement

d_v = effective shear depth

s = spacing of transverse reinforcement

The characteristic compressive strength of the concrete K-frames was identified to be 30 MPa. The need for strengthening of the girders can be determined by comparing the cross-sectional carrying capacity with the load demand described by AASHTO (1) as

$$\phi R_n \geq Q \tag{10}$$

where:

ϕ = strength reduction factor which is different in moment and shear

R_n = nominal strength defined in Eqs. (6) and (7) for moment and shear

Q = factored load defined by using Eqs. (1) to (5) for moment and shear.

When ϕR_n is less than Q, the girders needed to be strengthened for proper method. Fig. 13 to Fig. 16 show the factored moment and shear for *Strength I* and *Strength II* load combinations representing load demand for Bridges 7930 and 7937 for exterior and interior frames respectively. Moreover, Fig. 13 to 16 also showed the load carrying capacity for both bridges 7930 and 7937 for moment and shear carrying capacity. Tables A1 to A4 (Appendix A) present the factored moment and shear demand and the corresponding factored cross sectional capacity each 1 m along the bridge length for all bridges. In these Tables, only positive value of "*Shortage of Capacity*" indicates the need for strengthening.

STRENGTHENING NEEDS

Considering Figs. 13 to 16 and Table A1, it is obvious that there was a shortage in negative moment capacity for all girders around connection of the K-frames. This shortage only occurs when considering the NM-Permit load (Strength II) load combination. Therefore, negative moment strengthening of the K-frames was needed to meet AASHTO (1) requirements. There is no obvious need to provide shear strengthening of the K-frames. The large concrete depth at the K-frame connections enables high shear capacity at locations of high demand.

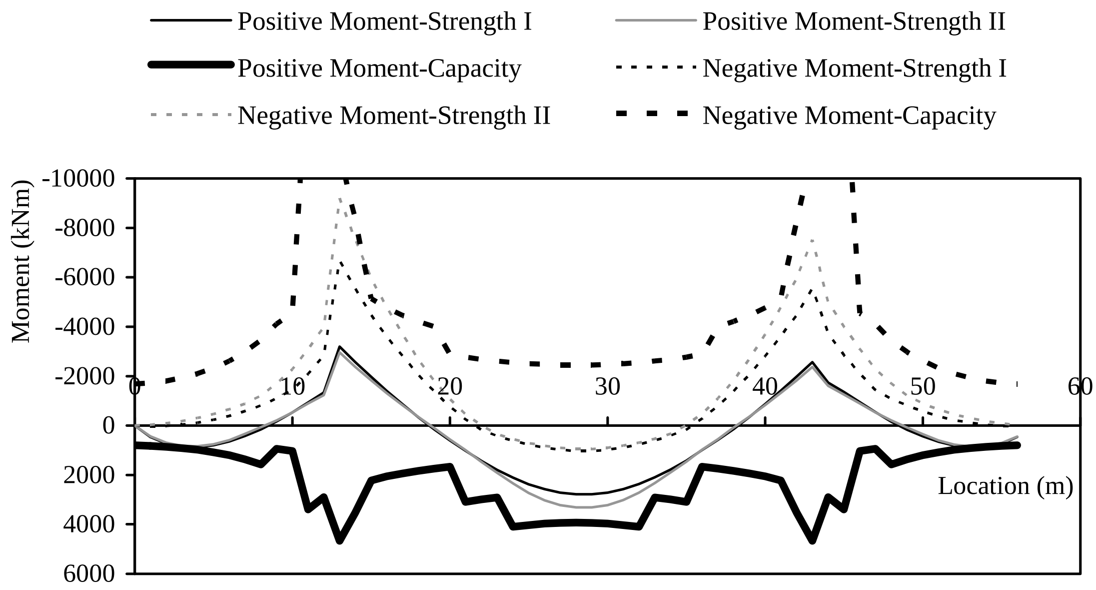

(a) Factored moment and capacity of exterior frame of bridge 7930

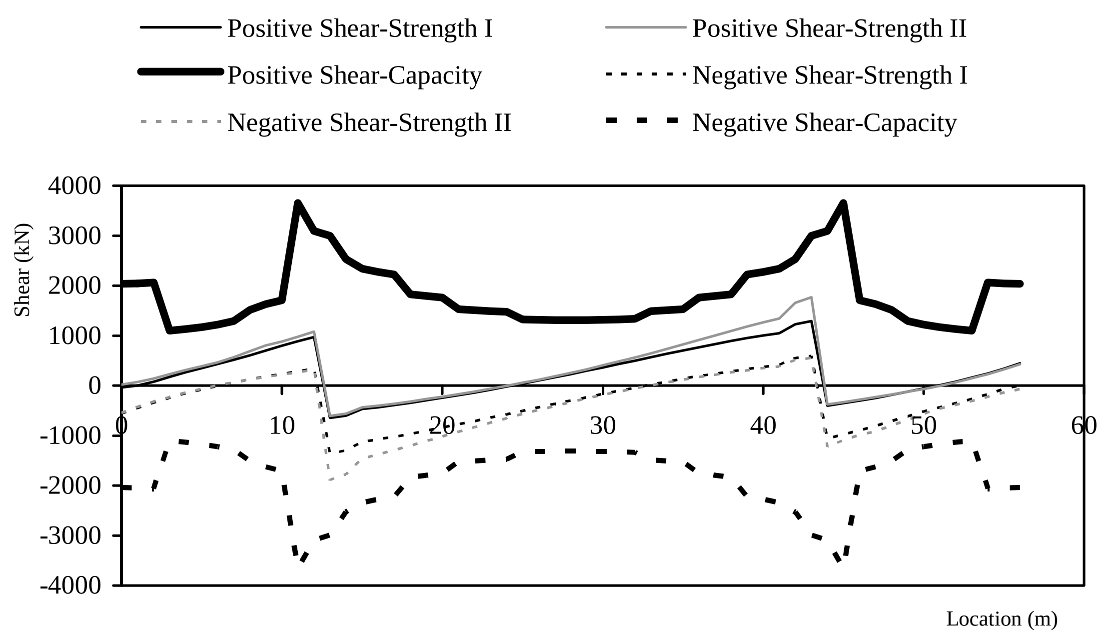

(b) Factored shear and capacity of exterior frame of bridge 7930

FIGURE **13** Factored load and capacity of exterior frames of bridge 7930.

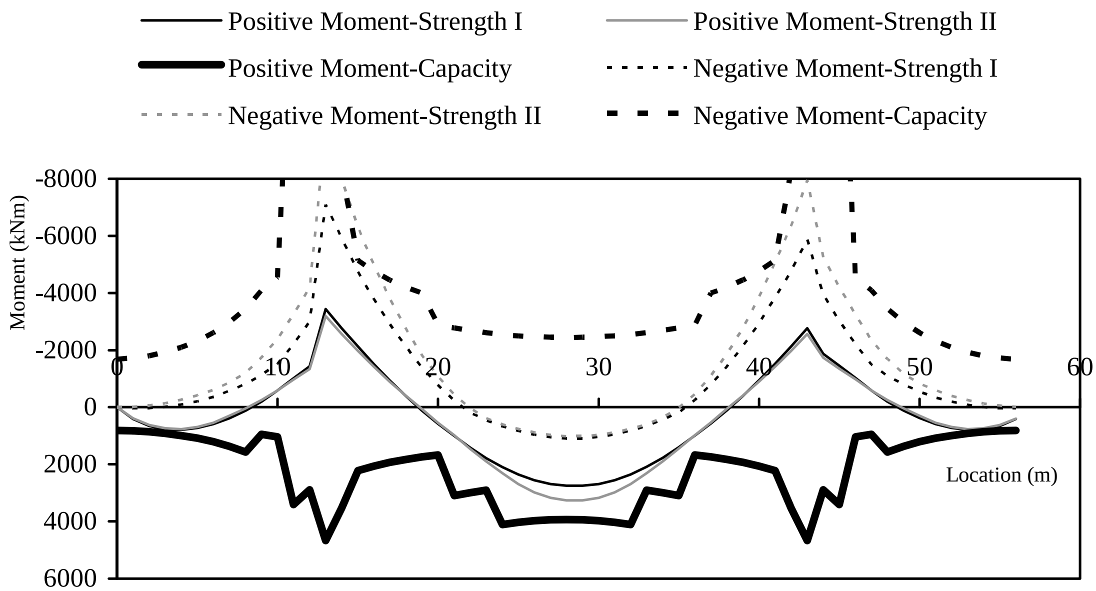

(a) Factored moment and capacity of interior frame of bridge 7930

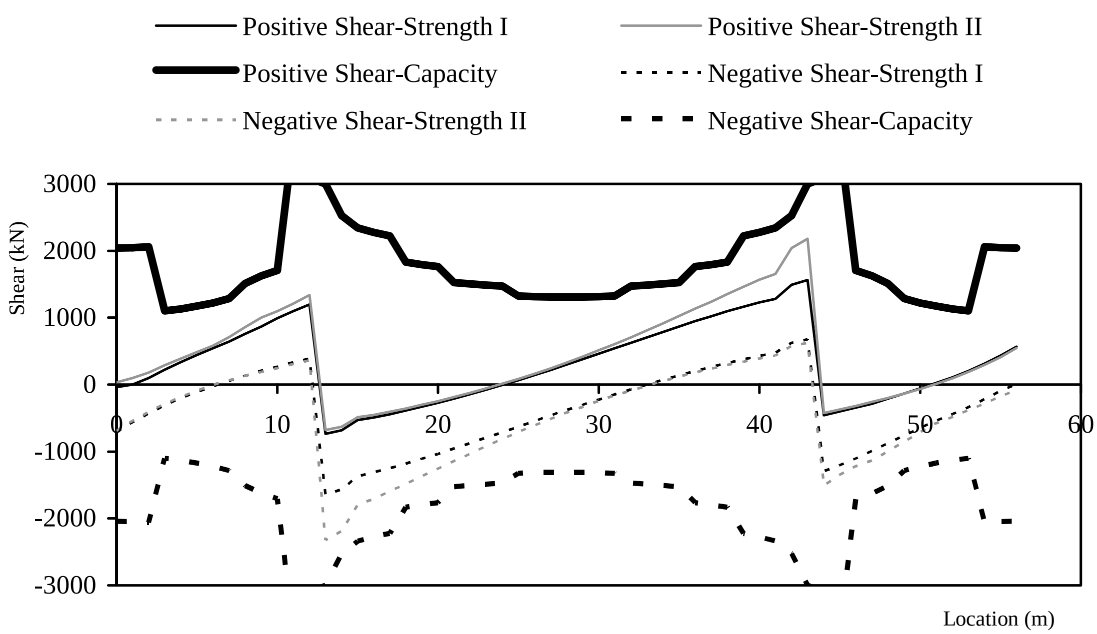

(b) Factored shear and capacity of interior frame of bridge 7930

FIGURE 14 Factored load and capacity of interior frame of bridge 7930.

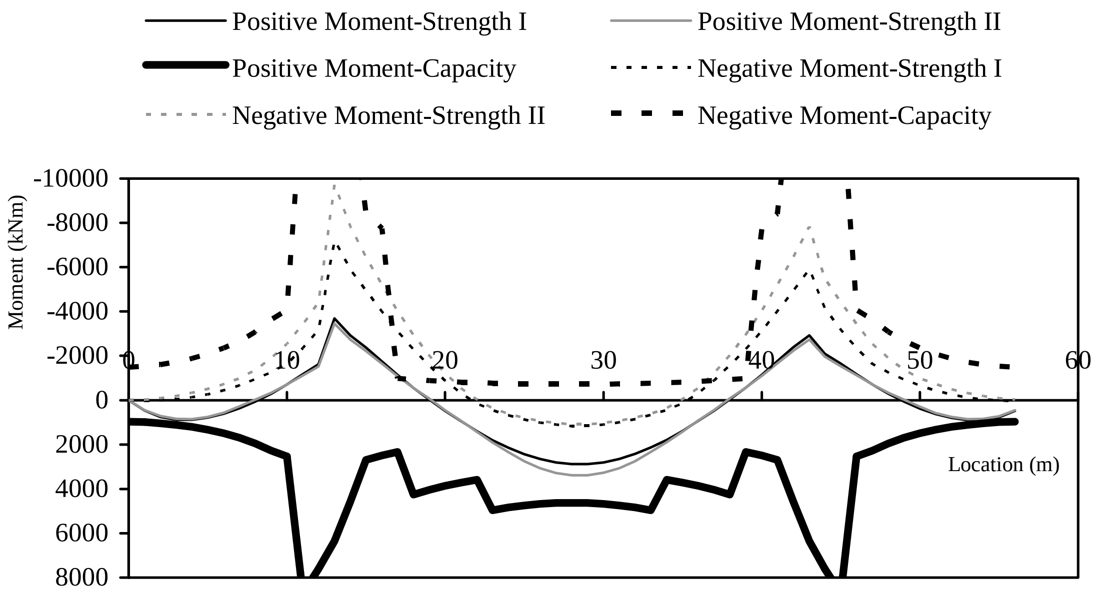

(a) Factored moment and capacity of exterior frame of bridge 7937

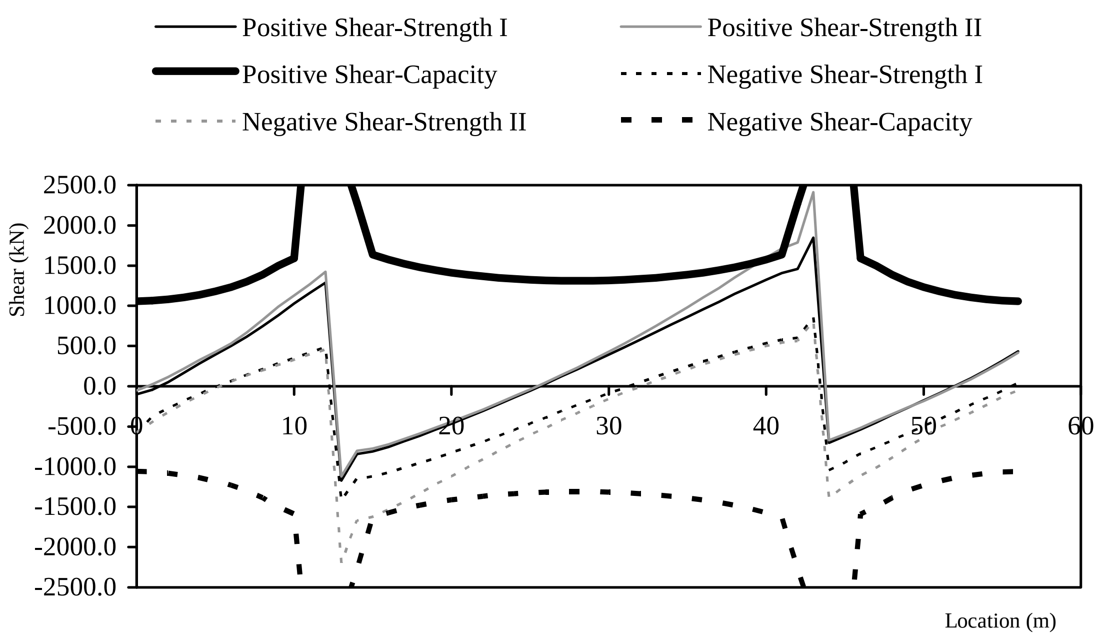

(b) Factored shear and capacity of Exterior beam of bridge 7937

FIGURE 15 Factored load and capacity of exterior frame of bridge 7937.

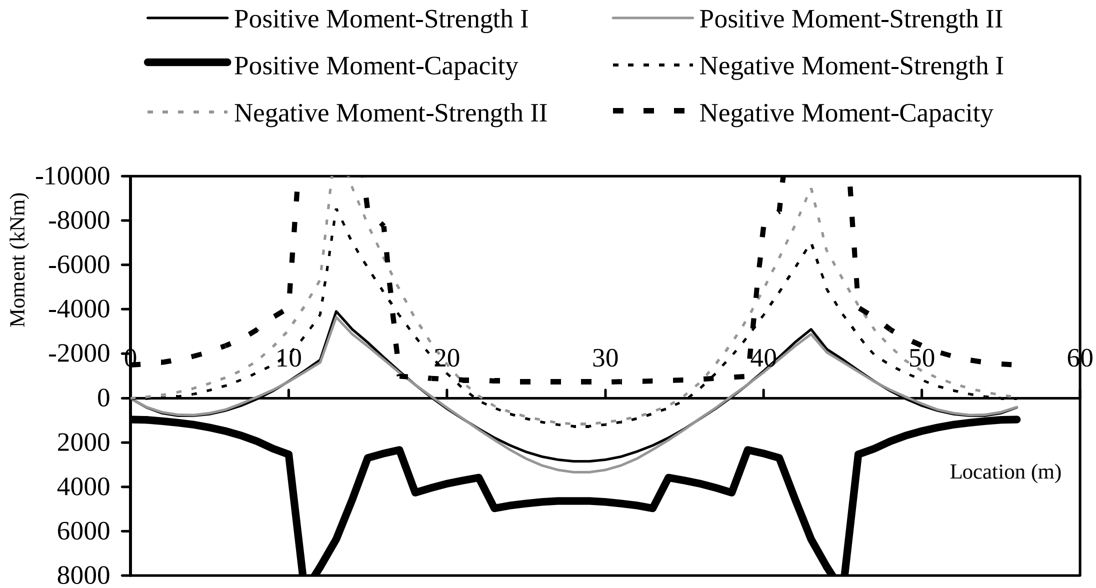

(a) Factored moment and capacity of interior frame of bridge 7937

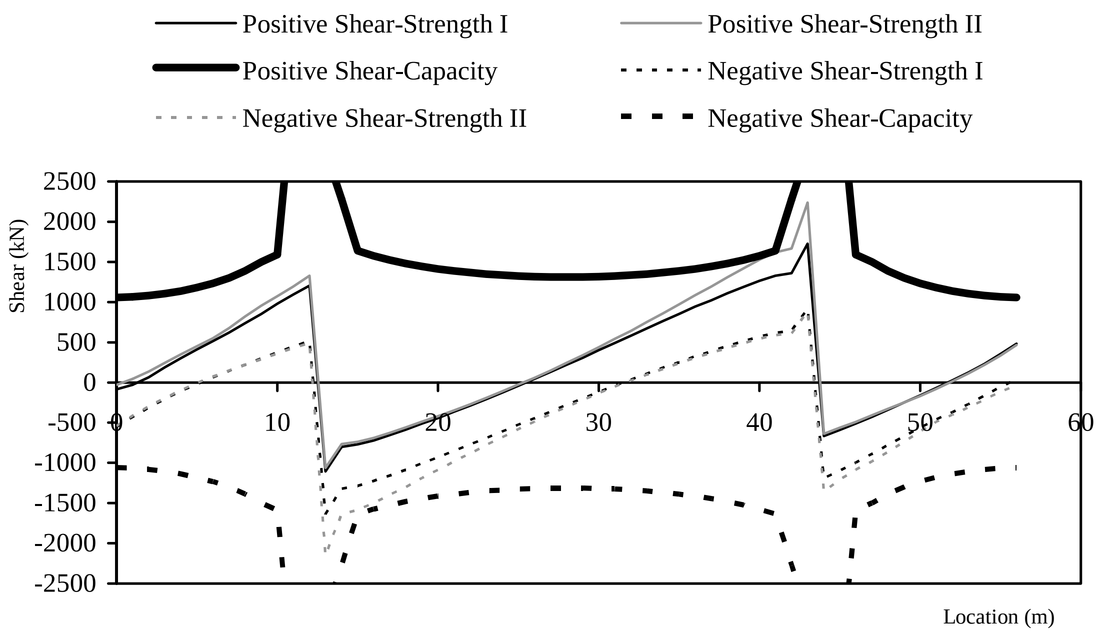

(b) Factored shear and capacity of interior frame of bridge 7937

FIGURE 16 Factored load and capacity of interior frame of bridge 7937.

FIELD TEST TO IDENTIFY BRIDGE CHARACTERISTICS

Step 1: Concrete Surface Milling

We consider bridge 7937 which has a concrete surface at the top of the exterior girders. One and one-half inches of concrete surface needed to be milled to enable installing the CFRP strips. For other locations on the bridge that are covered by asphalt instead of concrete, all asphalt in the FRP application zone needs to be completely milled if the bridge is to be strengthened by FRP.

Step 2: Concrete Surface Preparation

This is the most important step in the application of FRP strips because properly roughened and even concrete substrate is necessary for reliable performance of FRP strips (3 and 4). The acceptable unevenness, which indicates the maximum difference of the surface depth, is specified in current design provisions. In CEB-FIP code (3) and NCHRP Report (4), the allowable value of unevenness of the concrete surface is 4 mm (1/6 inch). If the surface is not even enough, putty needs to be applied to obtain better concrete surface. In addition, several aspects need to be considered. This includes the fact that the concrete substrate needs to be sound with proper tensile strength. In CEB-FIP (3), the minimum tensile strength of concrete is 1.5 N/mm^2. The crack width should be less than 0.2 mm. In addition, the concrete surface should be clean and free from oil, water, or dust before application of FRP.

Step 3: Rebound (Schmidt) Hammer Testing

After cleaning the surface, the rebound hammer (Schmidt) hammer test was performed at three different locations within the area of the milled concrete surface. Fig. 17 illustrates these locations schematically. Fig. 18 shows the Schmidt’s hammer test performed by University of New Mexico team.

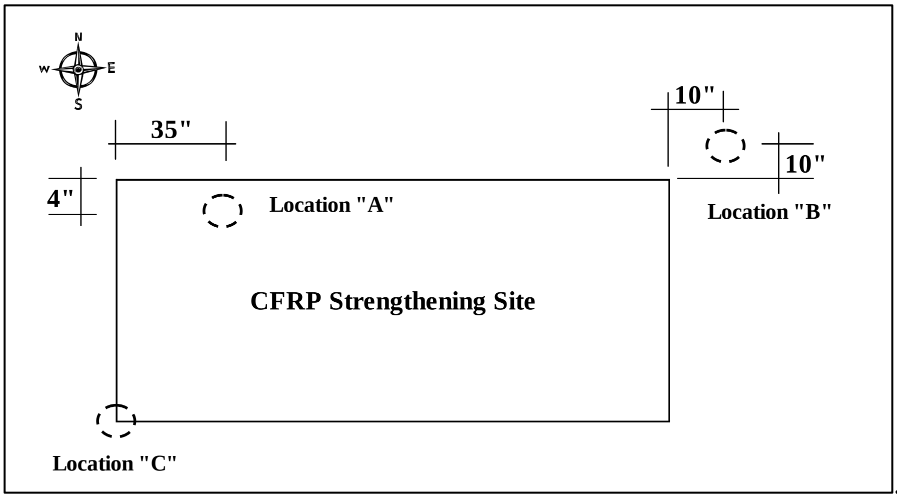

FIGURE 17 Locations considered for Schmidt’s hammer test.

FIGURE 18 Schmidt’s hammer testing on concrete surface.

The rebound hammer test allowed the researcher to determine the compressive strength of the concrete and thus its stiffness. This was an important step in comparing the measured strength to strength values on the bridge drawings. Moreover, realization of the concrete strength and stiffness is necessary for calibration of the FE model as discussed below. Example measurements of the rebound hammer test are presented in Table 2. The rebound hammer measurements were then converted to compressive strength using the hammer conversion charts with the hammer. The hammer was calibrated before being used as recommended by ASTM standards.

TABLE 2 Results of Schmidt's hammer test in different locations described in Fig. 17.

Location	A	B	C
1	34	40	36
2	44	36	38
3	35	49	38
4	48	40	38
5	35	41	42
6	30	45	48
7	40	38	40
8	34	32	36
9	30	40	42
10	48	37	44
11	37	42	44
12	38	42	40
13	50	38	40
14	38	44	40
15	30	40	38
Average	38.066667	40.266667	40.266667
Strength(psi)	5250	5700	5700

CALIBRATION OF FE MODELS BASED ON FIELD TEST DATA

To calibrate the analytical prediction by FE model developed using SAP 2000®, a load test was performed before the application of CFRP strips on concrete surface. First, the concrete strain of the top of the exterior girder was monitored when subjected to a 50 kip (220 kN) test truck (Fig. 19) with pre-determined weight. Details about the field tests before and after application of the FRP are provided in Report (3). Strain gauges at three locations within the area of interest are attached to the concrete surface. Fig. 20 shows schematically the area of interest and the location of concrete strain gauges. Fig. 21 shows the strain gauges after being attached to the concrete surface.

FIGURE 19 Mack 10 yard dump truck as test truck with weight of 50 kips.

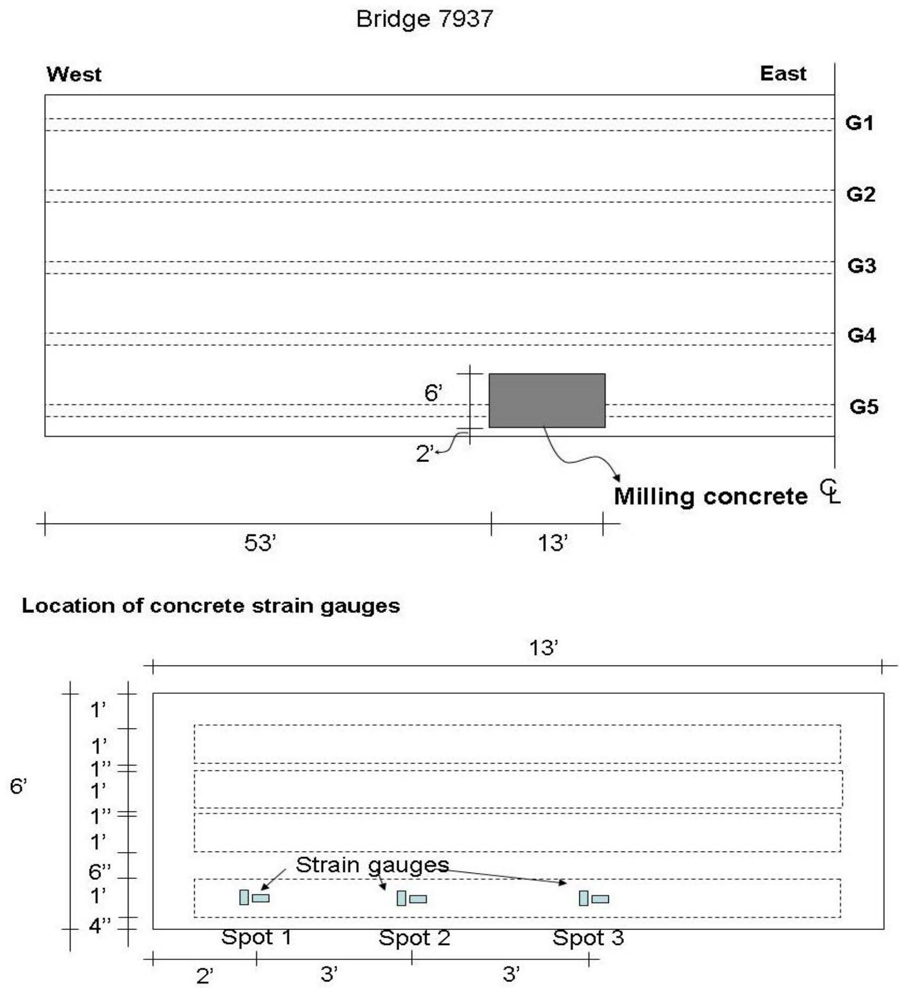

FIGURE 20 Schematic figure showing the area of concrete milling and the location of strain gauges to measure concrete surface strain.

FIGURE 21 Concrete strain gauges attached to the concrete surface.

Fig. 22 illustrates the concrete strain results at the top of the exterior girder. Based on the field test results shown in Fig. 22, the FE models were calibrated by modifying the concrete modulus of elasticity (E) such that concrete strain predictions using the FE model becomes as close as possible to field measured strains. Fig. 23 represents the strains field measured strains and FE predicted strains on the top of the concrete girders. Matching the field measured and FE strain data, it was concluded that concrete with the compression strength 50 MPa should be used in FE models to accurately represent the concrete in the K-frame bridges.

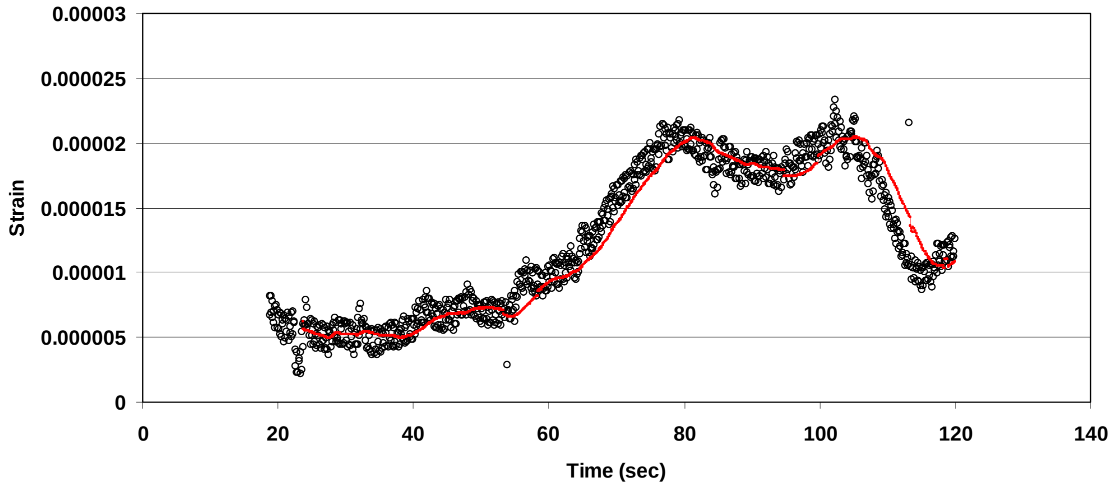

FIGURE 22 Concrete strain field measured at the top of the concrete surface before application of CFRP strips.

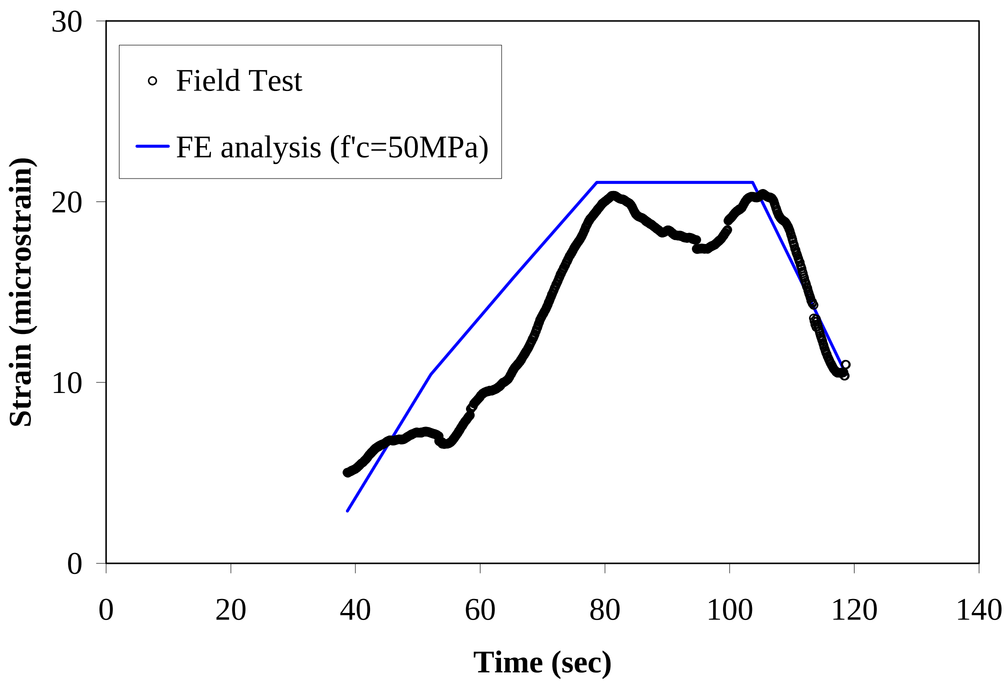

FIGURE 23 Concrete strains as predicted by the calibrated FE model and from field test.

REFERENCES

1. AASHTO. LRFD Bridge Design Specifications. *Manual for Condition Evaluation of Bridges*. American Association of State Highway and Transportation Officials. 2006 Interim revisions, Second Edition, Washington, D.C., 2006.

2. ACI 318 Committee. Building Code and Commentary. ACI 318-05/318R-05, 2005.

3. CEB-FIP. Externally bonded FRP reinforcement for RC structures. TRB 14, 2001, p. 124.

4. Shahawy, Mirmiran A., M. Shahawy, A. Nanni and V. Karbhari, Editors. *Bonded Repair and Retrofit of Concrete Structures using FRP Composites*. Recommended Construction Specifications and Process Control Manual. National Cooperative Highway Research Program: NCHRP Report 514, TRB National Research Council, Washington, D.C., 2004.

APPENDIX

TABLE A1 Positive factored moment and flexural capacity of exterior frame of bridge 7930.

Location (m)	Element	Beam thickness (m)	Factored moment-*Strength I* (kNm)	Factored moment-*Strength II* (kNm)	Flexural capacity (kNm)	Shortage of capacity (kNm)
0	1	0.765	0.0	0.0	806.2	-806.2
1	2	0.778	478.3	460.7	823.5	-345.2
2	3	0.804	768.9	729.1	858.6	-89.6
3	4	0.843	898.8	852.7	912.4	-13.6
4	5	0.898	902.6	867.0	986.5	-83.9
5	6	0.970	806.2	766.6	1083.5	-277.4
6	7	1.061	625.0	578.8	1207.6	-582.6
7	8	1.178	374.1	286.5	1365.5	-991.4
8	9	1.329	61.8	-27.4	1570.1	-1508.3
9	10	1.536	-310.8	-358.6	940.8	-1251.5
10	11	1.680	-748.1	-746.9	1038.1	-1785.0
11	12	5.169	-1219.7	-1175.5	3403.3	-4578.7
12	13	4.414	-1710.3	-1605.4	2891.8	-4497.2
13	14	3.617	-4124.8	-3889.8	4673.0	-8562.9
14	15	2.777	-3321.3	-3128.6	3534.0	-6662.6
15	16	1.807	-2562.4	-2412.6	2218.6	-4631.2
16	17	1.690	-1860.7	-1768.9	2059.7	-3828.6
17	18	1.597	-1192.4	-1153.8	1933.5	-3087.3
18	19	1.520	-564.7	-576.1	1829.6	-2394.3
19	20	1.456	21.4	-33.1	1742.6	-1721.2
20	21	1.402	559.8	525.5	1669.4	-1109.5
21	22	1.356	1053.8	1038.1	3093.0	-2039.1
22	23	1.319	1535.3	1582.2	2990.5	-1408.3
23	24	1.287	1960.5	2080.5	2906.4	-826.0
24	25	1.263	2324.0	2551.1	4104.8	-1553.8
25	26	1.244	2624.9	2976.3	4027.5	-1051.1
26	27	1.230	2858.2	3302.4	3973.0	-670.5
27	28	1.222	3013.2	3517.9	3940.6	-422.6
28	29	1.220	3087.4	3622.7	3929.8	-307.1
29	30	1.222	3085.6	3620.9	3940.6	-319.7
30	31	1.230	3007.7	3512.4	3973.0	-460.6
31	32	1.244	2849.2	3293.5	4027.5	-734.0
32	33	1.263	2612.8	2964.2	4104.8	-1140.7
33	34	1.287	2308.9	2536.0	2906.4	-370.4
34	35	1.319	1942.9	2062.9	2990.5	-927.6
35	36	1.356	1515.9	1562.8	3093.0	-1530.2
36	37	1.402	1033.2	1017.5	1669.4	-636.1
37	38	1.456	538.9	504.5	1742.6	-1203.7
38	39	1.520	1.1	-53.4	1829.6	-1828.5
39	40	1.597	-583.2	-594.5	1933.5	-2516.7
40	41	1.690	-1207.6	-1169.1	2059.7	-3228.8

41	42	1.807	-1870.9	-1779.1	2218.6	-3997.7
42	43	2.777	-2565.6	-2415.8	3534.0	-5949.8
43	44	3.617	-3316.6	-3123.8	4673.0	-7796.8
44	45	4.414	-2222.6	-2092.4	2891.8	-4984.2
45	46	5.169	-1739.1	-1634.2	3403.3	-5037.5
46	47	1.680	-1235.1	-1190.8	1038.1	-2229.0
47	48	1.536	-750.9	-749.6	940.8	-1690.4
48	49	1.329	-304.1	-352.0	1570.1	-1874.2
49	50	1.178	74.1	-15.0	1365.5	-1291.4
50	51	1.061	389.6	302.0	1207.6	-818.0
51	52	0.970	641.6	595.3	1083.5	-442.0
52	53	0.898	822.2	782.6	986.5	-164.3
53	54	0.843	916.8	881.2	912.4	**4.5**
54	55	0.804	910.2	864.2	858.6	**51.7**
55	56	0.778	777.0	737.2	823.5	-46.5
56	57	0.765	482.4	464.8	806.2	-323.8

TABLE A2 Negative factored moment and flexural capacity of exterior frame of bridge 7930.

Location (m)	Element	Beam thickness (m)	Factored moment-*Strength I* (kNm)	Factored moment-*Strength II* (kNm)	Flexural capacity (kNm)	Shortage of capacity (kNm)
0	1	0.765	0.0	0.0	-1682.5	-1682.5
1	2	0.778	37.1	-14.5	-1722.4	-1707.9
2	3	0.804	32.9	-67.8	-1803.4	-1735.6
3	4	0.843	-12.7	-160.0	-1927.6	-1767.6
4	5	0.898	-100.4	-291.6	-2098.7	-1807.1
5	6	0.970	-232.0	-464.2	-2322.8	-1858.6
6	7	1.061	-408.0	-678.4	-2609.1	-1930.8
7	8	1.178	-630.6	-936.4	-2973.7	-2037.2
8	9	1.329	-902.3	-1303.4	-3446.0	-2142.6
9	10	1.536	-1228.6	-1848.5	-4096.7	-2248.2
10	11	1.680	-1645.4	-2494.1	-4546.3	-2052.2
11	12	5.169	-2375.7	-3371.8	-15466.3	-12094.5
12	13	4.414	-3204.9	-4358.0	-13104.8	-8746.7
13	14	3.617	-7610.9	-10136.8	-11047.8	-911.0
14	15	2.777	-6291.3	-8271.4	-8306.1	-34.7
15	16	1.807	-5053.3	-6532.4	-5139.9	**1392.5**
16	17	1.690	-4061.7	-5227.1	-4757.6	**469.5**
17	18	1.597	-3132.2	-4014.2	-4453.7	-439.5
18	19	1.520	-2276.6	-2894.5	-4203.5	-1309.0
19	20	1.456	-1500.2	-1928.2	-3994.2	-2065.9
20	21	1.402	-811.3	-1120.4	-2883.6	-1763.2
21	22	1.356	-215.0	-414.8	-2774.3	-2359.5
22	23	1.319	282.0	105.2	-2683.1	-2788.3
23	24	1.287	587.0	507.6	-2608.4	-3116.0
24	25	1.263	829.6	770.8	-2548.7	-3319.4
25	26	1.244	1026.3	958.7	-2503.1	-3461.8
26	27	1.230	1177.4	1103.1	-2471.0	-3574.1
27	28	1.222	1283.3	1204.8	-2451.9	-3656.6
28	29	1.220	1343.0	1262.8	-2445.5	-3708.3
29	30	1.222	1341.1	1260.9	-2451.9	-3712.8
30	31	1.230	1277.8	1199.3	-2471.0	-3670.2
31	32	1.244	1168.4	1094.2	-2503.1	-3597.2
32	33	1.263	1014.1	946.6	-2548.7	-3495.2
33	34	1.287	814.5	755.7	-2608.4	-3364.1
34	35	1.319	569.4	490.1	-2683.1	-3173.2
35	36	1.356	262.6	85.8	-2774.3	-2860.0
36	37	1.402	-235.6	-435.4	-2883.6	-2448.2
37	38	1.456	-832.3	-1141.3	-3994.2	-2852.8
38	39	1.520	-1520.5	-1948.5	-4203.5	-2255.0
39	40	1.597	-2295.1	-2912.9	-4453.7	-1540.8
40	41	1.690	-3147.5	-4029.4	-4757.6	-728.1
41	42	1.807	-4071.9	-5237.3	-5139.9	**97.4**
42	43	2.777	-5056.4	-6535.5	-8306.1	-1770.6

43	44	3.617	-6286.5	-8266.7	-11047.8	-2781.1
44	45	4.414	-4207.2	-5467.5	-13104.8	-7637.2
45	46	5.169	-3233.7	-4386.8	-15466.3	-11079.5
46	47	1.680	-2391.1	-3387.2	-4546.3	-1159.1
47	48	1.536	-1648.1	-2496.8	-4096.7	-1599.9
48	49	1.329	-1222.0	-1841.9	-3446.0	-1604.1
49	50	1.178	-889.9	-1291.0	-2973.7	-1682.6
50	51	1.061	-615.1	-921.0	-2609.1	-1688.2
51	52	0.970	-391.4	-661.8	-2322.8	-1660.9
52	53	0.898	-216.0	-448.1	-2098.7	-1650.6
53	54	0.843	-86.2	-277.4	-1927.6	-1650.1
54	55	0.804	-1.2	-148.5	-1803.4	-1654.9
55	56	0.778	41.0	-59.8	-1722.4	-1662.6
56	57	0.765	41.2	-10.4	-1682.5	-1672.0

TABLE A3 Positive factored shear and shear capacity of exterior frame of bridge 7930.

Location (m)	Element	Beam thickness (m)	Factored shear-*Strength I* (kN)	Factored shear-*Strength II* (kN)	Shear capacity (kN)	Shortage of capacity (kN)
0	1	0.765	-57.1	-4.2	2040.0	-1982.9
1	2	0.778	-15.9	58.6	2047.1	-1988.5
2	3	0.804	69.7	136.1	2061.5	-1925.5
3	4	0.843	177.3	230.1	1101.2	-871.2
4	5	0.898	279.0	321.4	1131.7	-810.3
5	6	0.970	374.2	406.9	1171.6	-764.7
6	7	1.061	462.5	492.7	1222.6	-729.9
7	8	1.178	555.7	606.8	1287.6	-680.8
8	9	1.329	658.0	735.3	1512.1	-776.7
9	10	1.536	758.6	862.1	1628.0	-765.9
10	11	1.680	869.8	950.0	1708.1	-758.1
11	12	5.169	970.0	1056.4	3653.3	-2596.8
12	13	4.414	1063.6	1176.1	3092.2	-1916.1
13	14	3.617	-832.5	-789.2	2998.6	-2166.1
14	15	2.777	-773.7	-733.0	2530.2	-1756.5
15	16	1.807	-605.6	-571.9	2340.1	-1734.6
16	17	1.690	-561.6	-530.8	2274.8	-1713.2
17	18	1.597	-505.8	-477.9	2222.9	-1717.0
18	19	1.520	-449.6	-424.3	1829.3	-1379.7
19	20	1.456	-388.1	-365.3	1793.5	-1405.4
20	21	1.402	-329.4	-309.9	1763.4	-1434.0
21	22	1.356	-265.9	-248.4	1527.6	-1261.7
22	23	1.319	-201.5	-185.1	1506.5	-1305.0
23	24	1.287	-133.6	-118.5	1489.1	-1355.5
24	25	1.263	-64.5	-49.9	1475.3	-1410.9
25	26	1.244	6.1	20.6	1324.4	-1303.8
26	27	1.230	78.1	92.0	1317.0	-1225.0
27	28	1.222	153.2	170.9	1312.6	-1141.7
28	29	1.220	227.6	250.5	1311.1	-1060.6
29	30	1.222	303.0	333.2	1312.6	-979.4
30	31	1.230	381.1	420.5	1317.0	-896.5
31	32	1.244	458.0	507.7	1324.4	-816.7
32	33	1.263	535.2	597.4	1335.0	-737.6
33	34	1.287	612.6	692.1	1489.1	-797.1
34	35	1.319	689.8	788.8	1506.5	-717.6
35	36	1.356	764.9	885.9	1527.6	-641.7
36	37	1.402	841.4	987.7	1763.4	-775.7
37	38	1.456	911.9	1083.0	1793.5	-710.5
38	39	1.520	985.6	1187.0	1829.3	-642.3
39	40	1.597	1051.8	1283.7	2222.9	-939.2
40	41	1.690	1116.2	1379.5	2274.8	-895.3
41	42	1.807	1171.0	1461.8	2340.1	-878.3
42	43	2.777	1383.9	1811.2	2530.2	-719.0

43	44	3.617	1459.0	1940.0	2998.6	-1058.6
44	45	4.414	-512.8	-485.7	3092.2	-2579.4
45	46	5.169	-450.4	-428.2	3653.3	-3202.8
46	47	1.680	-384.3	-366.0	1708.1	-1323.8
47	48	1.536	-325.5	-303.4	1628.0	-1302.5
48	49	1.329	-247.5	-238.7	1512.1	-1264.6
49	50	1.178	-172.5	-172.6	1287.6	-1114.9
50	51	1.061	-97.9	-106.2	1222.6	-1116.5
51	52	0.970	-21.0	-33.2	1171.6	-1138.5
52	53	0.898	60.2	47.4	1131.7	-1071.5
53	54	0.843	147.1	133.9	1101.2	-954.1
54	55	0.804	242.4	227.2	2061.5	-1819.2
55	56	0.778	348.2	330.6	2047.1	-1698.9
56	57	0.765	462.3	446.0	2040.0	-1577.7

TABLE A4 Negative factored shear and shear capacity of exterior frame of bridge 7930.

Location (m)	Element	Beam thickness (m)	Factored shear-*Strength I* (kN)	Factored shear-*Strength II* (kN)	Shear capacity (kN)	Shortage of capacity (kN)
0	1	0.765	-580.4	-567.6	-2040.0	-1459.6
1	2	0.778	-458.6	-441.4	-2047.1	-1588.5
2	3	0.804	-344.8	-326.7	-2061.5	-1716.7
3	4	0.843	-239.5	-224.2	-1101.2	-861.7
4	5	0.898	-145.5	-131.4	-1131.7	-986.2
5	6	0.970	-59.4	-45.7	-1171.6	-1112.2
6	7	1.061	20.5	33.9	-1222.6	-1188.7
7	8	1.178	96.0	104.9	-1287.6	-1182.7
8	9	1.329	169.2	168.3	-1512.1	-1342.8
9	10	1.536	243.2	230.8	-1628.0	-1384.8
10	11	1.680	302.2	289.4	-1708.1	-1405.9
11	12	5.169	371.1	352.9	-3653.3	-3282.1
12	13	4.414	436.8	414.5	-3092.2	-2655.4
13	14	3.617	-1537.9	-2075.1	-2998.6	-923.5
14	15	2.777	-1466.6	-1947.5	-2530.2	-582.6
15	16	1.807	-1258.8	-1594.8	-2340.1	-745.3
16	17	1.690	-1201.3	-1507.4	-2274.8	-767.4
17	18	1.597	-1135.2	-1407.1	-2222.9	-815.8
18	19	1.520	-1067.9	-1306.7	-1829.3	-522.6
19	20	1.456	-993.7	-1198.4	-1793.5	-595.2
20	21	1.402	-922.8	-1098.0	-1763.4	-665.4
21	22	1.356	-846.0	-994.3	-1527.6	-533.3
22	23	1.319	-770.7	-893.9	-1506.5	-612.5
23	24	1.287	-693.3	-793.8	-1489.1	-695.4
24	25	1.263	-615.6	-696.3	-1475.3	-779.0
25	26	1.244	-537.9	-601.1	-1324.4	-723.4
26	27	1.230	-460.4	-510.9	-1317.0	-806.1
27	28	1.222	-381.3	-421.2	-1312.6	-891.4
28	29	1.220	-304.9	-335.6	-1311.1	-975.5
29	30	1.222	-229.5	-252.7	-1312.6	-1059.9
30	31	1.230	-153.2	-171.1	-1317.0	-1145.9
31	32	1.244	-80.1	-94.0	-1324.4	-1230.4
32	33	1.263	-8.2	-22.7	-1335.0	-1312.2
33	34	1.287	62.1	47.6	-1489.1	-1427.1
34	35	1.319	130.9	115.9	-1506.5	-1375.5
35	36	1.356	196.7	180.6	-1527.6	-1330.9
36	37	1.402	262.2	244.9	-1763.4	-1501.2
37	38	1.456	320.4	301.4	-1793.5	-1473.1
38	39	1.520	381.2	358.7	-1829.3	-1448.0
39	40	1.597	436.0	411.1	-2222.9	-1786.9
40	41	1.690	489.6	462.2	-2274.8	-1785.2
41	42	1.807	535.7	506.0	-2340.1	-1804.5
42	43	2.777	705.7	667.7	-2530.2	-1824.5

43	44	3.617	766.1	725.5	-2998.6	-2232.4
44	45	4.414	-1165.5	-1336.3	-3092.2	-1756.0
45	46	5.169	-1077.2	-1189.5	-3653.3	-2463.7
46	47	1.680	-983.0	-1069.7	-1708.1	-638.4
47	48	1.536	-876.9	-985.3	-1628.0	-642.7
48	49	1.329	-769.4	-861.4	-1512.1	-650.7
49	50	1.178	-664.0	-734.2	-1287.6	-553.4
50	51	1.061	-559.1	-605.4	-1222.6	-617.3
51	52	0.970	-463.7	-489.9	-1171.6	-681.8
52	53	0.898	-373.6	-403.9	-1131.7	-727.9
53	54	0.843	-277.4	-316.6	-1101.2	-784.6
54	55	0.804	-174.6	-225.1	-2061.5	-1836.5
55	56	0.778	-66.0	-130.7	-2047.1	-1916.4
56	57	0.765	21.1	-52.6	-2040.0	-1987.4

TABLE A5 Positive factored moment and flexural capacity of exterior frame of bridge 7931.

Location (m)	Element	Beam thickness (m)	Factored moment- *Strength I* (kNm)	Factored moment- *Strength II* (kNm)	Flexural capacity (kNm)	Shortage of capacity (kNm)
0	1	0.765	0.0	0.0	806.2	-806.2
1	2	0.778	446.5	430.2	823.5	-377.0
2	3	0.804	717.4	680.7	858.6	-141.1
3	4	0.843	837.7	795.2	912.4	-74.7
4	5	0.898	839.3	806.4	986.5	-147.2
5	6	0.970	745.9	709.4	1083.5	-337.7
6	7	1.061	571.8	529.1	1207.6	-635.8
7	8	1.178	330.7	249.8	1365.5	-1034.8
8	9	1.329	30.1	-52.2	1570.1	-1540.0
9	10	1.536	-329.1	-373.2	940.8	-1269.8
10	11	1.680	-751.3	-750.2	1038.1	-1788.3
11	12	5.169	-1208.2	-1167.3	3403.3	-4570.6
12	13	4.414	-1686.2	-1589.4	2891.8	-4481.3
13	14	3.617	-4073.8	-3857.1	4673.0	-8530.2
14	15	2.777	-3281.3	-3103.5	3534.0	-6637.5
15	16	1.807	-2533.6	-2395.4	2218.6	-4614.0
16	17	1.690	-1848.9	-1764.2	2059.7	-3823.9
17	18	1.597	-1197.7	-1162.2	1933.5	-3095.7
18	19	1.520	-587.1	-597.5	1829.6	-2416.7
19	20	1.456	-17.7	-67.9	1742.6	-1760.3
20	21	1.402	504.7	473.0	1669.4	-1164.7
21	22	1.356	983.1	968.6	3093.0	-2109.9
22	23	1.319	1446.9	1490.2	2990.5	-1500.3
23	24	1.287	1856.0	1966.7	2906.4	-939.7
24	25	1.263	2205.3	2414.8	4104.8	-1690.0
25	26	1.244	2494.0	2818.2	4027.5	-1209.3
26	27	1.230	2717.4	3127.3	3973.0	-845.7
27	28	1.222	2865.9	3331.5	3940.6	-609.0
28	29	1.220	2937.0	3430.8	3929.8	-499.0
29	30	1.222	2935.1	3429.0	3940.6	-511.6
30	31	1.230	2860.4	3326.0	3973.0	-646.9
31	32	1.244	2708.5	3118.3	4027.5	-909.2
32	33	1.263	2481.9	2806.0	4104.8	-1298.8
33	34	1.287	2190.3	2399.7	2906.4	-506.7
34	35	1.319	1838.5	1949.2	2990.5	-1041.3
35	36	1.356	1427.5	1470.8	3093.0	-1622.1
36	37	1.402	962.5	948.0	1669.4	-706.9
37	38	1.456	483.7	452.0	1742.6	-1258.9
38	39	1.520	-37.9	-88.2	1829.6	-1867.5
39	40	1.597	-605.6	-616.0	1933.5	-2539.1
40	41	1.690	-1213.0	-1177.4	2059.7	-3237.2

41	42	1.807	-1859.1	-1774.4	2218.6	-3993.0
42	43	2.777	-2536.8	-2398.6	3534.0	-5932.6
43	44	3.617	-3276.5	-3098.7	4673.0	-7771.7
44	45	4.414	-2191.2	-2071.2	2891.8	-4963.0
45	46	5.169	-1715.0	-1618.2	3403.3	-5021.5
46	47	1.680	-1223.5	-1182.7	1038.1	-2220.9
47	48	1.536	-754.1	-752.9	940.8	-1693.7
48	49	1.329	-322.4	-366.6	1570.1	-1892.5
49	50	1.178	42.4	-39.8	1365.5	-1323.1
50	51	1.061	346.2	265.3	1207.6	-861.4
51	52	0.970	588.4	545.7	1083.5	-495.2
52	53	0.898	761.9	725.4	986.5	-224.6
53	54	0.843	853.5	820.7	912.4	-58.8
54	55	0.804	849.1	806.6	858.6	-9.4
55	56	0.778	725.4	688.7	823.5	-98.1
56	57	0.765	450.6	434.3	806.2	-355.6

TABLE A6 Negative factored moment and flexural capacity of exterior frame of bridge 7931.

Location (m)	Element	Beam thickness (m)	Factored moment-*Strength I* (kNm)	Factored moment-*Strength II* (kNm)	Flexural capacity (kNm)	Shortage of capacity (kNm)
0	1	0.765	0.0	0.0	-1682.5	-1682.5
1	2	0.778	39.4	-8.2	-1722.4	-1714.2
2	3	0.804	38.4	-54.5	-1803.4	-1748.9
3	4	0.843	-3.2	-139.0	-1927.6	-1788.5
4	5	0.898	-86.0	-262.5	-2098.7	-1836.2
5	6	0.970	-211.9	-426.0	-2322.8	-1896.7
6	7	1.061	-381.2	-630.6	-2609.1	-1978.5
7	8	1.178	-596.2	-878.3	-2973.7	-2095.3
8	9	1.329	-859.3	-1229.3	-3446.0	-2216.7
9	10	1.536	-1175.8	-1747.7	-4096.7	-2349.0
10	11	1.680	-1579.0	-2362.0	-4546.3	-2184.3
11	12	5.169	-2274.7	-3193.6	-15466.3	-12272.7
12	13	4.414	-3065.0	-4128.8	-13104.8	-8976.0
13	14	3.617	-7289.9	-9620.2	-11047.8	-1427.6
14	15	2.777	-6021.2	-7848.0	-8306.1	-458.1
15	16	1.807	-4831.6	-6196.1	-5139.9	**1056.2**
16	17	1.690	-3879.4	-4954.5	-4757.6	**197.0**
17	18	1.597	-2987.3	-3801.0	-4453.7	-652.7
18	19	1.520	-2166.3	-2736.4	-4203.5	-1467.2
19	20	1.456	-1421.4	-1816.3	-3994.2	-2177.9
20	21	1.402	-760.3	-1045.4	-2883.6	-1838.2
21	22	1.356	-187.4	-371.8	-2774.3	-2402.5
22	23	1.319	290.7	127.6	-2683.1	-2810.7
23	24	1.287	588.9	515.7	-2608.4	-3124.1
24	25	1.263	826.7	772.4	-2548.7	-3321.1
25	26	1.244	1019.2	956.9	-2503.1	-3459.9
26	27	1.230	1166.9	1098.3	-2471.0	-3569.3
27	28	1.222	1270.0	1197.6	-2451.9	-3649.4
28	29	1.220	1327.7	1253.7	-2445.5	-3699.2
29	30	1.222	1325.9	1251.8	-2451.9	-3703.7
30	31	1.230	1264.5	1192.1	-2471.0	-3663.0
31	32	1.244	1157.9	1089.4	-2503.1	-3592.5
32	33	1.263	1007.0	944.7	-2548.7	-3493.4
33	34	1.287	811.6	757.4	-2608.4	-3365.7
34	35	1.319	571.4	498.2	-2683.1	-3181.3
35	36	1.356	271.3	108.2	-2774.3	-2882.5
36	37	1.402	-208.0	-392.4	-2883.6	-2491.3
37	38	1.456	-781.2	-1066.4	-3994.2	-2927.8
38	39	1.520	-1441.7	-1836.5	-4203.5	-2367.0
39	40	1.597	-2184.8	-2754.8	-4453.7	-1698.9
40	41	1.690	-3002.6	-3816.2	-4757.6	-941.3
41	42	1.807	-3889.6	-4964.8	-5139.9	-175.2
42	43	2.777	-4834.7	-6199.2	-8306.1	-2106.9

43	44	3.617	-6016.4	-7843.2	-11047.8	-3204.6
44	45	4.414	-4022.1	-5184.8	-13104.8	-7919.9
45	46	5.169	-3093.8	-4157.6	-15466.3	-11308.7
46	47	1.680	-2290.0	-3208.9	-4546.3	-1337.4
47	48	1.536	-1581.8	-2364.7	-4096.7	-1731.9
48	49	1.329	-1169.2	-1741.1	-3446.0	-1704.9
49	50	1.178	-846.9	-1217.0	-2973.7	-1756.7
50	51	1.061	-580.7	-862.9	-2609.1	-1746.3
51	52	0.970	-364.6	-614.1	-2322.8	-1708.7
52	53	0.898	-195.9	-410.0	-2098.7	-1688.7
53	54	0.843	-71.8	-248.3	-1927.6	-1679.3
54	55	0.804	8.3	-127.6	-1803.4	-1675.8
55	56	0.778	46.5	-46.5	-1722.4	-1675.9
56	57	0.765	43.5	-4.1	-1682.5	-1678.4

TABLE A7 Positive factored shear and shear capacity of exterior frame of bridge 7931.

Location (m)	Element	Beam thickness (m)	Factored shear-*Strength I* (kN)	Factored shear-*Strength II* (kN)	Shear capacity (kN)	Shortage of capacity (kN)
0	1	0.765	-59.1	-10.2	2040.0	-1980.9
1	2	0.778	-18.7	50.1	2047.1	-1997.0
2	3	0.804	62.6	123.9	2061.5	-1937.7
3	4	0.843	164.3	213.0	1101.2	-888.2
4	5	0.898	260.6	299.7	1131.7	-832.0
5	6	0.970	350.9	381.1	1171.6	-790.5
6	7	1.061	435.0	462.9	1222.6	-759.8
7	8	1.178	523.6	570.8	1287.6	-716.8
8	9	1.329	621.0	692.3	1512.1	-819.8
9	10	1.536	716.8	812.3	1628.0	-815.7
10	11	1.680	822.5	896.4	1708.1	-811.7
11	12	5.169	918.5	998.2	3653.3	-2655.1
12	13	4.414	1008.5	1112.3	3092.2	-1980.0
13	14	3.617	-821.2	-781.3	2998.6	-2177.3
14	15	2.777	-763.2	-725.7	2530.2	-1767.0
15	16	1.807	-597.9	-566.8	2340.1	-1742.2
16	17	1.690	-554.5	-526.1	2274.8	-1720.3
17	18	1.597	-500.1	-474.3	2222.9	-1722.8
18	19	1.520	-445.1	-421.8	1829.3	-1384.1
19	20	1.456	-385.3	-364.3	1793.5	-1408.2
20	21	1.402	-328.2	-310.2	1763.4	-1435.2
21	22	1.356	-266.6	-250.5	1527.6	-1261.0
22	23	1.319	-204.2	-189.1	1506.5	-1302.2
23	24	1.287	-138.8	-124.8	1489.1	-1350.4
24	25	1.263	-72.1	-58.6	1475.3	-1403.3
25	26	1.244	-4.1	9.3	1324.4	-1315.2
26	27	1.230	65.0	78.0	1317.0	-1239.0
27	28	1.222	137.2	153.5	1312.6	-1159.0
28	29	1.220	208.6	229.8	1311.1	-1081.3
29	30	1.222	280.9	308.8	1312.6	-1003.8
30	31	1.230	355.8	392.2	1317.0	-924.8
31	32	1.244	429.5	475.4	1324.4	-849.0
32	33	1.263	503.6	560.9	1335.0	-774.1
33	34	1.287	577.7	651.1	1489.1	-838.1
34	35	1.319	651.8	743.2	1506.5	-763.3
35	36	1.356	723.9	835.5	1527.6	-692.1
36	37	1.402	797.3	932.3	1763.4	-831.0
37	38	1.456	865.1	1023.0	1793.5	-770.5
38	39	1.520	936.1	1121.9	1829.3	-707.4
39	40	1.597	1000.0	1213.9	2222.9	-1009.0
40	41	1.690	1062.1	1305.1	2274.8	-969.7
41	42	1.807	1115.2	1383.5	2340.1	-956.7
42	43	2.777	1321.6	1715.9	2530.2	-814.3
43	44	3.617	1394.9	1838.6	2998.6	-1160.0

44	45	4.414	-505.2	-480.2	3092.2	-2587.1
45	46	5.169	-443.9	-423.3	3653.3	-3209.4
46	47	1.680	-379.1	-362.3	1708.1	-1328.9
47	48	1.536	-321.4	-301.0	1628.0	-1306.6
48	49	1.329	-245.8	-237.7	1512.1	-1266.2
49	50	1.178	-173.3	-173.4	1287.6	-1114.1
50	51	1.061	-101.5	-109.1	1222.6	-1113.6
51	52	0.970	-27.7	-38.9	1171.6	-1132.8
52	53	0.898	50.0	38.2	1131.7	-1081.7
53	54	0.843	132.8	120.5	1101.2	-968.5
54	55	0.804	223.1	209.2	2061.5	-1838.4
55	56	0.778	323.2	306.9	2047.1	-1723.9
56	57	0.765	430.9	415.8	2040.0	-1609.1

TABLE A8 Negative factored shear and shear capacity of exterior frame of bridge 7931.

Location (m)	Element	Beam thickness (m)	Factored shear-*Strength I* (kN)	Factored shear-*Strength II* (kN)	Shear capacity (kN)	Shortage of capacity (kN)
0	1	0.765	-541.8	-530.0	-2040.0	-1498.2
1	2	0.778	-427.1	-411.2	-2047.1	-1620.0
2	3	0.804	-319.8	-303.0	-2061.5	-1741.8
3	4	0.843	-220.2	-206.1	-1101.2	-881.0
4	5	0.898	-131.0	-118.1	-1131.7	-1000.7
5	6	0.970	-49.1	-36.5	-1171.6	-1122.5
6	7	1.061	27.2	39.6	-1222.6	-1183.1
7	8	1.178	99.6	107.8	-1287.6	-1179.8
8	9	1.329	170.0	169.2	-1512.1	-1342.0
9	10	1.536	241.3	229.9	-1628.0	-1386.6
10	11	1.680	298.7	287.0	-1708.1	-1409.3
11	12	5.169	366.0	349.1	-3653.3	-3287.3
12	13	4.414	430.3	409.6	-3092.2	-2662.0
13	14	3.617	-1472.0	-1967.6	-2998.6	-1031.0
14	15	2.777	-1402.4	-1846.1	-2530.2	-684.0
15	16	1.807	-1200.5	-1510.5	-2340.1	-829.6
16	17	1.690	-1144.7	-1427.1	-2274.8	-847.7
17	18	1.597	-1080.7	-1331.5	-2222.9	-891.4
18	19	1.520	-1015.6	-1235.9	-1829.3	-593.4
19	20	1.456	-944.0	-1132.8	-1793.5	-660.7
20	21	1.402	-875.7	-1037.3	-1763.4	-726.1
21	22	1.356	-801.8	-938.5	-1527.6	-589.0
22	23	1.319	-729.4	-843.1	-1506.5	-663.4
23	24	1.287	-655.0	-747.8	-1489.1	-741.4
24	25	1.263	-580.5	-655.0	-1475.3	-820.4
25	26	1.244	-506.0	-564.3	-1324.4	-760.2
26	27	1.230	-431.7	-478.3	-1317.0	-838.7
27	28	1.222	-355.9	-392.7	-1312.6	-919.9
28	29	1.220	-282.7	-310.9	-1311.1	-1000.2
29	30	1.222	-210.3	-231.7	-1312.6	-1080.8
30	31	1.230	-137.1	-153.6	-1317.0	-1163.4
31	32	1.244	-66.9	-79.8	-1324.4	-1244.7
32	33	1.263	2.2	-11.2	-1335.0	-1323.8
33	34	1.287	69.9	56.5	-1489.1	-1419.3
34	35	1.319	136.2	122.3	-1506.5	-1370.2
35	36	1.356	199.7	184.8	-1527.6	-1327.9
36	37	1.402	263.0	247.0	-1763.4	-1500.4
37	38	1.456	319.5	301.9	-1793.5	-1474.0
38	39	1.520	378.6	357.8	-1829.3	-1450.7
39	40	1.597	431.9	408.9	-2222.9	-1791.0
40	41	1.690	484.1	458.8	-2274.8	-1790.7
41	42	1.807	529.0	501.7	-2340.1	-1811.1
42	43	2.777	696.0	661.0	-2530.2	-1834.2

43	44	3.617	755.7	718.1	-2998.6	-2242.9
44	45	4.414	-1107.3	-1264.9	-3092.2	-1827.4
45	46	5.169	-1022.1	-1125.7	-3653.3	-2527.5
46	47	1.680	-931.5	-1011.4	-1708.1	-696.6
47	48	1.536	-830.1	-930.1	-1628.0	-697.9
48	49	1.329	-727.3	-812.2	-1512.1	-699.9
49	50	1.178	-626.7	-691.5	-1287.6	-596.1
50	51	1.061	-526.9	-569.6	-1222.6	-653.0
51	52	0.970	-436.0	-460.2	-1171.6	-711.5
52	53	0.898	-350.3	-378.1	-1131.7	-753.6
53	54	0.843	-258.9	-295.0	-1101.2	-806.2
54	55	0.804	-161.5	-208.1	-2061.5	-1853.4
55	56	0.778	-59.0	-118.6	-2047.1	-1928.5
56	57	0.765	23.8	-44.2	-2040.0	-1995.8

TABLE A9 Positive factored moment and flexural capacity of exterior frame of bridge 7937 and 7938.

Location (m)	Element	Beam thickness (m)	Factored moment-*Strength I* (kNm)	Factored moment-*Strength II* (kNm)	Flexural capacity (kNm)	Shortage of capacity (kNm)
0	1	0.765	0.0	0.0	967.8	-967.8
1	2	0.779	505.3	488.3	990.5	-485.3
2	3	0.807	808.3	769.3	1036.5	-228.2
3	4	0.850	936.4	891.5	1106.8	-170.4
4	5	0.908	924.2	889.8	1203.3	-279.1
5	6	0.984	798.9	761.0	1329.0	-530.1
6	7	1.080	575.8	531.0	1488.2	-912.5
7	8	1.201	269.7	185.1	1688.2	-1418.5
8	9	1.354	-111.3	-197.6	1941.1	-2052.4
9	10	1.554	-565.3	-610.5	2271.6	-2836.9
10	11	1.717	-1095.5	-1092.6	2542.1	-3634.7
11	12	5.449	-1683.8	-1635.2	8712.0	-10347.2
12	13	4.787	-2294.7	-2184.0	7618.5	-9802.5
13	14	4.027	-5232.4	-4998.4	6361.8	-11360.3
14	15	2.952	-4162.1	-3972.3	4583.2	-8555.5
15	16	1.807	-3398.6	-3241.1	2689.8	-5930.9
16	17	1.690	-2549.7	-2448.1	2496.1	-4944.2
17	18	1.597	-1737.0	-1687.3	2342.1	-4029.4
18	19	1.520	-974.6	-973.1	4254.8	-5227.9
19	20	1.456	-263.5	-310.6	4042.7	-4306.2
20	21	1.402	388.5	355.3	3864.1	-3475.5
21	22	1.356	983.4	968.1	3713.9	-2730.5
22	23	1.319	1548.5	1582.0	3588.8	-2006.7
23	24	1.287	2051.4	2157.8	4965.3	-2807.4
24	25	1.263	2480.4	2680.1	4842.3	-2162.1
25	26	1.244	2833.5	3156.5	4748.4	-1591.9
26	27	1.230	3107.4	3520.2	4682.3	-1162.0
27	28	1.222	3289.7	3762.0	4642.9	-880.9
28	29	1.220	3377.2	3880.1	4629.9	-749.8
29	30	1.222	3375.3	3878.1	4642.9	-764.8
30	31	1.230	3283.9	3756.2	4682.3	-926.1
31	32	1.244	3098.0	3510.8	4748.4	-1237.6
32	33	1.263	2820.7	3143.6	4842.3	-1698.7
33	34	1.287	2464.4	2664.2	4965.3	-2301.1
34	35	1.319	2032.8	2139.2	3588.8	-1449.6
35	36	1.356	1527.8	1561.3	3713.9	-2152.6
36	37	1.402	961.2	946.0	3864.1	-2902.8
37	38	1.456	365.8	332.6	4042.7	-3676.8
38	39	1.520	-285.7	-332.8	4254.8	-4540.5
39	40	1.597	-995.2	-993.7	2342.1	-3335.8
40	41	1.690	-1754.6	-1704.9	2496.1	-4200.9
41	42	1.807	-2562.5	-2460.9	2689.8	-5150.7

42	43	2.952	-3404.5	-3247.0	4583.2	-7830.2
43	44	4.027	-4158.1	-3968.3	6361.8	-10330.2
44	45	4.787	-2951.4	-2813.9	7618.5	-10432.4
45	46	5.449	-2323.5	-2212.8	8712.0	-10924.8
46	47	1.717	-1698.2	-1649.6	2542.1	-4191.6
47	48	1.554	-1097.2	-1094.2	2271.6	-3365.8
48	49	1.354	-557.6	-602.8	1941.1	-2498.7
49	50	1.201	-97.8	-184.1	1688.2	-1785.9
50	51	1.080	286.4	201.8	1488.2	-1201.8
51	52	0.984	593.5	548.8	1329.0	-735.5
52	53	0.908	816.0	778.1	1203.3	-387.3
53	54	0.850	939.4	905.0	1106.8	-167.4
54	55	0.807	948.6	903.7	1036.5	-87.9
55	56	0.779	816.8	777.9	990.5	-173.7
56	57	0.765	509.7	492.7	967.8	-458.2

TABLE A10 Negative factored moment and flexural capacity of exterior frame of bridges 7937 and 7938.

Location (m)	Element	Beam thickness (m)	Factored moment- *Strength I* (kNm)	Factored moment- *Strength II* (kNm)	Flexural capacity (kNm)	Shortage of capacity (kNm)
0	1	0.765	0.0	0.0	-1493.0	-1493.0
1	2	0.779	59.4	4.8	-1530.2	-1535.0
2	3	0.807	63.9	-42.6	-1605.4	-1562.8
3	4	0.850	13.2	-142.5	-1720.6	-1578.1
4	5	0.908	-93.5	-295.4	-1878.7	-1583.2
5	6	0.984	-257.7	-502.6	-2084.4	-1581.9
6	7	1.080	-479.9	-764.9	-2345.2	-1580.3
7	8	1.201	-762.7	-1084.5	-2672.6	-1588.1
8	9	1.354	-1108.0	-1534.7	-3086.7	-1552.0
9	10	1.554	-1520.7	-2170.7	-3627.9	-1457.2
10	11	1.717	-2017.8	-2918.1	-4070.8	-1152.7
11	12	5.449	-2864.1	-3925.8	-14174.0	-10248.2
12	13	4.787	-3822.7	-5058.2	-12383.6	-7325.3
13	14	4.027	-8753.2	-11253.6	-20839.4	-9585.8
14	15	2.952	-7141.3	-9070.7	-14814.2	-5743.5
15	16	1.807	-5948.5	-7458.5	-8400.3	-941.7
16	17	1.690	-4793.0	-5993.8	-7744.1	-1750.2
17	18	1.597	-3707.3	-4621.7	-980.4	**3641.4**
18	19	1.520	-2706.6	-3353.8	-928.5	**2425.3**
19	20	1.456	-1795.5	-2245.7	-885.0	**1360.7**
20	21	1.402	-986.7	-1314.2	-848.4	**465.8**
21	22	1.356	-279.2	-499.1	-817.7	-318.6
22	23	1.319	314.2	128.0	-792.1	-920.1
23	24	1.287	704.1	620.7	-771.1	-1391.8
24	25	1.263	1013.0	952.4	-754.3	-1706.7
25	26	1.244	1262.9	1198.0	-741.5	-1939.4
26	27	1.230	1454.4	1382.7	-732.4	-2115.1
27	28	1.222	1587.7	1511.8	-727.1	-2238.9
28	29	1.220	1661.5	1584.0	-725.3	-2309.2
29	30	1.222	1659.5	1582.0	-727.1	-2309.1
30	31	1.230	1581.9	1506.0	-732.4	-2238.4
31	32	1.244	1444.9	1373.3	-741.5	-2114.7
32	33	1.263	1250.0	1185.1	-754.3	-1939.4
33	34	1.287	997.0	936.5	-771.1	-1707.5
34	35	1.319	685.5	602.1	-792.1	-1394.2
35	36	1.356	293.4	107.3	-817.7	-925.0
36	37	1.402	-301.3	-521.3	-848.4	-327.2
37	38	1.456	-1009.4	-1336.9	-885.0	**451.8**
38	39	1.520	-1817.7	-2267.9	-928.5	**1339.5**
39	40	1.597	-2727.2	-3374.4	-980.4	**2394.0**
40	41	1.690	-3724.8	-4639.3	-7744.1	-3104.7
41	42	1.807	-4805.7	-6006.6	-8400.3	-2393.7

42	43	2.952	-5954.3	-7464.4	-14814.2	-7349.8
43	44	4.027	-7137.3	-9066.7	-20839.4	-11772.7
44	45	4.787	-4974.6	-6330.3	-12383.6	-6053.2
45	46	5.449	-3851.6	-5087.1	-14174.0	-9086.9
46	47	1.717	-2878.5	-3940.2	-4070.8	-130.6
47	48	1.554	-2019.5	-2919.7	-3627.9	-708.1
48	49	1.354	-1513.1	-2163.0	-3086.7	-923.7
49	50	1.201	-1094.5	-1521.2	-2672.6	-1151.4
50	51	1.080	-746.0	-1067.7	-2345.2	-1277.5
51	52	0.984	-462.2	-747.1	-2084.4	-1337.3
52	53	0.908	-240.6	-485.5	-1878.7	-1393.2
53	54	0.850	-78.4	-280.3	-1720.6	-1440.3
54	55	0.807	25.4	-130.3	-1605.4	-1475.2
55	56	0.779	72.5	-34.1	-1530.2	-1496.1
56	57	0.765	63.8	9.2	-1493.0	-1502.2

TABLE A11 Positive factored shear and shear capacity of exterior frame of bridges 7937 and 7938.

Location (m)	Element	Beam thickness (m)	Factored shear-*Strength I* (kN)	Factored shear-*Strength II* (kN)	Shear capacity (kN)	Shortage of capacity (kN)
0	1	0.765	-86.4	-30.4	1058.1	-971.6
1	2	0.779	-31.5	46.0	1065.7	-1019.7
2	3	0.807	64.6	137.2	1081.2	-944.1
3	4	0.850	186.8	245.5	1104.9	-859.4
4	5	0.908	302.8	350.8	1137.5	-786.7
5	6	0.984	412.0	450.1	1179.9	-729.8
6	7	1.080	514.1	549.5	1233.6	-684.0
7	8	1.201	621.4	676.9	1301.0	-624.0
8	9	1.354	737.7	818.3	1386.2	-567.9
9	10	1.554	852.5	956.1	1497.7	-541.6
10	11	1.717	979.4	1072.5	1588.9	-516.4
11	12	5.449	1094.5	1193.2	3669.4	-2476.2
12	13	4.787	1204.3	1329.6	3300.7	-1971.1
13	14	4.027	-1106.6	-1061.5	2876.9	-1770.3
14	15	2.952	-798.9	-762.8	2277.2	-1478.3
15	16	1.807	-769.9	-736.1	1638.7	-868.8
16	17	1.690	-718.9	-687.1	1573.4	-854.5
17	18	1.597	-652.6	-624.0	1521.5	-868.9
18	19	1.520	-585.4	-559.2	1478.7	-893.4
19	20	1.456	-511.5	-487.7	1443.0	-931.5
20	21	1.402	-441.0	-420.3	1412.9	-971.9
21	22	1.356	-364.6	-346.9	1387.5	-1023.0
22	23	1.319	-287.9	-271.1	1366.4	-1078.6
23	24	1.287	-207.1	-191.5	1349.1	-1142.0
24	25	1.263	-124.9	-109.8	1335.3	-1210.4
25	26	1.244	-41.3	-26.1	1324.8	-1283.5
26	27	1.230	43.9	58.6	1317.3	-1258.7
27	28	1.222	132.6	149.9	1312.9	-1163.0
28	29	1.220	220.4	242.6	1311.4	-1068.8
29	30	1.222	309.2	338.6	1312.9	-974.3
30	31	1.230	401.1	439.9	1317.3	-877.4
31	32	1.244	491.5	540.6	1324.8	-784.1
32	33	1.263	582.2	642.7	1335.3	-692.6
33	34	1.287	673.0	750.7	1349.1	-598.4
34	35	1.319	763.7	861.0	1366.4	-505.4
35	36	1.356	851.8	971.2	1387.5	-416.3
36	37	1.402	941.6	1086.8	1412.9	-326.1
37	38	1.456	1024.3	1194.6	1443.0	-248.4
38	39	1.520	1110.8	1310.4	1478.7	-168.3
39	40	1.597	1188.3	1418.5	1521.5	-103.0
40	41	1.690	1263.5	1525.6	1573.4	-47.8
41	42	1.807	1326.9	1616.8	1638.7	-21.9

42	43	2.952	1361.5	1664.8	2277.2	-612.4
43	44	4.027	1723.7	2239.1	2876.9	-637.8
44	45	4.787	-665.1	-636.9	3300.7	-2635.6
45	46	5.449	-589.0	-563.5	3669.4	-3080.5
46	47	1.717	-508.8	-489.7	1588.9	-1080.1
47	48	1.554	-428.2	-407.6	1497.7	-1069.5
48	49	1.354	-338.0	-328.9	1386.2	-1048.2
49	50	1.201	-249.8	-249.4	1301.0	-1051.2
50	51	1.080	-161.4	-169.2	1233.6	-1064.4
51	52	0.984	-70.8	-82.2	1179.9	-1097.7
52	53	0.908	24.3	12.2	1137.5	-1113.2
53	54	0.850	125.1	112.3	1104.9	-979.9
54	55	0.807	234.3	219.4	1081.2	-846.9
55	56	0.779	354.3	337.0	1065.7	-711.5
56	57	0.765	482.6	467.0	1058.1	-575.5

TABLE A12 Negative factored shear and shear capacity of exterior frame of bridges 7937 and 7938.

Location (m)	Element	Beam thickness (m)	Factored shear-*Strength I* (kN)	Factored shear-*Strength II* (kN)	Shear capacity (kN)	Shortage of capacity (kN)
0	1	0.765	-553.5	-542.5	-1058.1	-504.6
1	2	0.779	-431.0	-416.0	-1065.7	-634.7
2	3	0.807	-315.8	-299.8	-1081.2	-765.5
3	4	0.850	-208.4	-194.9	-1104.9	-896.6
4	5	0.908	-111.1	-98.9	-1137.5	-1026.4
5	6	0.984	-21.3	-9.5	-1179.9	-1158.6
6	7	1.080	63.0	74.6	-1233.6	-1159.0
7	8	1.201	143.2	150.7	-1301.0	-1150.2
8	9	1.354	221.0	219.8	-1386.2	-1165.3
9	10	1.554	298.6	288.1	-1497.7	-1199.1
10	11	1.717	370.7	358.2	-1588.9	-1218.2
11	12	5.449	445.8	428.5	-3669.4	-3223.6
12	13	4.787	516.3	493.3	-3300.7	-2784.5
13	14	4.027	-1640.0	-2156.0	-2876.9	-720.9
14	15	2.952	-1321.2	-1635.7	-2277.2	-641.5
15	16	1.807	-1285.5	-1587.8	-1638.7	-51.0
16	17	1.690	-1226.1	-1501.1	-1573.4	-72.3
17	18	1.597	-1157.0	-1400.7	-1521.5	-120.8
18	19	1.520	-1086.3	-1299.9	-1478.7	-178.8
19	20	1.456	-1008.2	-1190.8	-1443.0	-252.2
20	21	1.402	-933.4	-1090.4	-1412.9	-322.4
21	22	1.356	-852.4	-984.8	-1387.5	-402.7
22	23	1.319	-773.0	-882.5	-1366.4	-483.9
23	24	1.287	-691.2	-780.2	-1349.1	-568.9
24	25	1.263	-609.2	-680.3	-1335.3	-655.0
25	26	1.244	-527.2	-582.5	-1324.8	-742.2
26	27	1.230	-445.3	-490.2	-1317.3	-827.1
27	28	1.222	-361.7	-397.0	-1312.9	-915.9
28	29	1.220	-280.8	-307.7	-1311.4	-1003.7
29	30	1.222	-200.8	-221.1	-1312.9	-1091.8
30	31	1.230	-119.9	-135.5	-1317.3	-1181.8
31	32	1.244	-42.1	-55.3	-1324.8	-1269.5
32	33	1.263	34.5	20.8	-1335.3	-1300.9
33	34	1.287	109.6	96.0	-1349.1	-1239.6
34	35	1.319	183.2	169.2	-1366.4	-1183.2
35	36	1.356	253.7	238.8	-1387.5	-1133.8
36	37	1.402	324.1	308.2	-1412.9	-1088.8
37	38	1.456	387.1	368.9	-1443.0	-1055.8
38	39	1.520	453.1	431.9	-1478.7	-1025.6
39	40	1.597	512.3	489.1	-1521.5	-1009.2
40	41	1.690	570.0	544.8	-1573.4	-1003.4
41	42	1.807	619.1	591.6	-1638.7	-1019.6

42	43	2.952	641.7	611.6	-2277.2	-1635.5
43	44	4.027	917.1	878.9	-2876.9	-1959.8
44	45	4.787	-1193.9	-1357.5	-3300.7	-1943.2
45	46	5.449	-1097.8	-1210.8	-3669.4	-2458.6
46	47	1.717	-997.3	-1086.0	-1588.9	-502.9
47	48	1.554	-886.2	-984.1	-1497.7	-513.6
48	49	1.354	-777.3	-863.4	-1386.2	-522.8
49	50	1.201	-669.9	-737.4	-1301.0	-563.5
50	51	1.080	-562.7	-609.2	-1233.6	-624.4
51	52	0.984	-464.0	-492.4	-1179.9	-687.5
52	53	0.908	-370.5	-402.8	-1137.5	-734.7
53	54	0.850	-271.2	-311.8	-1104.9	-793.2
54	55	0.807	-165.8	-216.6	-1081.2	-864.7
55	56	0.779	-54.9	-118.8	-1065.7	-946.9
56	57	0.765	33.1	-36.0	-1058.1	-1022.1

NEW MEXICO DEPARTMENT OF TRANSPORTATION

RESEARCH BUREAU

Innovation in Transportation

Strengthening Reinforced Concrete Bridges in New Mexico Using Fiber Reinforced Polymers:

Report II – Design Method for Strengthening K-Frame Bridges Using FRP

Prepared by:
University of New Mexico
Department of Civil Engineering
Albuquerque, NM

Prepared for:
New Mexico Department of Transportation
Research Bureau
Albuquerque, New Mexico

In Cooperation with:
The US Department of Transportation
Federal Highway Administration

Report NM06TT-01

FEBRUARY 2009

orm DOT F 1700.7 (8-72)

1. Report No.	2. Government Accession No.	3. Recipient's Catalog No.
NM06TT-01		
4. Title and Subtitle Strengthening Reinforced Concrete Bridges in New Mexico Using Fiber Reinforced Polymers Report II: Design Method for Strengthening K-Frame Bridges Using FRP		5. Report Date March 2008 6. Performing Organization Code
7. Author(s) M. M. Reda Taha, K. K. Choi, M. Azarbayejani		8. Performing Organization Report No.
9. Performing Organization Name and Address University of New Mexico Department of Civil Engineering Albuquerque, NM 87131		10. Work Unit No. (TRAIS) 11. Contract or Grant No. CO4961
12. Sponsoring Agency Name and Address Research Bureau New Mexico Department of Transportation 7500-B Pan American Freeway NE Albuquerque, NM 87109		13. Type of Report and Period Covered 14. Sponsoring Agency Code
15. Supplementary Notes		

16. Abstract

The objective of this report is to provide detailed information about the design methods used to determine strengthening alternatives for the concrete frame bridges #7930, 7931, 7937 and 7938 at Tucumcari, New Mexico. Several strengthening alternatives were considered. Further details on the design of Fiber Reinforced Polymer (FRP) strips, the chosen strengthening alternative, are discussed. Locations and length requirements of the strengthening strips for the four bridges are identified. Guidelines for the application of the FRP material based on guidelines by the American Concrete Institute and other international agencies are provided.

17. Key Words:		18. Distribution Statement	
Concrete frame bridges, AASHTO LRFD Bridge Design Specification, Fiber reinforced polymers.		Available from NMDOT Research Bureau	
19. Security Classif. (of this report)	20. Security Classif. (of this page)	21. No. of Pages	22. Price
None	None	12	

STRENGTHENING REINFORCED CONCRETE BRIDGES IN NEW MEXICO USING FIBER REINFORCED POLYMERS

Report II: Design Method for Strengthening K-Frame Bridges Using FRP

by

M. M. Reda Taha
K. K. Choi
M. Azarbayejani
University of New Mexico
Department of Civil Engineering

Prepared for:
New Mexico Department of Transportation, Research Bureau

A Report on Research Sponsored by:
New Mexico Department of Transportation, Research Bureau

In Cooperation with the
U.S. Department of Transportation, Federal Highway Administration

March 2008

NMDOT, Research Bureau
7500-B Pan American Freeway NE
Albuquerque, NM 87109

PREFACE

The purpose of this research is to evaluate the structural capacity of the concrete frame bridges #7930, 7931, 7937 and 7938 at Tucumcari, New Mexico and evaluate their need for strengthening to meet AASHTO safety requirements. This report provides detailed information about the design methods used to determine the strengthening alternatives for these bridges.

NOTICE

DISCLAIMER

ABSTRACT

The objective of this report is to provide detailed information about the design methods used to determine strengthening alternatives for the concrete frame bridges #7930, 7931, 7937 and 7938 at Tucumcari, New Mexico. Several strengthening alternatives were considered. Further details on the design of Fiber Reinforced Polymer (FRP) strips, the chosen strengthening alternative, are discussed. Locations and length requirements of the strengthening strips for the four bridges are identified. Guidelines for the application of the FRP material based on guidelines by the American Concrete Institute and other international agencies are provided.

TABLE OF CONTENTS

TABLES

FIGURES

STRENGTHENING BRIDGES USING FRP

According to AASHTO (1), the need for strengthening of concrete structures can be determined by considering Eq. (1)

$$\phi M_n \geq M_u \tag{1}$$

where:

ϕ = strength reduction factor which is different in moment and shear

M_n = nominal flexural strength

M_u = factored applied moment.

when ϕM_n is less than M_u the concrete structures need to be strengthened by proper method. According to the results of calibrated FE analysis shown in Report (1), it was concluded that all the K-frames (Bridges # 7930, 7931, 7937 and 7937) require strengthening as they showed shortage in negative moment capacity around the K-frame connections. Such strengthening can be performed by providing additional negative moment reinforcement. It was suggested that strengthening be performed by attaching/bonding Fiber reinforced polymers (FRP) reinforcement to the top concrete fibers at the K-frame connections. Fiber Reinforced Polymer (FRP) reinforcement has been recommended as a strengthening material when the moment capacity of reinforced concrete sections is not sufficient (2). Numerous applications of FRP for strengthening bridges worldwide have shown FRP reinforcement to be an efficient strengthening method (2 and 3).

The moment resistance to be provided by FRP can be calculated as

$$M_u - \phi M_n \leq \phi M_{frp} \tag{2}$$

M_u = factored moment

M_n = nominal moment-carrying capacity.

According to the American Concrete Institute (ACI) Committee on FRP ACI 440 (2) and researchers Teng et al. (3), the moment capacity of a reinforced concrete section strengthened with FRP ϕM_{frp} can be computed as

$$\phi M_{frp} = \phi \varphi_{frp} A_f E_f \varepsilon_{fe} \cdot jd \qquad (3)$$

φ_{frp} = additional reduction factor (=0.85)

A_f = area of FRP reinforcement

ε_{fe} = effective ultimate strain developing at FRP

E_f = Young's modulus of FRP

jd = length of moment arm.

The ACI 440 (2) design method is similar to ACI 318 (4) design method, which is based on strain-compatibility and force equilibrium using the equivalent concrete stress block (Fig. 1).

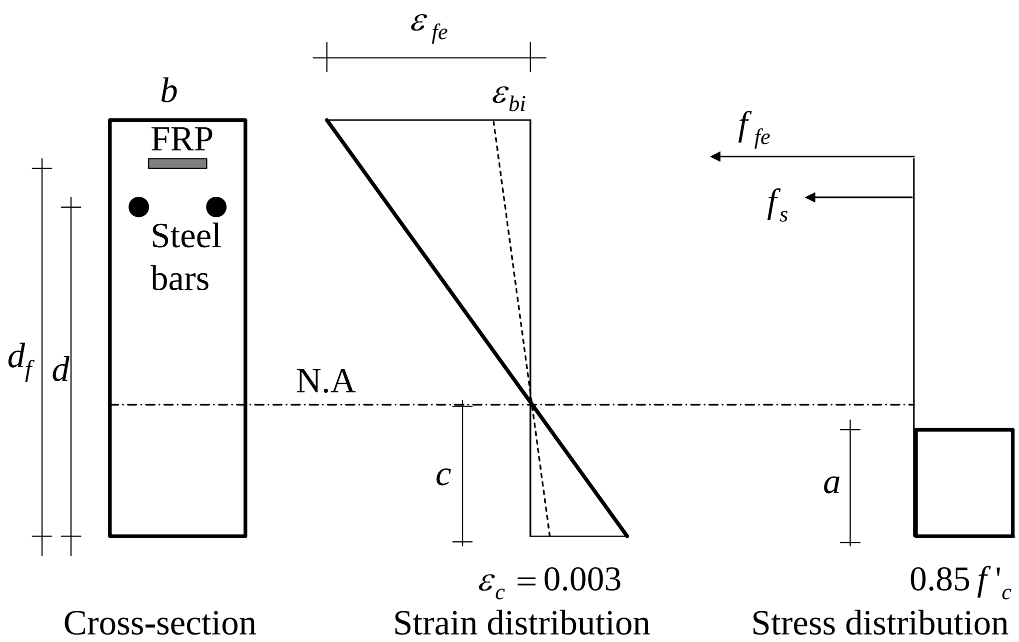

FIGURE 1 Stress and strain distribution of the concrete beam strengthened by FRP.

Considering that no tensile cracking was observed in the K-frames prior to strengthening, it can be assumed that the existing strain is negligible. Therefore, the effective strain of FRP at ultimate state is defined as

$$\varepsilon_{fe} = 0.003\left(\frac{d_f - c}{c}\right) \le \kappa_m \cdot \varepsilon_{fu} \qquad (4)$$

d_f = effective depth for FRP reinforcement

c = depth of compression zone

κ_m = bond-dependent coefficient for flexure

ε_{fu} = design rupture strain of the FRP reinforcement.

Durability experiments and experiences by ACI 440 (2) and the European code for strengthening of concrete structures using FRP (5) show Carbon Fiber Reinforced Polymer (CFRP) as the most durable FRP material. Strengthening using CFRP strips was considered. For this type of material ACI 440 design guidelines recommend using bond-dependent coefficient for flexure κ_m = 0.9.

DESIGN OF FRP STRENGTHENING STRIPS

In this section, first, the design method for an exterior frame of bridge 7937 is presented as an example. According to the results of Finite Element (FE) analysis shown in Report (1), the maximum shortage of negative moment ($M_u - \phi M_c$) in Eq. (2) is 3,788 kN.m at the connection (*x* = 17 m measured from the bridge end as shown in Figure 2). consider Two alternative types of FRP are considered: Carbon Fiber Reinforced Polymers (CFRP) and Glass Fiber Reinforced Polymers (GFRP). While CFRP is known for its high strength and durability, GFRP is known for its relatively low cost. Both materials have been used for strengthening bridges. From Eq. (3) and Eq. (4), the required area of FRP reinforcement can be evaluated as

For CFRP with $E_f = 150{,}000\,MPa$ and $\varepsilon_{fu} = 0.0134$

$$A_f = \frac{M_u - \phi M_c}{\kappa_m \cdot \varepsilon_{fu} E_f \phi\varphi_{frp} \cdot jd} = \frac{3788}{0.9 \cdot 0.0134 \cdot 150000 \cdot 0.85 \cdot 0.85 \cdot 0.9 \cdot 1.8} \times 1000 = 1789\,mm^2$$

For GFRP with $E_f = 42{,}000\,MPa$ and $\varepsilon_{fu} = 0.0165$

$$A_f = \frac{M_u - \phi M_c}{\kappa_m \cdot \varepsilon_{fu} E_f \phi\varphi_{frp} \cdot jd} = \frac{3788}{0.9 \cdot 0.0165 \cdot 42000 \cdot 0.85 \cdot 0.85 \cdot 0.9 \cdot 1.8} \times 1000 = 5190\,mm^2$$

It can be observed that the required amount of Glass Fiber Reinforced Polymer (GFRP) for strengthening the bridge is significantly large because of the relatively lower stiffness of GFRP compared with CFRP. Thus, it is recommended to use Carbon Fiber Reinforced Polymer (CFRP) strips with high stiffness and very high durability. In the above calculation, length of moment arm after application of FRP is assumed as

$jd = 0.85d$. Based on the calculation, CFRP needs to be applied between x = 16.2 m (53 inch) and 20.1 m (66 inch).

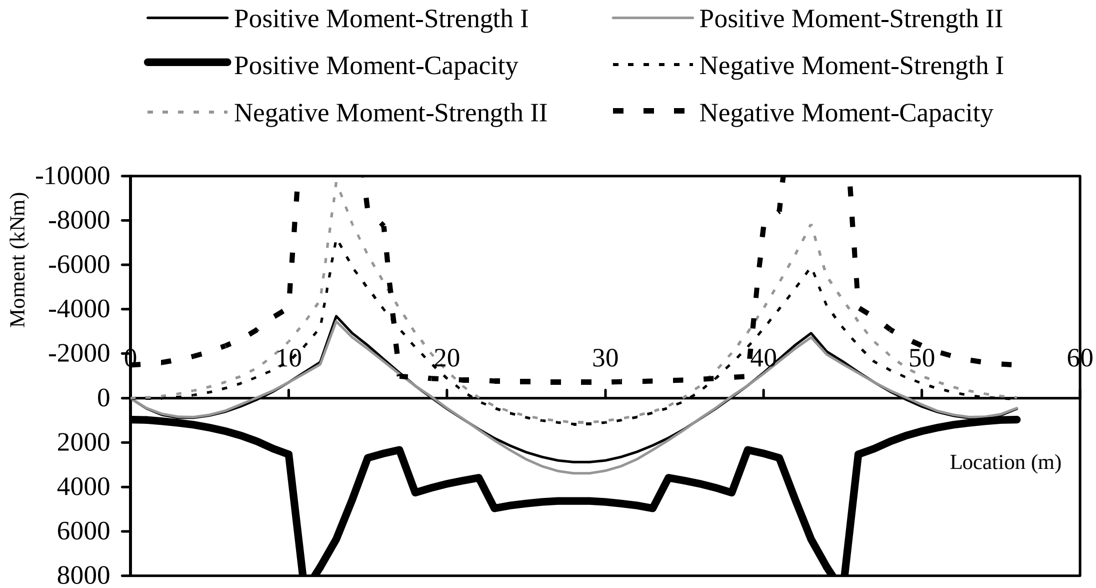

FIGURE 2 Factored moment and capacity of exterior beam of bridge 7937.

Considering the required area of CFRP material, it can be shown that 4 layers of CFRP strips, with each strip having a cross-section of 305 mm (1 feet) wide and 1.52 mm thick (0.06 inch) was sufficient to reinforce each K-frame. CFRP strips are typically produced with maximum length of 13 feet long (3.96 m). Fig. 3 presents a schematic figure showing the layout of CFRP strips for strengthening the exterior K-frame of bridge 7937. As shown in the figure, for strengthening the concrete frames for negative moment capacity, the FRP strips need to be applied at the connection of the K-frame.

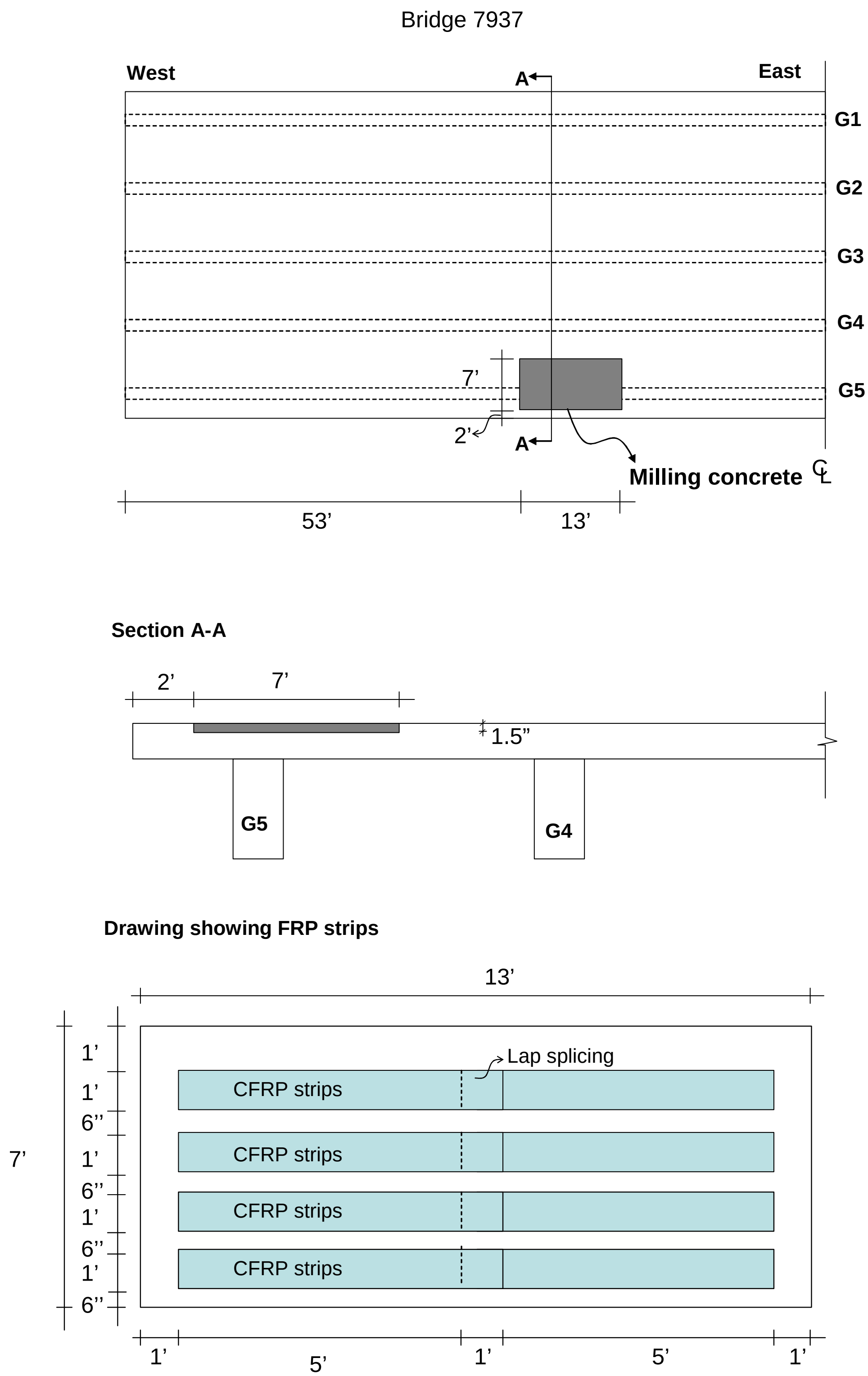

FIGURE 3 Schematic figure showing the layout of CFRP strips for strengthening the exterior girder of bridge 7937.

As the FRP strips provided by manufacturers were not long enough to cover the area that needed strengthening, two CFRP strips were overlapped considering the lap length defined by ACI 440, NCHRP Report (6) and recommended by other researchers (3). The total amount of CFRP strips required strengthening the four K-frame bridges at Tucumcari, New Mexico are presented in Table 1.

Table 1 Required amount of FRP strips and their locations for strengthening bridges.

		Required amount of FRP strips (mm^2)	Location of FRP strips, distance from the edge of the bridges
Bridge 7930	Exterior girder	1021	(13 m ~ 17 m) and (40 m ~ 44 m)
	Interior girder	828	(13 m ~ 17 m) and (40 m ~ 44 m)
Bridge 7931	Exterior girder	862	(13 m ~ 17 m) and (40 m ~ 44 m)
	Interior girder	1230	(13 m ~ 17 m) and (40 m ~ 44 m)
Bridge 7937	Exterior girder	1789	(16.2 m ~ 20.1 m) and (36.9 m ~ 40.8 m)
	Interior girder	2212	(15 m ~ 20 m) and (37 m ~ 42 m)
Bridge 7938	Exterior girder	1789	(17 m ~ 20 m) and (37 m ~ 40 m)
	Interior girder	2212	(15 m ~ 20 m) and (37 m ~ 42 m)

ALTERNATIVE STRENGTHENING METHODS

Recently, several alternative techniques using FRP materials for strengthening of reinforced concrete structures have been investigated and recommended by others. Near-surface mounted (NSM) reinforcement was recommended as a good alternative when large area of FRP is needed (7 and 8). A schematic figure showing the application of NSM-FRP bars is presented in Fig. 4. In this section, the design method for an exterior frame of bridge 7937 is presented as an example. As described in Report (1), the maximum shortage of negative moment ($M_u - \phi M_c$) is 3,788 kN.m at the K-frame connection (x = 17 m). From Eqs. (3) and (4), using CFRP with $E_f = 150{,}000\,MPa$ and

$\varepsilon_{fu} = 0.0134$, 7 layers of CFRP bars, whose diameters are 19 mm (0.75 inch) and length is 3.96 m (13 feet), are recommended.

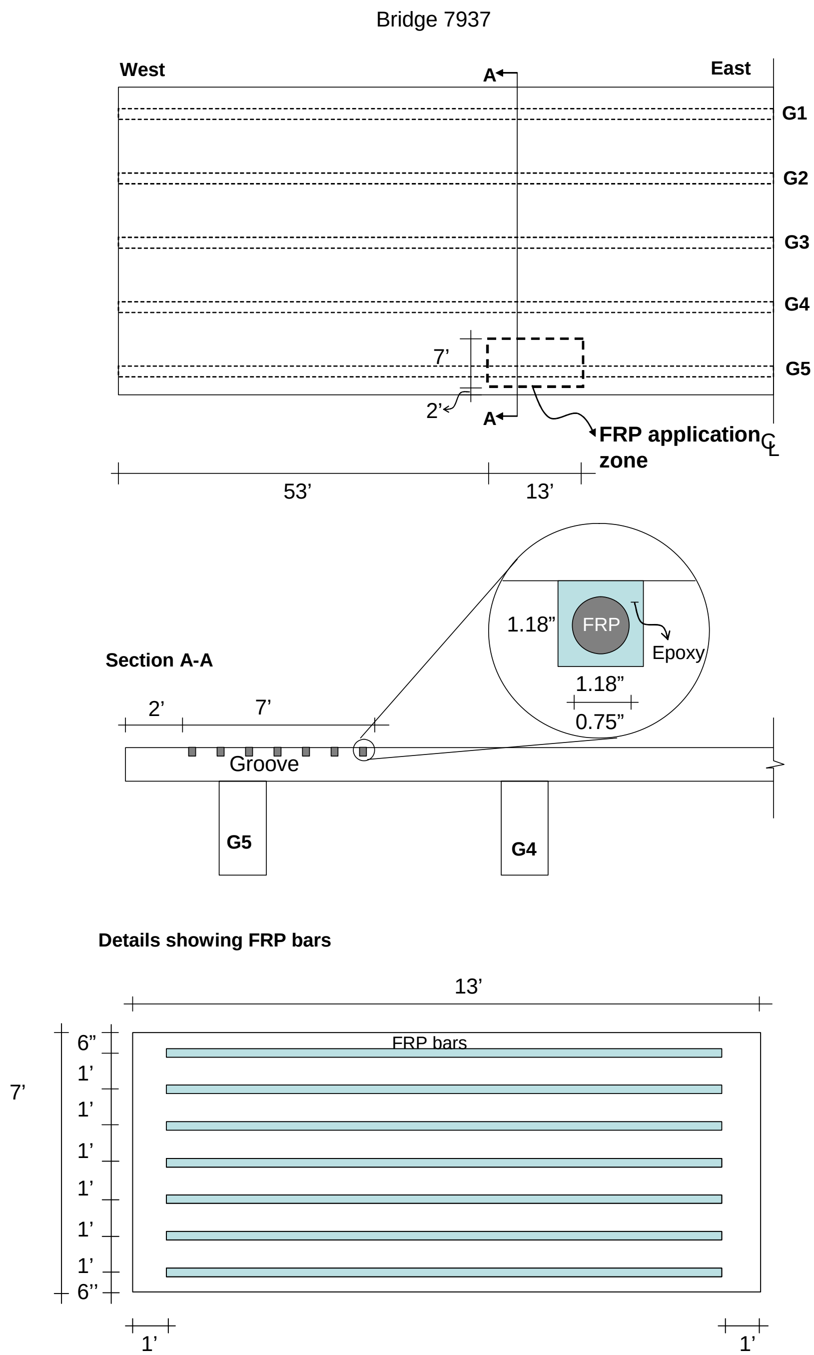

FIGURE 4 Schematic figure showing the layout of NSM-CFRP bars for strengthening the exterior girder of bridge 7937.

For the application of NSM FRP bars, the concrete grooves needed to be prepared were 30 mm (1.18 inch) in width and 3.96 m (13 feet) in length. Generally, application of NSM-FRP bars is similar to the application of FRP strips. However, instead of milling of whole concrete surface in construction zone, several grooves are needed by using saw cut machine. The FRP was installed with resin in the groove. Here it is noted that NSM FRP technique may not require finishing by other layers or topping such as asphalt or mortar because the FRP is not exposed to the air directly unlike the FRP strips method. The CFRP was applied from the top of the bridge, the ease of application enabled easy installation of wide CFRP strips. Therefore, it was decided that the CFRP strips strengthening alternative would be used for strengthening the K-frame bridges.

APPLICATION OF FRP STRIPS FOR STRENGTHENING BRIDGES

The application of FRP strips were performed according to standard methods as specified by ACI 440 (2) and the recent NCHRP Report 514 (6). Several different types of materials were used to install the FRP strips. These materials included putty for filling concrete cracks and providing a leveled concrete surface, epoxy adhesive, and CFRP strips. The major steps for application of FRP strips are as follows.

Step 1: Concrete Surface Milling

Bridge 7937 which has a concrete surface at the top of the exterior girders. 1.5 inch of concrete surface needed to be milled to enable installing the CFRP strips. For other locations on the bridge that are covered by asphalt instead of concrete, all asphalt in the FRP application zone needed to be completely milled as shown in Fig. 3. The investigation showed no need to provide positive moment strengthening at the K-frame soffits. If such strengthening is sought, the concrete surface of the K-frame soffit will need to be prepared without milling.

Step 2: Concrete Surface Preparation

This step is the most important step in application of FRP strips because properly roughened and even concrete substrate is necessary for reliable performance of FRP strips (5 and 6). The acceptable unevenness, which indicates the maximum difference of the surface depth, is specified in current design provisions. In CEB-FIP code (5) and NCHRP Report (6), the allowable value of unevenness of the concrete surface is 4 mm (1/6 inch). If the surface is not even enough, putty needs to be applied to obtain better concrete surface. In addition, several aspects need to be considered.

(1) The concrete substrate needs to be sound with proper tensile strength. In CEB-FIP (5), the minimum tensile strength of concrete is 1.5 N/mm^2. The crack width should be less than 0.2 mm. In addition, the concrete surface should be clean and free from oil, water, or dust before application of FRP.

(2) Moreover, special care is needed to ensure hardening of the putty. Usually, the hardening time depending on the putty type used may vary from 1 day to 14 days.

Step 3: Application of FRP Strips

To attach FRP strips to concrete substrate, epoxy adhesive with sufficient bond strength is used. For strips, usually, epoxy is recommended, which is composed of resin and hardener to obtain high bond and tensile strength. Here, the specific mixing ratio between resin and hardener must be used according to the specification of the materials. After mixing the resin and hardener, within 80 % of the allowable working time (pot life), the FRP strips need to be applied (6). The epoxy pot life is usually less than 30 minutes, therefore, care should be considered in preparing all materials in place before mixing epoxy. The epoxy mixture should then be applied to the clean and prepared concrete surface and the FRP attached. Rolling equipment might be needed to ensure getting rid of all air bubbles from the interface.

Step 4: Curing and Finishing

After applying FRP, the construction site should be properly covered by plastic sheets for curing. When the epoxy is hardened, the site needs to be finished by casting a concrete cover. Latex modified concrete/mortar is recommended for batching the concrete cover for its significantly high bond strength compared to conventional concrete mortar and for its enhanced durability criteria. LMC is also known to have a low permeability making it a good alternative for protecting the CFRP strips. More detailed information about the procedure for the application of FRP strips and general consideration for design and application is presented in Reports (3) and (4).

REFERENCES

1. AASHTO. LRFD Bridge Design Specifications. *Manual for Condition Evaluation of Bridges*. American Association of State Highway and Transportation Officials. 2006 Interim revisions, Second Edition, Washington, D.C., 2006.

2. ACI 440 Committee. *Guide for the Design and Construction of Externally Bonded FRP Systems for Strengthened Concrete Structures*, ACI 440.2R-02, American Concrete Institute, Farmington Hills, MI, 2002.

3. Teng, J. G., J. F. Chen, S. T. Smith and L. Lam. *FRP Strengthened RC Structures*. First Edition. John Wiley and Sons, West Sussex, England, 2002.

4. ACI 318 Committee. *Building Code and Commentary*. ACI 318-05/318R-05, American Concrete Institute, Farmington Hills, MI, 2005.

5. CEB-FIP. Externally bonded FRP reinforcement for RC structures. TRB 14, 2001, p.124.

6. NCHRP Report 514. Bonded Repair and Retrofit of Concrete Structures using FRP Composites. *Recommended Construction Specifications and Process Control Manual*. Mirmiran, A., M. Shahawy, A. Nani and V. Karbahari, Eds., 2004.

7. De Lorenzis, L., A. Nanni. Characterization of FRP Rods as Near-Surface Mounted Reinforcement. *ASCE J. Composite for Construction*, Vol. 5, Issue 2, 2001, pp. 114-121.

8. De Lorenzis, L., J. G. Teng. Near-surface mounted FRP reinforcement: An emerging technique for strengthening structures. *Composites Part B: Engineering*, Vol. 38, No. 2, 2007, pp. 119-143.

NEW MEXICO DEPARTMENT OF TRANSPORTATION

RESEARCH BUREAU

Innovation in Transportation

Strengthening Reinforced Concrete Bridges in New Mexico Using Fiber Reinforced Polymers:

Report III: Implementation of FRP
Design Alternative to K-Frame Bridge

Prepared by:
University of New Mexico
Department of Civil Engineering
Albuquerque, New Mexico 87131

Prepared for:
New Mexico Department of Transportation
Research Bureau
7500B Pan American Freeway NE
Albuquerque, New Mexico 87109

In Cooperation with:
The US Department of Transportation
Federal Highway Administration

Report
NM06TT-01

MARCH 2008

Form DOT F 1700.7 (8-72)

1. Report No.	2. Government Accession No.	3. Recipient's Catalog No.
NM06TT-01		

4. Title and Subtitle	5. Report Date
Strengthening Reinforced Concrete Bridges in New Mexico Using Fiber Reinforced Polymers Report III: Implementation of FRP Design Alternative to K-Frame Bridge	March 2008
	6. Performing Organization Code
7. Author(s)	**8. Performing Organization Report No.**
M. M. Reda Taha, K. K. Choi, M. Azarbayejani	
9. Performing Organization Name and Address	**10. Work Unit No. (TRAIS)**
University of New Mexico Department of Civil Engineering Albuquerque, NM 87131	**11. Contract or Grant No.** CO4961
12. Sponsoring Agency Name and Address	**13. Type of Report and Period Covered**
Research Bureau New Mexico Department of Transportation 7500-B Pan American Freeway NE Albuquerque, NM 87109	**14. Sponsoring Agency Code**

15. Supplementary Notes

16. Abstract

The purpose of this research is to evaluate the structural capacity of concrete frame bridges #7930, 7931, 7937 and 7938 at Tucumcari, New Mexico and to evaluate their need for strengthening to meet AASHTO safety requirements. This report provides detailed information about the implementation and installation of FRP strengthening alternative to one K-Frame bridge. The selected strengthening alternative is analyzed and details about implementation requirements are discussed. All installation steps are discussed and documented. Finally, information is provided about two field tests performed prior to and after the application of the FRP strengthening. The two field tests targeted calibrating the analytical model using the finite element method and validating the efficiency of the FRP strengthening.

17. Key Words:	18. Distribution Statement
Concrete frame bridges, AASHTO LRFD Bridge Design Specification, Fiber reinforced polymers.	Available from NMDOT Research Bureau

19. Security Classif. (of this report)	20. Security Classif. (of this page)	21. No. of Pages	22. Price
None	None	29	

STRENGTHENING REINFORCED CONCRETE BRIDGES IN NEW MEXICO USING FIBER REINFORCED POLYMERS

Report III: Implementation of FRP Design Alternative to K-Frame Bridge

by

M. M. Reda Taha
K. K. Choi
M. Azarbayejani
University of New Mexico
Department of Civil Engineering

Prepared for:
New Mexico Department of Transportation, Research Bureau

A Report on Research Sponsored by:
New Mexico Department of Transportation, Research Bureau

In Cooperation with the
U.S. Department of Transportation, Federal Highway Administration

March 2008

NMDOT Research Bureau
7500-B Pan American Freeway NE
Albuquerque, NM 87109

PREFACE

The purpose of this research is to evaluate the structural capacity of the concrete frame bridges #7930, 7931, 7937 and 7938 at Tucumcari, New Mexico and evaluate their need for strengthening to meet AASHTO safety requirements. This report provides detailed information about the implementation and installation of FRP strengthening alternative to one K-Frame.

NOTICE

DISCLAIMER

ABSTRACT

The purpose of this research is to evaluate the structural capacity of concrete frame bridges #7930, 7931, 7937 and 7938 at Tucumcari, New Mexico and to evaluate their need for strengthening to meet AASHTO safety requirements. This report provides detailed information about the implementation and installation of FRP strengthening alternative to one K-Frame bridge. The selected strengthening alternative is analyzed and details about implementation requirements are discussed. All installation steps are discussed and documented. Finally, information is provided about two field tests performed prior to and after the application of the FRP strengthening. The two field tests targeted calibrating the analytical model using the finite element method and validating the efficiency of the FRP strengthening.

TABLE OF CONTENTS

FIGURES

FRP DESIGN ALTERNATIVE FOR EXTERIOR GIRDER OF BRIDGE 7937

According to the results of FE analyses performed in Report (1), it was found that all the girders of Tucumcari, New Mexico bridges 7930, 7931, 7937 and 7938 showed shortage in negative moment capacity around the K-Frame connections. It was therefore recommended to strengthen these four bridges' girders using Fiber Reinforced Polymer (FRP). The moment resistance to be provided by FRP is calculated as

$$M_u - \phi M_n \leq \phi M_{frp} \quad (1)$$

where:

M_u = factored applied moment

M_n = nominal moment-carrying capacity.

In ACI 440, ϕM_{frp} is evaluated as

$$\phi M_{frp} = \phi \varphi_{frp} A_f E_f \varepsilon_{fe} \cdot jd \quad (2)$$

where:

φ_{frp} = additional reduction factor (=0.85)

A_f = area of FRP reinforcement

ε_{fe} = effective ultimate strain developing at FRP

E_f = Young's modulus of FRP

jd = length of moment arm.

The ACI 440 design method for FRP strengthened sections is basically similar to ACI 318 design method, which is based on strain-compatibility and equivalent concrete stress block (refer to Fig. 1). In this design, it is assumed that the existing strain is negligible compared with ultimate design strains. Moreover, considering the fact that no tension cracks were observed in the top of the K-Frame in the field inspection before strengthening, the existing service strains can be considered negligible. Therefore, the effective strain of FRP at ultimate state is defined as

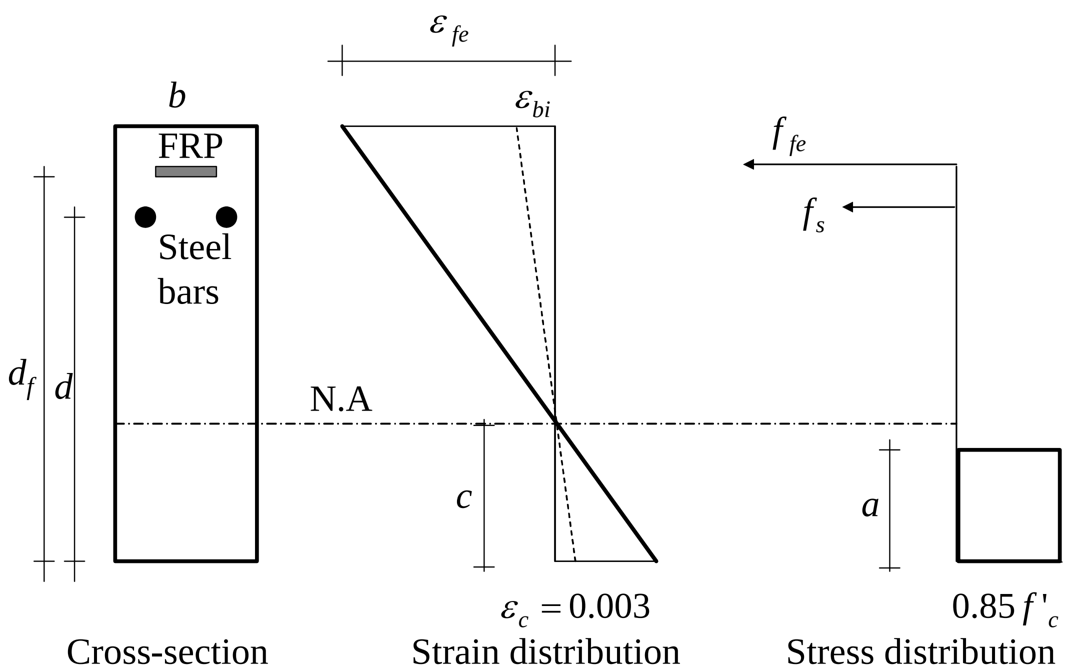

FIGURE 1 Stress and strain distribution of the concrete beam strengthened by FRP.

$$\varepsilon_{fe} = 0.003\left(\frac{d_f - c}{c}\right) \leq \kappa_m \cdot \varepsilon_{fu} \tag{3}$$

where:

d_f = effective depth for FRP reinforcement

c = depth of compression zone

κ_m = bond-dependent coefficient for flexure (=0.9 for Carbon Fiber Reinforced Polymer (CFRP) and Glass Fiber Reinforced Polymer (GFRP), ACI 440)

ε_{fu} = design rupture strain of the FRP reinforcement.

According to the results of Finite Element (FE) analyses, the exterior girder of bridge 7937, presented in Reports (1) and (2), the maximum shortage of negative moment capacity ($M_u - \phi M_c$) is 3,788 kN.m at the connection (x = 17 m). Please refer to Fig. 2.

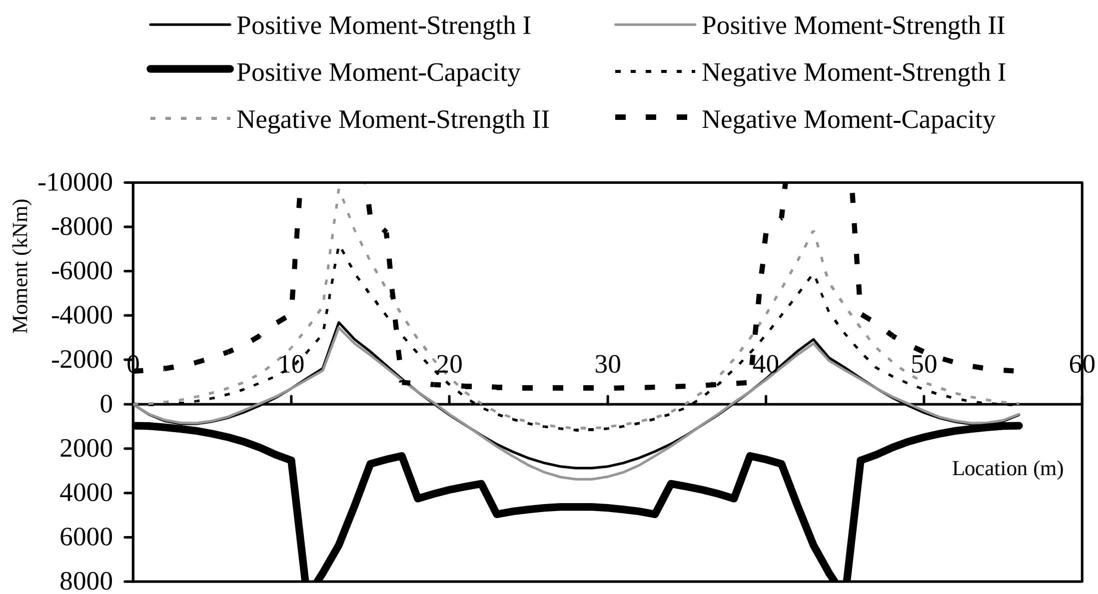

FIGURE 2 Factored moment and capacity of exterior beam of bridge 7937.

From Eqs. (2) and (3), the required amount of CFRP reinforcement can be evaluated as:

$$A_f = \frac{M_u - \phi M_c}{\kappa_m \cdot \varepsilon_{fu} E_f \phi \varphi_{frp} \cdot jd} = \frac{3788}{0.9 \cdot 0.0134 \cdot 150000 \cdot 0.85 \cdot 0.85 \cdot 0.9 \cdot 1.8} \times 1000 = 1789\, mm^2$$

CFRP was used (recommended in Report 2) for its enhanced strength and durability) with a Young's modulus of $E_f = 150{,}000\, MPa$ and an ultimate strain capacity of $\varepsilon_{fu} = 0.0134$. Moreover, it was assumed that the moment arm after application of FRP is *jd* to be *0.85d* . Based on the calculation, CFRP needed to be applied between x = 16.2 m (53 inch) and 20.1 m (66 inch). The required area of CFRP reinforcement was used for each K-Frame at both connections. In strengthening bridge 7937, one K-joint on one K-Frame only was reinforced for proof of method efficiency. The amount of CFRP reinforcement area required for strengthening one K-Frame at the K-connection on bridge 7937 was provided by means of 4 layers of CFRP strips, whose cross-section of CFRP strips is 1.52 mm thick (0.06 inch) and 305 mm (1 feet) wide. Since CFRP strips are not manufactured in 11 foot lengths to cover the entire application area, it was decided to overlap the CFRP strips using two 1.83 m (6 feet) CFRP strips.

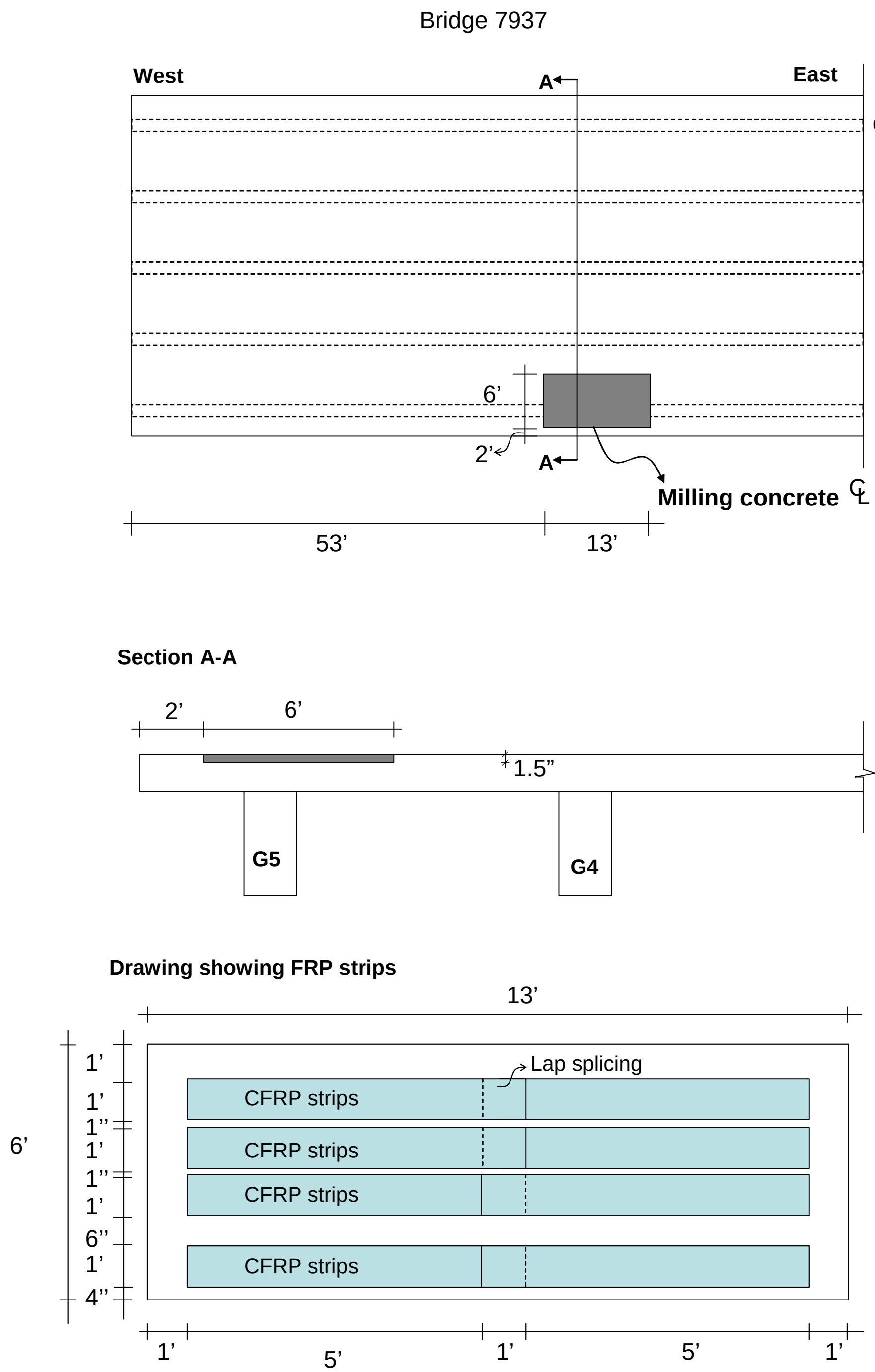

FIGURE 3 Schematic figure shows the layout of CFRP strips for strengthening the exterior girder of bridge 7937.

The CFRP strips were lap spliced to cover the entire strengthening zone. To ensure the performance of spliced CFRP strips, the lap splice location was alternated along the strengthening area such that no single section has more than 2 lap splices. This is shown in Fig. 3.

IMPLEMENTATION OF CFRP STRIPS TO EXTERIOR GIRDER OF BRIDGE 7937

Bridge 7937 was inspected and its concrete strength was evaluated. A structural analysis was performed (Report # 2) and the decision to strengthen one K-Frame connection on bridge 7937 was made. The bridge was to be strengthened using CFRP strips as shown in Fig. 3. Bridge strengthening preparation started on April 1st 2007 according to the original project schedule. The process continued between June 5th, 2007 and July 10th, 2007. The application of CFRP strips to an exterior girder of bridge 7937 as an example case for CFRP strengthening application was performed by the UNM research team, with the cooperation of New Mexico DOT in Tucumcari, New Mexico. It is worth noting that in the strengthening work of the bridge using CFRP strips, several different types of materials were used: putty, epoxy and CFRP. Therefore, the manufacturers' specifications of each material were considered in this installation. Moreover, the different material specifications were checked against the AASHTO (1) and ACI code requirements for CFRP materials.

Step 1: Concrete Surface Milling

As the bridge deck surface of the exterior girder of bridge 7937 was concrete, it needed to be milled to enable application of the CFRP strips. Approximately 1.5 inches of the concrete surface was milled according to the recommendation in Report (2). The milling process is shown in Fig. 4. The strengthening zone was marked first and then milled by a concrete milling machine attached to a wheel loader. The milled area was cleaned using air blowers and a construction vacuum as shown in Fig. 5. To obtain a surface with equal milling, the milling process was repeated twice.

FIGURE 4 Concrete surface milling showing the process of marking the zone and milling.

FIGURE 5 Concrete surface cleaning.

Step 2: Concrete Surface Preparation

The second step was to prepare the concrete surface. The procedure started by establishing an even surface with thickness differences less than 4 mm based on ACI 440 (2) and CEB-FIP code (3). Surface cracks formed due to the milling process were filled and the surface was made even. An even surface is essential to enable a good bond with the CFRP strips. To obtain an acceptable level of surface evenness, the concrete surface was first covered with a putty material in accordance with ACI 440 (1) and AASHTO (3) recommendations. The putty was applied to the application locations (Fig. 6) and then left to dry and bond to the concrete surface.

FIGURE 6 Application of putty material to obtain even concrete surface.

Here, several aspects need to be noted.

(3) Normally, putty material should be allowed to dry for a period dependent on the temperature at the time of application. The dry time will change significantly for low temperature versus high temperature application. Specifications by material manufactures should be carefully considered.

(4) The strengthening process was performed in June-July 2007, where high temperatures at the bridge site were observed (about 35 ^{o}C/90 ^{o}F). It was important to let the putty material dry for at least one week.

(5) If there are locations on the concrete surface where the putty application is too thick, the redundant putty needs to be removed before CFRP application.

Following the drying period, the concrete surface needs to be ground down to ensure evenness of the entire zone where CFRP will be applied. This process was performed using two different size grinding machines for overall and localized grinding as shown in Fig. 7(a) and 7(b) respectively. This step is very important for the application of CFRP strips because properly roughened and even concrete substrate is necessary for reliable performance of CFRP strips (4).

(a) Concrete grinder with double stone heads

(b) Concrete grinder with steel head

FIGURE 7 Concrete grinding.

Step 3: Application of CFRP Strips

After the concrete surface was ground and determined to not have any cracks, the epoxy adhesive was applied to bond the CFRP material. Epoxy is composed of resin and hardener in order to obtain the required bond and tensile strength. Epoxy 105 resin and slow hardener (206) produced by West System were used (Fig. 8). The epoxy resin was mixed as directed by the manufacturer At a mixing ratio (5 to 1) of resin to hardener. After mixing the resin and hardener to within 80 % of the allowable working time (pot life), the CFRP was applied (4). The pot life for the epoxy used was 20 to 25 minutes which represented enough time to lay down the CFRP strips on the locations identified on the bridge deck slab. Moreover, it is important to note that the epoxy hardening time is also a function of the temperature at time of mixing. The specifications by manufactures need to be considered carefully. During the hardening process (chemical reaction), epoxy becomes extremely hot, requiring special care by those applying it to the concrete surface.

FIGURE 8 Mixing resin and hardener according to specific mixing ratio.

Immediately after applying epoxy to the concrete surface, the CFRP strips were applied considering the locations marked and the lap splice alternating arrangement (Fig. 9). Here, because of the short pot life of the epoxy, it is recommended to mix enough resin and hardener to facilitate the application of one row of CFRP strips at a time.

FIGURE 9 CFRP strips attached to the concrete surface.

After applying the CFRP strips, proper pressure was applied to the CFRP for better attachment to the concrete surface (Fig. 10). Although not required the use of wood logs enabled uniform pressure distribution during the time of epoxy hardening.

FIGURE 10 Applying pressure for better attachment of CFRP strips.

Step 4: Curing and Finishing

After applying CFRP, the construction site was properly covered with plastic sheets to prevent exposure of the CFRP to rain and water. After the epoxy was fully hardened, on June 27th 2007, the construction site was covered by a cold dry asphalt mix. The asphalt mix was separated from the CFRP with a thick plastic sheet provided by NMDOT. The plastic sheet and the dry asphalt are shown in Fig. 11. The use of a dry asphalt mix was to prevent CFRP direct exposure to moisture, rain or traffic. This also enabled accessibility of the CFRP surface during the next phase of the project, which entailed the installation of monitoring sensors.

FIGURE 11 Construction zone covered with plastic sheets and dry asphalt mix.

ANALYSIS, VALIDATION OF FE MODELS AND CFRP EFFECTIVENESS

To validate the analytical prediction by FE analysis using SAP 2000®, a load test was performed before and after the application of CFRP strips. First, the concrete strain of the top of the exterior girder was monitored when subjected to a test truck (Fig. 12) with pre-determined weight. Detailed discussion on the calibration process is provided in Report 1. Moreover, strains on the top of the CFRP strips were monitored (after CFRP application) using the same test truck and weight. The ability of the CFRP strips to attain strain values in proportion with those strains observed at the concrete surface prior to strengthening ensured that the CFRP strips were properly attached to the concrete surface, they resisted the applied load and thus provide the needed strengthening for the K-Frame bridge. Fig. 13 shows the FE model of the exterior girder subjected to the truck load and the moment distribution obtained from the FE analysis. It is noted that in this analysis the bridge deck was taken into account in the calculation of effective width of the girder assuming elastic behavior during the loading test. This can be justified by the fact that the load of the test truck was significantly lower than the load carrying capacity of the bridge and thus the bridge behavior can be considered to follow linear elastic behavior.

FIGURE 12 Mack 10 yard dump truck as test truck with weight of 50 kips.

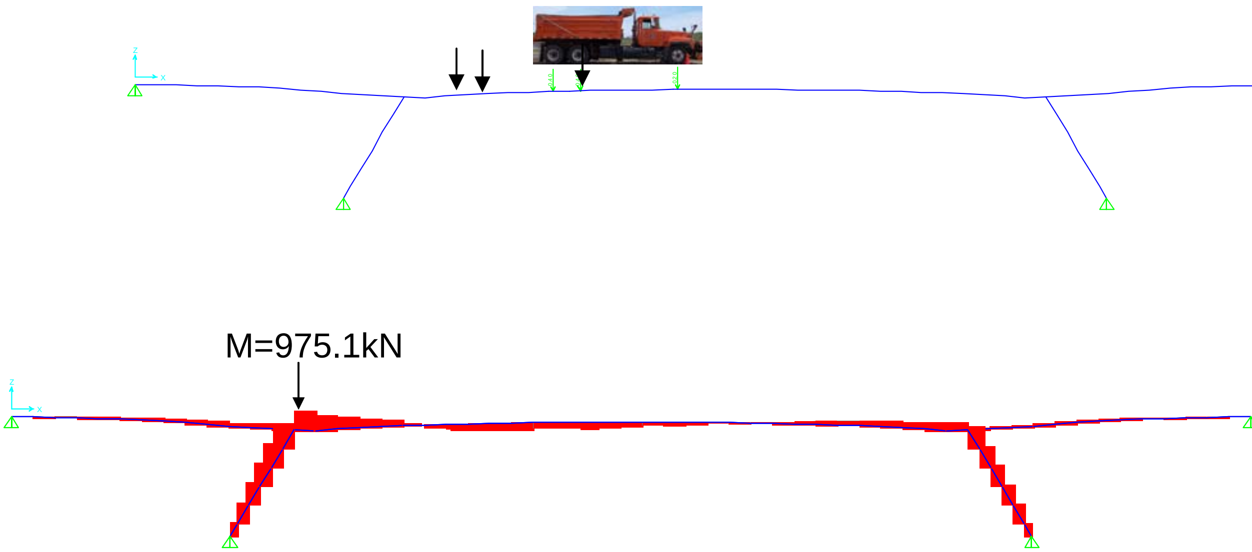

FIGURE 13 FE model of exterior girder subjected to truck load, and moment distribution throughout girder.

To compensate for the temperature effect, orthogonal strain gauges were placed as dummy gauges. The longitudinal gauges were used to measure the load effect and the dummy strain gauges were used to compensate temperature effects. The locations of strain gauges are shown in Fig. 14. The strain gauge on the top of concrete (prior to strengthening) and a dummy orthogonal gauge at this location are shown in Fig. 15. Moreover, strain gauges over the CFRP surface are shown in Fig. 16. User friendly data acquisition software under LabVIEW (4) programming environment was developed and used for measuring strain gauges on the concrete surface prior to CFRP strengthening and on the CFRP surface after strengthening. The strain gauges were connected to the data acquisition system which was connected to a Laptop computer (Fig. 17). Finally, a snap shot of the LabVIEW software for data analysis is shown in Fig. 18. The data acquisition system along with the developed LabVIEW software enabled observing and analyzing the data in the field during the load test.

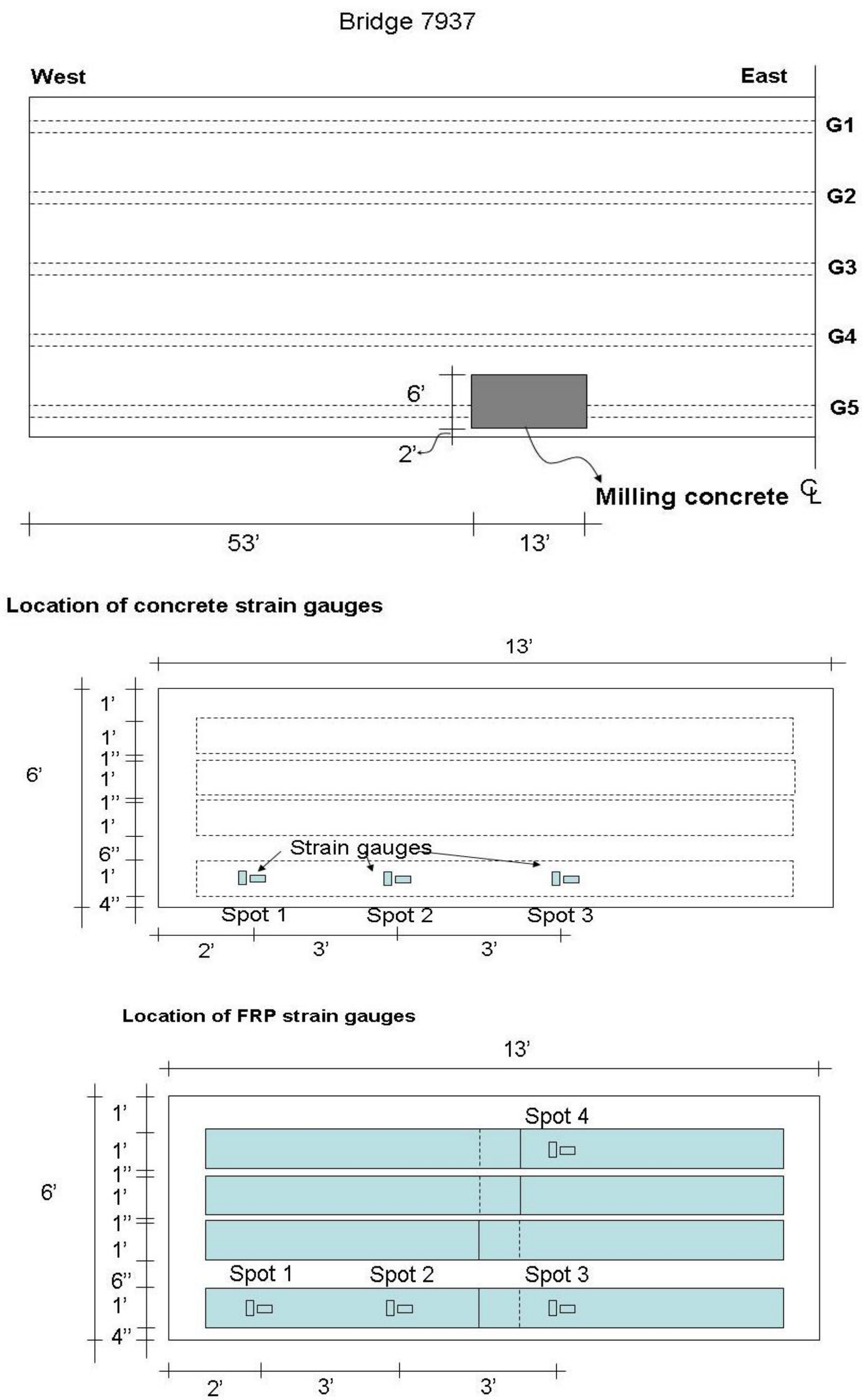

FIGURE 14 Schematic figure showing the location of strain gauges.

FIGURE 15 Concrete strain gauges attached to the concrete surface.

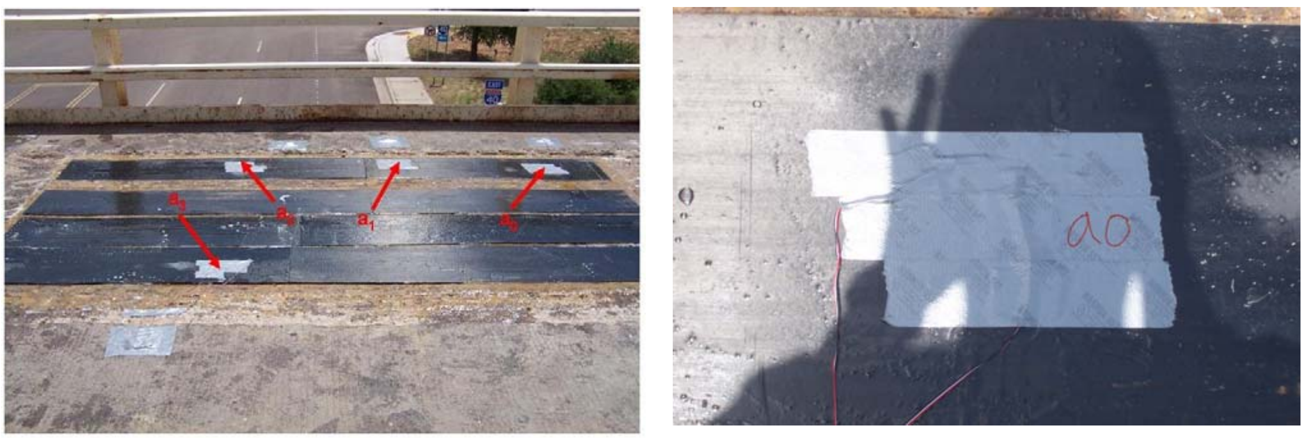

FIGURE 16 Strain gauges attached to CFRP strips.

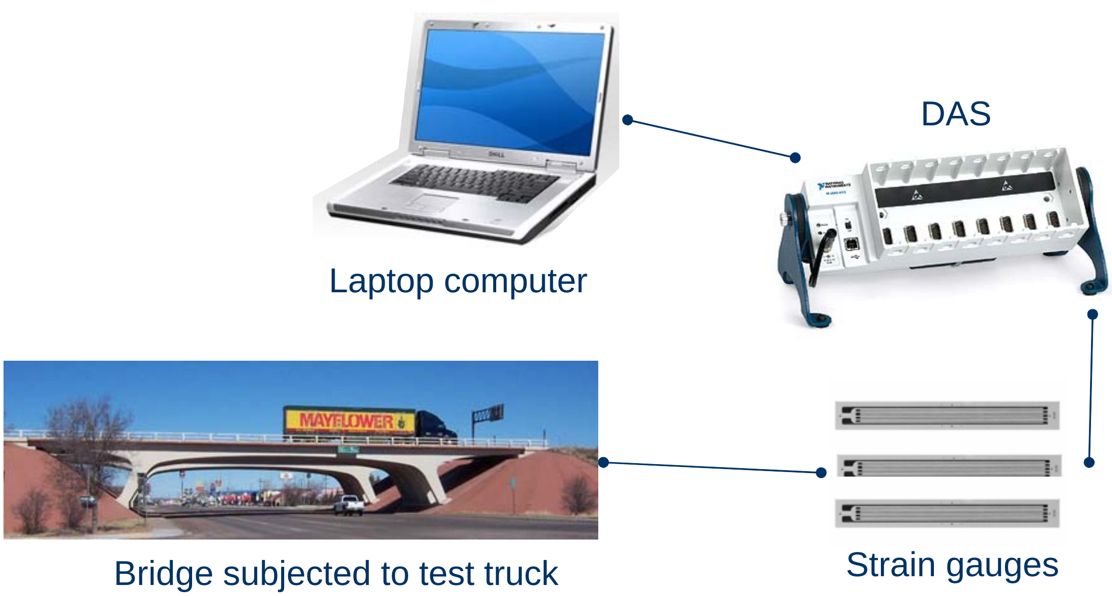

FIGURE 17 Data acquisition system and laptop computer used for data acquisition.

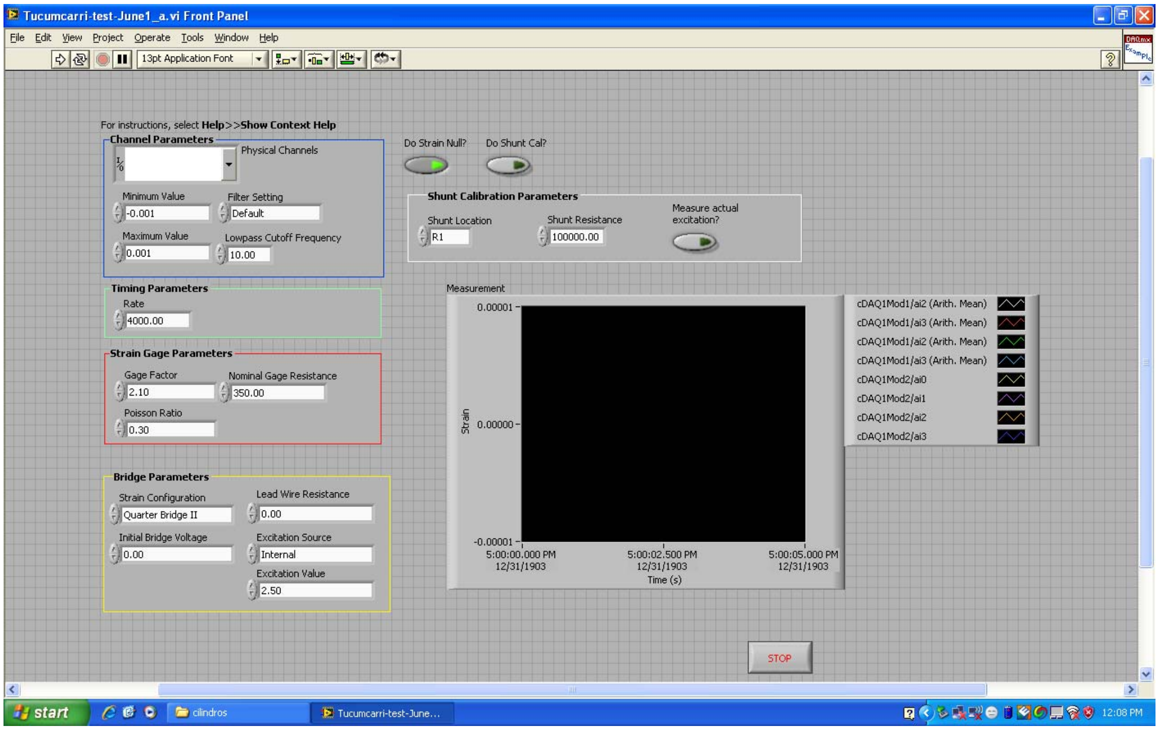

FIGURE 18 Snap shot of LabVIEW user-friendly software developed by research team and used for strain measurements based on dual strain measurements at each sensing location.

Here, a comparison of the strain measurements observed at spot 1 in Fig. 14 with that predicted by calibrated FE analysis was done. The strain measurements on the concrete surface prior to strengthening are shown in Fig. 19. It can be observed that under the designated test truck, 21.7 $\mu\varepsilon$ ($\mu\varepsilon$ = micro strain) was recorded as the maximum strain on the concrete surface. This number is very close to the maximum predicted strain on concrete surface of 23.2 $\mu\varepsilon$ predicted from the FE analysis. Similar FE predicted strains were confirmed by measurements at other locations of the bridge deck. These results validate the finite element model of the K-Frame bridge presented here and in Report 2. Validation of the finite element model was an essential step when designing the CFRP strengthening system. Fig. 19 shows the change in the strain at spot 1 as the truck was proceeding towards the construction/strengthening location at the K-Frame joint.

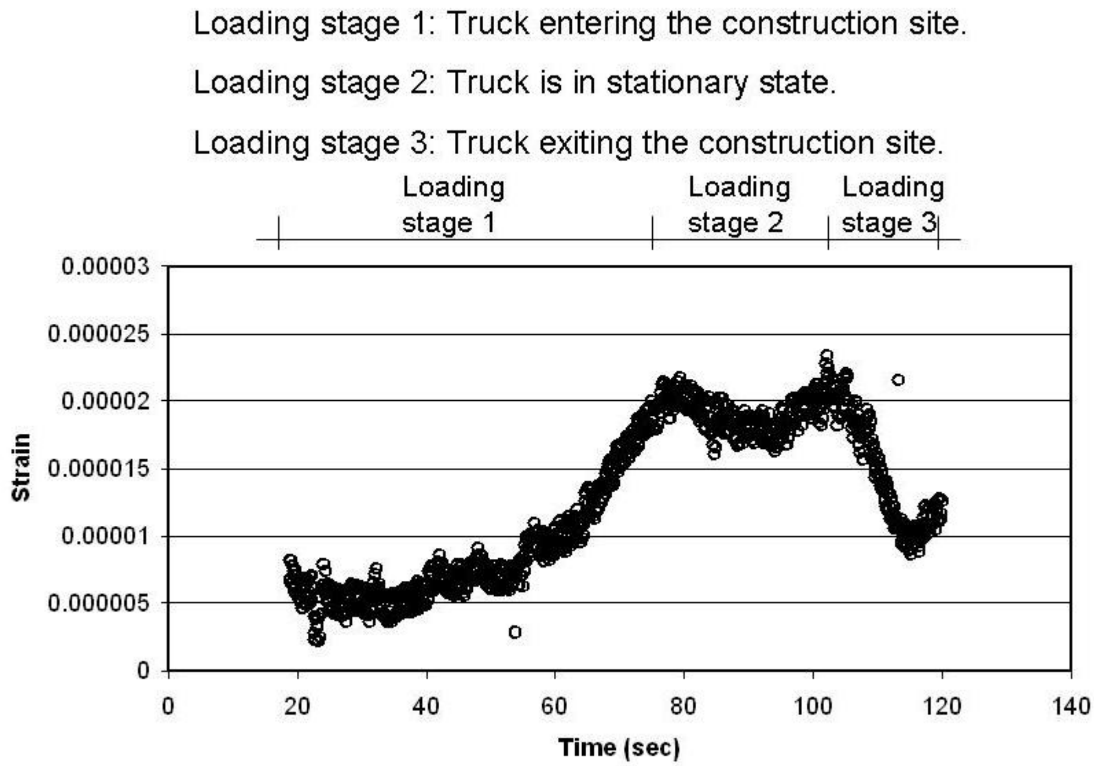

FIGURE 19 Strain measurements at spot 1 on concrete surface prior to strengthening.

The FE model was used to determine the strain in the CFRP strips after strengthening. The FE model predicted that the maximum strain in the CFRP strips for the test truck load should not exceed 23.2 $\mu\varepsilon$. Strains monitored using strain gauges glued above the CFRP strips at the second load-test observed strains on the CFRP strips changing with the motion of the test-truck along the bridge as shown in Fig. 22. The maximum observed strain on the CFRP surface was 20.5 $\mu\varepsilon$ which is close to the strains predicted from the FE analysis.

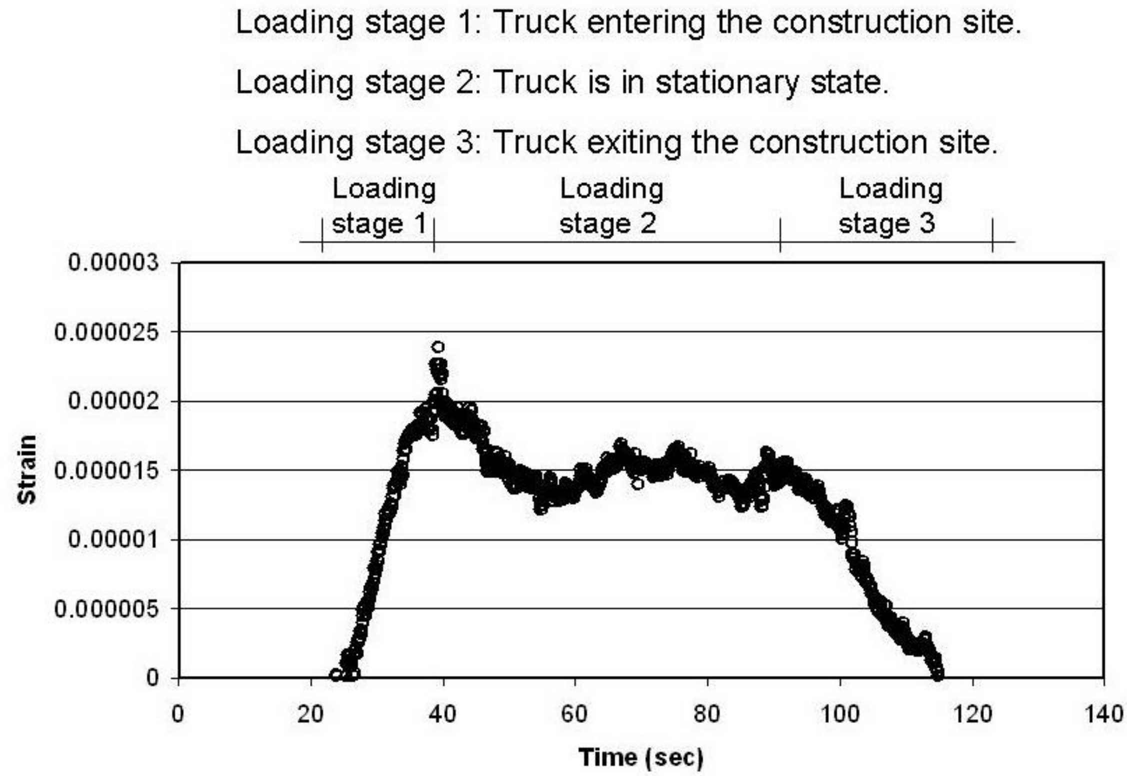

FIGURE 20 Strain measurements at spot 1 on CFRP surface after strengthening.

Moreover, the close proximity of both strains measured on the bridge surface prior to and after strengthening (20.5 $\mu\varepsilon$ on CFRP surface) and (21.7 $\mu\varepsilon$ in concrete prior to strengthening) under the same test truck load indicated the efficiency of the CFRP and its ability to resist the tensile stresses due to the test truck. Considering the strain compatibility, it was concluded that the CFRP strips are well attached to the concrete surface and will be able to enhance the girder carrying capacity. The load tests confirmed the objectives by enabling validation of the FE models and thus ensuring proper design of the strengthening system. It also confirmed the good bond between the CFRP strips and the K-Frame concrete surface and thus the ability of the CFRP strips to work as externally bonded reinforcement that are capable of enhancing the bridge carrying capacity.

SECOND FIELD TEST (FEB. 2008)

A second field test was organized and performed after 6 months of the CFRP strip applications. The field test was conducted on in February 2008 by the University of New Mexico team. New strain gauges were installed on CFRP strips and 4 new measurements were collected. It was interesting to note that that almost all the strain gauges installed on July 2007 were still operational. The following steps clarify this field test in more details.

Step 1: Cleaning the surface and investigate the conditions of CFRP strips

Fig. 21 shows the site before and after cleaning process.

FIGURE 21 CFRP strips before and after cleaning.

Step 2: Installing New Strain Gauges

The new strain gauges were installed on CFRP strips to get more measurements at different locations on CFRP strips. Fig. 22 illustrates the process of installing strain gauges. Fig. 23 shows the location of all strain gauges installed on CFRP strips schematically.

FIGURE 22 Installing new strain gauges.

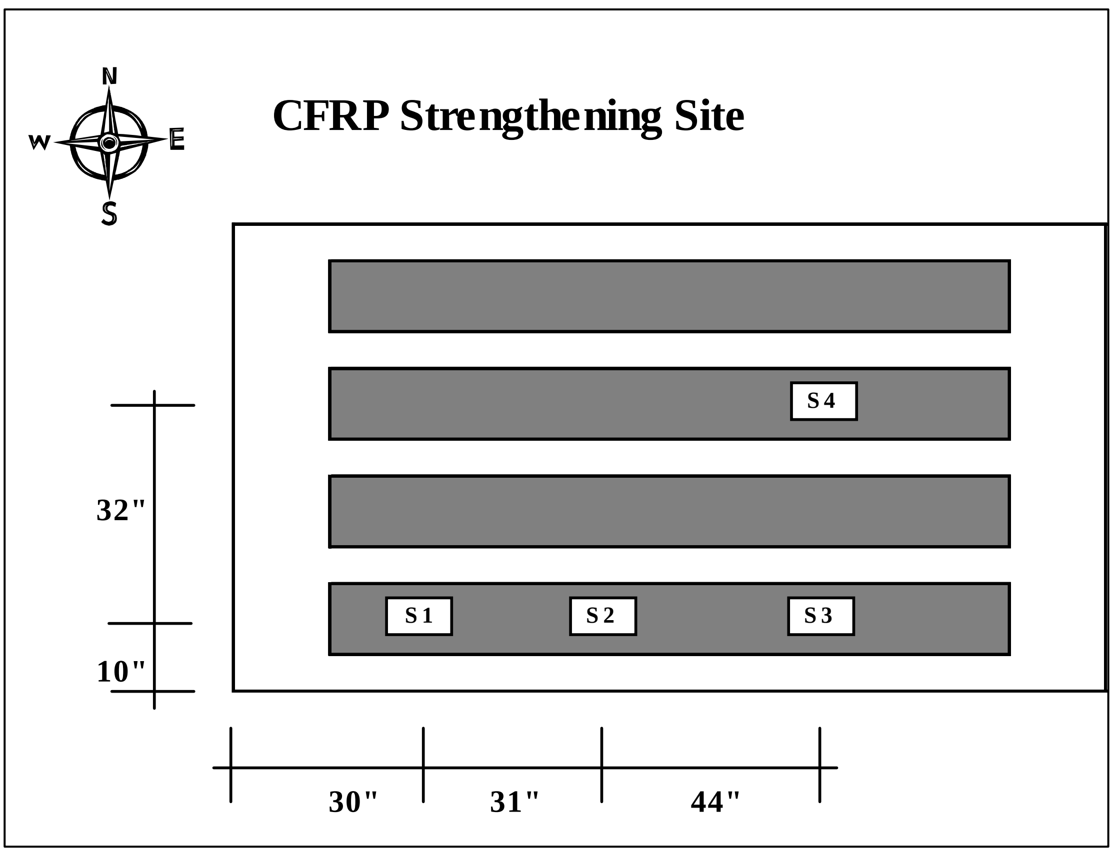

FIGURE 23 Location of strain gauges on CFRP strips.

Step 3: Load Test to Validate the Efficiency of CFRP Strips

After the installation of new strain gauges on CFRP strips, old and new strain gauges were connected to a data acquisition system. Using a 50 kips truck provided by NMDOT, new measurements were collected to demonstrate the efficiency of the CFRP strips in carrying load. Based on truck position at the field test, the FE model calibrated using concrete strain data (Report 1) was used to predict the strain in the CFRP strips. Predicted strains using the SAP 2000® FE model were then compared with the field test measurements. The new FE model is shown in Fig. 24. The strains were calculated at the location of strain gauges. Fig. 25 represents the strains at the locations shown in Fig. 23 based on different truck positions in the FE model. It should be noted that strain gauges 3 and 4 show the same results in the 2D FE model of the bridge girder because they are located at the same distance from the moving truck but at two different distances from the edge of the deck slab.

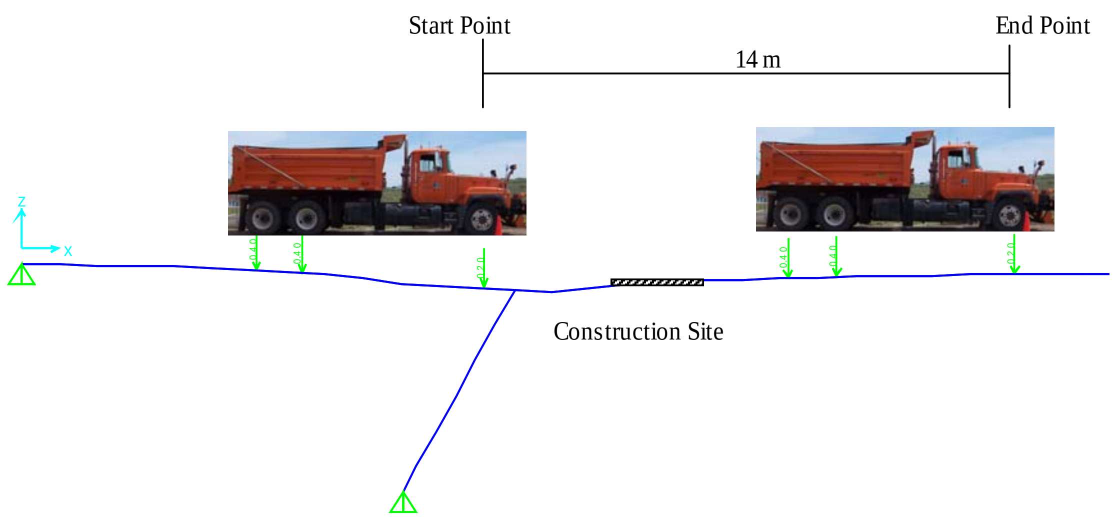

FIGURE 24 FE model based on the truck position in the field test.

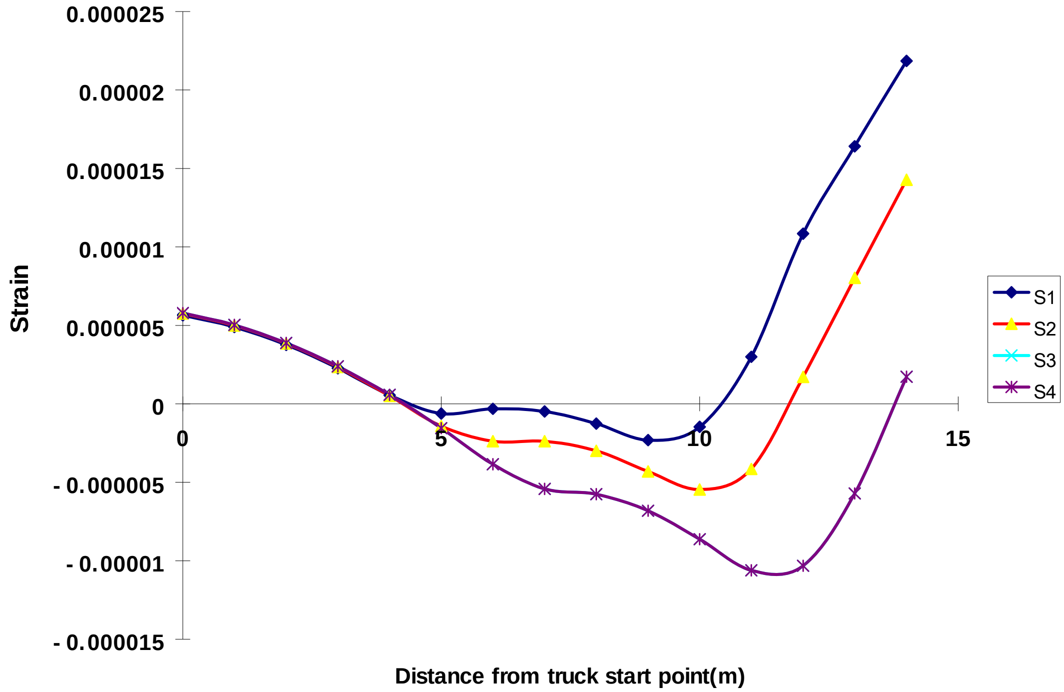

FIGURE 25 Strains predicted from SAP 2000 FE model at strain gauges locations.

VALIDATION

To validate the efficiency of the CFRP strips, a comparison between the strains from FE model and the strains collected in the site were made at four strain gauge locations. Figs 26, 27, 28 and 29 illustrate the strains predicted from FE model and measured from the field tests at strain gauges S1, S2, S3 and S4. The strains predicted from the FE model were similar to the strains collected from the field test as the truck moved along the bridge. The strains measured at the CFRP strips confirm complete bond between concrete surface and CFRP strips which indicates the ability of the CFRP strips to enhance the bridge carrying capacity.

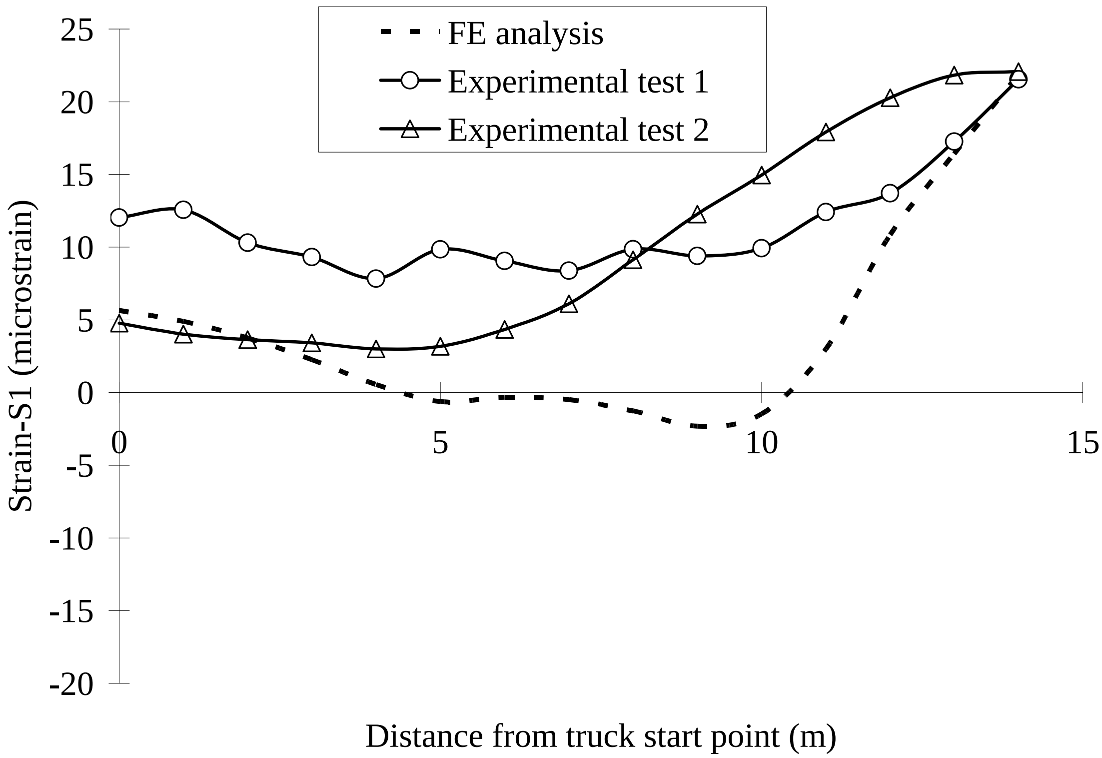

FIGURE 26 Strains calculated from FE model and field test at strain gauge 1 on CFRP strips.

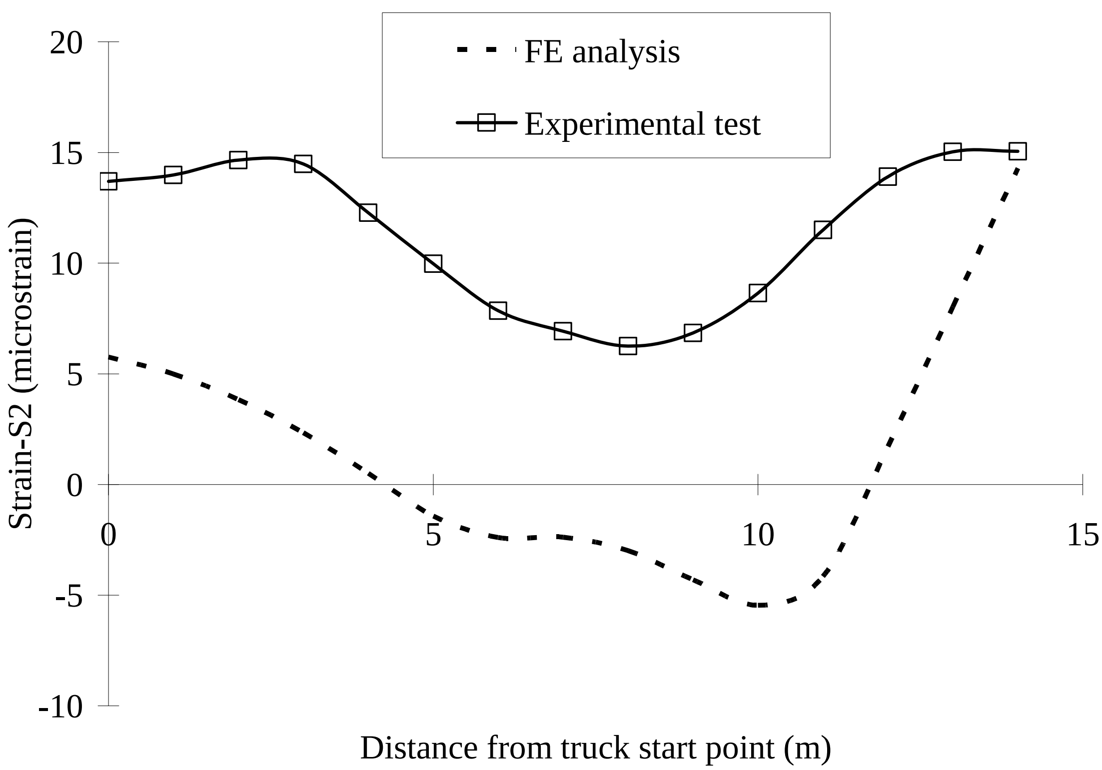

FIGURE 27 Strains calculated from FE model and field test at strain gauge 2 on CFRP strips.

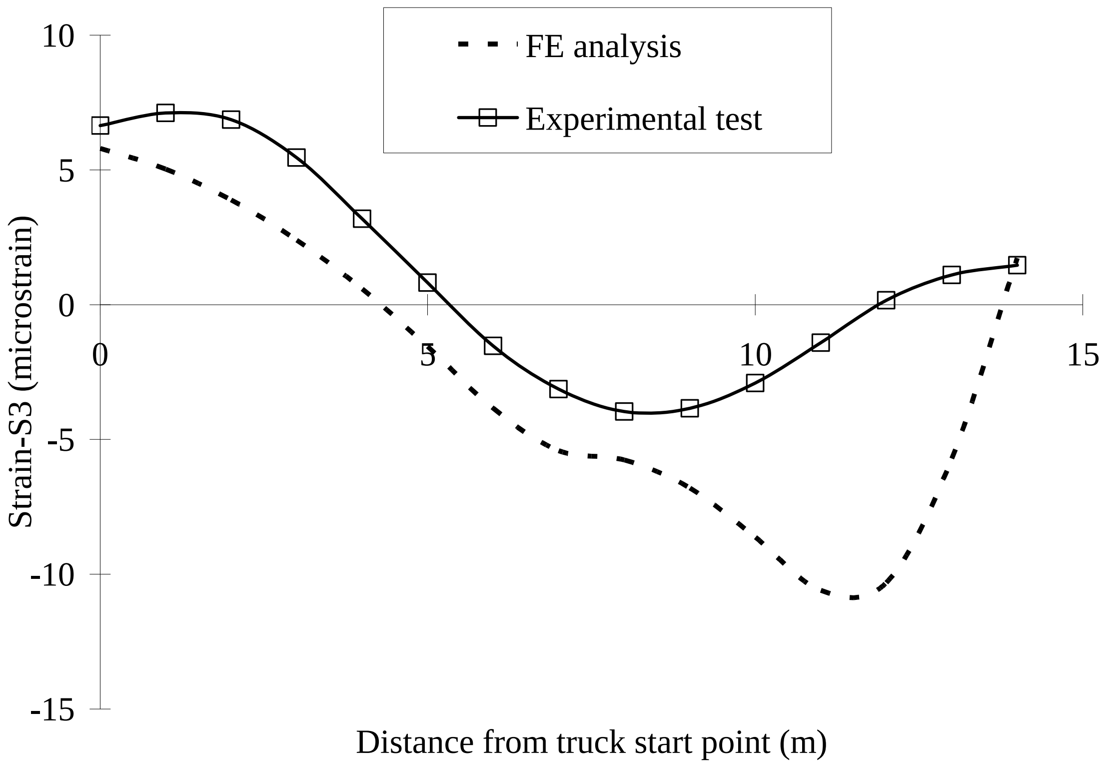

FIGURE 28 Strains calculated from FE model and field test at strain gauge 3 on CFRP strips.

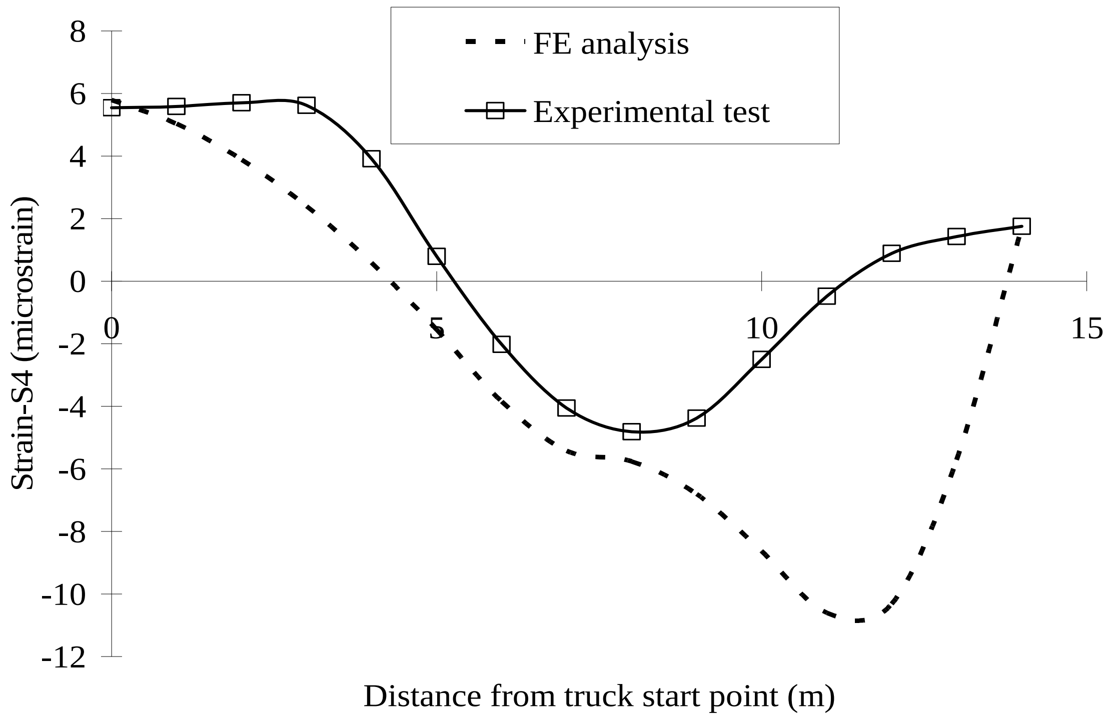

FIGURE 29 Strains calculated from FE model and field test at strain gauge 4 on CFRP strips.

RECOMMENDATION

Based on the above analysis and test observations, it is recommended that similar strengthening using CFRP should be applied to all four K-joints of the K-Frame bridges in Tucumcari, New Mexico bridges 7930, 7931, 7937 and 7938 once funding for such bridge enhancement becomes available.

REFERENCES

1. AASHTO. LRFD Bridge Design Specifications. *Manual for Condition Evaluation of Bridges*. American Association of State Highway and Transportation Officials. 2006 Interim Revisions, Second Edition, Washington, D.C., 2006.

2. ACI 440 Committee. *Guide for the Design and Construction of Externally Bonded FRP Systems for Strengthened Concrete Structures*, ACI 440.2R-02, American Concrete Institutes, Farmington Hills, MI, 2002.

3. CEB-FIP. Externally bonded FRP reinforcement for RC structures. TRB 14, 2001, p. 124.

4. National Instruments. LabVIEW Fundamentals, 2005.

5. ACI 318 Committee. Building Code and Commentary. ACI 318-05/318R-05, 2005.

NEW MEXICO DEPARTMENT OF TRANSPORTATION

RESEARCH BUREAU

Innovation in Transportation

Strengthening Reinforced Concrete Bridges in New Mexico Using Fiber Reinforced Polymers:

Report IV: Guidelines for Using FRP Technology for Strengthening Bridges

Prepared by:
University of New Mexico
Department of Civil Engineering
Albuquerque, NM 87131

Prepared for:
New Mexico Department of Transportation
Research Bureau
Albuquerque, NM 87109

In Cooperation with:
The US Department of Transportation
Federal Highway Administration

Report NM06TT-01

MARCH 2008

STRENGTHENING REINFORCED CONCRETE BRIDGES IN NEW MEXICO USING FIBER REINFORCED POLYMERS: A COMPILATION OF FOUR REPORTS

I. Structural Analysis and Evaluation of Bridges 7930, 7931, 7937 and 7938 in Tucumcari

II. Design Method for Strengthening K-Frame Bridges Using FRP

III. Implementation of FRP Design Alternative to K-Frame Bridge

IV. Guidelines for Using FRP Technology for Strengthening Bridges

by

M. M. Reda Taha
K. K. Choi
M. Azarbayejani
University of New Mexico
Department of Civil Engineering

Prepared for:
New Mexico Department of Transportation, Research Bureau

A Report on Research Sponsored by:
New Mexico Department of Transportation, Research Bureau

In Cooperation with the
U.S. Department of Transportation, Federal Highway Administration

March 2008

NMDOT, Research Bureau
7500-B Pan American Freeway NE
Albuquerque, NM 87109

Form DOT F 1700.7 (8-72)

1. Report No.	2. Government Accession No.	3. Recipient's Catalog No.
NM06TT-01		

4. Title and Subtitle	5. Report Date
Strengthening Reinforced Concrete Bridges in New Mexico Using Fiber Reinforced Polymers Report I: Structural Analysis and Evaluation of Bridges (7930, 7931, 7937 and 7938) in Tucumcari	March 2008 6. Performing Organization Code
7. Author(s) M. M. Reda Taha, K. K. Choi, M. Azarbayejani	8. Performing Organization Report No.
9. Performing Organization Name and Address University of New Mexico Department of Civil Engineering Albuquerque, NM 87131	10. Work Unit No. (TRAIS) 11. Contract or Grant No. CO4961
12. Sponsoring Agency Name and Address Research Bureau New Mexico Department of Transportation 7500-B Pan American Freeway NE Albuquerque, NM 87109	13. Type of Report and Period Covered 14. Sponsoring Agency Code

15. Supplementary Notes

16. Abstract

The objective of this report is to provide detailed evaluation of the structural capacity of the concrete frame bridges #7930, 7931, 7937 and 7938 at Tucumcari, New Mexico and evaluate their need for strengthening. Finite Element (FE) analysis using SAP 2000® was performed to estimate the moment and shear force demand and compare it to the existing capacity of the four bridges on I-40 at Tucumcari. The structural analysis and the strength evaluation were performed according to ASSHTO LRFD Bridge Design Specification with 2006 Interim Revision (AASHTO 2006).
The investigations showed that the four bridges do not meet the AASHTO requirements and need strengthening. The structural evaluation showed that the four bridges require strengthening at the top side (negative moment side) of the K-Frame joint. The report provides detailed information about the locations that require strengthening.

17. Key Words:	18. Distribution Statement
Concrete frame bridges, AASHTO LRFD Bridge Design Specification, Fiber reinforced polymers.	Available from NMDOT Research Bureau

19. Security Classif. (of this report)	20. Security Classif. (of this page)	21. No. of Pages	22. Price
None	None	54	

PREFACE

The purpose of this research is to evaluate the structural capacity of the concrete frame bridges #7930, 7931, 7937 and 7938 at Tucumcari, New Mexico and evaluate their need for strengthening to meet AASHTO safety requirements.

NOTICE

DISCLAIMER

ABSTRACT

The objective of this report is to provide detailed evaluation of the structural capacity of the concrete frame bridges #7930, 7931, 7937 and 7938 at Tucumcari, New Mexico and evaluate their need for strengthening. Finite Element (FE) analysis using SAP 2000® was performed to estimate the moment and shear force demand and compare it to the existing capacity of the four bridges on I-40 at Tucumcari. The structural analysis and the strength evaluation were performed according to ASSHTO LRFD Bridge Design Specification with 2006 Interim Revision (AASHTO 2006).

The investigations showed that the four bridges do not meet the AASHTO requirements and need strengthening. The structural evaluation showed that the four bridges require strengthening at the top side (negative moment side) of the K-Frame joint. The report provides detailed information about the locations that require strengthening.

TABLE OF CONTENTS

Report I: Structural Analysis and Evaluation of Bridges 7930, 7931, 7937 and 7938 in Tucumcari

TABLES

FIGURES

OBJECTIVE

The objective of this report is to provide details regarding the process of evaluation of the structural capacity of the concrete frame bridges 7930, 7931, 7937 and 7938 at Tucumcari and evaluate their need for strengthening. Finite Element (FE) analysis using SAP 2000® was performed to estimate the moment and shear force demand and compare it to the existing capacity of the four bridges on I-40 at Tucumcari. The structural analysis and the strength evaluation were performed according to ASSHTO LRFD Bridge Design Specification with 2006 Interim Revision (1).

DESCRIPTION OF BRIDGES

Bridges 7930, 7931, 7937 and 7938 at Tucumcari are four reinforced concrete K-Frame bridges located on Interstate I-40. Photos representing the four bridges are presented in Fig. 1 to Fig. 6. The four bridges have similar configurations and material properties as shown by their structural plans (Figs. 7 to 8). Each bridge consists of 5 to 6 K-frames (Bridge 7930 is composed of six reinforced concrete K-frames whiles the others three bridges 7931, 7937 and 7938 are composed of reinforced concrete 5 K-frames), reinforced concrete transverse beams, and a reinforced concrete deck. Asphalt overlay was used on bridges 7937 and 7938 while 7930 and 7931 did not have asphalt. It was noted that bridge 7931 was skewed by 7 degrees. Each K-frame has a rectangular-shaped cross-section the depth of which varies along the length of the bridge. Moreover, the longitudinal and transverse reinforcements vary along the length of the bridge.

During the last two decades since the bridges were constructed, the size and weight of trucks passing over I-40 increased dramatically. Therefore, it is expected that the moment and shear demand by the current traffic according to AASHTO 2006 (1) might exceed the bridge capacity. Our analysis aimed at investigating the moment and shear capacity of the four bridges compared to the current traffic loads according to AASHTO 2006 (1).

FIGURE 1 Tucumcari bridge 7930.

FIGURE 2 Tucumcari bridge 7931.

FIGURE 3 Tucumcari bridge 7937.

FIGURE 4 Tucumcari bridge 7938.

FIGURE 5 Tucumcari bridge 7930 showing tension cracking at the bottom of the deck at the K-frame connection.

FIGURE 6 Supporting condition at the end of the girder of bridge 7937.

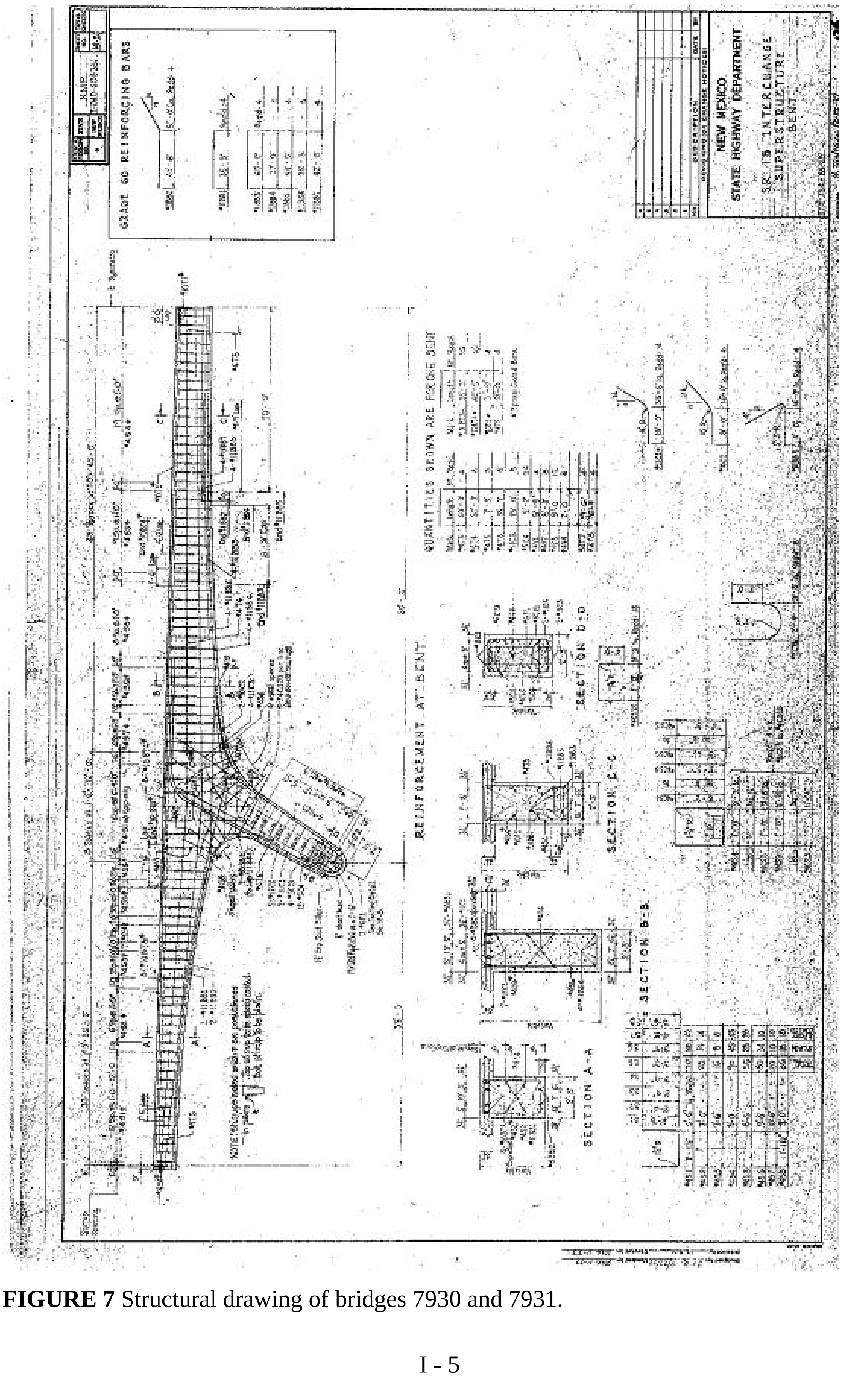

FIGURE 7 Structural drawing of bridges 7930 and 7931.

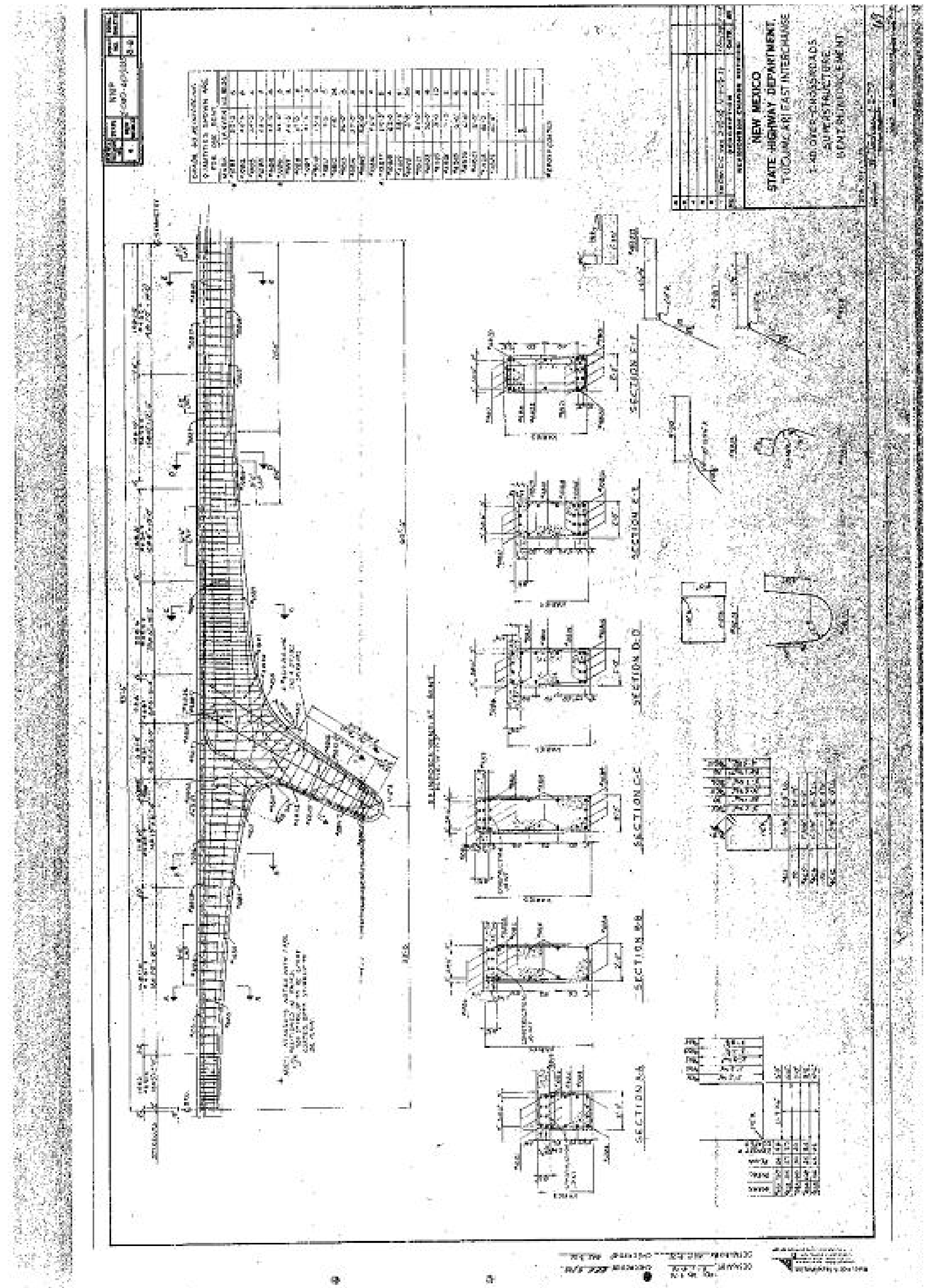

FIGURE 8 Structural drawing of bridges 7937 and 7938.

BRIDGE LOADING

Four different types of New Mexico Legal trucks were used in the FE analysis, in addition to Design truck by AASHTO and Tandem load. These four trucks included NMDOT Two-Axle Legal load truck, NMDOT Three-Axle Legal load truck, NMDOT Five-Axle Legal load truck, and NMDOT Permit truck P327-B. Characteristics of each truck including axle loading are presented in Fig. 9. Moreover, the distance between the two 145,000N axles in the AASHTO design truck was used as a variable from 4.3 m to 9.0 m as specified in AASHTO (1).

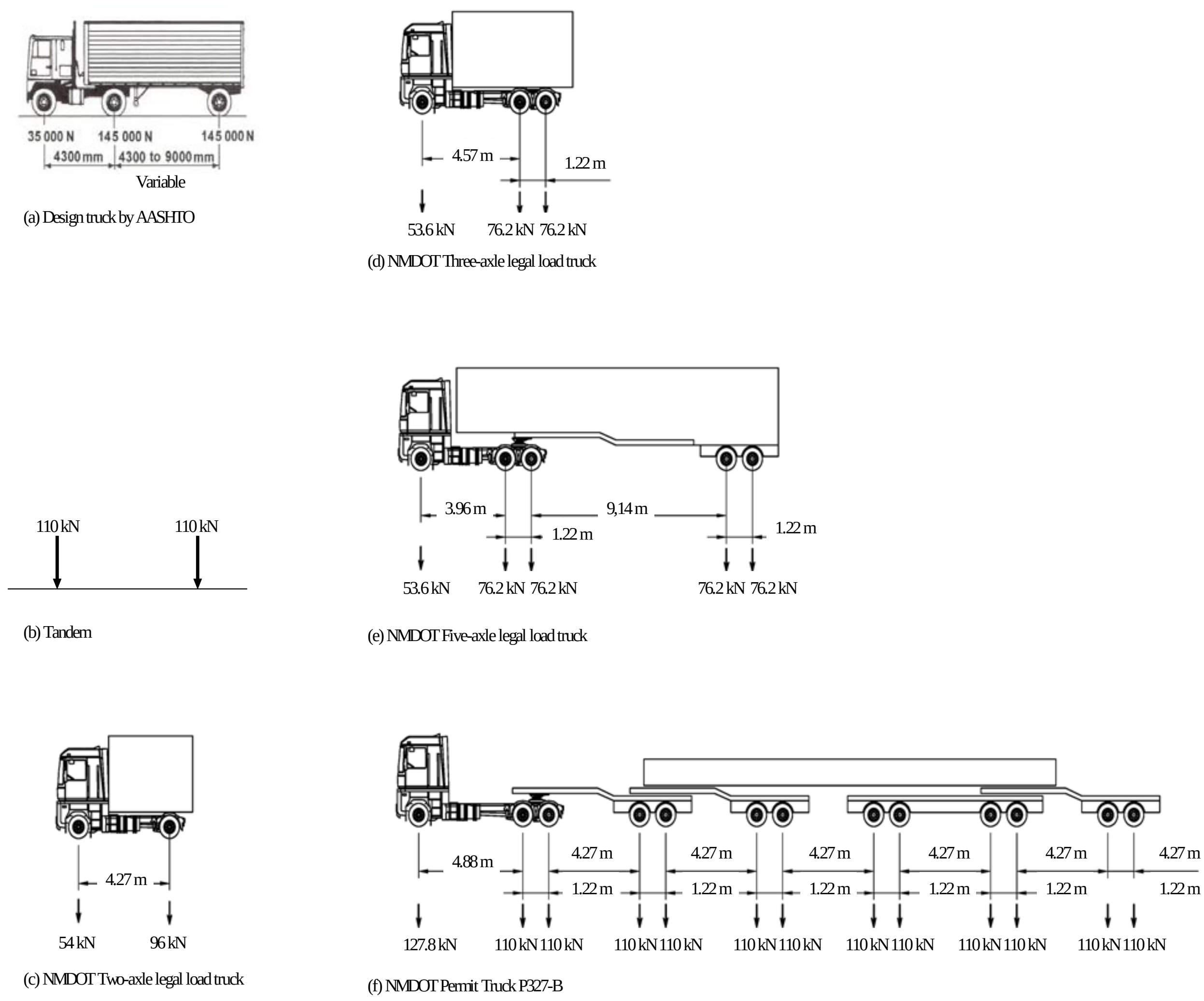

FIGURE 9 Characteristics of trucks used in FE analysis.

Furthermore, a 9.3 kN/m, uniformly distributed design lane load in the longitudinal direction was also considered as specified by AASHTO (1). The dynamic load allowance was computed to be (1.33) and was applied to the truck and tandem loads to consider the dynamic effect of traffic load. Finally, dead loads including self weight of the K-frames, concrete deck weight, rail load and asphalt weight were also included in the FE analysis.

LIVE LOAD DISTRIBUTION

In computing the total load on each K-frame bridge, traffic (live) load distribution between the frames needed to be calculated. The load distribution factors of the exterior and interior frames were computed separately. According to AASHTO (1), for exterior frames, the load distribution factors for moment and shear can be simply defined by using Eq. (1).

$$R = \frac{N_L}{N_b} + \frac{X_{ext} \sum^{N_L} e}{\sum^{N_L} x^2} \tag{1}$$

where

R = reaction on exterior beam in terms of lanes

N_L = number of loaded lanes under consideration

e = eccentricity of a design truck or a design lane load from the center of gravity of the pattern of frames (mm)

x = horizontal distance from the center of gravity of the pattern of frames to each frame (mm)

X_{ext} = horizontal distance from the center of gravity of the pattern of frames to the exterior frame (mm)

N_b = number of beams of frames.

The width of bridges 7930, 7931, 7937 and 7938 is 14.22 m, 11.78 m, 11.38 m, and 11.38 m, respectively. Therefore, four design lanes for bridge 7930 and three design lanes for the other bridges needed to be considered. Moreover, for exterior frames, the multiple presence factors m needed to be applied to address the effect of multiple presence of live load. The multiple presence factors are defined in Table 1 according to AASHTO (1). Finally, the load distribution factor is determined as a maximum value among the product of R [Eq. (1)] and m values (Table 1) using different N_L values.

TABLE 1 Multiple presence factors *m*.

Number of loaded lanes, N_L	Multiple presence factors *m*
1	1.20
2	1.00
3	0.85
> 3	0.65

For interior beams, the load distribution factors for moment and shear can be defined by Eqs. (2) and (3) respectively.

<u>*For moment*</u>

One design lane loaded

$$R = 0.06 + \left(\frac{S}{4300}\right)^{0.4}\left(\frac{S}{L}\right)^{0.3}\left(\frac{K_g}{Lt_s^3}\right)^{0.1} \tag{2a}$$

Two or more design lane loaded

$$R = 0.075 + \left(\frac{S}{2900}\right)^{0.6}\left(\frac{S}{L}\right)^{0.2}\left(\frac{K_g}{Lt_s^3}\right)^{0.1} \tag{2b}$$

For shear

One design lane loaded

$$R = 0.36 + \frac{S}{7600} \tag{3a}$$

Two or more design lane loaded

$$R = 0.2 + \frac{S}{3600} - \left(\frac{S}{10700}\right)^{2.0} \tag{3b}$$

where:

S = spacing of supporting components (mm)

L = span length of deck (mm)

K_g $[= n(I + Ae_g{}^2)]$ = longitudinal stiffness parameter (mm^4)

n = ratio between modulus of elasticity of beam material and modulus of elasticity of deck material

I = moment of inertia of beam

e_g = distance between the centers of gravity of the basic beam and deck (mm)

t_s = depth of concrete slab (mm).

As defined in Eq. (4), the load distribution factor of interior beams may vary according to its location along the length of the beams because the depth of beams varies along the length of the beams. It is also noted that the multiple presence factors need not be applied to interior beams because Eq. (4) already considers such multiple presence effect.

Finally, the skew of bridge 7931 needs to be considered in the load calculation. In such case, the load distribution factor needs to be revised by the following correction factor.

$$1.0 + 0.2\left(\frac{L{t_s}^3}{K_g}\right)^{0.3} \tan\theta \qquad (4)$$

where θ = skew angle.

FINITE ELEMENT (FE) ANALYSIS

Static structural analysis was performed for the four K-frame bridges. Considering the diaphragm action of bridges due to transverse beams and deck, each K-frame was analyzed as a separate frame instead of using an entire bridge model. Then, the load distribution between each frame was considered by using load distribution factors described above. Since the dead load (deck, asphalt, and bar railing load) was different in interior and exterior girders, two finite element models for each bridge were developed: one mode for interior frames and one model for exterior frames.

In general, bridge structures are analyzed assuming linear elastic behavior unless cracking is evident. No indication of cracks in the K-frames indicated the need for cracked/non-linear analysis. Therefore, according to AASHTO, the elastic material behavior was assumed in the FE analysis and the stiffness of the girder was calculated using an undamaged cross-section. Non-linear moving load analysis for live load was considered in order to identify the maximum effect of all moving loads considered in the analysis. Fig. 10 shows the FE model used in SAP 2000®. 58 nodes and 12 nodes were used to model the girder and inclined columns, respectively. Also 57 and 12 frame elements were used to model the girder and inclined columns, respectively. The girders and the columns were assumed to be monolithic, and enabling moment transfer. At each node, the FE model had the same depth of real K-frames shown in drawing.

Figures 11 and 12 show the moment and shear distribution of an exterior beam of bridge 7930 for several sources of loading: self weight of girders, Deck, design truck by AASHTO, Tandem, and NMDOT Permit truck P327-B. As shown in the figures, for moving load, the maximum and minimum effect was obtained directly from the non-linear moving load analysis in SAP 2000®.

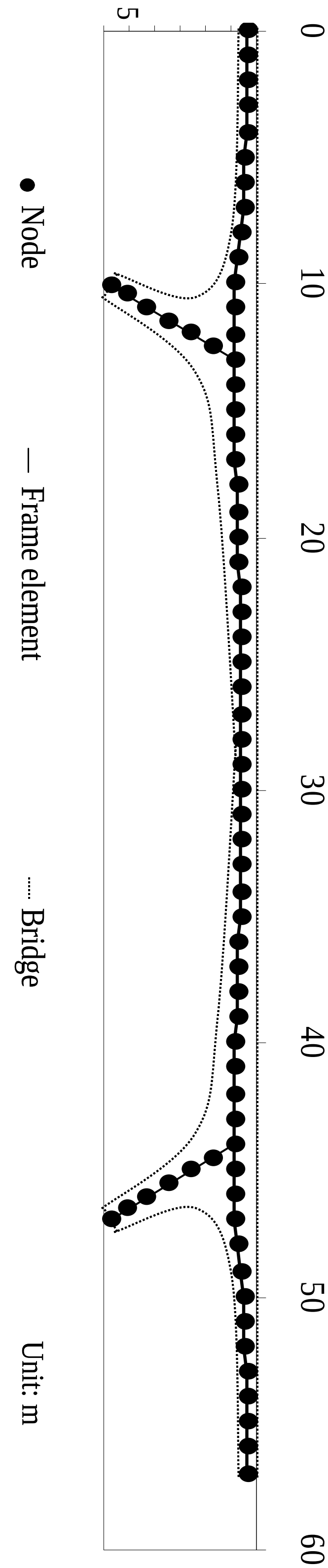

FIGURE 10 FE model showing nodes and frame elements.

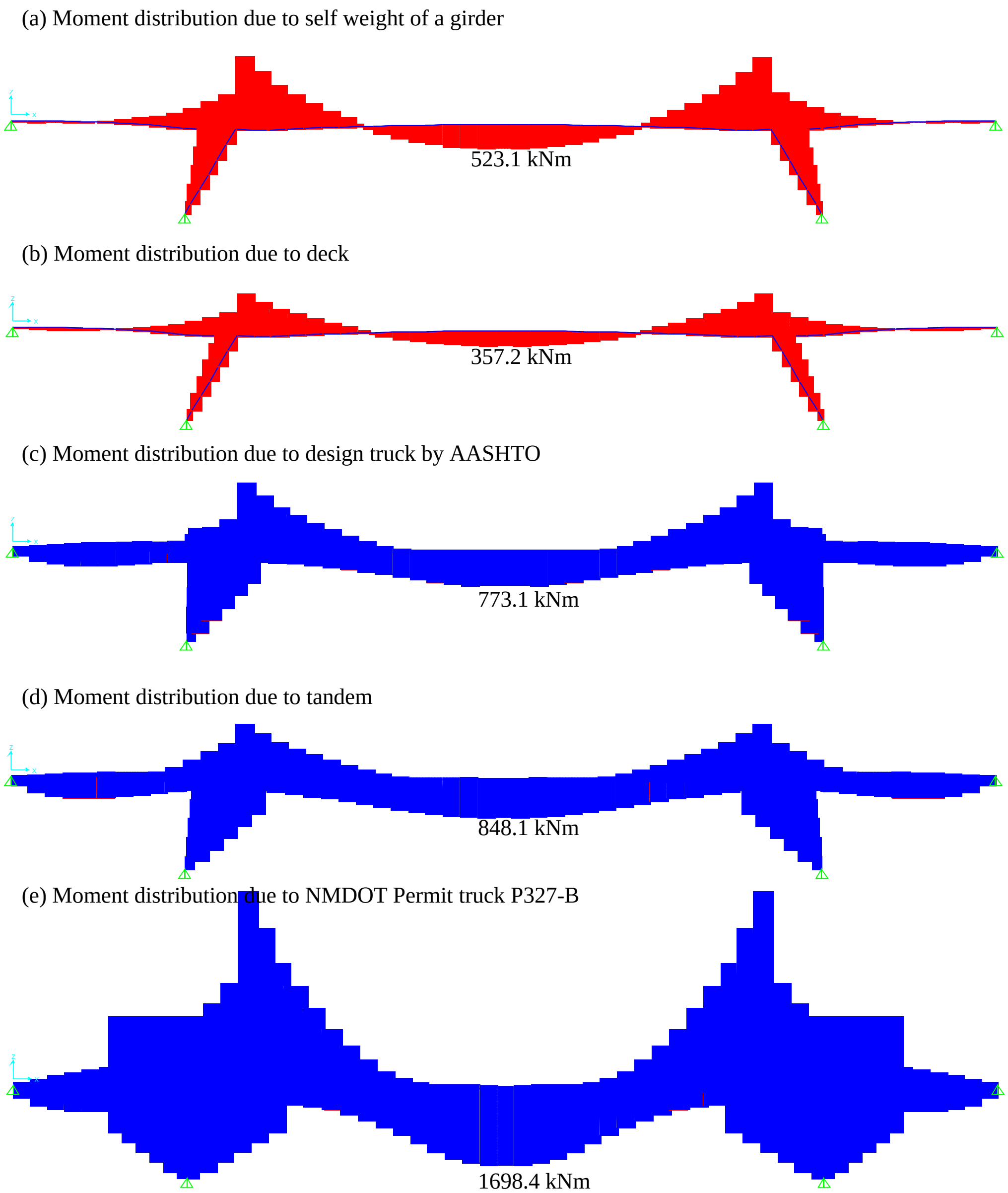

FIGURE 11 Moment distribution of an exterior beam of bridge 7937.

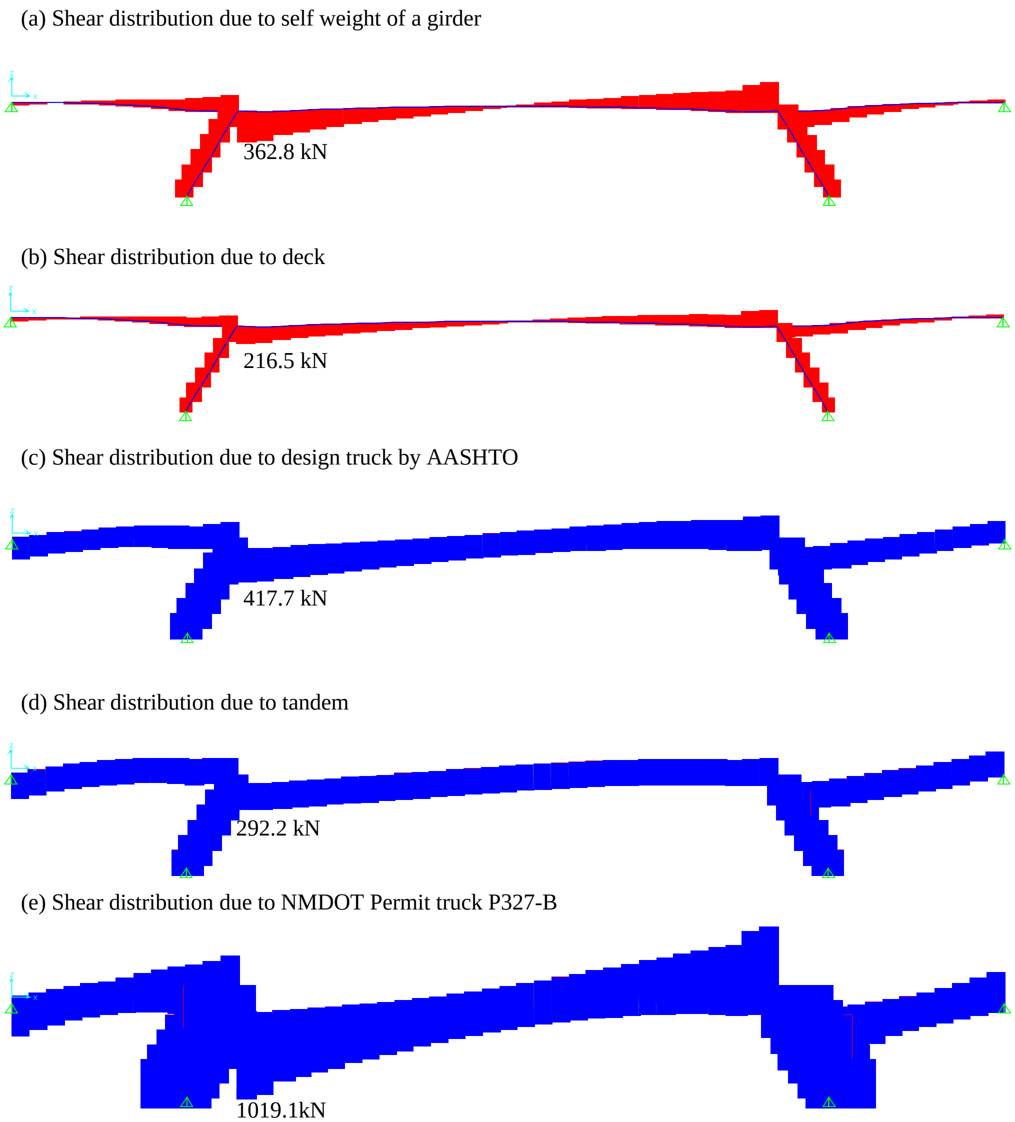

FIGURE 12 Shear distribution of an exterior beam of bridge 7937.

LOAD COMBINATIONS

The final shear and moment effects from all load cases were obtained from SAP 2000®. These values needed to be combined to represent the final straining action affecting the bridge structure. Based on AASHTO (1), several load combinations needed to be considered. This includes *Strength I* and *Strength II* load combinations which can be described as

Strength I

Factored load = 0.9*(Self weight of girder and deck load) + 0.65*(Asphalt and railing) + 1.75*Maximum moving loads and design lane load (5a)

Strength II

Factored load = 0.9*(Self weight of girder and deck load) + 0.65*(Asphalt and railing) + 1.35*Maximum moving loads and design lane load (5b)

Here, "*maximum moving loads and design lane load*" was defined as the maximum moment (or shear) of moving trucks and tandem plus design lane load. According to AASHTO, *Strength I* and *II* combinations include the basic load combination relating to the normal vehicular use of the bridges without wind and load combination relating to the use of the bridge by owner-specified special design vehicles, evaluation permit trucks, or both without wind. Therefore, in *Strength I*, AASHTO design truck and Tandem load were considered in calculation of "maximum moving loads and design lane load" while in *Strength II*, in addition to AASHTO design truck and Tandem load, NMDOT legal trucks (Two-Axle Legal load truck, NMDOT Three-Axle Legal load truck, NMDOT Five-Axle Legal load truck, NMDOT Permit truck P327-B) were considered.

BRIDGE CARRYING CAPACITY

The K-frames are reinforced concrete structures. The cross sectional dimensions and reinforcing details are provided in Figures 7 and 8 showing the as-built drawings. The flexural strength of the K-frames was defined according to AASHTO (1) specification (section 5) as

$$M_n = A_s f_y (d - a/2) \tag{6}$$

where:

A_s = area of tension reinforcement

f_y = yield strength of reinforcing bars

a = depth of the equivalent stress block determined based on compressive strength of concrete.

The shear capacity of the cross-section of girders was evaluated according to AASHTO (1) specification (section 5) as

$$V_n = V_c + V_s \tag{7}$$

where:

V_c = shear resistance of concrete

V_s = shear resistance of transverse reinforcement.

In this investigation, for simplicity, V_c is evaluated by using ACI 318 (2) design provision.

$$V_c = 0.33\sqrt{f'_c} \text{ (MPa)} \tag{8}$$

$$V_s = \frac{A_v f_{vy} d_v}{s} \tag{9}$$

where:

A_v = area of transverse reinforcement

f_{vy} = yield strength of transverse reinforcement

d_v = effective shear depth

s = spacing of transverse reinforcement

The characteristic compressive strength of the concrete K-frames was identified to be 30 MPa. The need for strengthening of the girders can be determined by comparing the cross-sectional carrying capacity with the load demand described by AASHTO (1) as

$$\phi R_n \geq Q \tag{10}$$

where:

ϕ = strength reduction factor which is different in moment and shear

R_n = nominal strength defined in Eqs. (6) and (7) for moment and shear

Q = factored load defined by using Eqs. (1) to (5) for moment and shear.

When ϕR_n is less than Q, the girders needed to be strengthened for proper method. Fig. 13 to Fig. 16 show the factored moment and shear for *Strength I* and *Strength II* load combinations representing load demand for Bridges 7930 and 7937 for exterior and interior frames respectively. Moreover, Fig. 13 to 16 also showed the load carrying capacity for both bridges 7930 and 7937 for moment and shear carrying capacity. Tables A1 to A4 (Appendix A) present the factored moment and shear demand and the corresponding factored cross sectional capacity each 1 m along the bridge length for all bridges. In these Tables, only positive value of "*Shortage of Capacity*" indicates the need for strengthening.

STRENGTHENING NEEDS

Considering Figs. 13 to 16 and Table A1, it is obvious that there was a shortage in negative moment capacity for all girders around connection of the K-frames. This shortage only occurs when considering the NM-Permit load (Strength II) load combination. Therefore, negative moment strengthening of the K-frames was needed to meet AASHTO (1) requirements. There is no obvious need to provide shear strengthening of the K-frames. The large concrete depth at the K-frame connections enables high shear capacity at locations of high demand.

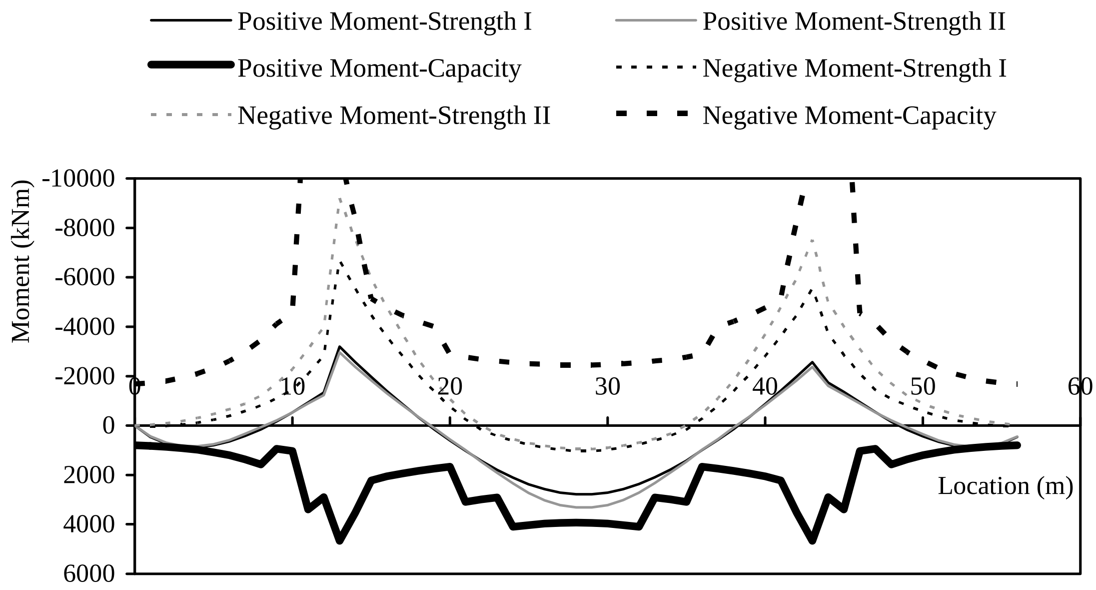

(a) Factored moment and capacity of exterior frame of bridge 7930

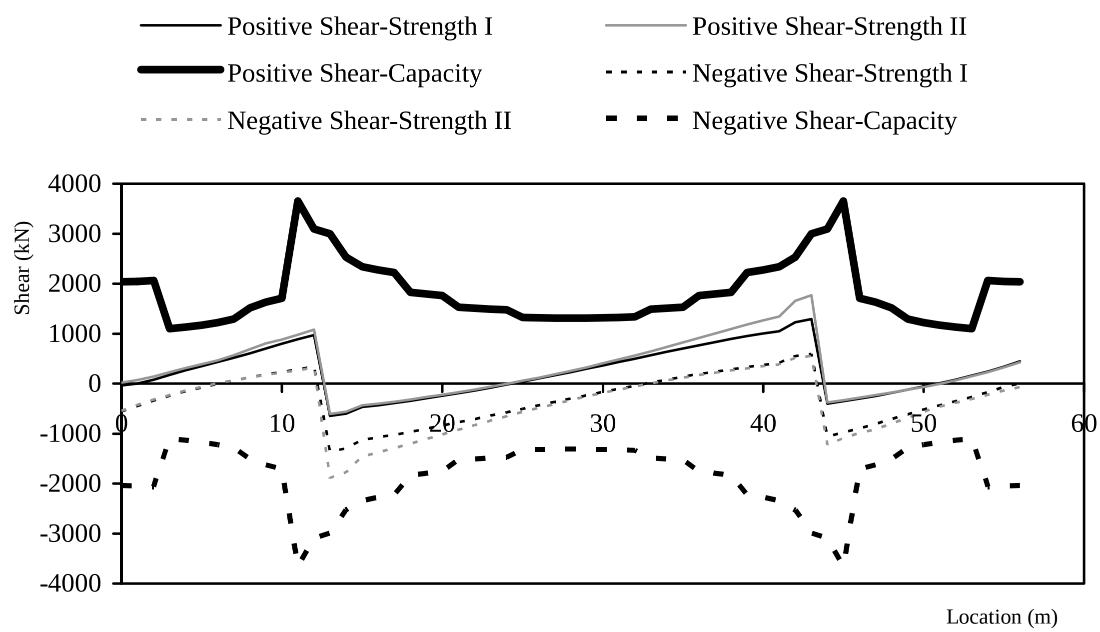

(b) Factored shear and capacity of exterior frame of bridge 7930

FIGURE **13** Factored load and capacity of exterior frames of bridge 7930.

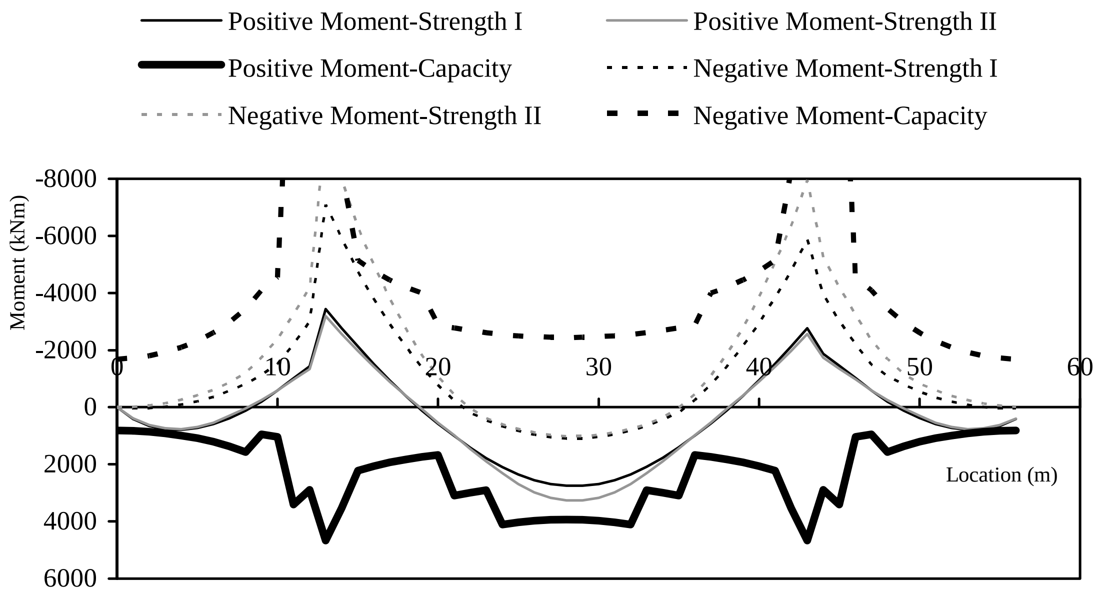

(a) Factored moment and capacity of interior frame of bridge 7930

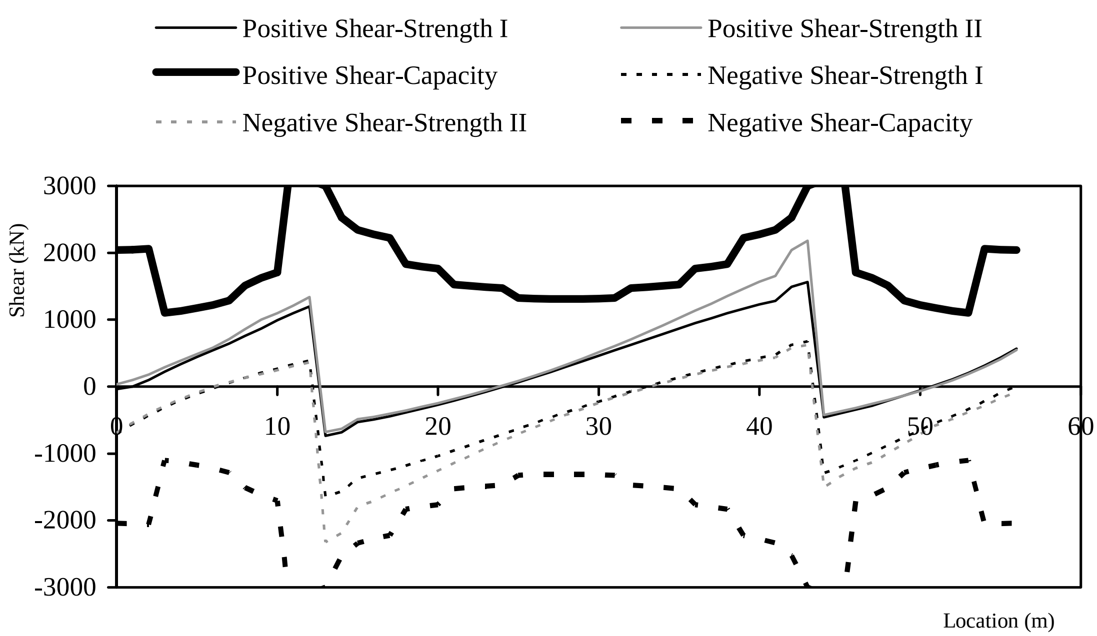

(b) Factored shear and capacity of interior frame of bridge 7930

FIGURE 14 Factored load and capacity of interior frame of bridge 7930.

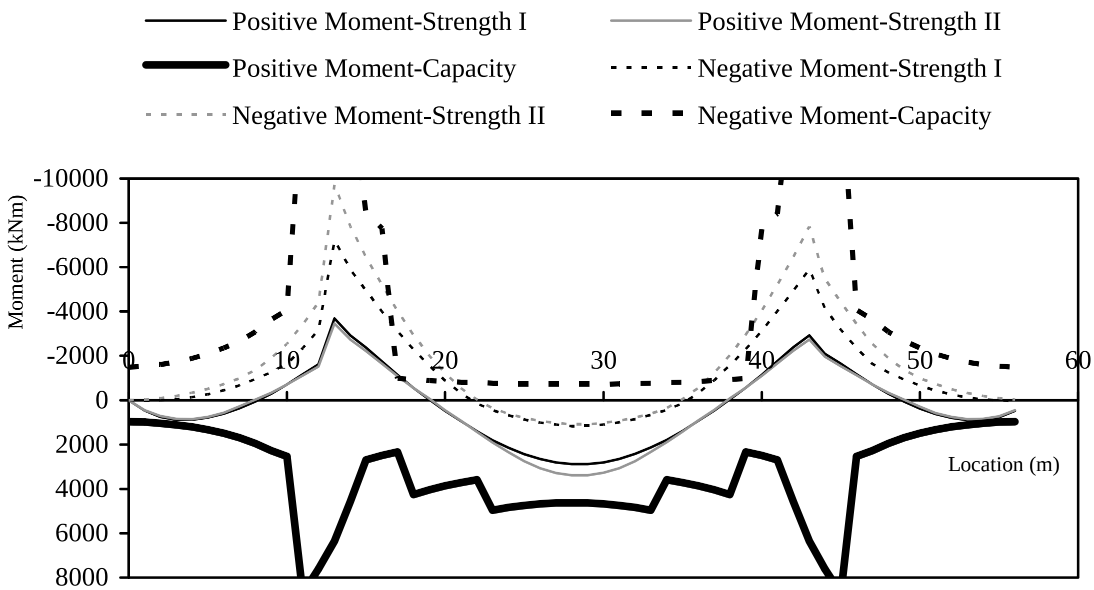

(a) Factored moment and capacity of exterior frame of bridge 7937

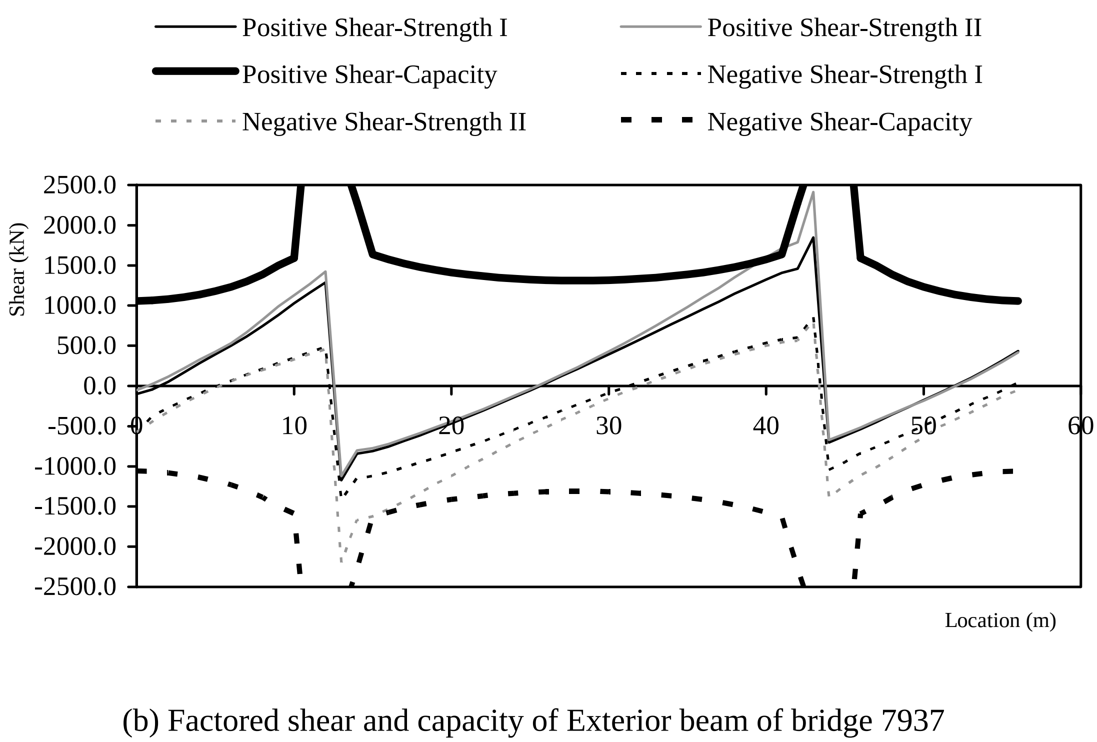

(b) Factored shear and capacity of Exterior beam of bridge 7937

FIGURE 15 Factored load and capacity of exterior frame of bridge 7937.

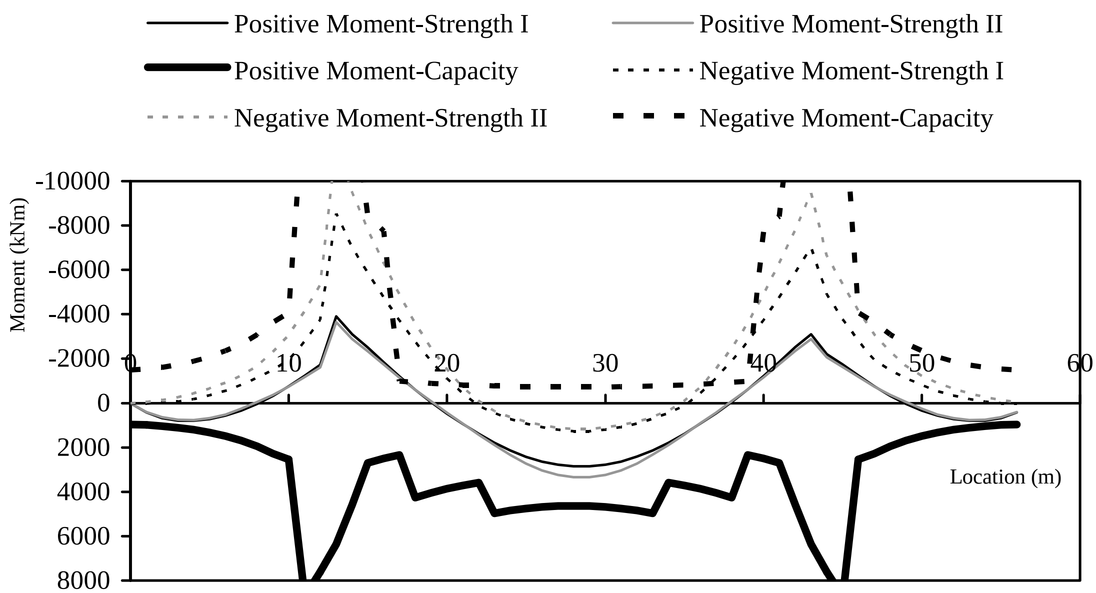

(a) Factored moment and capacity of interior frame of bridge 7937

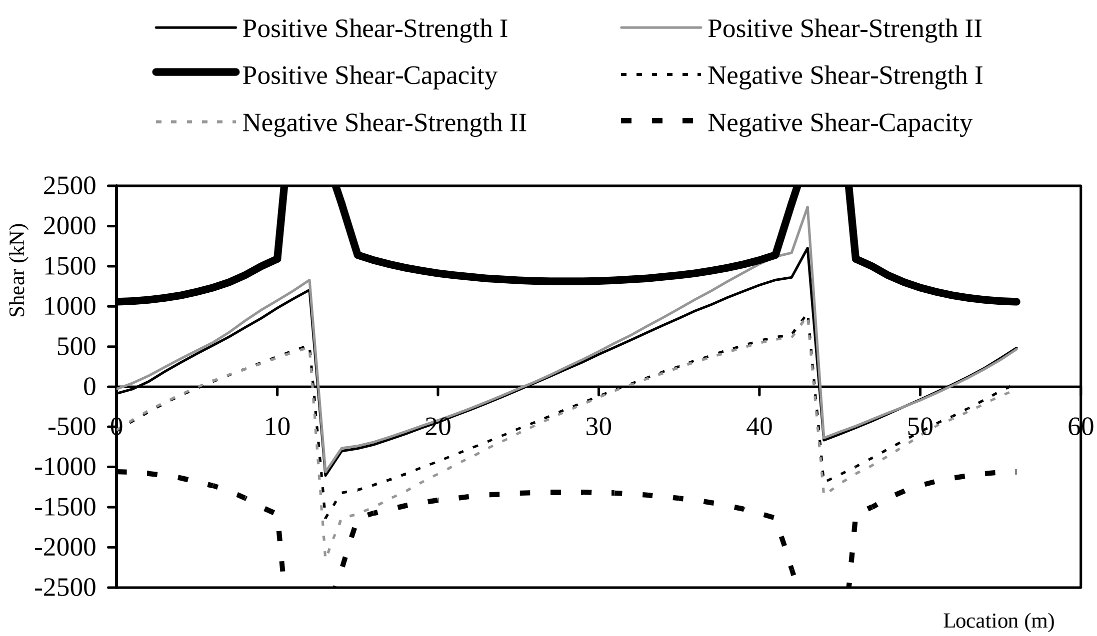

(b) Factored shear and capacity of interior frame of bridge 7937

FIGURE 16 Factored load and capacity of interior frame of bridge 7937.

FIELD TEST TO IDENTIFY BRIDGE CHARACTERISTICS

Step 1: Concrete Surface Milling

We consider bridge 7937 which has a concrete surface at the top of the exterior girders. One and one-half inches of concrete surface needed to be milled to enable installing the CFRP strips. For other locations on the bridge that are covered by asphalt instead of concrete, all asphalt in the FRP application zone needs to be completely milled if the bridge is to be strengthened by FRP.

Step 2: Concrete Surface Preparation

This is the most important step in the application of FRP strips because properly roughened and even concrete substrate is necessary for reliable performance of FRP strips (3 and 4). The acceptable unevenness, which indicates the maximum difference of the surface depth, is specified in current design provisions. In CEB-FIP code (3) and NCHRP Report (4), the allowable value of unevenness of the concrete surface is 4 mm (1/6 inch). If the surface is not even enough, putty needs to be applied to obtain better concrete surface. In addition, several aspects need to be considered. This includes the fact that the concrete substrate needs to be sound with proper tensile strength. In CEB-FIP (3), the minimum tensile strength of concrete is 1.5 N/mm^2. The crack width should be less than 0.2 mm. In addition, the concrete surface should be clean and free from oil, water, or dust before application of FRP.

Step 3: Rebound (Schmidt) Hammer Testing

After cleaning the surface, the rebound hammer (Schmidt) hammer test was performed at three different locations within the area of the milled concrete surface. Fig. 17 illustrates these locations schematically. Fig. 18 shows the Schmidt's hammer test performed by University of New Mexico team.

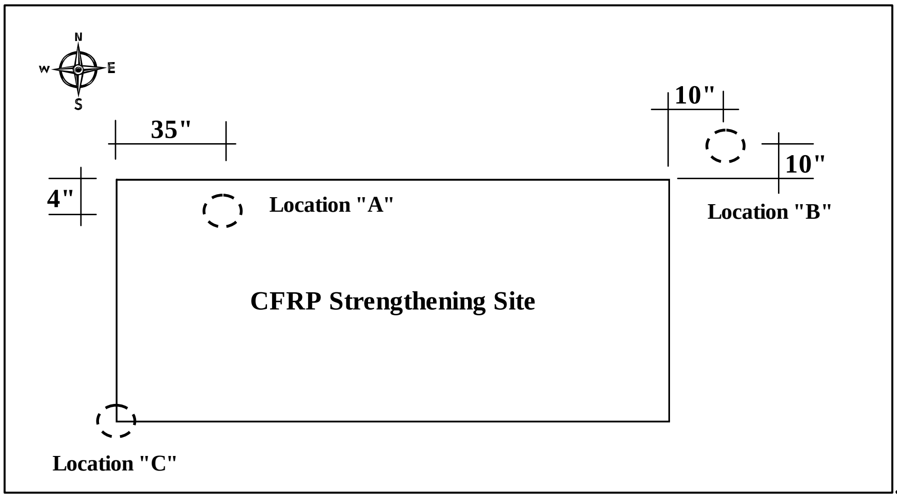

FIGURE 17 Locations considered for Schmidt's hammer test.

FIGURE 18 Schmidt's hammer testing on concrete surface.

The rebound hammer test allowed the researcher to determine the compressive strength of the concrete and thus its stiffness. This was an important step in comparing the measured strength to strength values on the bridge drawings. Moreover, realization of the concrete strength and stiffness is necessary for calibration of the FE model as discussed below. Example measurements of the rebound hammer test are presented in Table 2. The rebound hammer measurements were then converted to compressive strength using the hammer conversion charts with the hammer. The hammer was calibrated before being used as recommended by ASTM standards.

TABLE 2 Results of Schmidt's hammer test in different locations described in Fig. 17.

Location	A	B	C
1	34	40	36
2	44	36	38
3	35	49	38
4	48	40	38
5	35	41	42
6	30	45	48
7	40	38	40
8	34	32	36
9	30	40	42
10	48	37	44
11	37	42	44
12	38	42	40
13	50	38	40
14	38	44	40
15	30	40	38
Average	38.066667	40.266667	40.266667
Strength(psi)	5250	5700	5700

CALIBRATION OF FE MODELS BASED ON FIELD TEST DATA

To calibrate the analytical prediction by FE model developed using SAP 2000®, a load test was performed before the application of CFRP strips on concrete surface. First, the concrete strain of the top of the exterior girder was monitored when subjected to a 50 kip (220 kN) test truck (Fig. 19) with pre-determined weight. Details about the field tests before and after application of the FRP are provided in Report (3). Strain gauges at three locations within the area of interest are attached to the concrete surface. Fig. 20 shows schematically the area of interest and the location of concrete strain gauges. Fig. 21 shows the strain gauges after being attached to the concrete surface.

FIGURE 19 Mack 10 yard dump truck as test truck with weight of 50 kips.

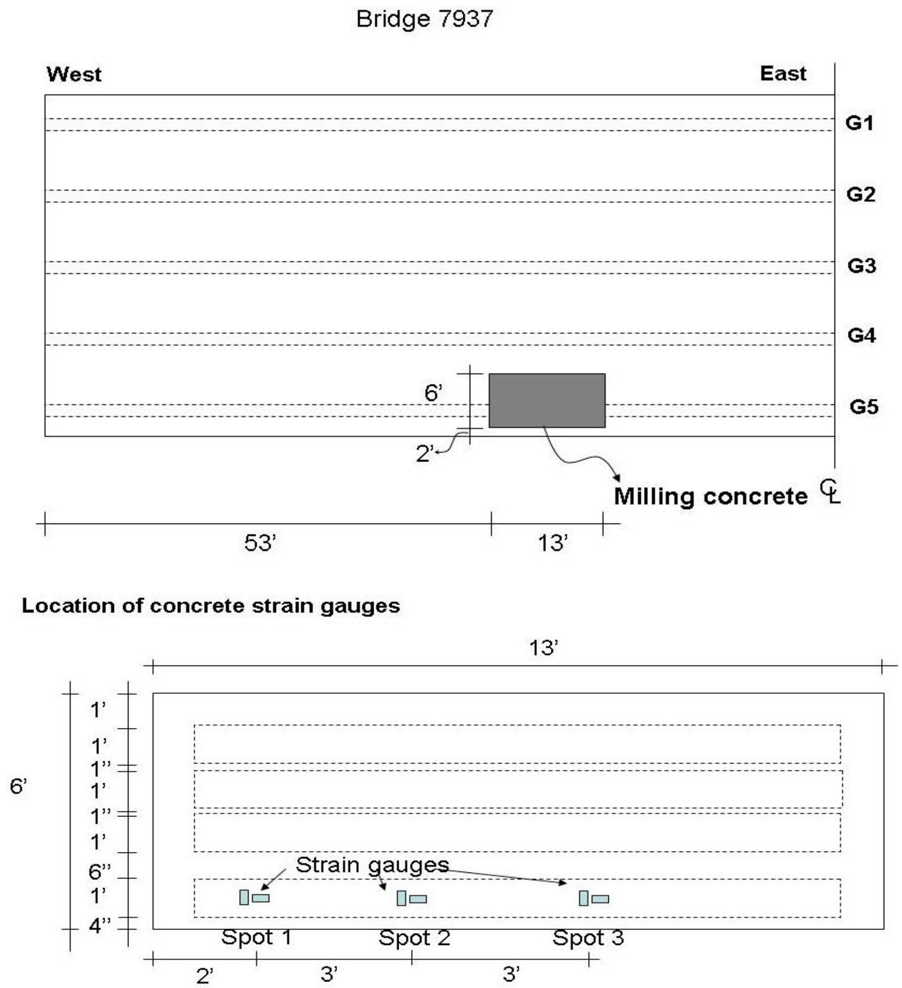

FIGURE 20 Schematic figure showing the area of concrete milling and the location of strain gauges to measure concrete surface strain.

FIGURE 21 Concrete strain gauges attached to the concrete surface.

Fig. 22 illustrates the concrete strain results at the top of the exterior girder. Based on the field test results shown in Fig. 22, the FE models were calibrated by modifying the concrete modulus of elasticity (E) such that concrete strain predictions using the FE model becomes as close as possible to field measured strains. Fig. 23 represents the strains field measured strains and FE predicted strains on the top of the concrete girders. Matching the field measured and FE strain data, it was concluded that concrete with the compression strength 50 MPa should be used in FE models to accurately represent the concrete in the K-frame bridges.

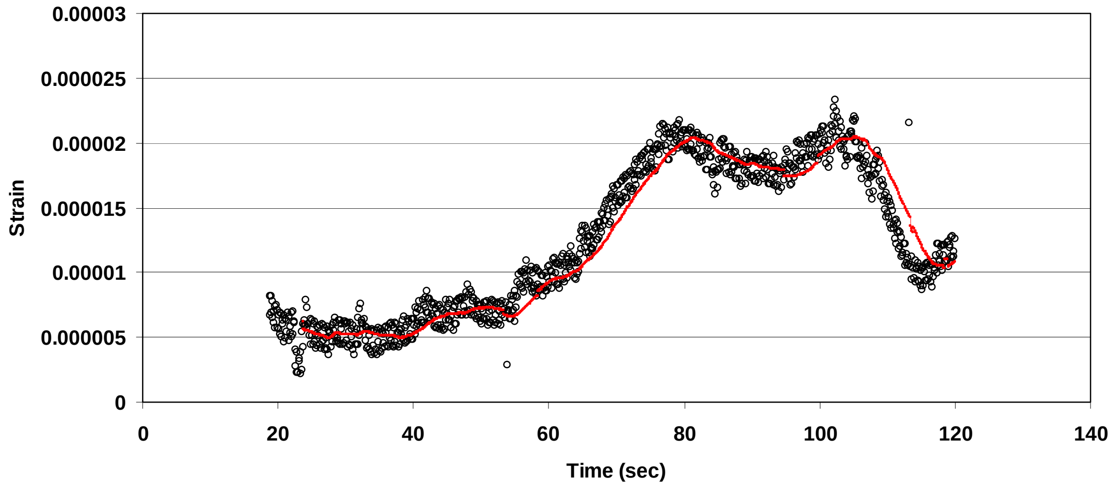

FIGURE 22 Concrete strain field measured at the top of the concrete surface before application of CFRP strips.

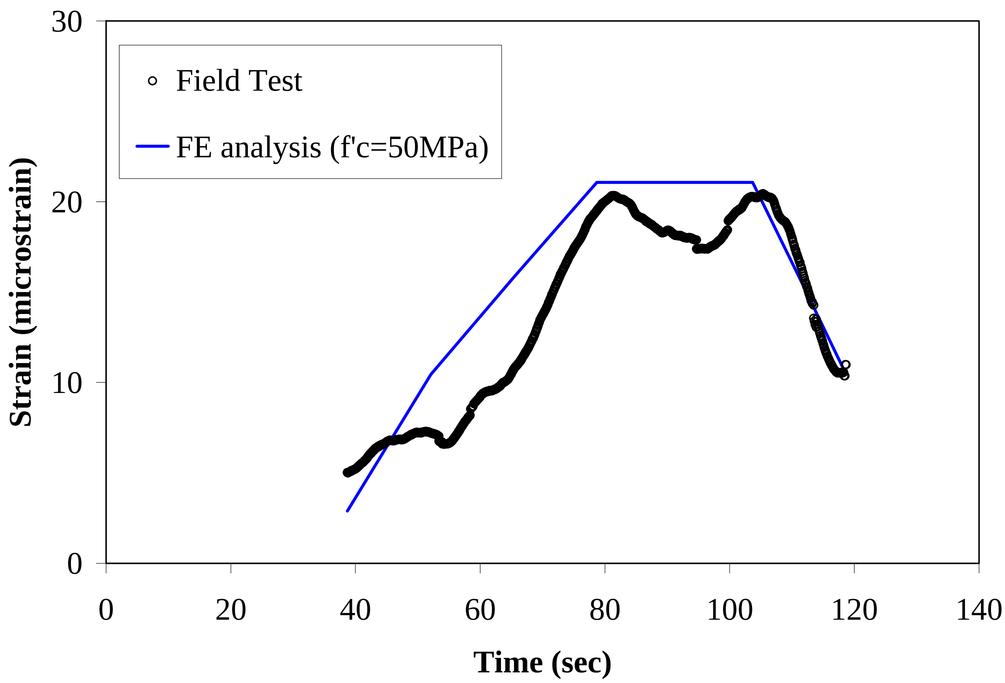

FIGURE 23 Concrete strains as predicted by the calibrated FE model and from field test.

REFERENCES

1. AASHTO. LRFD Bridge Design Specifications. *Manual for Condition Evaluation of Bridges*. American Association of State Highway and Transportation Officials. 2006 Interim revisions, Second Edition, Washington, D.C., 2006.

2. ACI 318 Committee. Building Code and Commentary. ACI 318-05/318R-05, 2005.

3. CEB-FIP. Externally bonded FRP reinforcement for RC structures. TRB 14, 2001, p. 124.

4. Shahawy, Mirmiran A., M. Shahawy, A. Nanni and V. Karbhari, Editors. *Bonded Repair and Retrofit of Concrete Structures using FRP Composites*. Recommended Construction Specifications and Process Control Manual. National Cooperative Highway Research Program: NCHRP Report 514, TRB National Research Council, Washington, D.C., 2004.

APPENDIX

TABLE A1 Positive factored moment and flexural capacity of exterior frame of bridge 7930.

Location (m)	Element	Beam thickness (m)	Factored moment-*Strength I* (kNm)	Factored moment-*Strength II* (kNm)	Flexural capacity (kNm)	Shortage of capacity (kNm)
0	1	0.765	0.0	0.0	806.2	-806.2
1	2	0.778	478.3	460.7	823.5	-345.2
2	3	0.804	768.9	729.1	858.6	-89.6
3	4	0.843	898.8	852.7	912.4	-13.6
4	5	0.898	902.6	867.0	986.5	-83.9
5	6	0.970	806.2	766.6	1083.5	-277.4
6	7	1.061	625.0	578.8	1207.6	-582.6
7	8	1.178	374.1	286.5	1365.5	-991.4
8	9	1.329	61.8	-27.4	1570.1	-1508.3
9	10	1.536	-310.8	-358.6	940.8	-1251.5
10	11	1.680	-748.1	-746.9	1038.1	-1785.0
11	12	5.169	-1219.7	-1175.5	3403.3	-4578.7
12	13	4.414	-1710.3	-1605.4	2891.8	-4497.2
13	14	3.617	-4124.8	-3889.8	4673.0	-8562.9
14	15	2.777	-3321.3	-3128.6	3534.0	-6662.6
15	16	1.807	-2562.4	-2412.6	2218.6	-4631.2
16	17	1.690	-1860.7	-1768.9	2059.7	-3828.6
17	18	1.597	-1192.4	-1153.8	1933.5	-3087.3
18	19	1.520	-564.7	-576.1	1829.6	-2394.3
19	20	1.456	21.4	-33.1	1742.6	-1721.2
20	21	1.402	559.8	525.5	1669.4	-1109.5
21	22	1.356	1053.8	1038.1	3093.0	-2039.1
22	23	1.319	1535.3	1582.2	2990.5	-1408.3
23	24	1.287	1960.5	2080.5	2906.4	-826.0
24	25	1.263	2324.0	2551.1	4104.8	-1553.8
25	26	1.244	2624.9	2976.3	4027.5	-1051.1
26	27	1.230	2858.2	3302.4	3973.0	-670.5
27	28	1.222	3013.2	3517.9	3940.6	-422.6
28	29	1.220	3087.4	3622.7	3929.8	-307.1
29	30	1.222	3085.6	3620.9	3940.6	-319.7
30	31	1.230	3007.7	3512.4	3973.0	-460.6
31	32	1.244	2849.2	3293.5	4027.5	-734.0
32	33	1.263	2612.8	2964.2	4104.8	-1140.7
33	34	1.287	2308.9	2536.0	2906.4	-370.4
34	35	1.319	1942.9	2062.9	2990.5	-927.6
35	36	1.356	1515.9	1562.8	3093.0	-1530.2
36	37	1.402	1033.2	1017.5	1669.4	-636.1
37	38	1.456	538.9	504.5	1742.6	-1203.7
38	39	1.520	1.1	-53.4	1829.6	-1828.5
39	40	1.597	-583.2	-594.5	1933.5	-2516.7
40	41	1.690	-1207.6	-1169.1	2059.7	-3228.8

41	42	1.807	-1870.9	-1779.1	2218.6	-3997.7
42	43	2.777	-2565.6	-2415.8	3534.0	-5949.8
43	44	3.617	-3316.6	-3123.8	4673.0	-7796.8
44	45	4.414	-2222.6	-2092.4	2891.8	-4984.2
45	46	5.169	-1739.1	-1634.2	3403.3	-5037.5
46	47	1.680	-1235.1	-1190.8	1038.1	-2229.0
47	48	1.536	-750.9	-749.6	940.8	-1690.4
48	49	1.329	-304.1	-352.0	1570.1	-1874.2
49	50	1.178	74.1	-15.0	1365.5	-1291.4
50	51	1.061	389.6	302.0	1207.6	-818.0
51	52	0.970	641.6	595.3	1083.5	-442.0
52	53	0.898	822.2	782.6	986.5	-164.3
53	54	0.843	916.8	881.2	912.4	**4.5**
54	55	0.804	910.2	864.2	858.6	**51.7**
55	56	0.778	777.0	737.2	823.5	-46.5
56	57	0.765	482.4	464.8	806.2	-323.8

TABLE A2 Negative factored moment and flexural capacity of exterior frame of bridge 7930.

Location (m)	Element	Beam thickness (m)	Factored moment-*Strength I* (kNm)	Factored moment-*Strength II* (kNm)	Flexural capacity (kNm)	Shortage of capacity (kNm)
0	1	0.765	0.0	0.0	-1682.5	-1682.5
1	2	0.778	37.1	-14.5	-1722.4	-1707.9
2	3	0.804	32.9	-67.8	-1803.4	-1735.6
3	4	0.843	-12.7	-160.0	-1927.6	-1767.6
4	5	0.898	-100.4	-291.6	-2098.7	-1807.1
5	6	0.970	-232.0	-464.2	-2322.8	-1858.6
6	7	1.061	-408.0	-678.4	-2609.1	-1930.8
7	8	1.178	-630.6	-936.4	-2973.7	-2037.2
8	9	1.329	-902.3	-1303.4	-3446.0	-2142.6
9	10	1.536	-1228.6	-1848.5	-4096.7	-2248.2
10	11	1.680	-1645.4	-2494.1	-4546.3	-2052.2
11	12	5.169	-2375.7	-3371.8	-15466.3	-12094.5
12	13	4.414	-3204.9	-4358.0	-13104.8	-8746.7
13	14	3.617	-7610.9	-10136.8	-11047.8	-911.0
14	15	2.777	-6291.3	-8271.4	-8306.1	-34.7
15	16	1.807	-5053.3	-6532.4	-5139.9	**1392.5**
16	17	1.690	-4061.7	-5227.1	-4757.6	**469.5**
17	18	1.597	-3132.2	-4014.2	-4453.7	-439.5
18	19	1.520	-2276.6	-2894.5	-4203.5	-1309.0
19	20	1.456	-1500.2	-1928.2	-3994.2	-2065.9
20	21	1.402	-811.3	-1120.4	-2883.6	-1763.2
21	22	1.356	-215.0	-414.8	-2774.3	-2359.5
22	23	1.319	282.0	105.2	-2683.1	-2788.3
23	24	1.287	587.0	507.6	-2608.4	-3116.0
24	25	1.263	829.6	770.8	-2548.7	-3319.4
25	26	1.244	1026.3	958.7	-2503.1	-3461.8
26	27	1.230	1177.4	1103.1	-2471.0	-3574.1
27	28	1.222	1283.3	1204.8	-2451.9	-3656.6
28	29	1.220	1343.0	1262.8	-2445.5	-3708.3
29	30	1.222	1341.1	1260.9	-2451.9	-3712.8
30	31	1.230	1277.8	1199.3	-2471.0	-3670.2
31	32	1.244	1168.4	1094.2	-2503.1	-3597.2
32	33	1.263	1014.1	946.6	-2548.7	-3495.2
33	34	1.287	814.5	755.7	-2608.4	-3364.1
34	35	1.319	569.4	490.1	-2683.1	-3173.2
35	36	1.356	262.6	85.8	-2774.3	-2860.0
36	37	1.402	-235.6	-435.4	-2883.6	-2448.2
37	38	1.456	-832.3	-1141.3	-3994.2	-2852.8
38	39	1.520	-1520.5	-1948.5	-4203.5	-2255.0
39	40	1.597	-2295.1	-2912.9	-4453.7	-1540.8
40	41	1.690	-3147.5	-4029.4	-4757.6	-728.1
41	42	1.807	-4071.9	-5237.3	-5139.9	**97.4**
42	43	2.777	-5056.4	-6535.5	-8306.1	-1770.6

43	44	3.617	-6286.5	-8266.7	-11047.8	-2781.1
44	45	4.414	-4207.2	-5467.5	-13104.8	-7637.2
45	46	5.169	-3233.7	-4386.8	-15466.3	-11079.5
46	47	1.680	-2391.1	-3387.2	-4546.3	-1159.1
47	48	1.536	-1648.1	-2496.8	-4096.7	-1599.9
48	49	1.329	-1222.0	-1841.9	-3446.0	-1604.1
49	50	1.178	-889.9	-1291.0	-2973.7	-1682.6
50	51	1.061	-615.1	-921.0	-2609.1	-1688.2
51	52	0.970	-391.4	-661.8	-2322.8	-1660.9
52	53	0.898	-216.0	-448.1	-2098.7	-1650.6
53	54	0.843	-86.2	-277.4	-1927.6	-1650.1
54	55	0.804	-1.2	-148.5	-1803.4	-1654.9
55	56	0.778	41.0	-59.8	-1722.4	-1662.6
56	57	0.765	41.2	-10.4	-1682.5	-1672.0

TABLE A3 Positive factored shear and shear capacity of exterior frame of bridge 7930.

Location (m)	Element	Beam thickness (m)	Factored shear-*Strength I* (kN)	Factored shear-*Strength II* (kN)	Shear capacity (kN)	Shortage of capacity (kN)
0	1	0.765	-57.1	-4.2	2040.0	-1982.9
1	2	0.778	-15.9	58.6	2047.1	-1988.5
2	3	0.804	69.7	136.1	2061.5	-1925.5
3	4	0.843	177.3	230.1	1101.2	-871.2
4	5	0.898	279.0	321.4	1131.7	-810.3
5	6	0.970	374.2	406.9	1171.6	-764.7
6	7	1.061	462.5	492.7	1222.6	-729.9
7	8	1.178	555.7	606.8	1287.6	-680.8
8	9	1.329	658.0	735.3	1512.1	-776.7
9	10	1.536	758.6	862.1	1628.0	-765.9
10	11	1.680	869.8	950.0	1708.1	-758.1
11	12	5.169	970.0	1056.4	3653.3	-2596.8
12	13	4.414	1063.6	1176.1	3092.2	-1916.1
13	14	3.617	-832.5	-789.2	2998.6	-2166.1
14	15	2.777	-773.7	-733.0	2530.2	-1756.5
15	16	1.807	-605.6	-571.9	2340.1	-1734.6
16	17	1.690	-561.6	-530.8	2274.8	-1713.2
17	18	1.597	-505.8	-477.9	2222.9	-1717.0
18	19	1.520	-449.6	-424.3	1829.3	-1379.7
19	20	1.456	-388.1	-365.3	1793.5	-1405.4
20	21	1.402	-329.4	-309.9	1763.4	-1434.0
21	22	1.356	-265.9	-248.4	1527.6	-1261.7
22	23	1.319	-201.5	-185.1	1506.5	-1305.0
23	24	1.287	-133.6	-118.5	1489.1	-1355.5
24	25	1.263	-64.5	-49.9	1475.3	-1410.9
25	26	1.244	6.1	20.6	1324.4	-1303.8
26	27	1.230	78.1	92.0	1317.0	-1225.0
27	28	1.222	153.2	170.9	1312.6	-1141.7
28	29	1.220	227.6	250.5	1311.1	-1060.6
29	30	1.222	303.0	333.2	1312.6	-979.4
30	31	1.230	381.1	420.5	1317.0	-896.5
31	32	1.244	458.0	507.7	1324.4	-816.7
32	33	1.263	535.2	597.4	1335.0	-737.6
33	34	1.287	612.6	692.1	1489.1	-797.1
34	35	1.319	689.8	788.8	1506.5	-717.6
35	36	1.356	764.9	885.9	1527.6	-641.7
36	37	1.402	841.4	987.7	1763.4	-775.7
37	38	1.456	911.9	1083.0	1793.5	-710.5
38	39	1.520	985.6	1187.0	1829.3	-642.3
39	40	1.597	1051.8	1283.7	2222.9	-939.2
40	41	1.690	1116.2	1379.5	2274.8	-895.3
41	42	1.807	1171.0	1461.8	2340.1	-878.3
42	43	2.777	1383.9	1811.2	2530.2	-719.0

43	44	3.617	1459.0	1940.0	2998.6	-1058.6
44	45	4.414	-512.8	-485.7	3092.2	-2579.4
45	46	5.169	-450.4	-428.2	3653.3	-3202.8
46	47	1.680	-384.3	-366.0	1708.1	-1323.8
47	48	1.536	-325.5	-303.4	1628.0	-1302.5
48	49	1.329	-247.5	-238.7	1512.1	-1264.6
49	50	1.178	-172.5	-172.6	1287.6	-1114.9
50	51	1.061	-97.9	-106.2	1222.6	-1116.5
51	52	0.970	-21.0	-33.2	1171.6	-1138.5
52	53	0.898	60.2	47.4	1131.7	-1071.5
53	54	0.843	147.1	133.9	1101.2	-954.1
54	55	0.804	242.4	227.2	2061.5	-1819.2
55	56	0.778	348.2	330.6	2047.1	-1698.9
56	57	0.765	462.3	446.0	2040.0	-1577.7

TABLE A4 Negative factored shear and shear capacity of exterior frame of bridge 7930.

Location (m)	Element	Beam thickness (m)	Factored shear-*Strength I* (kN)	Factored shear-*Strength II* (kN)	Shear capacity (kN)	Shortage of capacity (kN)
0	1	0.765	-580.4	-567.6	-2040.0	-1459.6
1	2	0.778	-458.6	-441.4	-2047.1	-1588.5
2	3	0.804	-344.8	-326.7	-2061.5	-1716.7
3	4	0.843	-239.5	-224.2	-1101.2	-861.7
4	5	0.898	-145.5	-131.4	-1131.7	-986.2
5	6	0.970	-59.4	-45.7	-1171.6	-1112.2
6	7	1.061	20.5	33.9	-1222.6	-1188.7
7	8	1.178	96.0	104.9	-1287.6	-1182.7
8	9	1.329	169.2	168.3	-1512.1	-1342.8
9	10	1.536	243.2	230.8	-1628.0	-1384.8
10	11	1.680	302.2	289.4	-1708.1	-1405.9
11	12	5.169	371.1	352.9	-3653.3	-3282.1
12	13	4.414	436.8	414.5	-3092.2	-2655.4
13	14	3.617	-1537.9	-2075.1	-2998.6	-923.5
14	15	2.777	-1466.6	-1947.5	-2530.2	-582.6
15	16	1.807	-1258.8	-1594.8	-2340.1	-745.3
16	17	1.690	-1201.3	-1507.4	-2274.8	-767.4
17	18	1.597	-1135.2	-1407.1	-2222.9	-815.8
18	19	1.520	-1067.9	-1306.7	-1829.3	-522.6
19	20	1.456	-993.7	-1198.4	-1793.5	-595.2
20	21	1.402	-922.8	-1098.0	-1763.4	-665.4
21	22	1.356	-846.0	-994.3	-1527.6	-533.3
22	23	1.319	-770.7	-893.9	-1506.5	-612.5
23	24	1.287	-693.3	-793.8	-1489.1	-695.4
24	25	1.263	-615.6	-696.3	-1475.3	-779.0
25	26	1.244	-537.9	-601.1	-1324.4	-723.4
26	27	1.230	-460.4	-510.9	-1317.0	-806.1
27	28	1.222	-381.3	-421.2	-1312.6	-891.4
28	29	1.220	-304.9	-335.6	-1311.1	-975.5
29	30	1.222	-229.5	-252.7	-1312.6	-1059.9
30	31	1.230	-153.2	-171.1	-1317.0	-1145.9
31	32	1.244	-80.1	-94.0	-1324.4	-1230.4
32	33	1.263	-8.2	-22.7	-1335.0	-1312.2
33	34	1.287	62.1	47.6	-1489.1	-1427.1
34	35	1.319	130.9	115.9	-1506.5	-1375.5
35	36	1.356	196.7	180.6	-1527.6	-1330.9
36	37	1.402	262.2	244.9	-1763.4	-1501.2
37	38	1.456	320.4	301.4	-1793.5	-1473.1
38	39	1.520	381.2	358.7	-1829.3	-1448.0
39	40	1.597	436.0	411.1	-2222.9	-1786.9
40	41	1.690	489.6	462.2	-2274.8	-1785.2
41	42	1.807	535.7	506.0	-2340.1	-1804.5
42	43	2.777	705.7	667.7	-2530.2	-1824.5

43	44	3.617	766.1	725.5	-2998.6	-2232.4
44	45	4.414	-1165.5	-1336.3	-3092.2	-1756.0
45	46	5.169	-1077.2	-1189.5	-3653.3	-2463.7
46	47	1.680	-983.0	-1069.7	-1708.1	-638.4
47	48	1.536	-876.9	-985.3	-1628.0	-642.7
48	49	1.329	-769.4	-861.4	-1512.1	-650.7
49	50	1.178	-664.0	-734.2	-1287.6	-553.4
50	51	1.061	-559.1	-605.4	-1222.6	-617.3
51	52	0.970	-463.7	-489.9	-1171.6	-681.8
52	53	0.898	-373.6	-403.9	-1131.7	-727.9
53	54	0.843	-277.4	-316.6	-1101.2	-784.6
54	55	0.804	-174.6	-225.1	-2061.5	-1836.5
55	56	0.778	-66.0	-130.7	-2047.1	-1916.4
56	57	0.765	21.1	-52.6	-2040.0	-1987.4

TABLE A5 Positive factored moment and flexural capacity of exterior frame of bridge 7931.

Location (m)	Element	Beam thickness (m)	Factored moment-*Strength I* (kNm)	Factored moment-*Strength II* (kNm)	Flexural capacity (kNm)	Shortage of capacity (kNm)
0	1	0.765	0.0	0.0	806.2	-806.2
1	2	0.778	446.5	430.2	823.5	-377.0
2	3	0.804	717.4	680.7	858.6	-141.1
3	4	0.843	837.7	795.2	912.4	-74.7
4	5	0.898	839.3	806.4	986.5	-147.2
5	6	0.970	745.9	709.4	1083.5	-337.7
6	7	1.061	571.8	529.1	1207.6	-635.8
7	8	1.178	330.7	249.8	1365.5	-1034.8
8	9	1.329	30.1	-52.2	1570.1	-1540.0
9	10	1.536	-329.1	-373.2	940.8	-1269.8
10	11	1.680	-751.3	-750.2	1038.1	-1788.3
11	12	5.169	-1208.2	-1167.3	3403.3	-4570.6
12	13	4.414	-1686.2	-1589.4	2891.8	-4481.3
13	14	3.617	-4073.8	-3857.1	4673.0	-8530.2
14	15	2.777	-3281.3	-3103.5	3534.0	-6637.5
15	16	1.807	-2533.6	-2395.4	2218.6	-4614.0
16	17	1.690	-1848.9	-1764.2	2059.7	-3823.9
17	18	1.597	-1197.7	-1162.2	1933.5	-3095.7
18	19	1.520	-587.1	-597.5	1829.6	-2416.7
19	20	1.456	-17.7	-67.9	1742.6	-1760.3
20	21	1.402	504.7	473.0	1669.4	-1164.7
21	22	1.356	983.1	968.6	3093.0	-2109.9
22	23	1.319	1446.9	1490.2	2990.5	-1500.3
23	24	1.287	1856.0	1966.7	2906.4	-939.7
24	25	1.263	2205.3	2414.8	4104.8	-1690.0
25	26	1.244	2494.0	2818.2	4027.5	-1209.3
26	27	1.230	2717.4	3127.3	3973.0	-845.7
27	28	1.222	2865.9	3331.5	3940.6	-609.0
28	29	1.220	2937.0	3430.8	3929.8	-499.0
29	30	1.222	2935.1	3429.0	3940.6	-511.6
30	31	1.230	2860.4	3326.0	3973.0	-646.9
31	32	1.244	2708.5	3118.3	4027.5	-909.2
32	33	1.263	2481.9	2806.0	4104.8	-1298.8
33	34	1.287	2190.3	2399.7	2906.4	-506.7
34	35	1.319	1838.5	1949.2	2990.5	-1041.3
35	36	1.356	1427.5	1470.8	3093.0	-1622.1
36	37	1.402	962.5	948.0	1669.4	-706.9
37	38	1.456	483.7	452.0	1742.6	-1258.9
38	39	1.520	-37.9	-88.2	1829.6	-1867.5
39	40	1.597	-605.6	-616.0	1933.5	-2539.1
40	41	1.690	-1213.0	-1177.4	2059.7	-3237.2

41	42	1.807	-1859.1	-1774.4	2218.6	-3993.0
42	43	2.777	-2536.8	-2398.6	3534.0	-5932.6
43	44	3.617	-3276.5	-3098.7	4673.0	-7771.7
44	45	4.414	-2191.2	-2071.2	2891.8	-4963.0
45	46	5.169	-1715.0	-1618.2	3403.3	-5021.5
46	47	1.680	-1223.5	-1182.7	1038.1	-2220.9
47	48	1.536	-754.1	-752.9	940.8	-1693.7
48	49	1.329	-322.4	-366.6	1570.1	-1892.5
49	50	1.178	42.4	-39.8	1365.5	-1323.1
50	51	1.061	346.2	265.3	1207.6	-861.4
51	52	0.970	588.4	545.7	1083.5	-495.2
52	53	0.898	761.9	725.4	986.5	-224.6
53	54	0.843	853.5	820.7	912.4	-58.8
54	55	0.804	849.1	806.6	858.6	-9.4
55	56	0.778	725.4	688.7	823.5	-98.1
56	57	0.765	450.6	434.3	806.2	-355.6

TABLE A6 Negative factored moment and flexural capacity of exterior frame of bridge 7931.

Location (m)	Element	Beam thickness (m)	Factored moment-*Strength I* (kNm)	Factored moment-*Strength II* (kNm)	Flexural capacity (kNm)	Shortage of capacity (kNm)
0	1	0.765	0.0	0.0	-1682.5	-1682.5
1	2	0.778	39.4	-8.2	-1722.4	-1714.2
2	3	0.804	38.4	-54.5	-1803.4	-1748.9
3	4	0.843	-3.2	-139.0	-1927.6	-1788.5
4	5	0.898	-86.0	-262.5	-2098.7	-1836.2
5	6	0.970	-211.9	-426.0	-2322.8	-1896.7
6	7	1.061	-381.2	-630.6	-2609.1	-1978.5
7	8	1.178	-596.2	-878.3	-2973.7	-2095.3
8	9	1.329	-859.3	-1229.3	-3446.0	-2216.7
9	10	1.536	-1175.8	-1747.7	-4096.7	-2349.0
10	11	1.680	-1579.0	-2362.0	-4546.3	-2184.3
11	12	5.169	-2274.7	-3193.6	-15466.3	-12272.7
12	13	4.414	-3065.0	-4128.8	-13104.8	-8976.0
13	14	3.617	-7289.9	-9620.2	-11047.8	-1427.6
14	15	2.777	-6021.2	-7848.0	-8306.1	-458.1
15	16	1.807	-4831.6	-6196.1	-5139.9	**1056.2**
16	17	1.690	-3879.4	-4954.5	-4757.6	**197.0**
17	18	1.597	-2987.3	-3801.0	-4453.7	-652.7
18	19	1.520	-2166.3	-2736.4	-4203.5	-1467.2
19	20	1.456	-1421.4	-1816.3	-3994.2	-2177.9
20	21	1.402	-760.3	-1045.4	-2883.6	-1838.2
21	22	1.356	-187.4	-371.8	-2774.3	-2402.5
22	23	1.319	290.7	127.6	-2683.1	-2810.7
23	24	1.287	588.9	515.7	-2608.4	-3124.1
24	25	1.263	826.7	772.4	-2548.7	-3321.1
25	26	1.244	1019.2	956.9	-2503.1	-3459.9
26	27	1.230	1166.9	1098.3	-2471.0	-3569.3
27	28	1.222	1270.0	1197.6	-2451.9	-3649.4
28	29	1.220	1327.7	1253.7	-2445.5	-3699.2
29	30	1.222	1325.9	1251.8	-2451.9	-3703.7
30	31	1.230	1264.5	1192.1	-2471.0	-3663.0
31	32	1.244	1157.9	1089.4	-2503.1	-3592.5
32	33	1.263	1007.0	944.7	-2548.7	-3493.4
33	34	1.287	811.6	757.4	-2608.4	-3365.7
34	35	1.319	571.4	498.2	-2683.1	-3181.3
35	36	1.356	271.3	108.2	-2774.3	-2882.5
36	37	1.402	-208.0	-392.4	-2883.6	-2491.3
37	38	1.456	-781.2	-1066.4	-3994.2	-2927.8
38	39	1.520	-1441.7	-1836.5	-4203.5	-2367.0
39	40	1.597	-2184.8	-2754.8	-4453.7	-1698.9
40	41	1.690	-3002.6	-3816.2	-4757.6	-941.3
41	42	1.807	-3889.6	-4964.8	-5139.9	-175.2
42	43	2.777	-4834.7	-6199.2	-8306.1	-2106.9

43	44	3.617	-6016.4	-7843.2	-11047.8	-3204.6
44	45	4.414	-4022.1	-5184.8	-13104.8	-7919.9
45	46	5.169	-3093.8	-4157.6	-15466.3	-11308.7
46	47	1.680	-2290.0	-3208.9	-4546.3	-1337.4
47	48	1.536	-1581.8	-2364.7	-4096.7	-1731.9
48	49	1.329	-1169.2	-1741.1	-3446.0	-1704.9
49	50	1.178	-846.9	-1217.0	-2973.7	-1756.7
50	51	1.061	-580.7	-862.9	-2609.1	-1746.3
51	52	0.970	-364.6	-614.1	-2322.8	-1708.7
52	53	0.898	-195.9	-410.0	-2098.7	-1688.7
53	54	0.843	-71.8	-248.3	-1927.6	-1679.3
54	55	0.804	8.3	-127.6	-1803.4	-1675.8
55	56	0.778	46.5	-46.5	-1722.4	-1675.9
56	57	0.765	43.5	-4.1	-1682.5	-1678.4

TABLE A7 Positive factored shear and shear capacity of exterior frame of bridge 7931.

Location (m)	Element	Beam thickness (m)	Factored shear-*Strength I* (kN)	Factored shear-*Strength II* (kN)	Shear capacity (kN)	Shortage of capacity (kN)
0	1	0.765	-59.1	-10.2	2040.0	-1980.9
1	2	0.778	-18.7	50.1	2047.1	-1997.0
2	3	0.804	62.6	123.9	2061.5	-1937.7
3	4	0.843	164.3	213.0	1101.2	-888.2
4	5	0.898	260.6	299.7	1131.7	-832.0
5	6	0.970	350.9	381.1	1171.6	-790.5
6	7	1.061	435.0	462.9	1222.6	-759.8
7	8	1.178	523.6	570.8	1287.6	-716.8
8	9	1.329	621.0	692.3	1512.1	-819.8
9	10	1.536	716.8	812.3	1628.0	-815.7
10	11	1.680	822.5	896.4	1708.1	-811.7
11	12	5.169	918.5	998.2	3653.3	-2655.1
12	13	4.414	1008.5	1112.3	3092.2	-1980.0
13	14	3.617	-821.2	-781.3	2998.6	-2177.3
14	15	2.777	-763.2	-725.7	2530.2	-1767.0
15	16	1.807	-597.9	-566.8	2340.1	-1742.2
16	17	1.690	-554.5	-526.1	2274.8	-1720.3
17	18	1.597	-500.1	-474.3	2222.9	-1722.8
18	19	1.520	-445.1	-421.8	1829.3	-1384.1
19	20	1.456	-385.3	-364.3	1793.5	-1408.2
20	21	1.402	-328.2	-310.2	1763.4	-1435.2
21	22	1.356	-266.6	-250.5	1527.6	-1261.0
22	23	1.319	-204.2	-189.1	1506.5	-1302.2
23	24	1.287	-138.8	-124.8	1489.1	-1350.4
24	25	1.263	-72.1	-58.6	1475.3	-1403.3
25	26	1.244	-4.1	9.3	1324.4	-1315.2
26	27	1.230	65.0	78.0	1317.0	-1239.0
27	28	1.222	137.2	153.5	1312.6	-1159.0
28	29	1.220	208.6	229.8	1311.1	-1081.3
29	30	1.222	280.9	308.8	1312.6	-1003.8
30	31	1.230	355.8	392.2	1317.0	-924.8
31	32	1.244	429.5	475.4	1324.4	-849.0
32	33	1.263	503.6	560.9	1335.0	-774.1
33	34	1.287	577.7	651.1	1489.1	-838.1
34	35	1.319	651.8	743.2	1506.5	-763.3
35	36	1.356	723.9	835.5	1527.6	-692.1
36	37	1.402	797.3	932.3	1763.4	-831.0
37	38	1.456	865.1	1023.0	1793.5	-770.5
38	39	1.520	936.1	1121.9	1829.3	-707.4
39	40	1.597	1000.0	1213.9	2222.9	-1009.0
40	41	1.690	1062.1	1305.1	2274.8	-969.7
41	42	1.807	1115.2	1383.5	2340.1	-956.7
42	43	2.777	1321.6	1715.9	2530.2	-814.3
43	44	3.617	1394.9	1838.6	2998.6	-1160.0

44	45	4.414	-505.2	-480.2	3092.2	-2587.1
45	46	5.169	-443.9	-423.3	3653.3	-3209.4
46	47	1.680	-379.1	-362.3	1708.1	-1328.9
47	48	1.536	-321.4	-301.0	1628.0	-1306.6
48	49	1.329	-245.8	-237.7	1512.1	-1266.2
49	50	1.178	-173.3	-173.4	1287.6	-1114.1
50	51	1.061	-101.5	-109.1	1222.6	-1113.6
51	52	0.970	-27.7	-38.9	1171.6	-1132.8
52	53	0.898	50.0	38.2	1131.7	-1081.7
53	54	0.843	132.8	120.5	1101.2	-968.5
54	55	0.804	223.1	209.2	2061.5	-1838.4
55	56	0.778	323.2	306.9	2047.1	-1723.9
56	57	0.765	430.9	415.8	2040.0	-1609.1

TABLE A8 Negative factored shear and shear capacity of exterior frame of bridge 7931.

Location (m)	Element	Beam thickness (m)	Factored shear-*Strength I* (kN)	Factored shear-*Strength II* (kN)	Shear capacity (kN)	Shortage of capacity (kN)
0	1	0.765	-541.8	-530.0	-2040.0	-1498.2
1	2	0.778	-427.1	-411.2	-2047.1	-1620.0
2	3	0.804	-319.8	-303.0	-2061.5	-1741.8
3	4	0.843	-220.2	-206.1	-1101.2	-881.0
4	5	0.898	-131.0	-118.1	-1131.7	-1000.7
5	6	0.970	-49.1	-36.5	-1171.6	-1122.5
6	7	1.061	27.2	39.6	-1222.6	-1183.1
7	8	1.178	99.6	107.8	-1287.6	-1179.8
8	9	1.329	170.0	169.2	-1512.1	-1342.0
9	10	1.536	241.3	229.9	-1628.0	-1386.6
10	11	1.680	298.7	287.0	-1708.1	-1409.3
11	12	5.169	366.0	349.1	-3653.3	-3287.3
12	13	4.414	430.3	409.6	-3092.2	-2662.0
13	14	3.617	-1472.0	-1967.6	-2998.6	-1031.0
14	15	2.777	-1402.4	-1846.1	-2530.2	-684.0
15	16	1.807	-1200.5	-1510.5	-2340.1	-829.6
16	17	1.690	-1144.7	-1427.1	-2274.8	-847.7
17	18	1.597	-1080.7	-1331.5	-2222.9	-891.4
18	19	1.520	-1015.6	-1235.9	-1829.3	-593.4
19	20	1.456	-944.0	-1132.8	-1793.5	-660.7
20	21	1.402	-875.7	-1037.3	-1763.4	-726.1
21	22	1.356	-801.8	-938.5	-1527.6	-589.0
22	23	1.319	-729.4	-843.1	-1506.5	-663.4
23	24	1.287	-655.0	-747.8	-1489.1	-741.4
24	25	1.263	-580.5	-655.0	-1475.3	-820.4
25	26	1.244	-506.0	-564.3	-1324.4	-760.2
26	27	1.230	-431.7	-478.3	-1317.0	-838.7
27	28	1.222	-355.9	-392.7	-1312.6	-919.9
28	29	1.220	-282.7	-310.9	-1311.1	-1000.2
29	30	1.222	-210.3	-231.7	-1312.6	-1080.8
30	31	1.230	-137.1	-153.6	-1317.0	-1163.4
31	32	1.244	-66.9	-79.8	-1324.4	-1244.7
32	33	1.263	2.2	-11.2	-1335.0	-1323.8
33	34	1.287	69.9	56.5	-1489.1	-1419.3
34	35	1.319	136.2	122.3	-1506.5	-1370.2
35	36	1.356	199.7	184.8	-1527.6	-1327.9
36	37	1.402	263.0	247.0	-1763.4	-1500.4
37	38	1.456	319.5	301.9	-1793.5	-1474.0
38	39	1.520	378.6	357.8	-1829.3	-1450.7
39	40	1.597	431.9	408.9	-2222.9	-1791.0
40	41	1.690	484.1	458.8	-2274.8	-1790.7
41	42	1.807	529.0	501.7	-2340.1	-1811.1
42	43	2.777	696.0	661.0	-2530.2	-1834.2

43	44	3.617	755.7	718.1	-2998.6	-2242.9
44	45	4.414	-1107.3	-1264.9	-3092.2	-1827.4
45	46	5.169	-1022.1	-1125.7	-3653.3	-2527.5
46	47	1.680	-931.5	-1011.4	-1708.1	-696.6
47	48	1.536	-830.1	-930.1	-1628.0	-697.9
48	49	1.329	-727.3	-812.2	-1512.1	-699.9
49	50	1.178	-626.7	-691.5	-1287.6	-596.1
50	51	1.061	-526.9	-569.6	-1222.6	-653.0
51	52	0.970	-436.0	-460.2	-1171.6	-711.5
52	53	0.898	-350.3	-378.1	-1131.7	-753.6
53	54	0.843	-258.9	-295.0	-1101.2	-806.2
54	55	0.804	-161.5	-208.1	-2061.5	-1853.4
55	56	0.778	-59.0	-118.6	-2047.1	-1928.5
56	57	0.765	23.8	-44.2	-2040.0	-1995.8

TABLE A9 Positive factored moment and flexural capacity of exterior frame of bridge 7937 and 7938.

Location (m)	Element	Beam thickness (m)	Factored moment-*Strength I* (kNm)	Factored moment-*Strength II* (kNm)	Flexural capacity (kNm)	Shortage of capacity (kNm)
0	1	0.765	0.0	0.0	967.8	-967.8
1	2	0.779	505.3	488.3	990.5	-485.3
2	3	0.807	808.3	769.3	1036.5	-228.2
3	4	0.850	936.4	891.5	1106.8	-170.4
4	5	0.908	924.2	889.8	1203.3	-279.1
5	6	0.984	798.9	761.0	1329.0	-530.1
6	7	1.080	575.8	531.0	1488.2	-912.5
7	8	1.201	269.7	185.1	1688.2	-1418.5
8	9	1.354	-111.3	-197.6	1941.1	-2052.4
9	10	1.554	-565.3	-610.5	2271.6	-2836.9
10	11	1.717	-1095.5	-1092.6	2542.1	-3634.7
11	12	5.449	-1683.8	-1635.2	8712.0	-10347.2
12	13	4.787	-2294.7	-2184.0	7618.5	-9802.5
13	14	4.027	-5232.4	-4998.4	6361.8	-11360.3
14	15	2.952	-4162.1	-3972.3	4583.2	-8555.5
15	16	1.807	-3398.6	-3241.1	2689.8	-5930.9
16	17	1.690	-2549.7	-2448.1	2496.1	-4944.2
17	18	1.597	-1737.0	-1687.3	2342.1	-4029.4
18	19	1.520	-974.6	-973.1	4254.8	-5227.9
19	20	1.456	-263.5	-310.6	4042.7	-4306.2
20	21	1.402	388.5	355.3	3864.1	-3475.5
21	22	1.356	983.4	968.1	3713.9	-2730.5
22	23	1.319	1548.5	1582.0	3588.8	-2006.7
23	24	1.287	2051.4	2157.8	4965.3	-2807.4
24	25	1.263	2480.4	2680.1	4842.3	-2162.1
25	26	1.244	2833.5	3156.5	4748.4	-1591.9
26	27	1.230	3107.4	3520.2	4682.3	-1162.0
27	28	1.222	3289.7	3762.0	4642.9	-880.9
28	29	1.220	3377.2	3880.1	4629.9	-749.8
29	30	1.222	3375.3	3878.1	4642.9	-764.8
30	31	1.230	3283.9	3756.2	4682.3	-926.1
31	32	1.244	3098.0	3510.8	4748.4	-1237.6
32	33	1.263	2820.7	3143.6	4842.3	-1698.7
33	34	1.287	2464.4	2664.2	4965.3	-2301.1
34	35	1.319	2032.8	2139.2	3588.8	-1449.6
35	36	1.356	1527.8	1561.3	3713.9	-2152.6
36	37	1.402	961.2	946.0	3864.1	-2902.8
37	38	1.456	365.8	332.6	4042.7	-3676.8
38	39	1.520	-285.7	-332.8	4254.8	-4540.5
39	40	1.597	-995.2	-993.7	2342.1	-3335.8
40	41	1.690	-1754.6	-1704.9	2496.1	-4200.9
41	42	1.807	-2562.5	-2460.9	2689.8	-5150.7

42	43	2.952	-3404.5	-3247.0	4583.2	-7830.2
43	44	4.027	-4158.1	-3968.3	6361.8	-10330.2
44	45	4.787	-2951.4	-2813.9	7618.5	-10432.4
45	46	5.449	-2323.5	-2212.8	8712.0	-10924.8
46	47	1.717	-1698.2	-1649.6	2542.1	-4191.6
47	48	1.554	-1097.2	-1094.2	2271.6	-3365.8
48	49	1.354	-557.6	-602.8	1941.1	-2498.7
49	50	1.201	-97.8	-184.1	1688.2	-1785.9
50	51	1.080	286.4	201.8	1488.2	-1201.8
51	52	0.984	593.5	548.8	1329.0	-735.5
52	53	0.908	816.0	778.1	1203.3	-387.3
53	54	0.850	939.4	905.0	1106.8	-167.4
54	55	0.807	948.6	903.7	1036.5	-87.9
55	56	0.779	816.8	777.9	990.5	-173.7
56	57	0.765	509.7	492.7	967.8	-458.2

TABLE A10 Negative factored moment and flexural capacity of exterior frame of bridges 7937 and 7938.

Location (m)	Element	Beam thickness (m)	Factored moment-*Strength I* (kNm)	Factored moment-*Strength II* (kNm)	Flexural capacity (kNm)	Shortage of capacity (kNm)
0	1	0.765	0.0	0.0	-1493.0	-1493.0
1	2	0.779	59.4	4.8	-1530.2	-1535.0
2	3	0.807	63.9	-42.6	-1605.4	-1562.8
3	4	0.850	13.2	-142.5	-1720.6	-1578.1
4	5	0.908	-93.5	-295.4	-1878.7	-1583.2
5	6	0.984	-257.7	-502.6	-2084.4	-1581.9
6	7	1.080	-479.9	-764.9	-2345.2	-1580.3
7	8	1.201	-762.7	-1084.5	-2672.6	-1588.1
8	9	1.354	-1108.0	-1534.7	-3086.7	-1552.0
9	10	1.554	-1520.7	-2170.7	-3627.9	-1457.2
10	11	1.717	-2017.8	-2918.1	-4070.8	-1152.7
11	12	5.449	-2864.1	-3925.8	-14174.0	-10248.2
12	13	4.787	-3822.7	-5058.2	-12383.6	-7325.3
13	14	4.027	-8753.2	-11253.6	-20839.4	-9585.8
14	15	2.952	-7141.3	-9070.7	-14814.2	-5743.5
15	16	1.807	-5948.5	-7458.5	-8400.3	-941.7
16	17	1.690	-4793.0	-5993.8	-7744.1	-1750.2
17	18	1.597	-3707.3	-4621.7	-980.4	**3641.4**
18	19	1.520	-2706.6	-3353.8	-928.5	**2425.3**
19	20	1.456	-1795.5	-2245.7	-885.0	**1360.7**
20	21	1.402	-986.7	-1314.2	-848.4	**465.8**
21	22	1.356	-279.2	-499.1	-817.7	-318.6
22	23	1.319	314.2	128.0	-792.1	-920.1
23	24	1.287	704.1	620.7	-771.1	-1391.8
24	25	1.263	1013.0	952.4	-754.3	-1706.7
25	26	1.244	1262.9	1198.0	-741.5	-1939.4
26	27	1.230	1454.4	1382.7	-732.4	-2115.1
27	28	1.222	1587.7	1511.8	-727.1	-2238.9
28	29	1.220	1661.5	1584.0	-725.3	-2309.2
29	30	1.222	1659.5	1582.0	-727.1	-2309.1
30	31	1.230	1581.9	1506.0	-732.4	-2238.4
31	32	1.244	1444.9	1373.3	-741.5	-2114.7
32	33	1.263	1250.0	1185.1	-754.3	-1939.4
33	34	1.287	997.0	936.5	-771.1	-1707.5
34	35	1.319	685.5	602.1	-792.1	-1394.2
35	36	1.356	293.4	107.3	-817.7	-925.0
36	37	1.402	-301.3	-521.3	-848.4	-327.2
37	38	1.456	-1009.4	-1336.9	-885.0	**451.8**
38	39	1.520	-1817.7	-2267.9	-928.5	**1339.5**
39	40	1.597	-2727.2	-3374.4	-980.4	**2394.0**
40	41	1.690	-3724.8	-4639.3	-7744.1	-3104.7
41	42	1.807	-4805.7	-6006.6	-8400.3	-2393.7

42	43	2.952	-5954.3	-7464.4	-14814.2	-7349.8
43	44	4.027	-7137.3	-9066.7	-20839.4	-11772.7
44	45	4.787	-4974.6	-6330.3	-12383.6	-6053.2
45	46	5.449	-3851.6	-5087.1	-14174.0	-9086.9
46	47	1.717	-2878.5	-3940.2	-4070.8	-130.6
47	48	1.554	-2019.5	-2919.7	-3627.9	-708.1
48	49	1.354	-1513.1	-2163.0	-3086.7	-923.7
49	50	1.201	-1094.5	-1521.2	-2672.6	-1151.4
50	51	1.080	-746.0	-1067.7	-2345.2	-1277.5
51	52	0.984	-462.2	-747.1	-2084.4	-1337.3
52	53	0.908	-240.6	-485.5	-1878.7	-1393.2
53	54	0.850	-78.4	-280.3	-1720.6	-1440.3
54	55	0.807	25.4	-130.3	-1605.4	-1475.2
55	56	0.779	72.5	-34.1	-1530.2	-1496.1
56	57	0.765	63.8	9.2	-1493.0	-1502.2

TABLE A11 Positive factored shear and shear capacity of exterior frame of bridges 7937 and 7938.

Location (m)	Element	Beam thickness (m)	Factored shear-*Strength I* (kN)	Factored shear-*Strength II* (kN)	Shear capacity (kN)	Shortage of capacity (kN)
0	1	0.765	-86.4	-30.4	1058.1	-971.6
1	2	0.779	-31.5	46.0	1065.7	-1019.7
2	3	0.807	64.6	137.2	1081.2	-944.1
3	4	0.850	186.8	245.5	1104.9	-859.4
4	5	0.908	302.8	350.8	1137.5	-786.7
5	6	0.984	412.0	450.1	1179.9	-729.8
6	7	1.080	514.1	549.5	1233.6	-684.0
7	8	1.201	621.4	676.9	1301.0	-624.0
8	9	1.354	737.7	818.3	1386.2	-567.9
9	10	1.554	852.5	956.1	1497.7	-541.6
10	11	1.717	979.4	1072.5	1588.9	-516.4
11	12	5.449	1094.5	1193.2	3669.4	-2476.2
12	13	4.787	1204.3	1329.6	3300.7	-1971.1
13	14	4.027	-1106.6	-1061.5	2876.9	-1770.3
14	15	2.952	-798.9	-762.8	2277.2	-1478.3
15	16	1.807	-769.9	-736.1	1638.7	-868.8
16	17	1.690	-718.9	-687.1	1573.4	-854.5
17	18	1.597	-652.6	-624.0	1521.5	-868.9
18	19	1.520	-585.4	-559.2	1478.7	-893.4
19	20	1.456	-511.5	-487.7	1443.0	-931.5
20	21	1.402	-441.0	-420.3	1412.9	-971.9
21	22	1.356	-364.6	-346.9	1387.5	-1023.0
22	23	1.319	-287.9	-271.1	1366.4	-1078.6
23	24	1.287	-207.1	-191.5	1349.1	-1142.0
24	25	1.263	-124.9	-109.8	1335.3	-1210.4
25	26	1.244	-41.3	-26.1	1324.8	-1283.5
26	27	1.230	43.9	58.6	1317.3	-1258.7
27	28	1.222	132.6	149.9	1312.9	-1163.0
28	29	1.220	220.4	242.6	1311.4	-1068.8
29	30	1.222	309.2	338.6	1312.9	-974.3
30	31	1.230	401.1	439.9	1317.3	-877.4
31	32	1.244	491.5	540.6	1324.8	-784.1
32	33	1.263	582.2	642.7	1335.3	-692.6
33	34	1.287	673.0	750.7	1349.1	-598.4
34	35	1.319	763.7	861.0	1366.4	-505.4
35	36	1.356	851.8	971.2	1387.5	-416.3
36	37	1.402	941.6	1086.8	1412.9	-326.1
37	38	1.456	1024.3	1194.6	1443.0	-248.4
38	39	1.520	1110.8	1310.4	1478.7	-168.3
39	40	1.597	1188.3	1418.5	1521.5	-103.0
40	41	1.690	1263.5	1525.6	1573.4	-47.8
41	42	1.807	1326.9	1616.8	1638.7	-21.9

42	43	2.952	1361.5	1664.8	2277.2	-612.4
43	44	4.027	1723.7	2239.1	2876.9	-637.8
44	45	4.787	-665.1	-636.9	3300.7	-2635.6
45	46	5.449	-589.0	-563.5	3669.4	-3080.5
46	47	1.717	-508.8	-489.7	1588.9	-1080.1
47	48	1.554	-428.2	-407.6	1497.7	-1069.5
48	49	1.354	-338.0	-328.9	1386.2	-1048.2
49	50	1.201	-249.8	-249.4	1301.0	-1051.2
50	51	1.080	-161.4	-169.2	1233.6	-1064.4
51	52	0.984	-70.8	-82.2	1179.9	-1097.7
52	53	0.908	24.3	12.2	1137.5	-1113.2
53	54	0.850	125.1	112.3	1104.9	-979.9
54	55	0.807	234.3	219.4	1081.2	-846.9
55	56	0.779	354.3	337.0	1065.7	-711.5
56	57	0.765	482.6	467.0	1058.1	-575.5

TABLE A12 Negative factored shear and shear capacity of exterior frame of bridges 7937 and 7938.

Location (m)	Element	Beam thickness (m)	Factored shear-*Strength I* (kN)	Factored shear-*Strength II* (kN)	Shear capacity (kN)	Shortage of capacity (kN)
0	1	0.765	-553.5	-542.5	-1058.1	-504.6
1	2	0.779	-431.0	-416.0	-1065.7	-634.7
2	3	0.807	-315.8	-299.8	-1081.2	-765.5
3	4	0.850	-208.4	-194.9	-1104.9	-896.6
4	5	0.908	-111.1	-98.9	-1137.5	-1026.4
5	6	0.984	-21.3	-9.5	-1179.9	-1158.6
6	7	1.080	63.0	74.6	-1233.6	-1159.0
7	8	1.201	143.2	150.7	-1301.0	-1150.2
8	9	1.354	221.0	219.8	-1386.2	-1165.3
9	10	1.554	298.6	288.1	-1497.7	-1199.1
10	11	1.717	370.7	358.2	-1588.9	-1218.2
11	12	5.449	445.8	428.5	-3669.4	-3223.6
12	13	4.787	516.3	493.3	-3300.7	-2784.5
13	14	4.027	-1640.0	-2156.0	-2876.9	-720.9
14	15	2.952	-1321.2	-1635.7	-2277.2	-641.5
15	16	1.807	-1285.5	-1587.8	-1638.7	-51.0
16	17	1.690	-1226.1	-1501.1	-1573.4	-72.3
17	18	1.597	-1157.0	-1400.7	-1521.5	-120.8
18	19	1.520	-1086.3	-1299.9	-1478.7	-178.8
19	20	1.456	-1008.2	-1190.8	-1443.0	-252.2
20	21	1.402	-933.4	-1090.4	-1412.9	-322.4
21	22	1.356	-852.4	-984.8	-1387.5	-402.7
22	23	1.319	-773.0	-882.5	-1366.4	-483.9
23	24	1.287	-691.2	-780.2	-1349.1	-568.9
24	25	1.263	-609.2	-680.3	-1335.3	-655.0
25	26	1.244	-527.2	-582.5	-1324.8	-742.2
26	27	1.230	-445.3	-490.2	-1317.3	-827.1
27	28	1.222	-361.7	-397.0	-1312.9	-915.9
28	29	1.220	-280.8	-307.7	-1311.4	-1003.7
29	30	1.222	-200.8	-221.1	-1312.9	-1091.8
30	31	1.230	-119.9	-135.5	-1317.3	-1181.8
31	32	1.244	-42.1	-55.3	-1324.8	-1269.5
32	33	1.263	34.5	20.8	-1335.3	-1300.9
33	34	1.287	109.6	96.0	-1349.1	-1239.6
34	35	1.319	183.2	169.2	-1366.4	-1183.2
35	36	1.356	253.7	238.8	-1387.5	-1133.8
36	37	1.402	324.1	308.2	-1412.9	-1088.8
37	38	1.456	387.1	368.9	-1443.0	-1055.8
38	39	1.520	453.1	431.9	-1478.7	-1025.6
39	40	1.597	512.3	489.1	-1521.5	-1009.2
40	41	1.690	570.0	544.8	-1573.4	-1003.4
41	42	1.807	619.1	591.6	-1638.7	-1019.6

42	43	2.952	641.7	611.6	-2277.2	-1635.5
43	44	4.027	917.1	878.9	-2876.9	-1959.8
44	45	4.787	-1193.9	-1357.5	-3300.7	-1943.2
45	46	5.449	-1097.8	-1210.8	-3669.4	-2458.6
46	47	1.717	-997.3	-1086.0	-1588.9	-502.9
47	48	1.554	-886.2	-984.1	-1497.7	-513.6
48	49	1.354	-777.3	-863.4	-1386.2	-522.8
49	50	1.201	-669.9	-737.4	-1301.0	-563.5
50	51	1.080	-562.7	-609.2	-1233.6	-624.4
51	52	0.984	-464.0	-492.4	-1179.9	-687.5
52	53	0.908	-370.5	-402.8	-1137.5	-734.7
53	54	0.850	-271.2	-311.8	-1104.9	-793.2
54	55	0.807	-165.8	-216.6	-1081.2	-864.7
55	56	0.779	-54.9	-118.8	-1065.7	-946.9
56	57	0.765	33.1	-36.0	-1058.1	-1022.1

NEW MEXICO DEPARTMENT OF TRANSPORTATION

RESEARCH BUREAU

Innovation in Transportation

Strengthening Reinforced Concrete Bridges in New Mexico Using Fiber Reinforced Polymers:

Report II – Design Method for Strengthening K-Frame Bridges Using FRP

Prepared by:
University of New Mexico
Department of Civil Engineering
Albuquerque, NM

Prepared for:
New Mexico Department of Transportation
Research Bureau
Albuquerque, New Mexico

In Cooperation with:
The US Department of Transportation
Federal Highway Administration

Report NM06TT-01

FEBRUARY 2009

orm DOT F 1700.7 (8-72)

1. Report No.	2. Government Accession No.	3. Recipient's Catalog No.
NM06TT-01		

4. Title and Subtitle	5. Report Date
Strengthening Reinforced Concrete Bridges in New Mexico Using Fiber Reinforced Polymers Report II: Design Method for Strengthening K-Frame Bridges Using FRP	March 2008 6. Performing Organization Code
7. Author(s) M. M. Reda Taha, K. K. Choi, M. Azarbayejani	8. Performing Organization Report No.
9. Performing Organization Name and Address University of New Mexico Department of Civil Engineering Albuquerque, NM 87131	10. Work Unit No. (TRAIS) 11. Contract or Grant No. CO4961
12. Sponsoring Agency Name and Address Research Bureau New Mexico Department of Transportation 7500-B Pan American Freeway NE Albuquerque, NM 87109	13. Type of Report and Period Covered 14. Sponsoring Agency Code

15. Supplementary Notes

16. Abstract

The objective of this report is to provide detailed information about the design methods used to determine strengthening alternatives for the concrete frame bridges #7930, 7931, 7937 and 7938 at Tucumcari, New Mexico. Several strengthening alternatives were considered. Further details on the design of Fiber Reinforced Polymer (FRP) strips, the chosen strengthening alternative, are discussed. Locations and length requirements of the strengthening strips for the four bridges are identified. Guidelines for the application of the FRP material based on guidelines by the American Concrete Institute and other international agencies are provided.

17. Key Words:	18. Distribution Statement
Concrete frame bridges, AASHTO LRFD Bridge Design Specification, Fiber reinforced polymers.	Available from NMDOT Research Bureau

19. Security Classif. (of this report)	20. Security Classif. (of this page)	21. No. of Pages	22. Price
None	None	12	

STRENGTHENING REINFORCED CONCRETE BRIDGES IN NEW MEXICO USING FIBER REINFORCED POLYMERS

Report II: Design Method for Strengthening K-Frame Bridges Using FRP

by

M. M. Reda Taha
K. K. Choi
M. Azarbayejani
University of New Mexico
Department of Civil Engineering

Prepared for:
New Mexico Department of Transportation, Research Bureau

A Report on Research Sponsored by:
New Mexico Department of Transportation, Research Bureau

In Cooperation with the
U.S. Department of Transportation, Federal Highway Administration

March 2008

NMDOT, Research Bureau
7500-B Pan American Freeway NE
Albuquerque, NM 87109

PREFACE

The purpose of this research is to evaluate the structural capacity of the concrete frame bridges #7930, 7931, 7937 and 7938 at Tucumcari, New Mexico and evaluate their need for strengthening to meet AASHTO safety requirements. This report provides detailed information about the design methods used to determine the strengthening alternatives for these bridges.

NOTICE

DISCLAIMER

ABSTRACT

The objective of this report is to provide detailed information about the design methods used to determine strengthening alternatives for the concrete frame bridges #7930, 7931, 7937 and 7938 at Tucumcari, New Mexico. Several strengthening alternatives were considered. Further details on the design of Fiber Reinforced Polymer (FRP) strips, the chosen strengthening alternative, are discussed. Locations and length requirements of the strengthening strips for the four bridges are identified. Guidelines for the application of the FRP material based on guidelines by the American Concrete Institute and other international agencies are provided.

TABLE OF CONTENTS

TABLES

FIGURES

STRENGTHENING BRIDGES USING FRP

According to AASHTO (1), the need for strengthening of concrete structures can be determined by considering Eq. (1)

$$\phi M_n \geq M_u \tag{1}$$

where:

ϕ = strength reduction factor which is different in moment and shear

M_n = nominal flexural strength

M_u = factored applied moment.

when ϕM_n is less than M_u the concrete structures need to be strengthened by proper method. According to the results of calibrated FE analysis shown in Report (1), it was concluded that all the K-frames (Bridges # 7930, 7931, 7937 and 7937) require strengthening as they showed shortage in negative moment capacity around the K-frame connections. Such strengthening can be performed by providing additional negative moment reinforcement. It was suggested that strengthening be performed by attaching/bonding Fiber reinforced polymers (FRP) reinforcement to the top concrete fibers at the K-frame connections. Fiber Reinforced Polymer (FRP) reinforcement has been recommended as a strengthening material when the moment capacity of reinforced concrete sections is not sufficient (2). Numerous applications of FRP for strengthening bridges worldwide have shown FRP reinforcement to be an efficient strengthening method (2 and 3).

The moment resistance to be provided by FRP can be calculated as

$$M_u - \phi M_n \leq \phi M_{frp} \tag{2}$$

M_u = factored moment

M_n = nominal moment-carrying capacity.

According to the American Concrete Institute (ACI) Committee on FRP ACI 440 (2) and researchers Teng et al. (3), the moment capacity of a reinforced concrete section strengthened with FRP ϕM_{frp} can be computed as

$$\phi M_{frp} = \phi \varphi_{frp} A_f E_f \varepsilon_{fe} \cdot jd \qquad (3)$$

φ_{frp} = additional reduction factor (=0.85)

A_f = area of FRP reinforcement

ε_{fe} = effective ultimate strain developing at FRP

E_f = Young's modulus of FRP

jd = length of moment arm.

The ACI 440 (2) design method is similar to ACI 318 (4) design method, which is based on strain-compatibility and force equilibrium using the equivalent concrete stress block (Fig. 1).

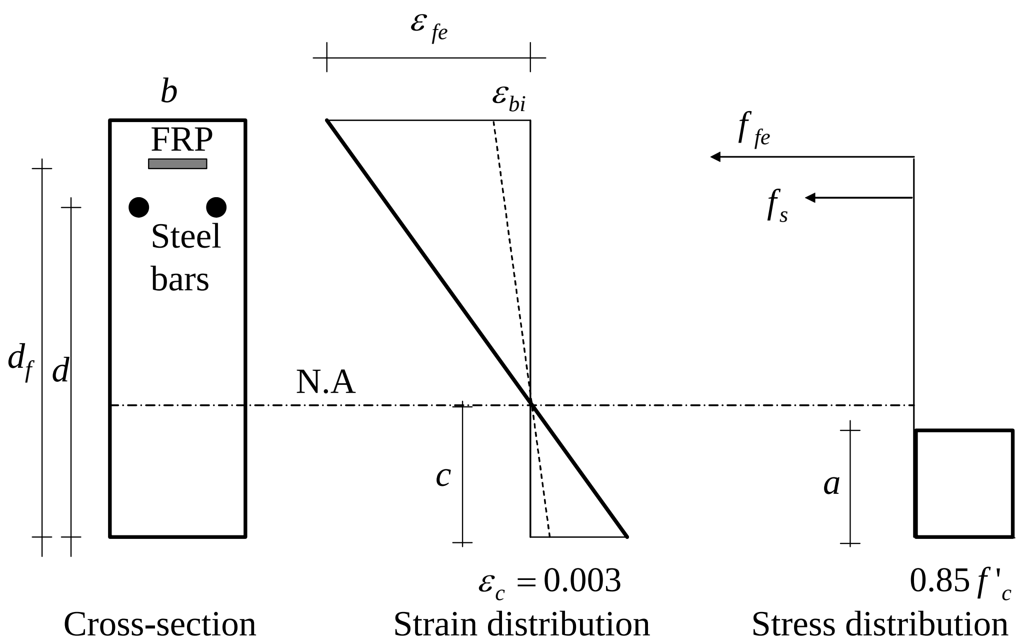

FIGURE 1 Stress and strain distribution of the concrete beam strengthened by FRP.

Considering that no tensile cracking was observed in the K-frames prior to strengthening, it can be assumed that the existing strain is negligible. Therefore, the effective strain of FRP at ultimate state is defined as

$$\varepsilon_{fe} = 0.003\left(\frac{d_f - c}{c}\right) \le \kappa_m \cdot \varepsilon_{fu} \tag{4}$$

d_f = effective depth for FRP reinforcement

c = depth of compression zone

κ_m = bond-dependent coefficient for flexure

ε_{fu} = design rupture strain of the FRP reinforcement.

Durability experiments and experiences by ACI 440 (2) and the European code for strengthening of concrete structures using FRP (5) show Carbon Fiber Reinforced Polymer (CFRP) as the most durable FRP material. Strengthening using CFRP strips was considered. For this type of material ACI 440 design guidelines recommend using bond-dependent coefficient for flexure κ_m = 0.9.

DESIGN OF FRP STRENGTHENING STRIPS

In this section, first, the design method for an exterior frame of bridge 7937 is presented as an example. According to the results of Finite Element (FE) analysis shown in Report (1), the maximum shortage of negative moment ($M_u - \phi M_c$) in Eq. (2) is 3,788 kN.m at the connection (x = 17 m measured from the bridge end as shown in Figure 2). consider Two alternative types of FRP are considered: Carbon Fiber Reinforced Polymers (CFRP) and Glass Fiber Reinforced Polymers (GFRP). While CFRP is known for its high strength and durability, GFRP is known for its relatively low cost. Both materials have been used for strengthening bridges. From Eq. (3) and Eq. (4), the required area of FRP reinforcement can be evaluated as

For CFRP with $E_f = 150{,}000\, MPa$ and $\varepsilon_{fu} = 0.0134$

$$A_f = \frac{M_u - \phi M_c}{\kappa_m \cdot \varepsilon_{fu} E_f \phi \varphi_{frp} \cdot jd} = \frac{3788}{0.9 \cdot 0.0134 \cdot 150000 \cdot 0.85 \cdot 0.85 \cdot 0.9 \cdot 1.8} \times 1000 = 1789\, mm^2$$

For GFRP with $E_f = 42{,}000\, MPa$ and $\varepsilon_{fu} = 0.0165$

$$A_f = \frac{M_u - \phi M_c}{\kappa_m \cdot \varepsilon_{fu} E_f \phi \varphi_{frp} \cdot jd} = \frac{3788}{0.9 \cdot 0.0165 \cdot 42000 \cdot 0.85 \cdot 0.85 \cdot 0.9 \cdot 1.8} \times 1000 = 5190\, mm^2$$

It can be observed that the required amount of Glass Fiber Reinforced Polymer (GFRP) for strengthening the bridge is significantly large because of the relatively lower stiffness of GFRP compared with CFRP. Thus, it is recommended to use Carbon Fiber Reinforced Polymer (CFRP) strips with high stiffness and very high durability. In the above calculation, length of moment arm after application of FRP is assumed as

$jd = 0.85d$. Based on the calculation, CFRP needs to be applied between x = 16.2 m (53 inch) and 20.1 m (66 inch).

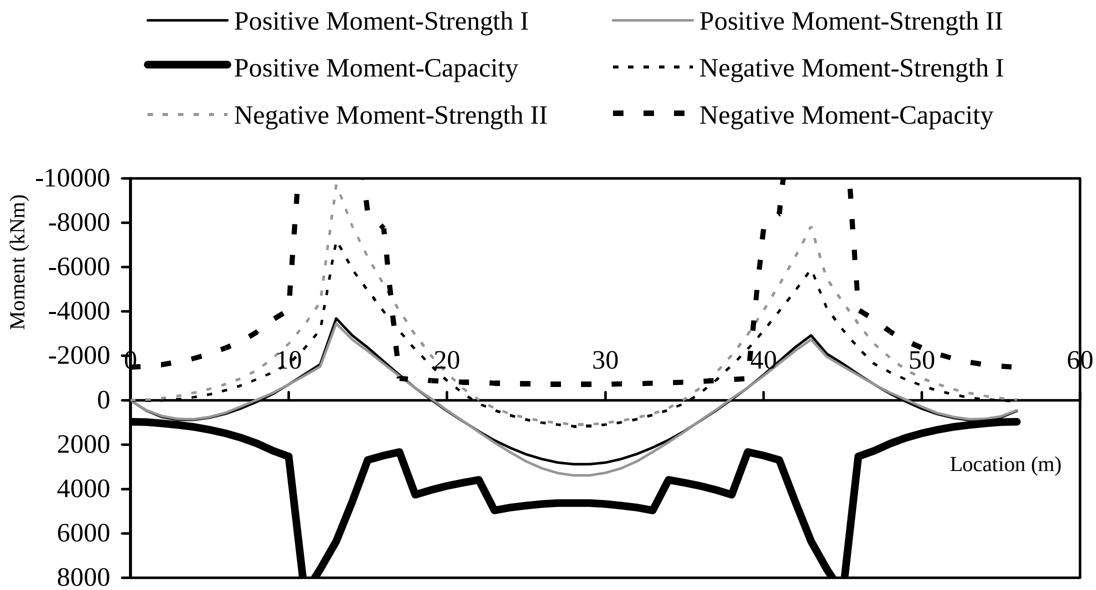

FIGURE 2 Factored moment and capacity of exterior beam of bridge 7937.

Considering the required area of CFRP material, it can be shown that 4 layers of CFRP strips, with each strip having a cross-section of 305 mm (1 feet) wide and 1.52 mm thick (0.06 inch) was sufficient to reinforce each K-frame. CFRP strips are typically produced with maximum length of 13 feet long (3.96 m). Fig. 3 presents a schematic figure showing the layout of CFRP strips for strengthening the exterior K-frame of bridge 7937. As shown in the figure, for strengthening the concrete frames for negative moment capacity, the FRP strips need to be applied at the connection of the K-frame.

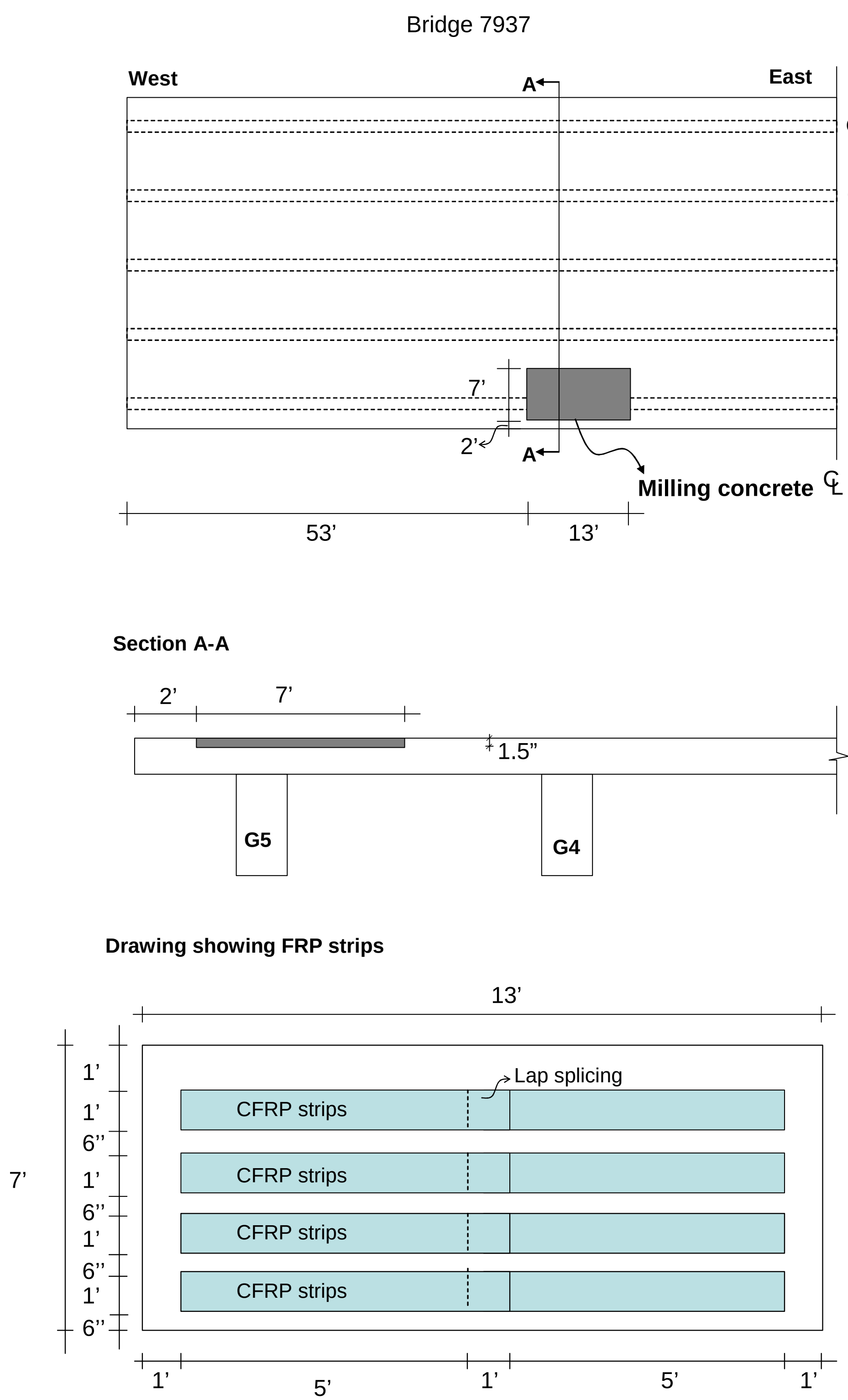

FIGURE 3 Schematic figure showing the layout of CFRP strips for strengthening the exterior girder of bridge 7937.

As the FRP strips provided by manufacturers were not long enough to cover the area that needed strengthening, two CFRP strips were overlapped considering the lap length defined by ACI 440, NCHRP Report (6) and recommended by other researchers (3). The total amount of CFRP strips required strengthening the four K-frame bridges at Tucumcari, New Mexico are presented in Table 1.

Table 1 Required amount of FRP strips and their locations for strengthening bridges.

		Required amount of FRP strips (mm^2)	Location of FRP strips, distance from the edge of the bridges
Bridge 7930	Exterior girder	1021	(13 m ~ 17 m) and (40 m ~ 44 m)
	Interior girder	828	(13 m ~ 17 m) and (40 m ~ 44 m)
Bridge 7931	Exterior girder	862	(13 m ~ 17 m) and (40 m ~ 44 m)
	Interior girder	1230	(13 m ~ 17 m) and (40 m ~ 44 m)
Bridge 7937	Exterior girder	1789	(16.2 m ~ 20.1 m) and (36.9 m ~ 40.8 m)
	Interior girder	2212	(15 m ~ 20 m) and (37 m ~ 42 m)
Bridge 7938	Exterior girder	1789	(17 m ~ 20 m) and (37 m ~ 40 m)
	Interior girder	2212	(15 m ~ 20 m) and (37 m ~ 42 m)

ALTERNATIVE STRENGTHENING METHODS

Recently, several alternative techniques using FRP materials for strengthening of reinforced concrete structures have been investigated and recommended by others. Near-surface mounted (NSM) reinforcement was recommended as a good alternative when large area of FRP is needed (7 and 8). A schematic figure showing the application of NSM-FRP bars is presented in Fig. 4. In this section, the design method for an exterior frame of bridge 7937 is presented as an example. As described in Report (1), the maximum shortage of negative moment ($M_u - \phi M_c$) is 3,788 kN.m at the K-frame connection (*x* = 17 m). From Eqs. (3) and (4), using CFRP with $E_f = 150{,}000\,MPa$ and

$\varepsilon_{fu} = 0.0134$, 7 layers of CFRP bars, whose diameters are 19 mm (0.75 inch) and length is 3.96 m (13 feet), are recommended.

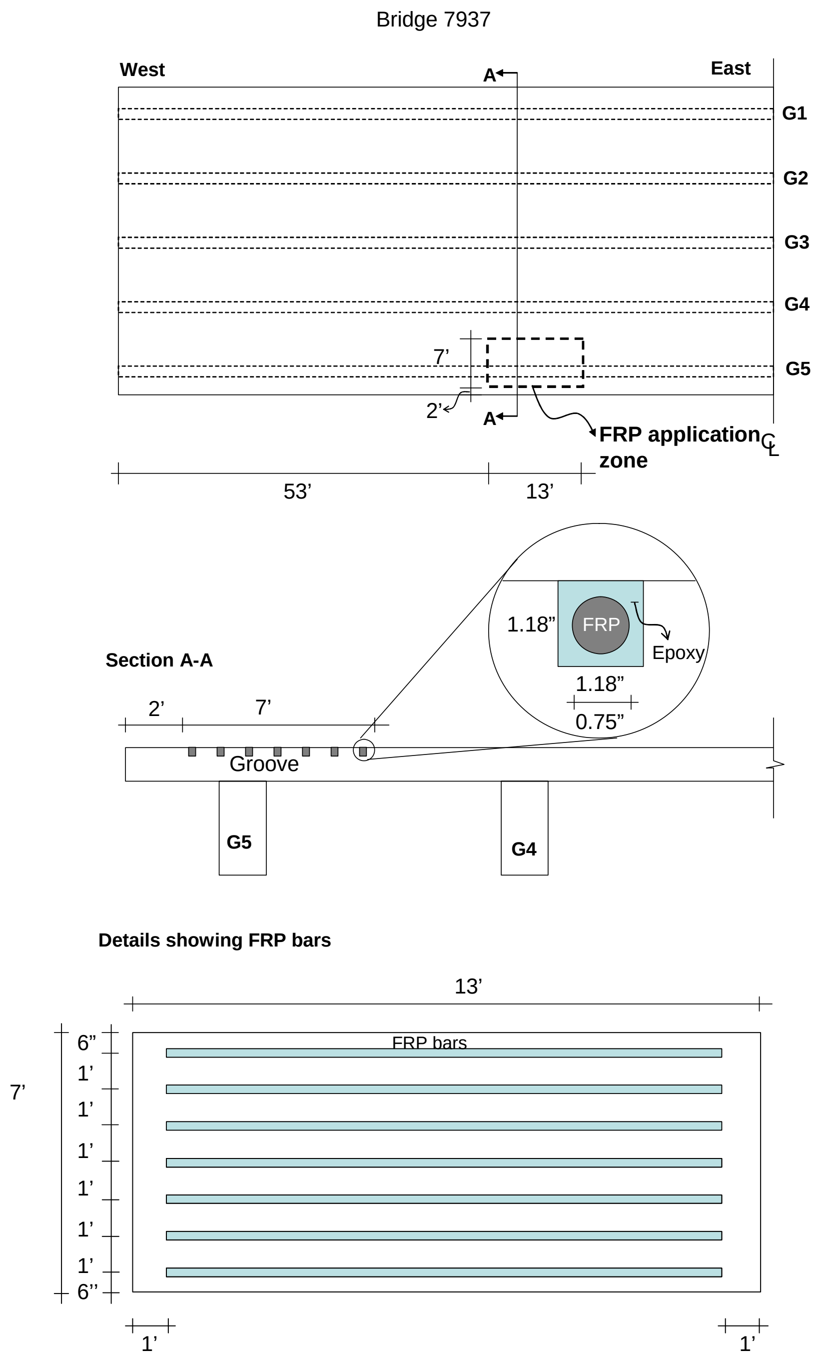

FIGURE 4 Schematic figure showing the layout of NSM-CFRP bars for strengthening the exterior girder of bridge 7937.

For the application of NSM FRP bars, the concrete grooves needed to be prepared were 30 mm (1.18 inch) in width and 3.96 m (13 feet) in length. Generally, application of NSM-FRP bars is similar to the application of FRP strips. However, instead of milling of whole concrete surface in construction zone, several grooves are needed by using saw cut machine. The FRP was installed with resin in the groove. Here it is noted that NSM FRP technique may not require finishing by other layers or topping such as asphalt or mortar because the FRP is not exposed to the air directly unlike the FRP strips method. The CFRP was applied from the top of the bridge, the ease of application enabled easy installation of wide CFRP strips. Therefore, it was decided that the CFRP strips strengthening alternative would be used for strengthening the K-frame bridges.

APPLICATION OF FRP STRIPS FOR STRENGTHENING BRIDGES

The application of FRP strips were performed according to standard methods as specified by ACI 440 (2) and the recent NCHRP Report 514 (6). Several different types of materials were used to install the FRP strips. These materials included putty for filling concrete cracks and providing a leveled concrete surface, epoxy adhesive, and CFRP strips. The major steps for application of FRP strips are as follows.

Step 1: Concrete Surface Milling

Bridge 7937 which has a concrete surface at the top of the exterior girders. 1.5 inch of concrete surface needed to be milled to enable installing the CFRP strips. For other locations on the bridge that are covered by asphalt instead of concrete, all asphalt in the FRP application zone needed to be completely milled as shown in Fig. 3. The investigation showed no need to provide positive moment strengthening at the K-frame soffits. If such strengthening is sought, the concrete surface of the K-frame soffit will need to be prepared without milling.

Step 2: Concrete Surface Preparation

This step is the most important step in application of FRP strips because properly roughened and even concrete substrate is necessary for reliable performance of FRP strips (5 and 6). The acceptable unevenness, which indicates the maximum difference of the surface depth, is specified in current design provisions. In CEB-FIP code (5) and NCHRP Report (6), the allowable value of unevenness of the concrete surface is 4 mm (1/6 inch). If the surface is not even enough, putty needs to be applied to obtain better concrete surface. In addition, several aspects need to be considered.

(6) The concrete substrate needs to be sound with proper tensile strength. In CEB-FIP (5), the minimum tensile strength of concrete is 1.5 N/mm^2. The crack width should be less than 0.2 mm. In addition, the concrete surface should be clean and free from oil, water, or dust before application of FRP.

(7) Moreover, special care is needed to ensure hardening of the putty. Usually, the hardening time depending on the putty type used may vary from 1 day to 14 days.

Step 3: Application of FRP Strips

To attach FRP strips to concrete substrate, epoxy adhesive with sufficient bond strength is used. For strips, usually, epoxy is recommended, which is composed of resin and hardener to obtain high bond and tensile strength. Here, the specific mixing ratio between resin and hardener must be used according to the specification of the materials. After mixing the resin and hardener, within 80 % of the allowable working time (pot life), the FRP strips need to be applied (6). The epoxy pot life is usually less than 30 minutes, therefore, care should be considered in preparing all materials in place before mixing epoxy. The epoxy mixture should then be applied to the clean and prepared concrete surface and the FRP attached. Rolling equipment might be needed to ensure getting rid of all air bubbles from the interface.

Step 4: Curing and Finishing

After applying FRP, the construction site should be properly covered by plastic sheets for curing. When the epoxy is hardened, the site needs to be finished by casting a concrete cover. Latex modified concrete/mortar is recommended for batching the concrete cover for its significantly high bond strength compared to conventional concrete mortar and for its enhanced durability criteria. LMC is also known to have a low permeability making it a good alternative for protecting the CFRP strips. More detailed information about the procedure for the application of FRP strips and general consideration for design and application is presented in Reports (3) and (4).

REFERENCES

1. AASHTO. LRFD Bridge Design Specifications. *Manual for Condition Evaluation of Bridges*. American Association of State Highway and Transportation Officials. 2006 Interim revisions, Second Edition, Washington, D.C., 2006.

2. ACI 440 Committee. *Guide for the Design and Construction of Externally Bonded FRP Systems for Strengthened Concrete Structures*, ACI 440.2R-02, American Concrete Institute, Farmington Hills, MI, 2002.

3. Teng, J. G., J. F. Chen, S. T. Smith and L. Lam. *FRP Strengthened RC Structures*. First Edition. John Wiley and Sons, West Sussex, England, 2002.

4. ACI 318 Committee. *Building Code and Commentary*. ACI 318-05/318R-05, American Concrete Institute, Farmington Hills, MI, 2005.

5. CEB-FIP. Externally bonded FRP reinforcement for RC structures. TRB 14, 2001, p.124.

6. NCHRP Report 514. Bonded Repair and Retrofit of Concrete Structures using FRP Composites. *Recommended Construction Specifications and Process Control Manual*. Mirmiran, A., M. Shahawy, A. Nani and V. Karbahari, Eds., 2004.

7. De Lorenzis, L., A. Nanni. Characterization of FRP Rods as Near-Surface Mounted Reinforcement. *ASCE J. Composite for Construction*, Vol. 5, Issue 2, 2001, pp. 114-121.

8. De Lorenzis, L., J. G. Teng. Near-surface mounted FRP reinforcement: An emerging technique for strengthening structures. *Composites Part B: Engineering*, Vol. 38, No. 2, 2007, pp. 119-143.

NEW MEXICO DEPARTMENT OF TRANSPORTATION

RESEARCH BUREAU

Innovation in Transportation

Strengthening Reinforced Concrete Bridges in New Mexico Using Fiber Reinforced Polymers:

Report III: Implementation of FRP Design Alternative to K-Frame Bridge

Prepared by:
University of New Mexico
Department of Civil Engineering
Albuquerque, New Mexico 87131

Prepared for:
New Mexico Department of Transportation
Research Bureau
7500B Pan American Freeway NE
Albuquerque, New Mexico 87109

In Cooperation with:
The US Department of Transportation

Report
NM06TT-01

MARCH 2008

Form DOT F 1700.7 (8-72)

1. Report No.	2. Government Accession No.	3. Recipient's Catalog No.
NM06TT-01		

4. Title and Subtitle	5. Report Date
Strengthening Reinforced Concrete Bridges in New Mexico Using Fiber Reinforced Polymers Report III: Implementation of FRP Design Alternative to K-Frame Bridge	March 2008
	6. Performing Organization Code
7. Author(s)	**8. Performing Organization Report No.**
M. M. Reda Taha, K. K. Choi, M. Azarbayejani	
9. Performing Organization Name and Address	**10. Work Unit No. (TRAIS)**
University of New Mexico Department of Civil Engineering Albuquerque, NM 87131	**11. Contract or Grant No.** CO4961
12. Sponsoring Agency Name and Address	**13. Type of Report and Period Covered**
Research Bureau New Mexico Department of Transportation 7500-B Pan American Freeway NE Albuquerque, NM 87109	**14. Sponsoring Agency Code**

15. Supplementary Notes

16. Abstract

The purpose of this research is to evaluate the structural capacity of concrete frame bridges #7930, 7931, 7937 and 7938 at Tucumcari, New Mexico and to evaluate their need for strengthening to meet AASHTO safety requirements. This report provides detailed information about the implementation and installation of FRP strengthening alternative to one K-Frame bridge. The selected strengthening alternative is analyzed and details about implementation requirements are discussed. All installation steps are discussed and documented. Finally, information is provided about two field tests performed prior to and after the application of the FRP strengthening. The two field tests targeted calibrating the analytical model using the finite element method and validating the efficiency of the FRP strengthening.

17. Key Words:	18. Distribution Statement
Concrete frame bridges, AASHTO LRFD Bridge Design Specification, Fiber reinforced polymers.	Available from NMDOT Research Bureau

19. Security Classif. (of this report)	20. Security Classif. (of this page)	21. No. of Pages	22. Price
None	None	29	

STRENGTHENING REINFORCED CONCRETE BRIDGES IN NEW MEXICO USING FIBER REINFORCED POLYMERS

Report III: Implementation of FRP Design Alternative to K-Frame Bridge

by

M. M. Reda Taha
K. K. Choi
M. Azarbayejani
University of New Mexico
Department of Civil Engineering

Prepared for:
New Mexico Department of Transportation, Research Bureau

A Report on Research Sponsored by:
New Mexico Department of Transportation, Research Bureau

In Cooperation with the
U.S. Department of Transportation, Federal Highway Administration

March 2008

NMDOT Research Bureau
7500-B Pan American Freeway NE
Albuquerque, NM 87109

PREFACE

The purpose of this research is to evaluate the structural capacity of the concrete frame bridges #7930, 7931, 7937 and 7938 at Tucumcari, New Mexico and evaluate their need for strengthening to meet AASHTO safety requirements. This report provides detailed information about the implementation and installation of FRP strengthening alternative to one K-Frame.

NOTICE

DISCLAIMER

ABSTRACT

The purpose of this research is to evaluate the structural capacity of concrete frame bridges #7930, 7931, 7937 and 7938 at Tucumcari, New Mexico and to evaluate their need for strengthening to meet AASHTO safety requirements. This report provides detailed information about the implementation and installation of FRP strengthening alternative to one K-Frame bridge. The selected strengthening alternative is analyzed and details about implementation requirements are discussed. All installation steps are discussed and documented. Finally, information is provided about two field tests performed prior to and after the application of the FRP strengthening. The two field tests targeted calibrating the analytical model using the finite element method and validating the efficiency of the FRP strengthening.

TABLE OF CONTENTS

FIGURES

FRP DESIGN ALTERNATIVE FOR EXTERIOR GIRDER OF BRIDGE 7937

According to the results of FE analyses performed in Report (1), it was found that all the girders of Tucumcari, New Mexico bridges 7930, 7931, 7937 and 7938 showed shortage in negative moment capacity around the K-Frame connections. It was therefore recommended to strengthen these four bridges' girders using Fiber Reinforced Polymer (FRP). The moment resistance to be provided by FRP is calculated as

$$M_u - \phi M_n \leq \phi M_{frp} \qquad (1)$$

where:

M_u = factored applied moment

M_n = nominal moment-carrying capacity.

In ACI 440, ϕM_{frp} is evaluated as

$$\phi M_{frp} = \phi \varphi_{frp} A_f E_f \varepsilon_{fe} \cdot jd \qquad (2)$$

where:

φ_{frp} = additional reduction factor (=0.85)

A_f = area of FRP reinforcement

ε_{fe} = effective ultimate strain developing at FRP

E_f = Young's modulus of FRP

jd = length of moment arm.

The ACI 440 design method for FRP strengthened sections is basically similar to ACI 318 design method, which is based on strain-compatibility and equivalent concrete stress block (refer to Fig. 1). In this design, it is assumed that the existing strain is negligible compared with ultimate design strains. Moreover, considering the fact that no tension cracks were observed in the top of the K-Frame in the field inspection before strengthening, the existing service strains can be considered negligible. Therefore, the effective strain of FRP at ultimate state is defined as

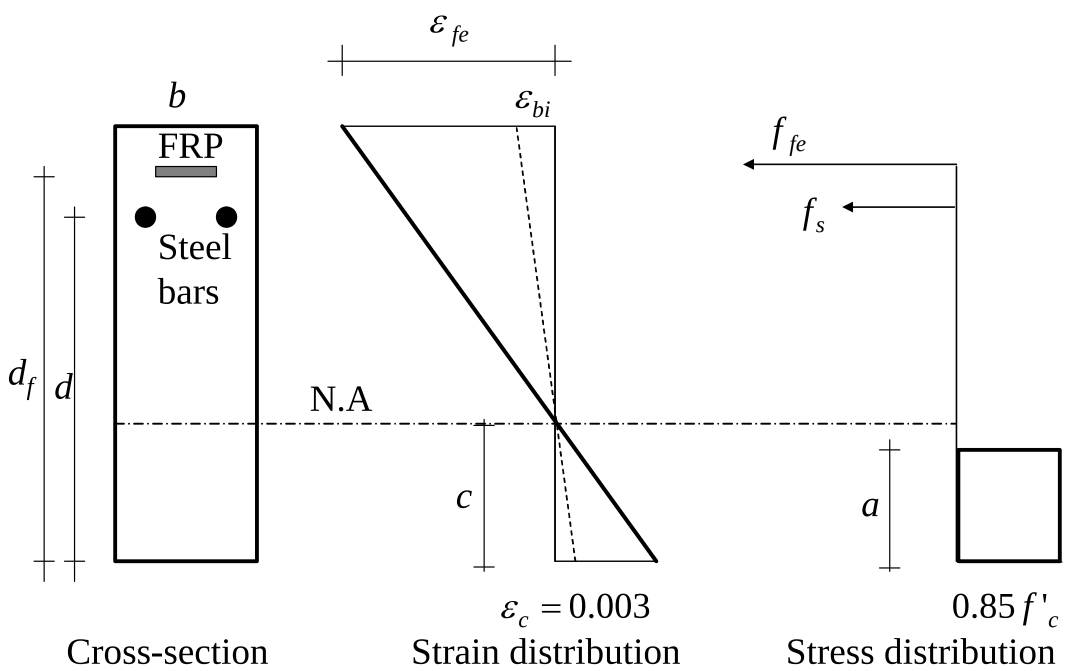

FIGURE 1 Stress and strain distribution of the concrete beam strengthened by FRP.

$$\varepsilon_{fe} = 0.003\left(\frac{d_f - c}{c}\right) \leq \kappa_m \cdot \varepsilon_{fu} \tag{3}$$

where:

d_f = effective depth for FRP reinforcement

c = depth of compression zone

κ_m = bond-dependent coefficient for flexure (=0.9 for Carbon Fiber Reinforced Polymer (CFRP) and Glass Fiber Reinforced Polymer (GFRP), ACI 440)

ε_{fu} = design rupture strain of the FRP reinforcement.

According to the results of Finite Element (FE) analyses, the exterior girder of bridge 7937, presented in Reports (1) and (2), the maximum shortage of negative moment capacity ($M_u - \phi M_c$) is 3,788 kN.m at the connection (x = 17 m). Please refer to Fig. 2.

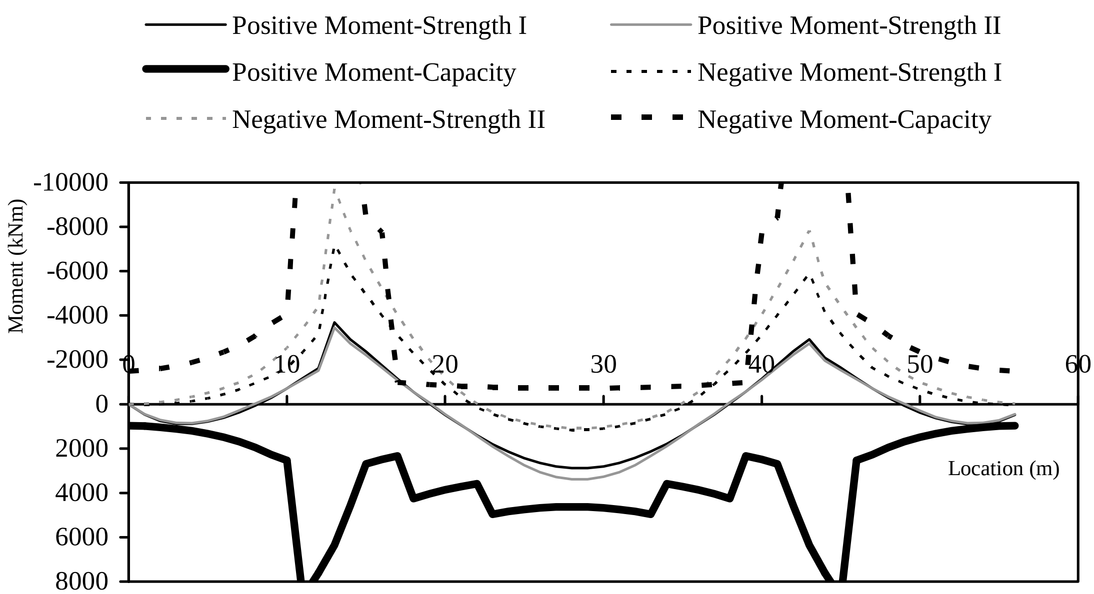

FIGURE 2 Factored moment and capacity of exterior beam of bridge 7937.

From Eqs. (2) and (3), the required amount of CFRP reinforcement can be evaluated as:

$$A_f = \frac{M_u - \phi M_c}{\kappa_m \cdot \varepsilon_{fu} E_f \phi \varphi_{frp} \cdot jd} = \frac{3788}{0.9 \cdot 0.0134 \cdot 150000 \cdot 0.85 \cdot 0.85 \cdot 0.9 \cdot 1.8} \times 1000 = 1789\, mm^2$$

CFRP was used (recommended in Report 2) for its enhanced strength and durability) with a Young's modulus of $E_f = 150{,}000\, MPa$ and an ultimate strain capacity of $\varepsilon_{fu} = 0.0134$. Moreover, it was assumed that the moment arm after application of FRP is *jd* to be *0.85d*. Based on the calculation, CFRP needed to be applied between x = 16.2 m (53 inch) and 20.1 m (66 inch). The required area of CFRP reinforcement was used for each K-Frame at both connections. In strengthening bridge 7937, one K-joint on one K-Frame only was reinforced for proof of method efficiency. The amount of CFRP reinforcement area required for strengthening one K-Frame at the K-connection on bridge 7937 was provided by means of 4 layers of CFRP strips, whose cross-section of CFRP strips is 1.52 mm thick (0.06 inch) and 305 mm (1 feet) wide. Since CFRP strips are not manufactured in 11 foot lengths to cover the entire application area, it was decided to overlap the CFRP strips using two 1.83 m (6 feet) CFRP strips.

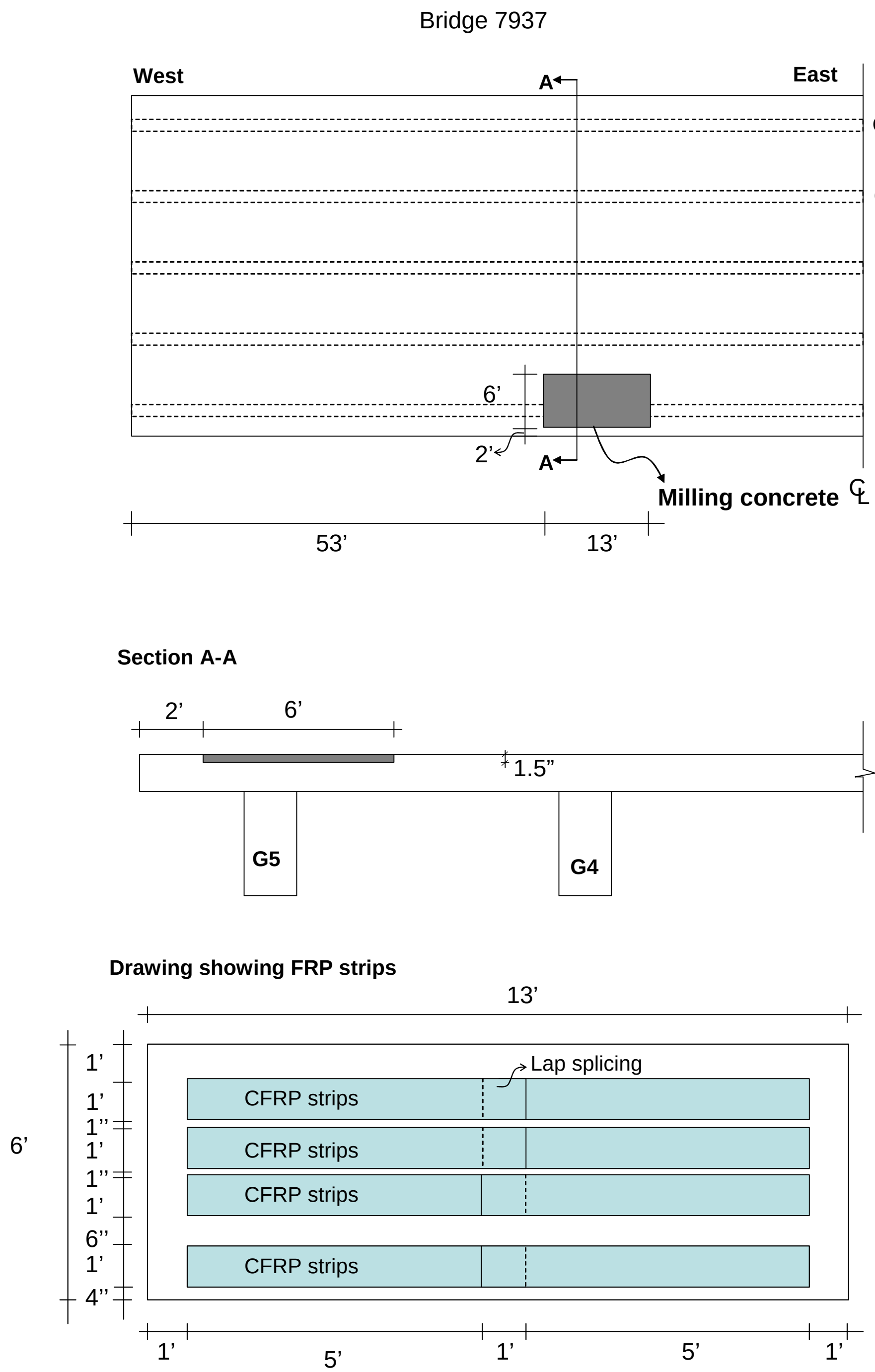

FIGURE 3 Schematic figure shows the layout of CFRP strips for strengthening the exterior girder of bridge 7937.

The CFRP strips were lap spliced to cover the entire strengthening zone. To ensure the performance of spliced CFRP strips, the lap splice location was alternated along the strengthening area such that no single section has more than 2 lap splices. This is shown in Fig. 3.

IMPLEMENTATION OF CFRP STRIPS TO EXTERIOR GIRDER OF BRIDGE 7937

Bridge 7937 was inspected and its concrete strength was evaluated. A structural analysis was performed (Report # 2) and the decision to strengthen one K-Frame connection on bridge 7937 was made. The bridge was to be strengthened using CFRP strips as shown in Fig. 3. Bridge strengthening preparation started on April 1st 2007 according to the original project schedule. The process continued between June 5th, 2007 and July 10th, 2007. The application of CFRP strips to an exterior girder of bridge 7937 as an example case for CFRP strengthening application was performed by the UNM research team, with the cooperation of New Mexico DOT in Tucumcari, New Mexico. It is worth noting that in the strengthening work of the bridge using CFRP strips, several different types of materials were used: putty, epoxy and CFRP. Therefore, the manufacturers' specifications of each material were considered in this installation. Moreover, the different material specifications were checked against the AASHTO (1) and ACI code requirements for CFRP materials.

Step 1: Concrete Surface Milling

As the bridge deck surface of the exterior girder of bridge 7937 was concrete, it needed to be milled to enable application of the CFRP strips. Approximately 1.5 inches of the concrete surface was milled according to the recommendation in Report (2). The milling process is shown in Fig. 4. The strengthening zone was marked first and then milled by a concrete milling machine attached to a wheel loader. The milled area was cleaned using air blowers and a construction vacuum as shown in Fig. 5. To obtain a surface with equal milling, the milling process was repeated twice.

FIGURE 4 Concrete surface milling showing the process of marking the zone and milling.

FIGURE 5 Concrete surface cleaning.

Step 2: Concrete Surface Preparation

The second step was to prepare the concrete surface. The procedure started by establishing an even surface with thickness differences less than 4 mm based on ACI 440 (2) and CEB-FIP code (3). Surface cracks formed due to the milling process were filled and the surface was made even. An even surface is essential to enable a good bond with the CFRP strips. To obtain an acceptable level of surface evenness, the concrete surface was first covered with a putty material in accordance with ACI 440 (1) and AASHTO (3) recommendations. The putty was applied to the application locations (Fig. 6) and then left to dry and bond to the concrete surface.

FIGURE 6 Application of putty material to obtain even concrete surface.

Here, several aspects need to be noted.

(8) Normally, putty material should be allowed to dry for a period dependent on the temperature at the time of application. The dry time will change significantly for low temperature versus high temperature application. Specifications by material manufactures should be carefully considered.

(9) The strengthening process was performed in June-July 2007, where high temperatures at the bridge site were observed (about 35 ^{o}C/90 ^{o}F). It was important to let the putty material dry for at least one week.

(10) If there are locations on the concrete surface where the putty application is too thick, the redundant putty needs to be removed before CFRP application.

Following the drying period, the concrete surface needs to be ground down to ensure evenness of the entire zone where CFRP will be applied. This process was performed using two different size grinding machines for overall and localized grinding as shown in Fig. 7(a) and 7(b) respectively. This step is very important for the application of CFRP strips because properly roughened and even concrete substrate is necessary for reliable performance of CFRP strips (4).

(a) Concrete grinder with double stone heads

(b) Concrete grinder with steel head

FIGURE 7 Concrete grinding.

Step 3: Application of CFRP Strips

After the concrete surface was ground and determined to not have any cracks, the epoxy adhesive was applied to bond the CFRP material. Epoxy is composed of resin and hardener in order to obtain the required bond and tensile strength. Epoxy 105 resin and slow hardener (206) produced by West System were used (Fig. 8). The epoxy resin was mixed as directed by the manufacturer At a mixing ratio (5 to 1) of resin to hardener. After mixing the resin and hardener to within 80 % of the allowable working time (pot life), the CFRP was applied (4). The pot life for the epoxy used was 20 to 25 minutes which represented enough time to lay down the CFRP strips on the locations identified on the bridge deck slab. Moreover, it is important to note that the epoxy hardening time is also a function of the temperature at time of mixing. The specifications by manufactures need to be considered carefully. During the hardening process (chemical reaction), epoxy becomes extremely hot, requiring special care by those applying it to the concrete surface.

FIGURE 8 Mixing resin and hardener according to specific mixing ratio.

Immediately after applying epoxy to the concrete surface, the CFRP strips were applied considering the locations marked and the lap splice alternating arrangement (Fig. 9). Here, because of the short pot life of the epoxy, it is recommended to mix enough resin and hardener to facilitate the application of one row of CFRP strips at a time.

FIGURE 9 CFRP strips attached to the concrete surface.

After applying the CFRP strips, proper pressure was applied to the CFRP for better attachment to the concrete surface (Fig. 10). Although not required the use of wood logs enabled uniform pressure distribution during the time of epoxy hardening.

FIGURE 10 Applying pressure for better attachment of CFRP strips.

Step 4: Curing and Finishing

After applying CFRP, the construction site was properly covered with plastic sheets to prevent exposure of the CFRP to rain and water. After the epoxy was fully hardened, on June 27th 2007, the construction site was covered by a cold dry asphalt mix. The asphalt mix was separated from the CFRP with a thick plastic sheet provided by NMDOT. The plastic sheet and the dry asphalt are shown in Fig. 11. The use of a dry asphalt mix was to prevent CFRP direct exposure to moisture, rain or traffic. This also enabled accessibility of the CFRP surface during the next phase of the project, which entailed the installation of monitoring sensors.

FIGURE 11 Construction zone covered with plastic sheets and dry asphalt mix.

ANALYSIS, VALIDATION OF FE MODELS AND CFRP EFFECTIVENESS

To validate the analytical prediction by FE analysis using SAP 2000®, a load test was performed before and after the application of CFRP strips. First, the concrete strain of the top of the exterior girder was monitored when subjected to a test truck (Fig. 12) with pre-determined weight. Detailed discussion on the calibration process is provided in Report 1. Moreover, strains on the top of the CFRP strips were monitored (after CFRP application) using the same test truck and weight. The ability of the CFRP strips to attain strain values in proportion with those strains observed at the concrete surface prior to strengthening ensured that the CFRP strips were properly attached to the concrete surface, they resisted the applied load and thus provide the needed strengthening for the K-Frame bridge. Fig. 13 shows the FE model of the exterior girder subjected to the truck load and the moment distribution obtained from the FE analysis. It is noted that in this analysis the bridge deck was taken into account in the calculation of effective width of the girder assuming elastic behavior during the loading test. This can be justified by the fact that the load of the test truck was significantly lower than the load carrying capacity of the bridge and thus the bridge behavior can be considered to follow linear elastic behavior.

FIGURE 12 Mack 10 yard dump truck as test truck with weight of 50 kips.

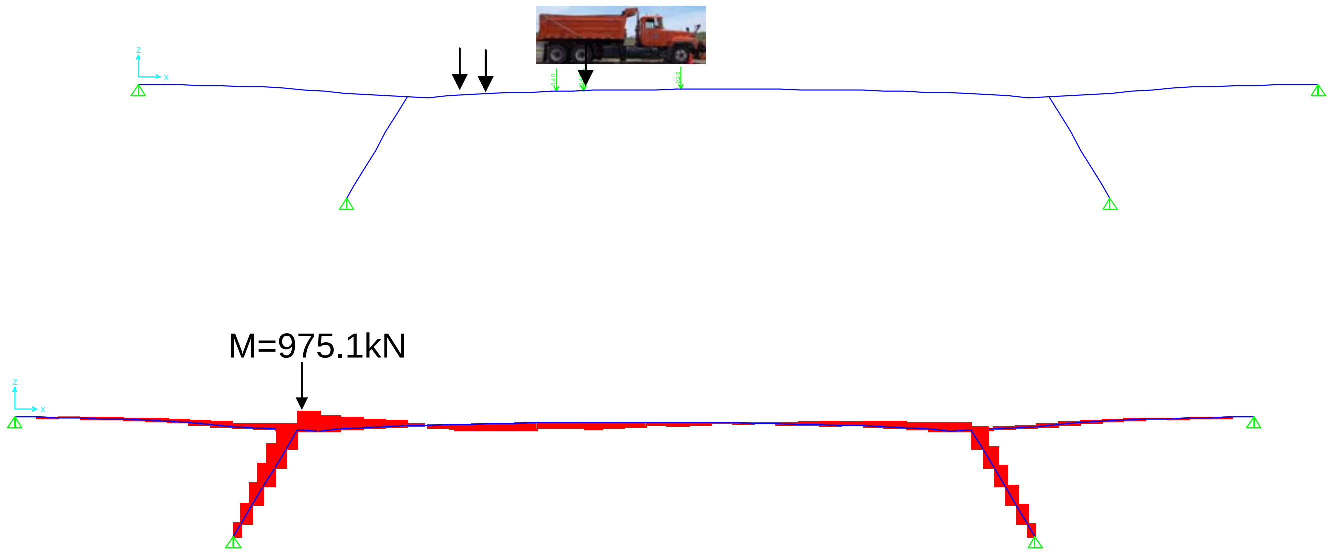

FIGURE 13 FE model of exterior girder subjected to truck load, and moment distribution throughout girder.

To compensate for the temperature effect, orthogonal strain gauges were placed as dummy gauges. The longitudinal gauges were used to measure the load effect and the dummy strain gauges were used to compensate temperature effects. The locations of strain gauges are shown in Fig. 14. The strain gauge on the top of concrete (prior to strengthening) and a dummy orthogonal gauge at this location are shown in Fig. 15. Moreover, strain gauges over the CFRP surface are shown in Fig. 16. User friendly data acquisition software under LabVIEW (4) programming environment was developed and used for measuring strain gauges on the concrete surface prior to CFRP strengthening and on the CFRP surface after strengthening. The strain gauges were connected to the data acquisition system which was connected to a Laptop computer (Fig. 17). Finally, a snap shot of the LabVIEW software for data analysis is shown in Fig. 18. The data acquisition system along with the developed LabVIEW software enabled observing and analyzing the data in the field during the load test.

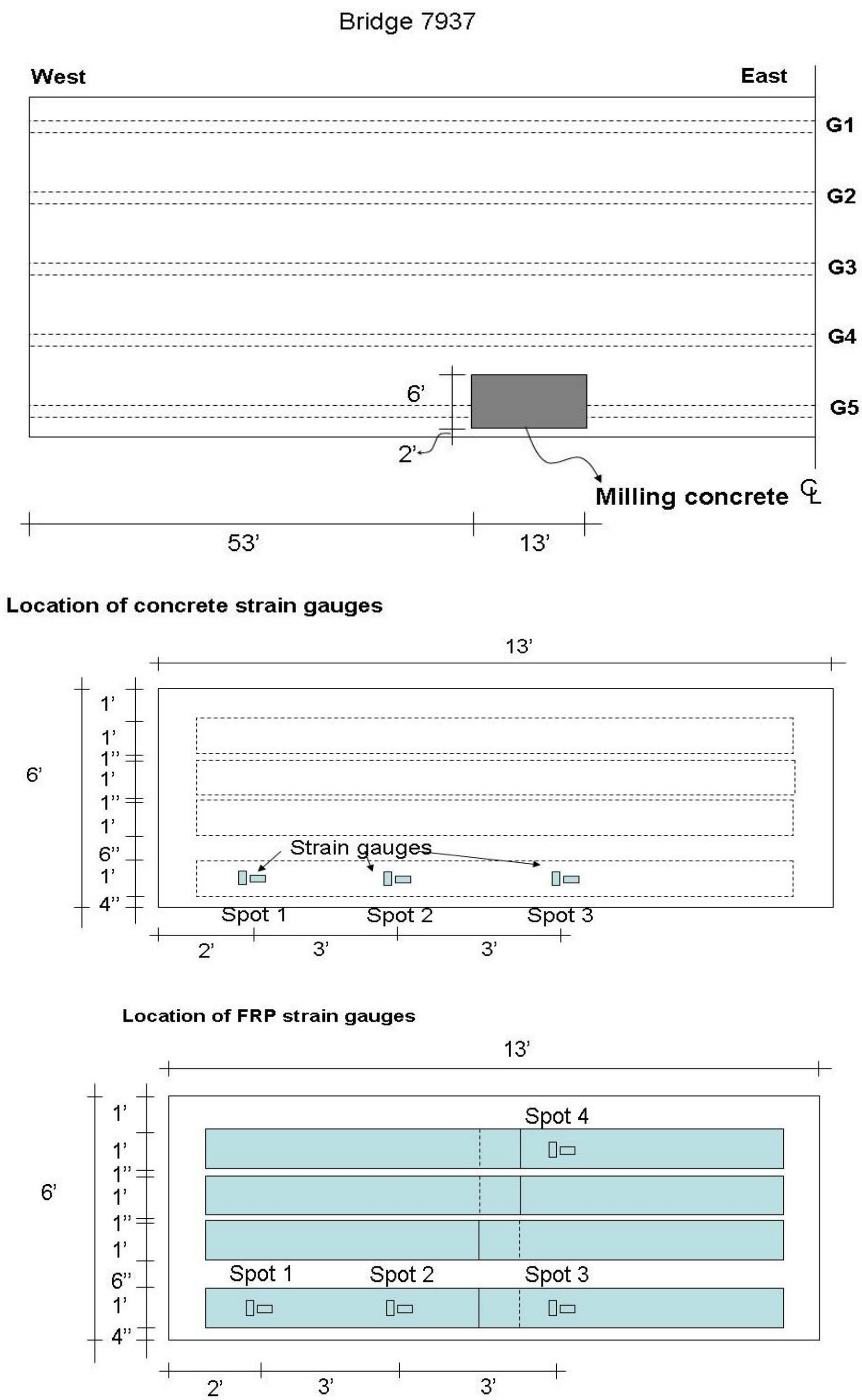

FIGURE 14 Schematic figure showing the location of strain gauges.

FIGURE 15 Concrete strain gauges attached to the concrete surface.

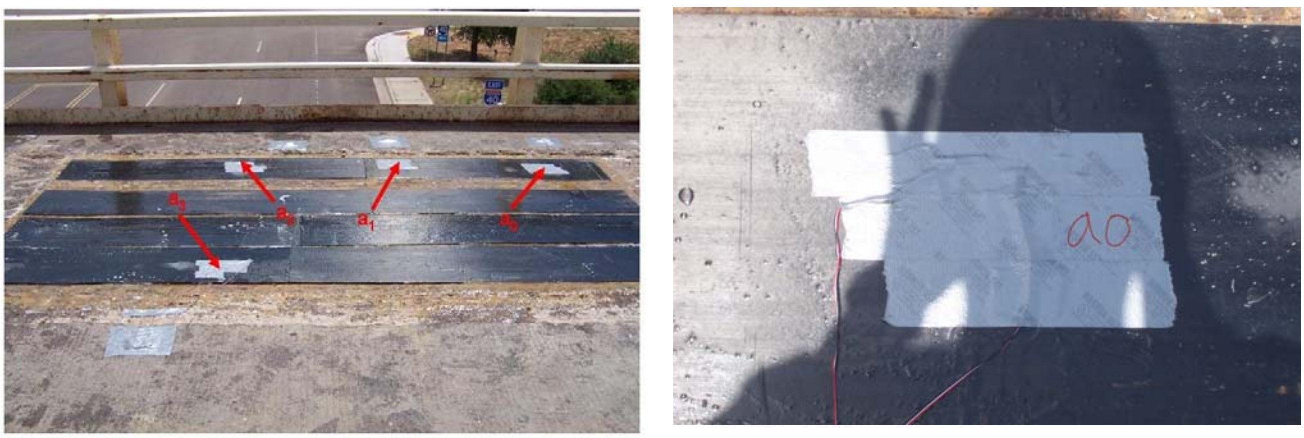

FIGURE 16 Strain gauges attached to CFRP strips.

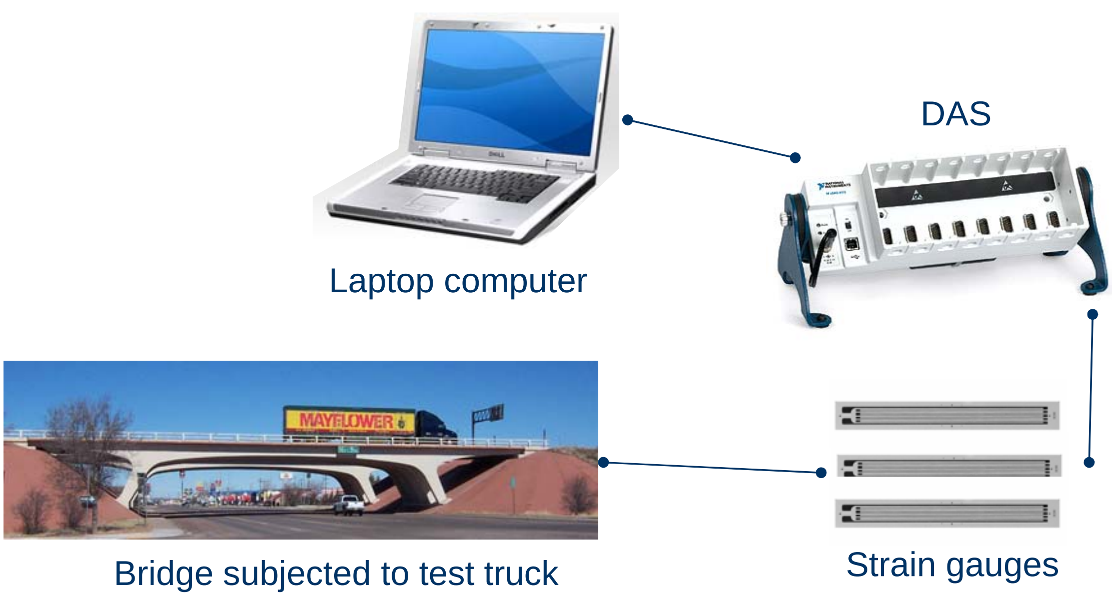

FIGURE 17 Data acquisition system and laptop computer used for data acquisition.

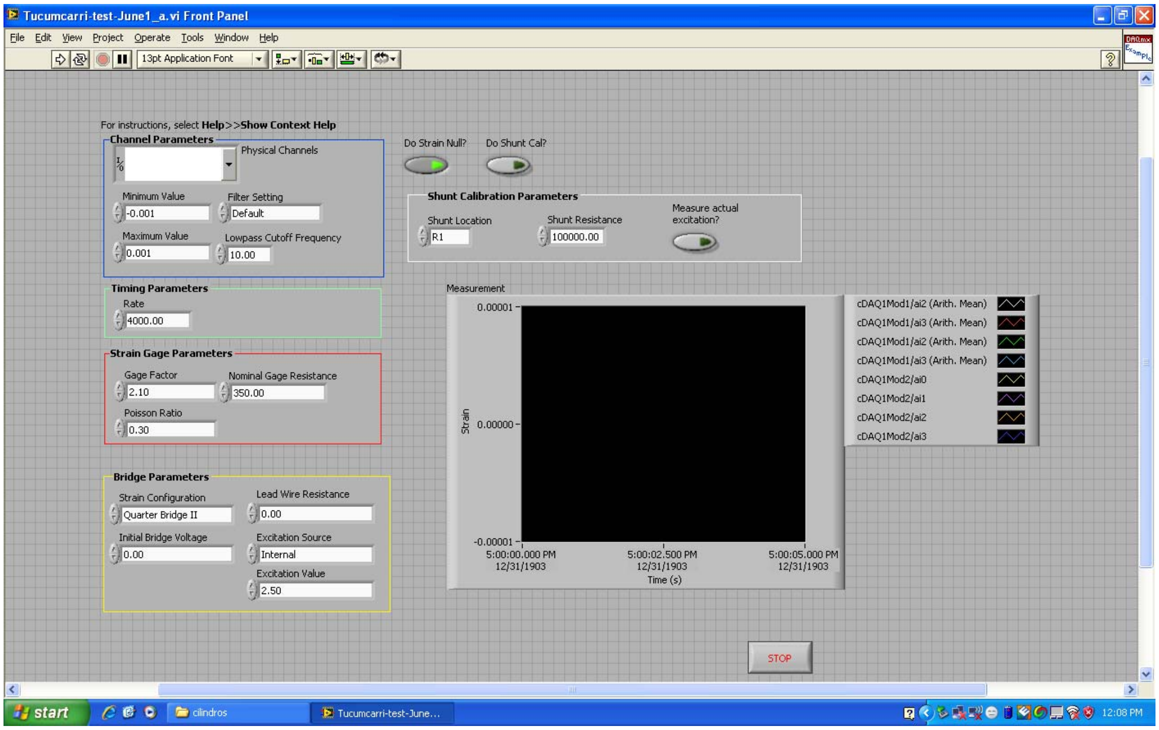

FIGURE 18 Snap shot of LabVIEW user-friendly software developed by research team and used for strain measurements based on dual strain measurements at each sensing location.

Here, a comparison of the strain measurements observed at spot 1 in Fig. 14 with that predicted by calibrated FE analysis was done. The strain measurements on the concrete surface prior to strengthening are shown in Fig. 19. It can be observed that under the designated test truck, 21.7 με (με = micro strain) was recorded as the maximum strain on the concrete surface. This number is very close to the maximum predicted strain on concrete surface of 23.2 με predicted from the FE analysis. Similar FE predicted strains were confirmed by measurements at other locations of the bridge deck. These results validate the finite element model of the K-Frame bridge presented here and in Report 2. Validation of the finite element model was an essential step when designing the CFRP strengthening system. Fig. 19 shows the change in the strain at spot 1 as the truck was proceeding towards the construction/strengthening location at the K-Frame joint.

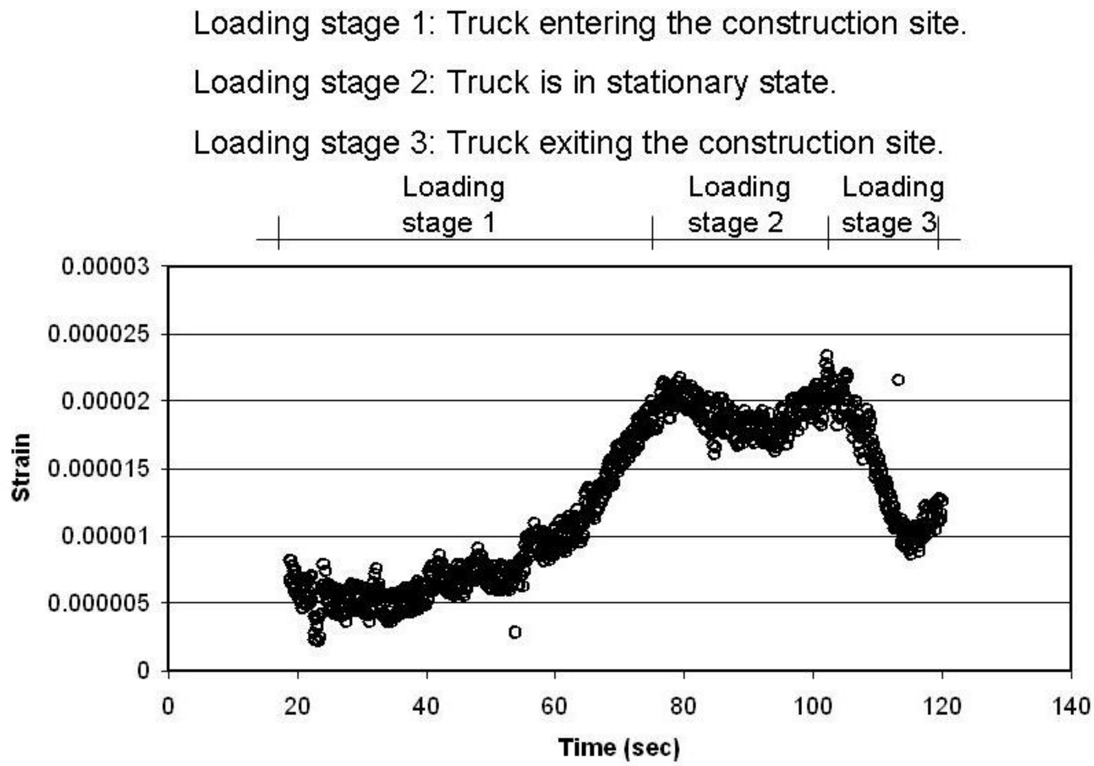

FIGURE 19 Strain measurements at spot 1 on concrete surface prior to strengthening.

The FE model was used to determine the strain in the CFRP strips after strengthening. The FE model predicted that the maximum strain in the CFRP strips for the test truck load should not exceed 23.2 με. Strains monitored using strain gauges glued above the CFRP strips at the second load-test observed strains on the CFRP strips changing with the motion of the test-truck along the bridge as shown in Fig. 22. The maximum observed strain on the CFRP surface was 20.5 με which is close to the strains predicted from the FE analysis.

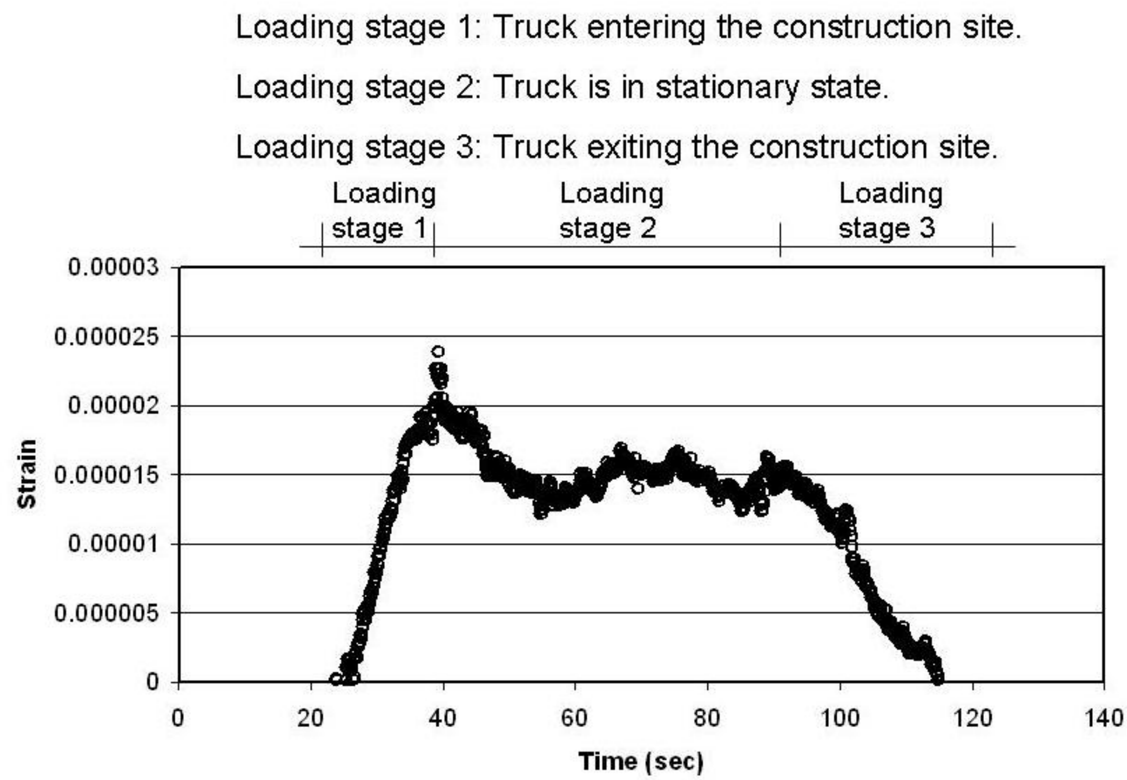

FIGURE 20 Strain measurements at spot 1 on CFRP surface after strengthening.

Moreover, the close proximity of both strains measured on the bridge surface prior to and after strengthening (20.5 $\mu\varepsilon$ on CFRP surface) and (21.7 $\mu\varepsilon$ in concrete prior to strengthening) under the same test truck load indicated the efficiency of the CFRP and its ability to resist the tensile stresses due to the test truck. Considering the strain compatibility, it was concluded that the CFRP strips are well attached to the concrete surface and will be able to enhance the girder carrying capacity. The load tests confirmed the objectives by enabling validation of the FE models and thus ensuring proper design of the strengthening system. It also confirmed the good bond between the CFRP strips and the K-Frame concrete surface and thus the ability of the CFRP strips to work as externally bonded reinforcement that are capable of enhancing the bridge carrying capacity.

SECOND FIELD TEST (FEB. 2008)

A second field test was organized and performed after 6 months of the CFRP strip applications. The field test was conducted on in February 2008 by the University of New Mexico team. New strain gauges were installed on CFRP strips and 4 new measurements were collected. It was interesting to note that that almost all the strain gauges installed on July 2007 were still operational. The following steps clarify this field test in more details.

Step 1: Cleaning the surface and investigate the conditions of CFRP strips

Fig. 21 shows the site before and after cleaning process.

FIGURE 21 CFRP strips before and after cleaning.

Step 2: Installing New Strain Gauges

The new strain gauges were installed on CFRP strips to get more measurements at different locations on CFRP strips. Fig. 22 illustrates the process of installing strain gauges. Fig. 23 shows the location of all strain gauges installed on CFRP strips schematically.

FIGURE 22 Installing new strain gauges.

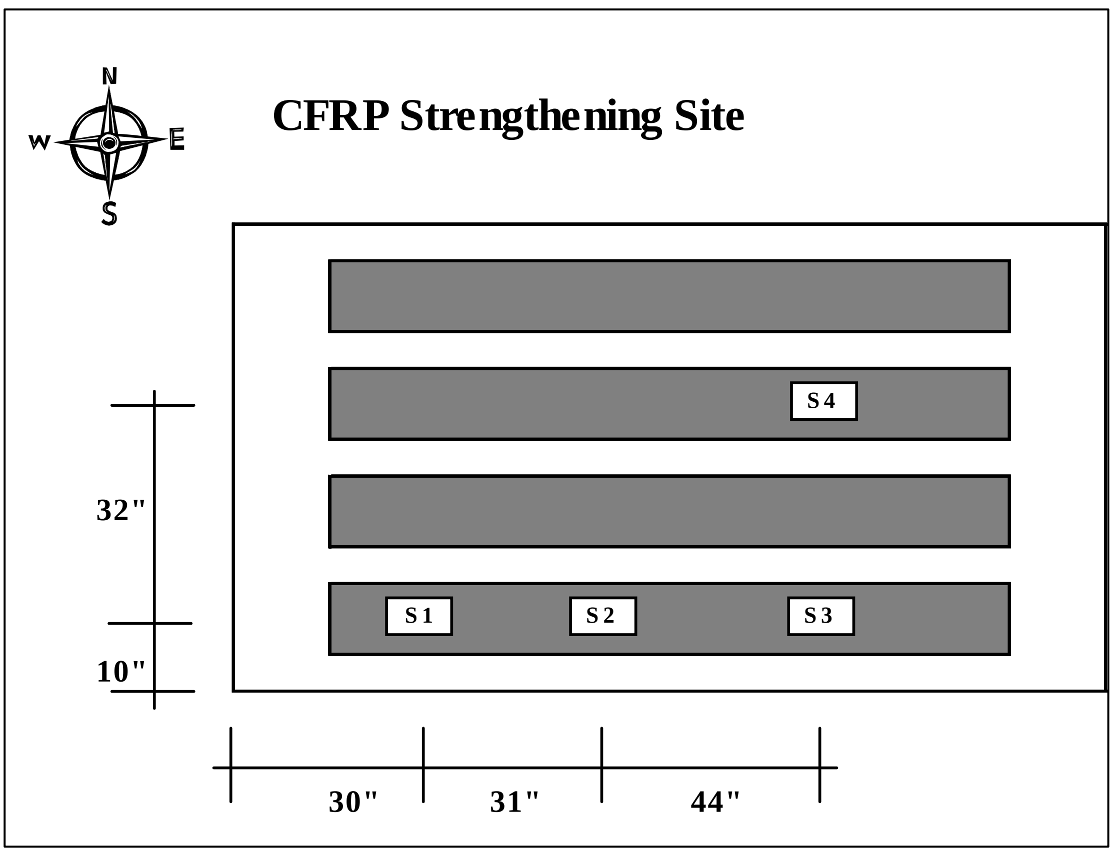

FIGURE 23 Location of strain gauges on CFRP strips.

Step 3: Load Test to Validate the Efficiency of CFRP Strips

After the installation of new strain gauges on CFRP strips, old and new strain gauges were connected to a data acquisition system. Using a 50 kips truck provided by NMDOT, new measurements were collected to demonstrate the efficiency of the CFRP strips in carrying load. Based on truck position at the field test, the FE model calibrated using concrete strain data (Report 1) was used to predict the strain in the CFRP strips. Predicted strains using the SAP 2000® FE model were then compared with the field test measurements. The new FE model is shown in Fig. 24. The strains were calculated at the location of strain gauges. Fig. 25 represents the strains at the locations shown in Fig. 23 based on different truck positions in the FE model. It should be noted that strain gauges 3 and 4 show the same results in the 2D FE model of the bridge girder because they are located at the same distance from the moving truck but at two different distances from the edge of the deck slab.

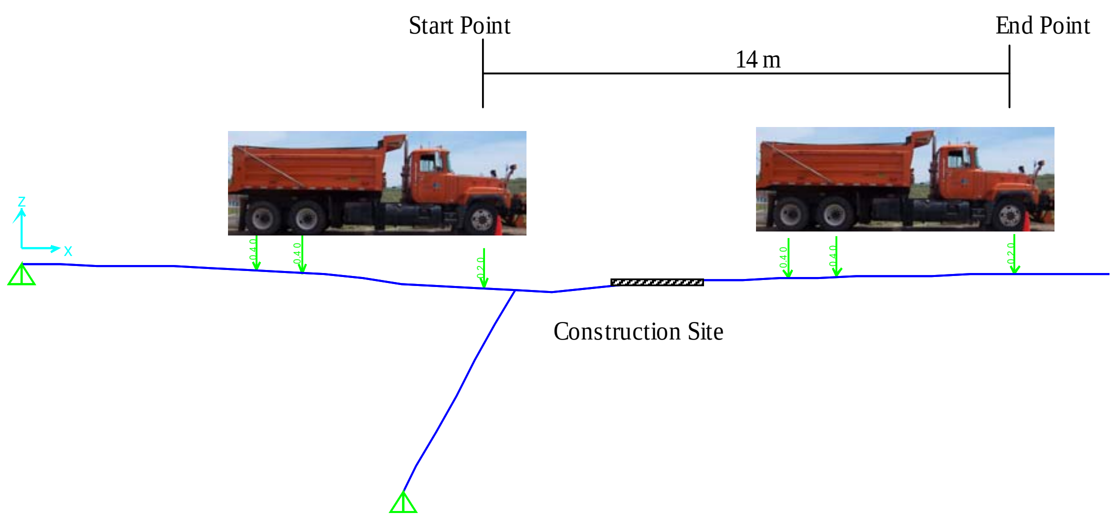

FIGURE 24 FE model based on the truck position in the field test.

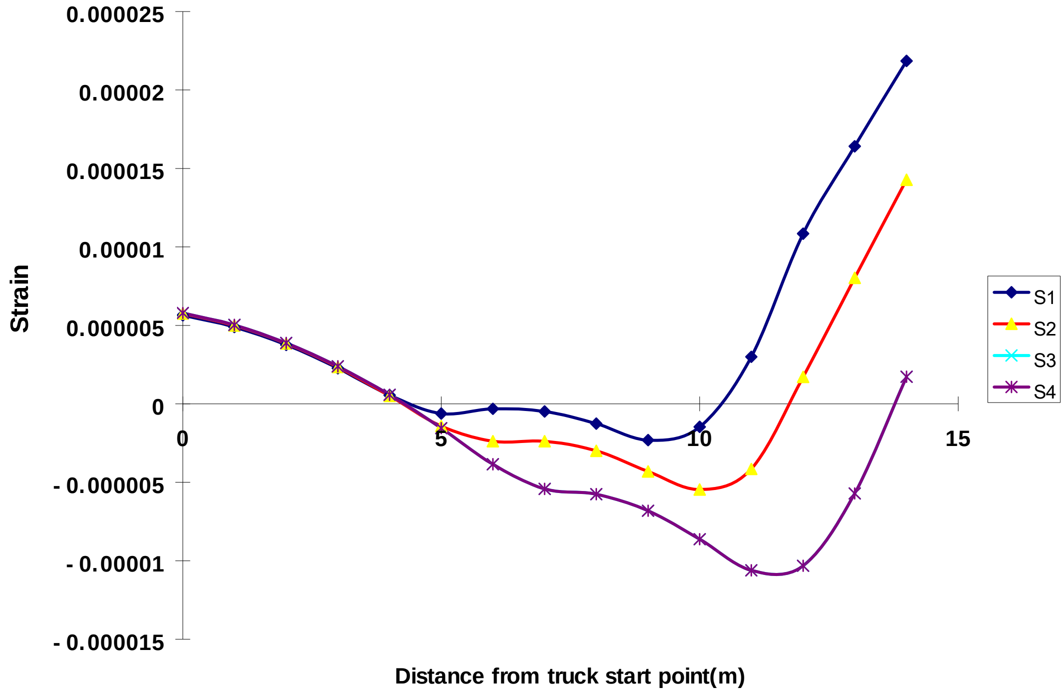

FIGURE 25 Strains predicted from SAP 2000 FE model at strain gauges locations.

VALIDATION

To validate the efficiency of the CFRP strips, a comparison between the strains from FE model and the strains collected in the site were made at four strain gauge locations. Figs 26, 27, 28 and 29 illustrate the strains predicted from FE model and measured from the field tests at strain gauges S1, S2, S3 and S4. The strains predicted from the FE model were similar to the strains collected from the field test as the truck moved along the bridge. The strains measured at the CFRP strips confirm complete bond between concrete surface and CFRP strips which indicates the ability of the CFRP strips to enhance the bridge carrying capacity.

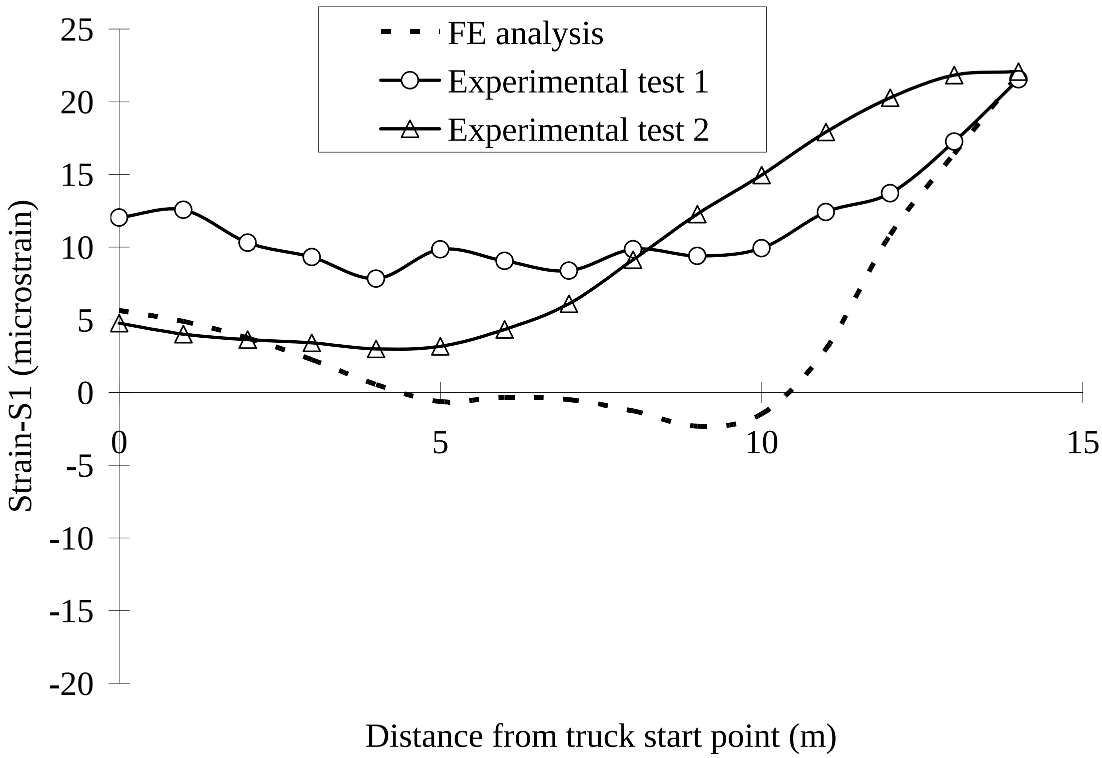

FIGURE 26 Strains calculated from FE model and field test at strain gauge 1 on CFRP strips.

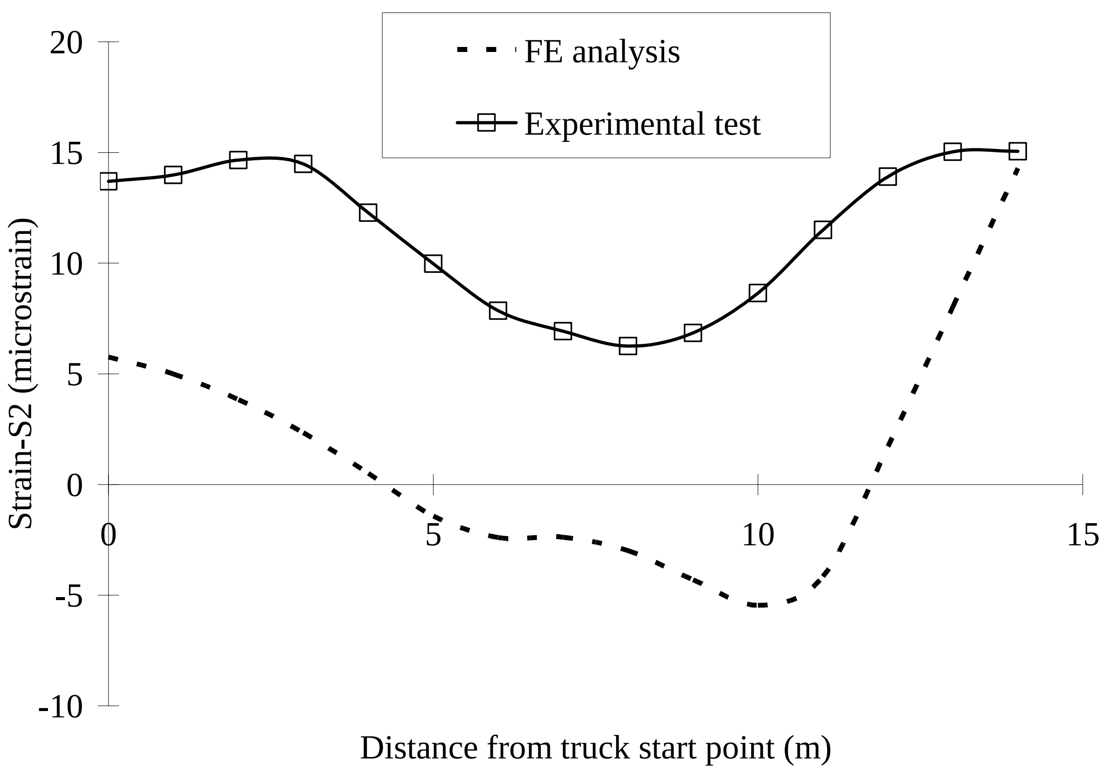

FIGURE 27 Strains calculated from FE model and field test at strain gauge 2 on CFRP strips.

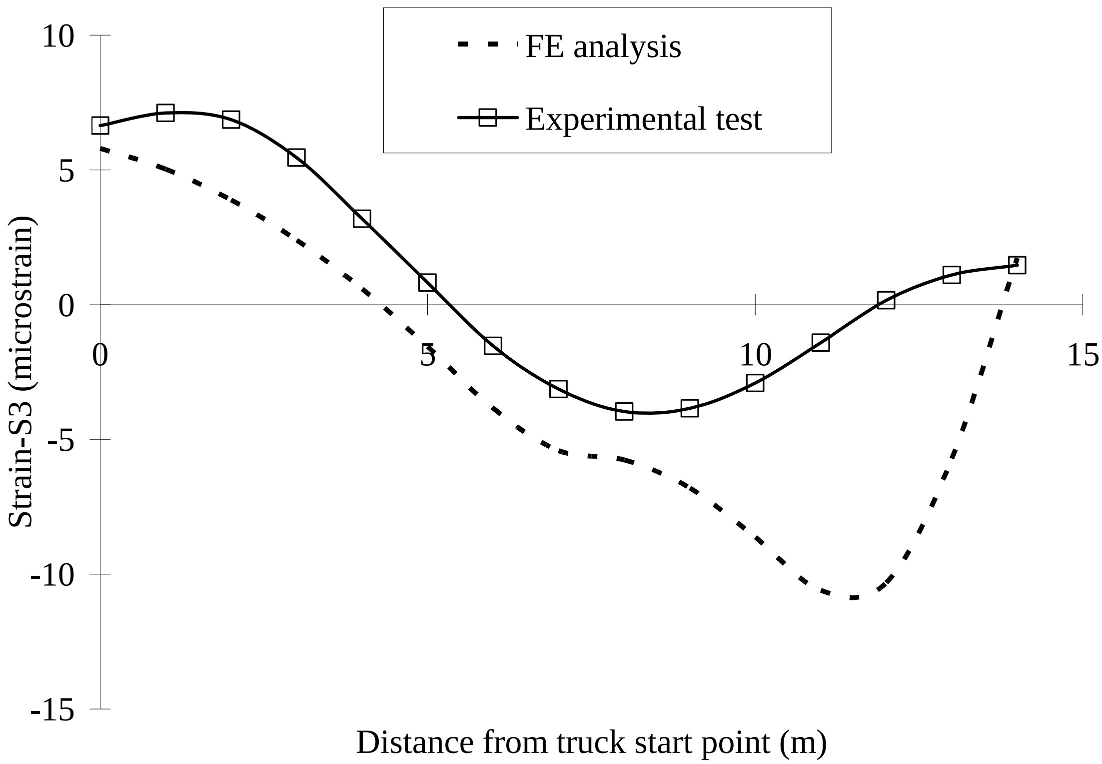

FIGURE 28 Strains calculated from FE model and field test at strain gauge 3 on CFRP strips.

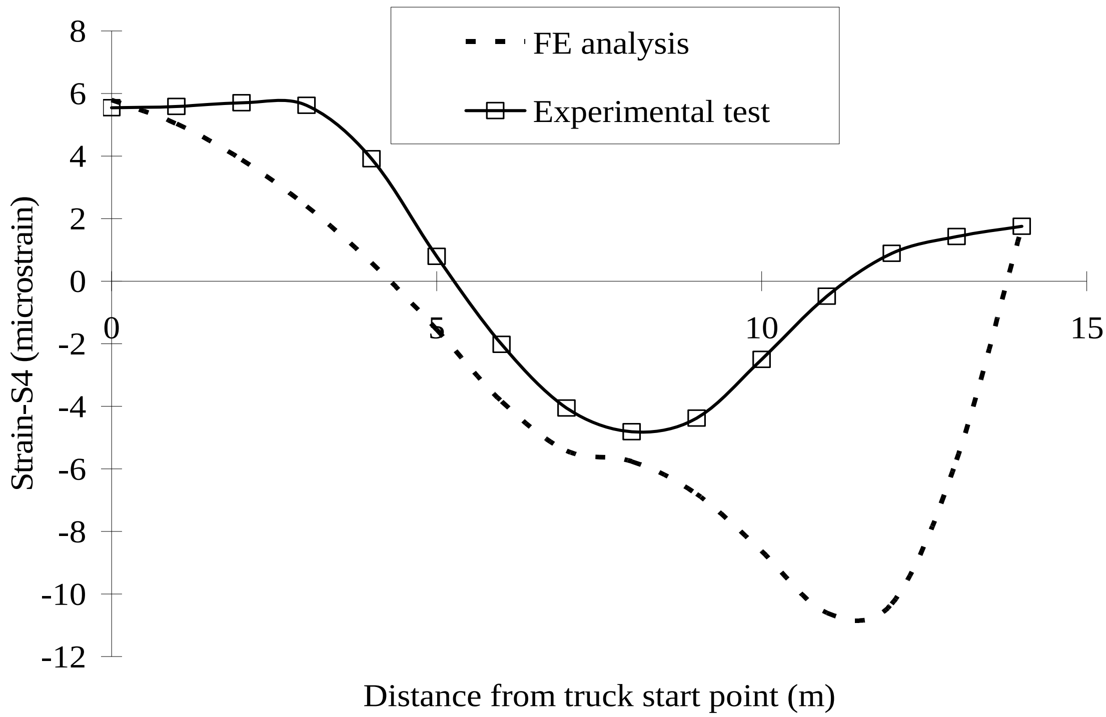

FIGURE 29 Strains calculated from FE model and field test at strain gauge 4 on CFRP strips.

RECOMMENDATION

Based on the above analysis and test observations, it is recommended that similar strengthening using CFRP should be applied to all four K-joints of the K-Frame bridges in Tucumcari, New Mexico bridges 7930, 7931, 7937 and 7938 once funding for such bridge enhancement becomes available.

REFERENCES

1. AASHTO. LRFD Bridge Design Specifications. *Manual for Condition Evaluation of Bridges*. American Association of State Highway and Transportation Officials. 2006 Interim Revisions, Second Edition, Washington, D.C., 2006.

2. ACI 440 Committee. *Guide for the Design and Construction of Externally Bonded FRP Systems for Strengthened Concrete Structures*, ACI 440.2R-02, American Concrete Institutes, Farmington Hills, MI, 2002.

3. CEB-FIP. Externally bonded FRP reinforcement for RC structures. TRB 14, 2001, p. 124.

4. National Instruments. LabVIEW Fundamentals, 2005.

5. ACI 318 Committee. Building Code and Commentary. ACI 318-05/318R-05, 2005.

New Mexico Department of Transportation

Research Bureau

Innovation in Transportation

Strengthening Reinforced Concrete Bridges in New Mexico Using fiber Reinforced Polymers:

Report IV: Guidelines for Using FRP Technology for Strengthening Bridges

Prepared by:
University of New Mexico
Department of Civil Engineering
Albuquerque, NM 87131

Prepared for:
New Mexico Department of Transportation
Research Bureau
Albuquerque, NM 87109

In Cooperation with:
The US Department of Transportation
Federal Highway Administration

Report
NM06TT-01

MARCH 2008

Form DOT F 1700.7 (8-72)

1. Report No.
NM06TT-01

2. Government Accession No.

3. Recipient's Catalog No.

4. Title and Subtitle
Strengthening Reinforced Concrete Bridges in New Mexico Using Fiber Reinforced Polymers
Report IV: Guidelines for Using FRP Technology for Strengthening Bridges

5. Report Date
March 20[illegible]

6. Performing Organization Code

7. Author(s)
M. M. Reda Taha, K. K. Choi, M. Azarbayejani

8. Performing Organization Report No.

9. Performing Organization Name and Address
University of New Mexico
Department of Civil Engineering
Albuquerque, NM 87131

10. Work Unit No. (TRAIS)

11. Contract or Grant No.
CO4961

12. Sponsoring Agency Name and Address
Research Bureau
New Mexico Department of Transportation
7500-B Pan American Freeway NE
Albuquerque, NM 87109

13. Type of Report and Period Covered

14. Sponsoring Agency Code

15. Supplementary Notes

16. Abstract

The purpose of this research was to evaluate the structural capacity of concrete frame bridges #7930, 7931, 7937 and 7938 at Tucumcari, New Mexico and evaluate the need for strengthening to meet AASHTO safety requirements. The report provides detailed guidelines for the design and implantation of FRP technology to strengthen reinforced concrete bridges. Special considerations to guarantee the efficiency of the FRP strengthening system are also discussed.

17. Key Words:
Concrete frame bridges, AASHTO LRFD Bridge Design Specification, Fiber reinforced polymers.

18. Distribution Statement
Available from NMDOT Research Bureau

19. Security Classif. (of this report)	20. Security Classif. (of this page)	21. No. of Pages	22. Price
None	None	17	

STRENGTHENING REINFORCED CONCRETE BRIDGES IN NEW MEXICO USING FIBER REINFORCED POLYMERS

Report IV: Guidelines for Using FRP Technology for Strengthening Bridges

by

M. M. Reda Taha
K. K. Choi
M. Azarbayejani
University of New Mexico
Department of Civil Engineering

Prepared for:
New Mexico Department of Transportation, Research Bureau

A Report on Research Sponsored by:
New Mexico Department of Transportation, Research Bureau

In Cooperation with the
U.S. Department of Transportation, Federal Highway Administration

March 2008

NMDOT Research Bureau
7500-B Pan American Freeway NE
Albuquerque, NM 87109

PREFACE

The purpose of this research is to evaluate the structural capacity of concrete frame bridges #7930, 7931, 7937 and 7938 at Tucumcari, New Mexico and evaluate their need for strengthening to meet AASHTO safety requirements. This report provides detailed guidelines for the design and implantation of FRP technology to strengthen reinforced concrete bridges.

ABSTRACT

The purpose of this research was to evaluate the structural capacity of concrete frame bridges #7930, 7931, 7937 and 7938 at Tucumcari, New Mexico and evaluate the need for strengthening to meet AASHTO safety requirements. The report provides detailed guidelines for the design and implantation of FRP technology to strengthen reinforced concrete bridges. Special considerations to guarantee the efficiency of the FRP strengthening system are also discussed.

TABLE OF CONTENTS

TABLES

FIGURES

INTRODUCTION

For several decades, rehabilitation of existing reinforced concrete (RC) structures has emerged as a primary issue in civil engineering. Concrete aging, service in harsh environmental conditions, poor maintenance and an increase in traffic loads might cause the trend of deterioration of concrete infrastructure. Conventional rehabilitation methods have been applied using externally bonded steel plates and jackets with little results. Recently, the use of fiber reinforced polymer (FRP) sheets and plates appeared as a promising strengthening and rehabilitation alternative material with significant advantages compared with common strengthening and rehabilitation materials including high corrosion resistance, durability and high strength to weight ratio (1 and 2). Moreover, the ease of application of FRP materials enabled its use to increase the flexural and shear capacity of a number of existing concrete structures (3).

This document aims at providing guidelines for the design and installation of FRP systems, and for the external strengthening of reinforced concrete structures. Overall design guidelines and recommendations are based on design methods developed by design committees (4) and (5) and strengthening the K-frame reinforced concrete bridges in Tucumcari, New Mexico. The flexural strengthening method is reported in detail.

FRP STRENGTHENING MATERIALS

FRP strengthening systems can be classified into three groups according to their resin curing:

- Group I: Wet lay-up systems composed of dry FRP sheets. FRP sheets are saturated by resin and cured in-site.

- Group II: Prepreg systems composed of uncured but pre-impregnated with resin in the manufacturer's facility. The systems may or may not require additional resin for its application to concrete surface. After application of FRP, these systems need time for the curing process to properly take effect.
- Group III: Pre-cured systems, which are composed of pre-cured FRP with various shapes according to their purposes. These systems may require putty and resin for FRP application. The FRP strips which are used for external strengthening are one example of the pre-cured systems.

The performance of FRP systems is dependent on several parameters including fiber type and volume, and resin type. Emphasis is given to the 1pre-cured FRP systems.

Adhesives

To bond FRP strips to the concrete surface, adhesives with sufficient bond strength are crucial for satisfactory composite action between concrete and FRP. Epoxy, which is formed by mixing epoxy resin and hardener, is the typical adhesive recommended for use with FRP. In CEB-FIP repost (5), epoxy shows several advantages over other types of polymer adhesives. Such advantages include:

- High surface activity for various substrates
- High bond strength after curing
- Relatively low shrinkage and creep

Typical properties of cured epoxy are provided in Table 1 (5) comparing them with those of concrete and mild steel.

Table 1 Comparison of material properties of epoxy, concrete and steel.

Properties (at 20^{o}C)	Epoxy	Concrete	Mild steel
Density (kg/m^3)	1100-1700	2350	7800
Young's modulus (GPa)	0.5-20	20-50	205
Tensile strength (MPa)	9-30	1-4	200-600
Shear strength (MPa)	10-30	2-5	200-600
Compressive strength (MPa)	55-110	25-150	200-600
Coefficient of thermal expansion ($10^{-6}/^{o}$C)	25-100	11-13	10-15
Glass transition temperature (^{o}C)	45-80	-	-

FRP

FRP materials are relatively light matter compared with typical construction materials (i.e. concrete and steel). FRP density varies from 1200 kg/m^3 to 2100 kg/m^3 according to the type of fiber. The tensile strength and stiffness of FRP are dependent mainly on the fiber type, orientation and fiber volume fraction. The ultimate tensile strength and rupture strain of several types of FRP are summarized in Table 2 (4). It is noted in Table 2 that manufacturers should report the properties of FRP as the mean tensile strength (or rupture strain) of the sample tests minus three times the standard deviation (4). The FRP materials show the coefficient of thermal expansion compared with concrete. FRP materials do not show identical coefficient for longitudinal and transverse directions as presented in Table 3. For reference, the coefficients of thermal expansion of concrete and steel are $7x10^{-6}$ to $11x10^{-6}/ ^{o}$C and $11.7x10^{-6}/^{o}$C, respectively, while that of CFRP seems to be -1 x 10^{-6}.

Table 2 Tensile strength and rupture strain of FRP.

Fiber	Elastic modulus, GPa	Ultimate strength ,GPa	Rupture strain, %
Carbon			
General purpose	220 to 240	2050 to 3790	1.2
High strength	220 to 240	3790 to 6200	1.4 to 1.5
High modulus	340 to 690	1380 to 3100	0.2 to 0.5
Glass			
E-glass	69 to 72	1860 to 2680	4.5
S-glass	86 to 90	3440 to 4140	5.4
Aramid			
General purpose	69 to 83	3440 to 4140	2.5
High performance	110 to 124	3440 to 4140	1.6

Table 3 Coefficients of thermal expansion of FRP.

	GFRP, $10^{-6}/^{o}C$	CFRP, $10^{-6}/^{o}C$	AFRP, $10^{-6}/^{o}C$
Longitudinal direction	6 to 10	-1 to 0	-6 to -2
Transverse direction	19 to 23	22 to 50	60 to 80

Mixed results of time dependent properties have been reported with different FRP materials. While GFRP seem to have creep rupture limitations and deteriorates under significant fatigue stress range, CFRP showed no sign of creep and does not deteriorate under fatigue. Creep rupture limitations shall be considered in design of GFRP as recommended by ACI 440 (4) and CEB-FIP (5).

DESIGN RECOMMENDATIONS

General Design Concept

The design concept of FRP strengthening systems are based on typical design of RC structures in ACI 318-05 (6). The design recommendation is therefore also based on similar RC strength design principles listed by AASHTO (7), ACI 318-05 design code (6) and ACI 440 guide (4). Design is based on load and resistance factors which consider a strength reduction (ϕ) factor as required by ACI 318-05 (6) and AASHTO (7). Other reduction factors to consider are brittle behavior of FRP compared with steel reinforcement and significance of other environmental conditions on performance.

For careful consideration of FRP strengthening systems, ACI 440 (4) recommends strengthening limits as

$$(\phi R_n)_{existing} \geq (1.2S_{DL} + 0.85S_{LL})_{new} \quad (1)$$

where:

ϕ = strength reduction factor

R_n = nominal strength

S_{DL} and S_{LL} = factored dead load and live load.

In design of FRP strengthening systems, the environmental reduction factor C_E is considered. The ultimate tensile strength and rupture strain are determined as

$$f_{fu} = C_E f_{fu}^* \quad (2a)$$

$$\varepsilon_{fu} = C_E \varepsilon_{fu}^* \quad (2b)$$

where:

f_{fu} = ultimate tensile strength considering the environmental reduction

f_{fu}^* = ultimate tensile strength without considering the environmental reduction

ε_{fu} = rupture strain considering the environmental reduction

ε_{fu}^* = rupture strain without considering the environmental reduction.

The environmental reduction factor CE for exterior exposure condition is 0.85, 0.65, and 0.75 for Carbon, Glass, and Aramid, respectively while that for aggressive environment is 0.85, 0.50, and 0.70 for Carbon, Glass, and Aramid, respectively. Stiffness of FRP would then be obtained as $E_f = f_{fu} / \varepsilon_{fu}$ which would be similar if f^*_{fu} and ε^*_{fu} are considered.

Flexural Strengthening

The flexural resistance of the RC girders was defined according to AASHTO specification (section 5) as

$$M_n = A_s f_y (d - a/2) \tag{3}$$

where:

A_s = area of tension reinforcement

f_y = yield strength of reinforcing bars

a = depth of the equivalent stress block.

In AASHTO, the need for strengthening of concrete structures can be determined by the following equation.

$$\phi M_n \geq M_u \tag{4}$$

where:

ϕ = strength reduction factor which is different in moment and shear

M_n = nominal flexural strength

M_u = factored moment.

When ϕM_n is less than M_u, the concrete structures need to be strengthened by proper methods. According to the results of FE analysis shown in Report (1), it was found that as expected all the K-frame bridges 7930, 7931, 7937, and 7938 in Tucumcari, New Mexico showed shortage in negative moment capacity around the K-frame connections and would require strengthening. Based on Report (1) and Report (2), it was decided to use Fiber Reinforced Polymer (FRP) sheets as a strengthening material to increase the moment capacity of the RC K-frames in Tucumcari, New Mexico. The moment resistance to be provided by FRP is calculated as

$$M_u - \phi M_n \leq \phi M_{frp} \tag{5}$$

where:

M_u = factored moment

M_n = nominal moment-carrying capacity.

In ACI 440, ϕM_{frp} is evaluated as

$$\phi M_{frp} = \phi \varphi_{frp} A_f E_f \varepsilon_{fe} \cdot jd \tag{6}$$

where:

φ_{frp} = additional reduction factor (=0.85)

A_f = area of FRP reinforcement

ε_{fe} = effective ultimate strain developing at FRP

E_f = Young's modulus of FRP

jd = length of moment arm.

The design process was similar to that used by AASHTO and ACI for RC sections and is based on strain-compatibility and equivalent concrete block concept (refer to Fig. 1). In this design, it is assumed that the existing strain is negligible considering that no tensile cracking was observed in the girders during the field visit before strengthening. Therefore, the effective strain of FRP at ultimate state is defined as

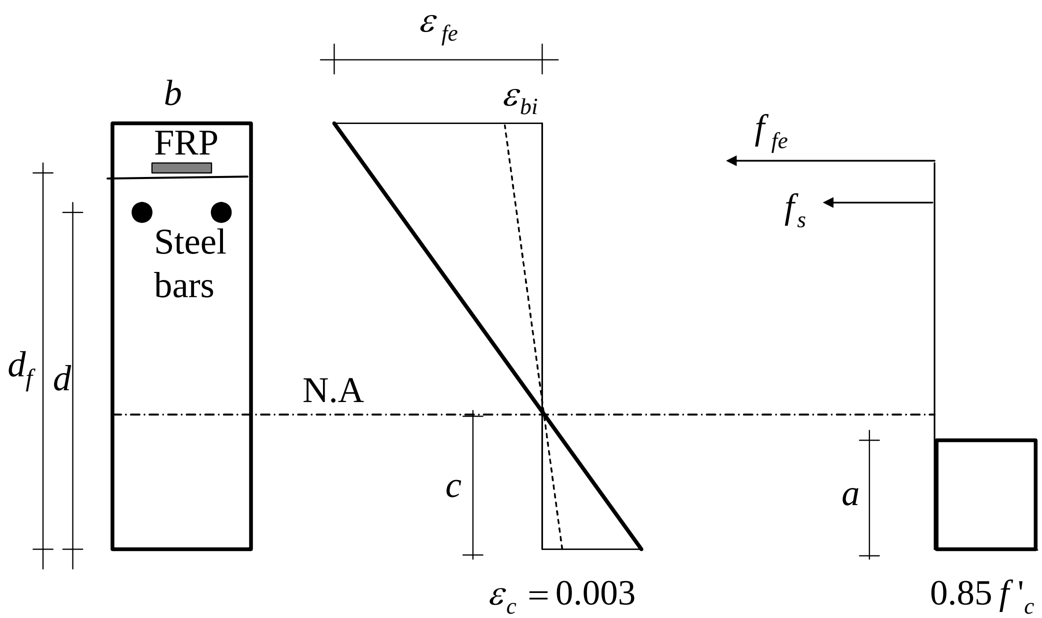

Figure 1 Stress and strain distribution of the concrete beam strengthened by FRP.

$$\varepsilon_{fe} = 0.003\left(\frac{d_f - c}{c}\right) \le \kappa_m \cdot \varepsilon_{fu} \qquad (7)$$

where:

d_f = effective depth for FRP reinforcement

c = depth of compression zone

κ_m = bond-dependent coefficient for flexure

ε_{fu} = design rupture strain of the FRP reinforcement.

The bond-dependent coefficient for flexure is defined as ACI 440 2002 (4)

$$k_m = \frac{1}{60\varepsilon_{fu}}\left(1 - \frac{nE_f t_f}{360000}\right) \le 0.90 \qquad \text{for} \quad nE_f t_f \le 180{,}000 \qquad (8a)$$

$$k_m = \frac{1}{60\varepsilon_{fu}}\left(\frac{90}{nE_f t_f}\right) \leq 0.90 \qquad \text{for} \quad nE_f t_f > 180{,}000 \tag{8b}$$

where:

E_f = tensile modulus of elasticity of FRP (MPa)

n = number of plies of FRP reinforcement

t_f = nominal thickness of one ply of the FRP reinforcement (mm)

For convenience in calculation, for Carbon Fiber Reinforced Polymer (CFRP) and Glass Fiber Reinforced Polymer (GFRP), κ_m = 0.9 is recommended in the design practice. Using the results of structural analysis presented in Report (1), the maximum negative moment demand ($M_u - \phi M_n$) needs to be resisted by the CFRP strengthening systems. The required amount of CFRP is calculated as

$$A_f = \frac{M_u - \phi M_n}{\kappa_m \cdot \varepsilon_{fu} E_f \phi \varphi_{frp} \cdot jd} \tag{9}$$

The moment arm after application of CFRP can be assumed to be $jd = 0.85d$. If the CFRP strips provided by manufacturers are not long enough to cover the entire application range, two or three strips can be used with lap splicing. The exterior beam in bridge 7937 is considered as the design example. According to the results of Finite Element (FE) analysis shown in Report (1), the maximum negative moment demand ($M_u - \phi M_n$) in Eq. (5) is 3,788 kN.m. Thus, the required area of FRP reinforcement can be evaluated as follows.

For CFRP with $E_f = 150{,}000\,MPa$ and $\varepsilon_{fu} = 0.0134$

$$A_f = \frac{M_u - \phi M_n}{\kappa_m \cdot \varepsilon_{fu} E_f \phi \varphi_{frp} \cdot jd} = \frac{3788}{0.9 \cdot 0.0134 \cdot 150000 \cdot 0.85 \cdot 0.85 \cdot 0.9 \cdot 1.8} \times 1000 = 1789\,mm^2$$

If GFRP with $E_f = 42{,}000\,MPa$ and $\varepsilon_{fu} = 0.0165$

$$A_f = \frac{M_u - \phi M_n}{\kappa_m \cdot \varepsilon_{fu} E_f \phi \varphi_{frp} \cdot jd} = \frac{3788}{0.9 \cdot 0.0165 \cdot 42000 \cdot 0.85 \cdot 0.85 \cdot 0.9 \cdot 1.8} \times 1000 = 5190\,mm^2$$

CFRP was chosen as the strengthening alternative for its enhanced mechanical characteristics. The choice of CFRP was also based on its excellent durability characteristics and reported performance in harsh service environment. Other design considerations include checking the limit state on fatigue rupture by limiting the stress in the FRP under service loads. These details are provided in Report (2) for designing of the FRP strengthening system and is also discussed elsewhere (4).

APPLICATION OF FRP STRIPS AS STRENGTHENING MATERIAL

Application of FRP strips should be performed according to Steps 1 through 4 on Pgs IV – 11 to 15. The FRP strip strengthening method uses various materials: putty, adhesive (epoxy), and FRP strips. During installation, each material's manufacturers' specification must be considered. Three basic materials are as follows.

Substrate: this is the concrete surface to which the FRP is bonded. The status and material properties including cracks, tensile strength and unevenness need to be identified. Results of the rebound hammer (Report (1) proved the soundness of the concrete substrate.

Adhesive: this is a bonding agent to bond FRP to the substrate. In some bonding agents, they may impregnate wet lay-up of FRP. Epoxy is the most common adhesive used with FRP.

FRP: this is a strengthening material which is bonded to the substrate. See Chapter (2).

As discussed in Chapter (2) of this report, two types of FRP are used depending on the technique selected; strips (or laminates) for the pre-cured technique, and sheets (or fabrics) for the wet lay-up technique (see Table 4). FRP strips are already cured composites of resin and fibers. When using FRP strips for the pre-cured technique, epoxy adhesive can be used to bond the strips to the concrete substrate. However, since FRP sheets do not include resin, the wet lay-up process requires an application of epoxy adhesive in order to bond the FRP sheets to the substrate. This additional process of impregnating the FRP sheets in epoxy adhesive is a requirement of the wet lay-up process.

Table 4 Comparison of two types of FRP systems (CEB-FRP 2001).

	Pre-cured system	Wet lay-up system
Type of FRP used	Strips or laminates	Sheets or fabrics
Thickness	1.0 – 1.5 mm	0.1 to 0.5 mm
Use of resin	To bond strips (or laminates) and substrate	To bond sheets (or fabrics) and substrate, and to impregnate resin inside the sheet
Basic application	* It is usually used for the flat surface of a substrate. For a special shaped substrate, it should be pre-shaped. * 1 layer and multi-layer fibers. * High quality guaranteed	* It can be used regardless of the surface shape of a substrate. * Multi-layers are common * Accurate application is needed due to its flexibility

.

The following four steps are therefore fundamental for the application of FRP.

Step 1: Check Possible use of FRP as a Strengthening Material

Before applying FRP as a strengthening material, the applicability of FRP strengthening to be used with the concrete structure of interest needs to be carefully checked. This includes checking the soundness of the concrete surface. According to CEB-FIP (5), the minimum concrete tensile strength must be greater than 1.5 MPa. If the deteriorated concrete is too deep, all deteriorated concrete surfaces need to be replaced. The crack width should be less that 0.2 mm. If the crack is larger than 0.2 mm, it should be filled and sealed properly by a low viscosity resin before applying FRP.

Step 2: Concrete Surface Preparation

This is the most important step in application of FRP because properly roughened and even concrete substrate is crucial for reliable performance of FRP strengthening (5). Milling of the concrete/asphalt top surface will be necessary if the FRP is to be used as top reinforcement so that the final FRP material is embedded and not exposed to the outer environment. If FRP is to be applied to the bottom side of concrete girders, the FRP strips can be applied to concrete substrate directly with proper surface preparation shown in the next steps.

The acceptable unevenness, which indicates the maximum difference of the surface depth, is specified in current design provisions. In CEB-FIP code (5), the allowable value of unevenness of the concrete surface is 4 mm (1/6 in). If the surface is not sufficiently even, a putty (filling material) needs to be applied to obtain an even concrete surface. Moreover, several aspects need to be considered.

(11) The concrete surface should be dry and needs to be contamination free from oil, water or dust before application of FRP. In CEB-FIP code (5), the

minimum recommended temperature for FRP application is 5^{o} C, otherwise the temperature and humidity need to be controlled artificially.

(12) Special care is needed to ensure hardening of the putty material when used. Usually, the hardening time may vary from 1 day to 14 days depending on the putty material used. Fast hardening putty materials are recommended.

Step 3: Application of FRP Strips

To attach FRP strips to concrete substrate, epoxy adhesive with sufficient bond strength is used. The epoxy adhesive is made by mixing a resin and a hardener, determined by the manufacturer's specifications. Epoxy has a limited pot life (15 – 30 minutes) and it significantly shortens in hot weather. Therefore, after mixing the resin and hardener, the FRP needs to be quickly applied within 80% of the allowable working time or pot life (5). Moreover, epoxy material hardening is sensitive to temperature. The specifications by manufactures need to be considered carefully. Other aspects that need to be taken into account include:

(1) To insure better bonding, FRP strips need proper abrading and wiping, and must be completely dry before their application. FRP strips need to be carefully handled using clean gloves. In addition, installers need to check for possible damage during the delivery of the FRP to the construction site. The adhesive normally needs to be applied to both the concrete substrate and FRP strips. After applying the FRP strips to the concrete, proper pressure should be applied using a rubber roller for intimate contact. Any excess, oozing adhesive should be removed. The proper thickness of adhesive is 1.5 to 2.0 mm.

(2) A high viscosity adhesive is used for FRP strips, and a low viscosity adhesive is used for FRP sheets.

(3) FRP sheets and fabrics should be checked to be free from twists or fiber misalignment.

(4) FRP sheets — adhesive is applied to the concrete surface (known as undercoating) by a roller brush. Then, the FRP sheets are applied. Finally,

adhesive needs to be applied on top of the FRP sheets for impregnation (known as over coating).

Step 4: Curing and Finishing

After FRP application, the construction site should be properly covered by plastic sheets for curing. A concrete topping is then applied to cover the FRP strips after the epoxy has hardened. The curing time specified by the epoxy's manufacture should be followed to ensure the epoxy develops its maximum strength. No external heating shall be applied. To ensure proper quality control for FRP application, the following shall be considered:

(1) Quality control for strengthening materials.

All the materials used should be properly checked with the manufacturer's testing data. The test data needs to be based on standard test methods. For epoxy adhesives, the pot life should exceed 40 minutes at 20^{o}C. The glass transition temperature, Tg, should be greater than 45^{o}C. The modulus of elasticity of adhesive should be 2000-15000 MPa and the shear strength, and bond strength of adhesives should be greater than 12 MPa and 15 MPa at 20^{o}C. For durability of the adhesive, the performance should be ensured by proper laboratory accelerated tests for a minimum of 15 years. Finally, manufacturer reported properties of FRP shall meet or exceed those reported by design standards by AASHTO and ACI.

(2) Quality control for practical execution.

The FRP application should be performed by qualified and experienced workers. The minimum tensile strength of the concrete surface and sound condition discussed above must be checked. In particular, the direction of FRP application and unevenness of concrete surface should be carefully checked.

(3) Bond quality control after FRP application.

The bond quality of FRP-concrete interfaces should be tested by standard test methods (4). Usually, at least 3 bond tests are recommended to be performed at 3 days and/or at 7 days. Destructive tests will be performed partially for the critical zone with voids. Surface adherence pull-off test, surface adherence shear test, and surface adherence torque test are the representative destructive tests. For detailed information, please refer to CEB-FIP (5). Non-destructive tests include tapping, ultrasonic pulsed echo techniques and ultrasonic transparency techniques.

SPECIAL CONSIDERATIONS

Previous research showed that FRP strengthening systems exposed to harsh environments show poor performance. The following issues pertaining to the FRP exposure environment should be considered.

Moisture Effect

In the interface of concrete, FRP and resin there may be voids which can absorb water. The water absorption of resin lowers the glass transition temperature (Tg). Tg indicates the temperature above which FRP does not develop its original performance (8). Moreover, the water absorbed into concrete may propagate the peeling action (or debonding of FRP-concrete interface), which deteriorates the durability of the FRP strengthening systems. According to the results of research performed by the UNM team, it was found that using Latex Modified Concrete (LMC) as an overlay can significantly prevent the moisture absorption. The combined performance of FRP strengthening systems and LMC overlay need further research.

Temperature Effect

At low temperature, the water absorbed at FRP-concrete interface and resin can expand and cause micro-cracking. At the high temperature beyond Tg, the FRP-Concrete interface does not develop its full bond strength (9). Therefore, in design of FRP systems, high or low temperature effects shall be considered.

Sunlight Effect

In addition, UV light may reduce the durability of resin and FRP performances (10). So, the FRP systems need to be protected by proper topping or overlay and shall not be left to sunlight exposure.

Creep of Epoxy

It is evident that epoxy creeps. Recent research investigations by the UNM team (11) showed that such epoxy creep at the FRP-concrete interfaces is critical when thick epoxy resins and high stress to ultimate shear strength ratios take place. The stress in the FRP sheets shall also be sustained. In this project, FRP is used against live load only and no creep effects should be noticed. Careful checks are recommended if stress in the FRP shall be sustained. Further research is definitely needed in this area.

REFERENCES

1. Emmons, P. H., A. M. Vaysburd and J. Thomas. Strengthening concrete structure, Part II. *Concrete International*, Vol. 20, No. 4, 1998, pp. 56-60.

2. Rizkalla, S., T. Hassan and N. Hassan. Design recommendations for the use of FRP for reinforcement and strengthening of concrete structures. *Progress in Structural Engineering and Materials*, Vol. 5, No. 1, 2003, pp. 16-28.

3. Reda Taha, M.M., E. Tromposch, G. Tadros, A. Mufti and C. Klowak. "Performance Based Design for FRP Strengthening of The Roof Panels of Calgary Saddledome". ACI Special Publication SP-215: Field Application of FRP Reinforcement: Case studies. S. Rizkalla et al., Eds., 2003, pp. 385-398.

4. ACI 440 Committee. *Guide for the Design and Construction of Externally Bonded FRP Systems for Strengthened Concrete Structures*, ACI 440.2R-02, American Concrete Institute, Farmington Hills, MI, 2002.

5. CEB-FIP. Externally Bonded FRP Reinforcement for RC Structures. TRB 14, 2001, p. 124.

6. ACI Committee 318. Building Code Requirements for Structural Concrete (ACI 318M-05) and Commentary (ACI 318R-05), American Concrete Institute, Farmington Hills, MI, 2005, p. 436.

7. AASHTO. LRFD Bridge Design Specifications. *Manual for Condition Evaluation of Bridges*. American Association of State Highway and Transportation Officials. 2006 Interim Revisions, Second Edition, Washington, D.C., 2006.

8. Lubin, G. and P. Donohue Real life ageing properties of composites. In Proceedings of 35th Annual Technical Conference of the Reinforce Plastics and Composites Institute, Section 17E, 21, 1980.

9. Pantuso, A., U. Neubauer and F.S. Rostasy. Effects of thermal mismatch between FRP and concrete on bond. In Minutes of 4th ConFibreCrete Meeting, Lille, France, 2000.

10. Ahmad, S. H. and J. M. Plecnik. Transfer of composites technology to design and construction of bridges. Report of the California State University, 1989.

11. Choi, K., P. Meshgin and M. M. Reda Taha. Shear creep of epoxy at the concrete-FRP interfaces, *Composites Part B: Engineering*, 38(5-6), 2007, pp. 772-780.

New Mexico Department of Transportation
RESEARCH BUREAU
7500B Pan American Freeway NE
PO Box 94690
Albuquerque, NM 87199-4690
Tel: (505) 841-9145